Targeting APC loss using synthetic lethality in Colorectal Cancer

Hannah Shailes

Submitted in partial fulfilment of the requirements of the

Degree of Doctor of Philosophy

February 2018

Centre for Molecular Oncology

Barts Cancer Institute

Barts and The London School of Medicine and Dentistry

Queen Mary University of London

Charterhouse Square

London

EC1M 6BQ

Declaration

I, Hannah Shailes, confirm that the research included within this thesis is my own work or that where it has been carried out in collaboration with, or supported by others, that this is duly acknowledged below and my contribution indicated. Previously published material is also acknowledged below.

I attest that I have exercised reasonable care to ensure that the work is original, and does not to the best of my knowledge break any UK law, infringe any third party's copyright or other Intellectual Property Right, or contain any confidential material.

I accept that the College has the right to use plagiarism detection software to check the electronic version of the thesis.

I confirm that this thesis has not been previously submitted for the award of a degree by this or any other university.

Signature: 

Date: 28.02.18

Details of collaboration and publications:

Acknowledgements

I would like to thank Bowel and Cancer Research, and the Rosetree trust for providing the funding for this PhD project. My supervisor Dr Sarah Martin has been great, offering her guidance, expertise and support throughout the project. Also to my second supervisor for supporting the project, Dr Andrew Silver. Marta Freitas and Betty Tse have helped me with the final push of lab work and I cannot thank them enough. Every member of the Martin lab past and present have contributed, especially during the highs and lows of a PhD.

Many members of Molecular Oncology at Barts Cancer Institute have helped provide invaluable advice. Dr Tyson Sharp and Daniel Foxler were key to guiding me with the CRISPR-cas9 process. Additionally, everyone in the Sharp lab were always on hand to help in the lab, they even solved one of many problems I had with my APC blots throughout the PhD!

I'd like to thank everyone in the two offices I've worked in, sharing the PhD experience has been enjoyable and made it easier. Discussing data and learning little lab tips have hugely helped.

I'd like to thank Pam Charles for helping me with things outside of the lab. I'd like to thank both Vips Bhakta and Ashley Browne for their lab management. Also thank you to all the laboratory assistants who do a lot of work behind the scenes, keeping the labs organised and consumables topped up. They also contributed to the friendly atmosphere in the lab.

Outside of the lab I'd like to thank my family for supporting me and to Iain Goulding for keeping me fed during the final few months of lab work. Also my friends outside of the lab, who quietly wonder to themselves why a thesis consumes so much time!

Abstract

Mutations in the tumour suppressor gene *Adenomatous polyposis coli (APC)* are found in 80 % of sporadic colorectal cancer (CRC) tumours and are also responsible for the inherited form of CRC, Familial adenomatous polyposis (FAP). In order to identify novel therapeutic targets for the treatment of APC mutated CRC, we have generated an *in vitro* model of APC mutant CRC using CRISPR-cas9 gene editing. Using the APC wildtype colorectal carcinoma cell line RKO, we targeted the cells with guide RNA (gRNA) targeting exon 2 or exon 15 (encodes 80 % of APC) of the *APC* gene. We generated isogenic cell lines which differed in the expression of APC, the controls were APC wildtype and the APC mutant (APC Lys736fs) cell lines expressed a truncated ~80 kDa APC protein.

We used these cell lines to perform an siRNA screen against 720 kinases and kinase-related genes. We selected seven genes to investigate further, unfortunately none of the potential hits validated. Additionally, we performed an FDA-approved compound screen targeting over 1000 compounds. From this, we identified a group of HMG-CoA reductase (HMGCR) inhibitors known as statins, which selectively cause a greater loss in cell viability in the APC mutated cell lines, compared to the APC wildtype cells. Mechanistically, our data suggests this synthetic lethal relationship is due to a greater decrease in the anti-apoptotic protein survivin. We propose this is due to statins altering the localisation of Rac1, reducing Pak1 activation and reducing the level of Wnt signalling. This results in the reduction of the Wnt target gene survivin. We have successfully identified an FDA-approved family of compounds, which show synthetic lethality with the APC mutation in our *in vitro* model.

Abbreviations

aa	Amino acids
15aa	15 amino acid repeats
20aa	20 amino acid repeats
AFAP	Attenuated familial adenomatous polyposis
AML	Acute myloid leukemia
AMPK	AMP-activated protein kinase
APC	Adenomatous polyposis coli
AP1	Activator protein 1
ARF6	GTPase ADP-ribosylation factor 6
5-ASA	5-Aminosalicyclic acid
ASEF1	APC-stimulated guanine nucleotide exchange factor 1
ASEF2	APC-stimulated guanine nucleotide exchange factor 2
A.terreus	Aspergillus terreus
ATG13	Autophagy related 13
BCI	Barts Cancer Institute
Bcl-2	B-cell lymphoma 2
BER	Base excision repair
BID	B3 interacting-domain death agonist
BIRC5	Baculoviral IAP repeat containing 5
BMP	Bone morphogenic protein
Bp	Base pair
BRCA1	Breast cancer 1
BRCA2	Breast cancer 2
BSA	Bovine serum albumin
CAC	Colitis associated colon cancer model
Cas	CRISPR associated protein
CBP	CREB binding protein
CD40	Cluster of differentiation 40
Cdc42	Cell division cycle 42
CDK1	Cyclin dependent kinase 1
C.elegans	Caenorhabditis elegans
cIAP1	Cellular inhibitor of apoptosis protein 1
cIAP2	Cellular inhibitor of apoptosis protein 2
CIN	Chromosomal instability
CK1	Casein kinase 1
CK1α	Casein kinase 1α
CMS	Consensus molecular subtypes
CPC	Chromosomal passenger complex
cPPT	Central polypurine tract
CRC	Colorectal cancer
CRISPR	Clustered regularly interspaced short palindromic repeats
CRP	C-reactive protein
crRNA	CRISPR RNA
CTG	CellTiter-glo
CTLA4	Cytotoxic T-lymphocyte associated protein 4
CTNNB1	Catenin beta 1
CTT	Cholesterol treatment trialists
COX2	Cyclooxygenase 2
CVD	Cardiovascular disease
DCC	Deleted in colorectal cancer
DLG	Discs large

D.melanogaster	Drosophila melanogaster
DMEM	Dulbecco's Modified Eagles Medium
DMSO	Dimethyl sulfoxide
DNA-Pkcs	DNA dependent protein kinase catalytic subunit
dsRNA	Double stranded RNA
DTT	Dithiothreitol
DYRK2	Dual-specificity tyrosine (y) phosphorylation regulated kinase 2
EB1	End-binding protein 1
4E-BP1	Eukaryotic translation initiation factor 4E-binding protein 1
EBP	Emopamil-binding protein
E-cadherin	Epithelial-cadherin
E.coli	Escherichia coli
eEF2	Eukaryotic elongation factor 2
EGFR	Epidermal growth factor receptor
eIF4E	Inhibition of eukaryotic translation initiation factor 4E
EMT	Epithelial to mesenchyal transition
EphB4	EPH receptor B4
ER	Endoplasmic reticulum
ERBB2	Erb-B2 receptor tyrosine kinase 2
FA	Folinic acid
FAP	Famalial adenomatous polyposis
FBS	Fetal bovine serum
FDA	Food and drug administration
Fen-1	Flap endonuclease 1
FIP200	FAK family kinase-interacting protein of 200 kDa
FLT3	Fms related tyrosine kinase 3
FN3KRP	Fructosamine 3 kinase related protein
Fox01	Forkhead box O1
Fox03a	Forkhead box O3a
FPP	Farnesyl pyrophosphate
FTase	Farnesyl transferase
FTI	Farnesyl transferase inhibitor
5-FU	5-fluorouracil
GAP	GTPase-activating proteins
GDI	Guanine nucleotide dissociation inhibitors
GDP	Guanosine diphosphate
GEF	Guanine nucleotide exchange factors
GGPP	Geranylgeranyl pyrophosphate
GGTase	Geranylgeranyl transferase
GGTI	Geranylgeranyltransferase inhibitor
GlcNAc	N-acetylglucosamine
gRNA	Guide RNA
GSK3β	Glycogen synthase kinase 3β
GTP	Guanosine triphosphate
HCEC	Human colonic epithelial cell lines
HDAC	Histone deacetylases
HDL	High density lipoprotein
HDR	Homology directed repair
HMG-CoA	3-hydroxyl-3-methylglutaryl coenzyme
HMGCR	3-hydroxyl-3-methylglutaryl coenzyme A reductase
HNPCC	Hereditary nonpolyposis colorectal cancer
HR	Homologous recombination
hTERT	Human telomerase reverse transcriptase
IAP	Inhibitor of apoptosis
IBD	Inflammatory bowel disease
ICAM1	Intercellular adhesion molecule 1
Icm1	Isoprenylcysteine-O-carboxyl methyltransferase

IL-1B	Interleukin1 beta
IL6	Interleukin 6
IQGAP1	IQ motif containing GTPase activating protein 1
JNK2	C-jun N-terminal kinase 2
Kap3	Kinesin associated protein 3
KB	Kilobase
kDa	Kilodaltons
Kif3	Kinesin superfamily protein 3
KLF2	Kruppel like factor 2
LB	Lysogeny broth
LDL	Low density lipoprotein
LFA1	Lymphocyte functions-associated antigen 1
LRP5	Low density lipoprotein receptor related proteins 5
LRP6	Low density lipoprotein receptor related proteins 6
MAD	Median absolute deviation
MAPK	Mitogen activated protein kinase
MAP3K12	Mitogen activated protein kinase kinase kinase 12
MCR	Mutation cluster region
mDia	Diaphanous-related formin-1
MHC-II	Major histocompatibility class II
miRNA	Micro RNA
MLH1	MutL homolog 1
mLST8	Mammalian lethal with SEC13 protein 8
MMR	Mismatch repair
MNP	Micellar nanoparticles
MSH2	MutS protein homolog 2
MSH6	MutS homolog 6
MSI	Microsatellite instability
Msin1	Mammalian stress-activated map kinase-interacting protein 1
mTOR	Mammalian target of rapamycin
mTORC1	Mammalian target of rapamycin complex 1
mTORC2	Mammalian target of rapamycin complex 2
MVA	Mevalonic acid
NAGK	N-acetylglucosamine kinase
N4BP2	NEDD4 binding protein 2
NES	Nuclear export signal
NF-kB	NF-kappaB
NHEJ	Non-homologous end joining
NKD1	Naked cuticle homolog 1
NLS	Nuclear localisation sequence
NMD	Non-sense mediated mRNA decay
NSAID	Non-steroidal anti-inflammatory drug
NSCLC	Non-small cell lung cancer
NT	Nucleotides
NTC	No template control
8-oxo G	8-Oxoguanine
PA	Phosphatidic acid
Pak1	p21 activated kinase 1
PAM	Protospacer adjacent motif
PARP	Poly (ADP-ribose) polymerase
PBD	p21(rac1)-binding domain
PBS	Phosphate buffered saline
PCNA	Proliferating cell nuclear antigen
PD1	Programmed cell death protein 1
PD-L1	Programmed death ligand 1
P.citrinum	Penicillium citrinum
PFA	Paraformaldehyde

PGC1α	Peroxisome proliferator-activated receptor gamma coactivator 1 alpha
PI3K	Phosphoinositide 3-kinase
PIM2	Proviral integrations of moloney virus 2
PINK1	PTEN induced putative kinase 1
PKCα	Protein kinase C alpha
PLD	Phospholipase D
PLK1	Polo like kinase 1
PMS2	PMS1 homolog 2
Pol- β	Polymerase β
Pol-γ	DNA polymerase γ
PP2A	Protein phosphatase 2A
PPARα	Peroxisome proliferator-activated receptor alpha
PPAR β	Peroxisome proliferator-activated receptor beta
PPARγ	Peroxisome proliferator-activated receptor gamma
pras40	Proline-rich Akt substrate of 40kDa
pre-miRNA	Precursor miRNA
pri-miRNA	Primary miRNA
PrxII	Peroxiredoxin type II
Ptgs2	Prostaglandin-endoperoxide synthase 2
Rac1	Rac family small GTPase 1
RBD	Rhotekin-binding domain
Rce1	Endoprotease Ras-converting enzyme 1
Rheb	Ras homolog enriched in brain
RhoA	Ras homolog gene family member A
RISC	RNA-induced silencing complex
RNAi	RNA interference
RNF146	Ring finger protein 146
RPMI	Roswell Park Memorial Institute
RRE	Rev response element
RTK	Receptor tyrosine kinase
S6	Ribosomal protein s6
S.cerevisiae	Saccharomyces cerevisiae
SCID	Severely compromised immunodeficient
SCNA	Somatic copy number alterations
Scr	Non-targeting gRNA
SD	Standard deviation
SEM	Standard error of the mean
shRNA	Short hairpin RNA
siCON	Non-targeting siRNA control
siRNA	Short interfering RNA
S6K1	S6 kinase beta-1
SMG1	Suppressor with morphogenetic effect on genitalia
S.pyogenes	Streptococcus pyogenes
SREBP1	Sterol regulatory element-binding protein 1
SREBP2	Sterol regulatory element-binding protein 2
TALENS	Transcription activator-like effector nuclease
TASIN-1	Truncated APC selective inhibitor-1
TCF/LEF	T cell factor/Lymphoid enhancer factor
TGF-β	Transforming growth factor beta
TNFα	Tumour necrosis factor alpha
TNKS	Tankyrase
TNKS1	Tankyrase 1
TNKS2	Tankyrase 2
Topo IIα	Topoisomerase IIα
TP53	Tumour protein p53
tracrRNA	Trans-activating crRNA

βTrCP	β-transducing repeat containing protein
TRE	TCF response element
TSC	Tuberous sclerosis complex
TSC1	Tuberous sclerosis 1
TSC2	Tuberous sclerosis 2
UKL1	Uridine kinase-like protein 1
VEGF	Vascular endothelial growth factor
VEGF-A	Vascular endothelial growth factor A
WPRE	WHP post transcriptional regulatory element
XIAP	X-linked inhibitor of apoptosis
YY1	Ying yang 1
ZFN	Zinc finger nuclease

Contents

List of figures

List of tables

Introduction

1 Introduction to colorectal cancer

1.1 Colorectal cancer

Colorectal cancer (CRC) is divided into colon or rectal cancer depending on the anatomical location of the tumour (Pabla 2015). CRC has the second highest cancer mortality worldwide and over 20 % of patients develop metastatic disease, with under 15 % of patients surviving past 5 years (Rao & Kühl 2010; Pabla 2015). This high mortality rate highlights why many countries have screening programs to help prevent and increase early diagnosis, therefore reducing incidence and levels of metastatic disease. Screening programs help to identify adenomatous polyps which can be removed during colonscopy before they become carcinomas, which is a type of cancer arising from the epithelium (Pabla 2015). Early diagnosis increases the chance that the tumour can be entirely removed and can increase the disease free period.

CRC risk is determined by the complex interaction of environmental and genetic factors. The risk for all cancers increases with age, due to the accumulation of cancer causing mutations. Dietary and lifestyle factors play an important role in CRC risk, a diet high in unsaturated fats, red meats, high alcohol intake and a low level of physical exercise is associated with an increased risk (Fearon 2011). Some patients have CRC related syndromes such as Famalial adenomatous polyposis (FAP) and Hereditary nonpolyposis colorectal cancer (HNPCC) caused by germline mutations in key tumour suppressors, Adenomatous polyposis coli (APC) and DNA mismatch repair genes respectively. Both syndromes are responsible for causing an extremely high risk, in patients with FAP the risk of developing CRC is 100 % and for HNPCC patients the risk is 50-80 % if left untreated (Jasperson et al. 2010). Inflammatory bowel disease (IBD) is the 3rd highest condition risk factor and the risk increases with disease duration, after 30 years the risk is thought to be up to 30 % (Kim & Chang 2014). Other conditions increasing the risk of CRC include type 2 diabetes and obesity (Pabla 2015). Type 2 diabetes is believed to cause a 1.3 fold higher risk of CRC, whilst for obesity studies are inconclusive and suggest an increased risk ranging from 7-60 % (Peeters et al. 2015; Ma et al. 2013).

1.2 Colorectal cancer subtypes

To help treat patients with cancer it helps to be able to group patients according to certain characteristics. Breast cancer has well studied distinct subtypes, guiding treatment for patients, in comparison CRC does not have clear subtypes. Many groups have used gene expression studies to suggest CRC subtypes and recently a large

collaboration has combined six of these studies to derive a new classification system called Consensus molecular subtypes (CMSs) (Guinney et al. 2015). The system highlights the poor genotype-phenotype correlation in CRC because none of the subtypes can be defined by either gene mutations or somatic copy number alterations, instead all common drivers of CRC (discussed in 1.3) are found in all of the suggested subtypes. This system divides CRC into four subtypes; CMS1 (microsatellite instability and immune - 14 %), CMS2 (canonical - 37 %), CMS3 (metabolic - 13 %) and CMS4 (mesenchymal - 23 %) (Guinney et al. 2015).

The CMS1 subtype is characterised by microsatellite instability (MSI) caused by mutations in the DNA mismatch repair genes, immune activation, widespread hypermethylation, hypermutated, low prevelance of somatic copy number alterations (SCNA), activation of receptor tyrosine kinase (RTK) and mitogen activated protein kinase (MAPK) pathways (Guinney et al. 2015). This subtype harbours more mutations in *BRAF* in comparison to the other subtypes. This subtype has been associated with very poor survival rates after relapse and this reinforces other studies showing MSI tumours in combination with *BRAF* mutations confer a poorer prognosis (Guinney et al. 2015). Whereas most CMS1 show MSI, the other three subtypes are all characterised by higher chromosomal instability (CIN), supporting the traditional view that CIN and MSI are mutually exclusive (Walther et al. 2009).

CMS2 is known as the canonical subtype because this group is characterised by strong Wnt and c-myc activation, which is seen as a key driver in the progression to tumourigenesis in CRC (Guinney et al. 2015). Wnt activation is not unique to this subtype because it is found in over 90 % of patients with CRC (Cancer Genom Atlas 2012). In addition to strong Wnt activation, this subtype has a high rate of SCNA and the best survival rates after relapse (Guinney et al. 2015).

The CMS3 group shares some features with the subtype CMS1 including hypermutated, MSI, low prevalence of SCNA and activation of the RTK and MAPK pathways. Unique features of this subtype are the over-representation of mutations in *KRAS* and metabolic deregulation (Guinney et al. 2015).

The CMS4 subtype is characterised by an increase in the activation of genes involved in the epithelial to mesenchyal transition (EMT), which is part of the process of metastasis (Guinney et al. 2015). EMT involves the activation of transforming growth factor beta (TGF-β) signalling, angiogensis, matrix re-modelling and activation of the complement mediated inflammatory system. Extracellular matrix proteins are also overexpressed. Due to the pro-metastasis signature of this subtype, patients are often diagnosed later and survival rates are the lowest (Guinney et al. 2015). Understanding

potential groups of patients can help to develop more targeted therapies depending on the key characteristics of the group, for example CMS2 could potentially benefit from drugs targeting the Wnt pathway whilst CMS4 could potentially benefit from drugs targeting the TGF-β pathway.

1.3 The adenoma – carcinoma sequence

A unique feature of CRC is typically the development of tumourgenesis is characterised by a specific set of mutations, which drive initiation and progression. In 1990, Fearon and Vogelstein first presented their ideas in the multistep progression of CRC (Fearon & Vogelstein 1990). This model is based on the idea that most colorectal carcinomas develop from pre-existing benign tumours (adenoma) in the glandular epithelium. Progression from an adenoma involves mutations in at least 4 to 5 genes causing activation of oncogenes and inactivation of tumour suppressors (Fearon & Vogelstein 1990). The mutations generally occur in a specific order, but they are not restricted to the order shown in the model. Loss of chromosomal regions can also be responsible for the inactivation of tumour suppressors. The genes/regions lost in the model include chromosome 5 (now known to be loss of *APC*), *KRAS*, 18q loss (Deleted in Colorectal Cancer (*DCC)*), 17p loss (Tumour protein p53 (*TP53)*) and additional mutations allow the carcinoma to metastasise (Fearon & Vogelstein 1990). The model presented by Fearon and Vogelstein (1990) is still applicable today and an updated version is shown in figure 1.

A useful way to look at the adenoma - carcinoma sequence is in terms of pathways affected. The first pathway altered is the Wnt pathway, this becomes hyperactivated. In 80 % of patients this occurs through a mutation in *APC* (Fearon 2011). Hyperactivation of the Wnt pathway can also occur through mutations in *catenin beta 1 (CTNNB1),* this gene encodes β-catenin (Fearon 2011). Deregulation of the Wnt pathway occurs in over 90 % of patients with CRC, highlighting the importance of this pathway (Cancer Genom Atlas 2012). The next pathway hyperactivated is the epidermal growth factor receptor (EGFR) pathway and this mostly occurs through mutations in *RAS* or *RAF* or *Phosphoinositide 3-kinase* (*PI3K*) (Fearon 2011). A member of the RAS superfamily, *KRAS* is the most frequently mutated gene in this pathway (40 % of CRC patients). Mutated KRAS remains in its active form, causing hyperactivation of the pathway (Schubbert et al. 2007). The next pathway, TGF-β pathway is inactivated to promote tumourgenesis, the genes commonly mutated include *SMAD2*, *SMAD3* and *SMAD4* (Fearon 2011). The next tumour suppressor to be mutated is *TP53* and this occurs in over 60 % of CRC patients (Fearon 2011). Alongside these mutations the transition to

carcinoma involves an increasing level of genomic instability through either MSI or CIN (Walther et al. 2009). The adenoma - carcinoma pathway described highlights the key mutations which occur in CRC, but it does not reflect all the mutations found in patients, many contributing mutations occur at lower frequencies and it is important to consider these as well.

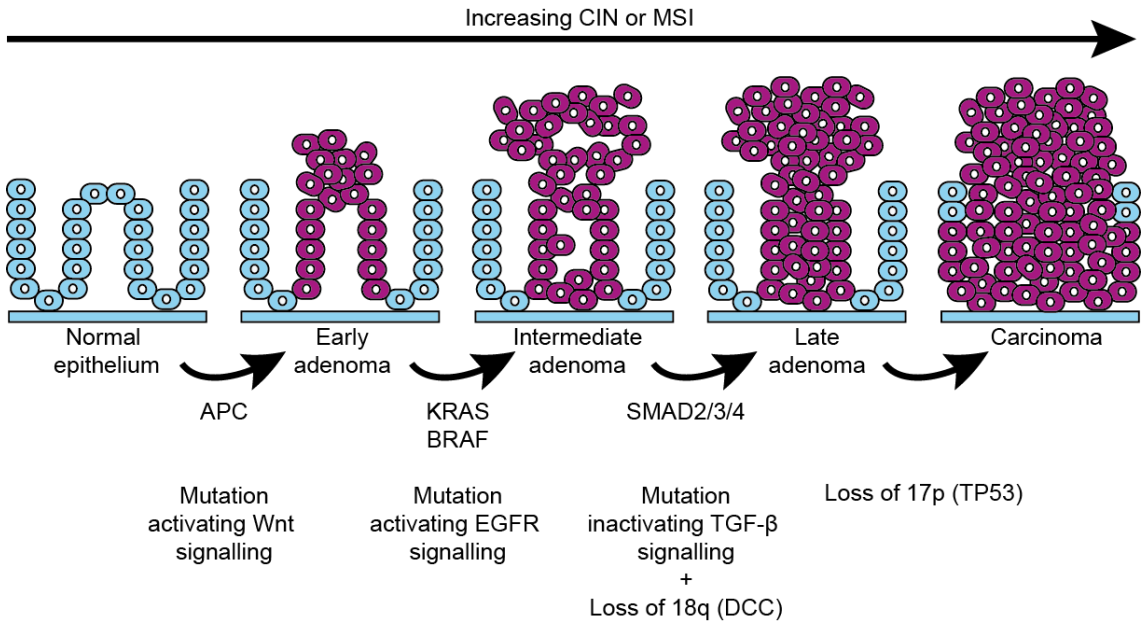

Figure 1 The adenoma - carcinoma sequence

The typical progression for the development of colorectal cancer. The genes commonly mutated include; *APC*, *KRAS/BRAF*, *SMAD2/3/4* and *TP53*. The mutations frequently occur in the order shown but are not restricted to this. Adapted from (Walther et al. 2009; Fearon & Vogelstein 1990).

1.4 Inherited and somatic colorectal cancer

Both inherited and somatic CRC follow the adenoma - carcinoma pathway, however, inherited forms develop earlier and some progress more quickly. There are a number of inherited syndromes which predispose to CRC and the germline mutations responsible also occur in sporadic CRC. Studying inherited forms of CRC has significantly helped our understanding of sporadic CRC. The main inherited syndromes are either caused by mutations in *APC* or the DNA mismatch repair genes (Fearon 2011). Over 90 % of FAP patients have mutations in *APC* and if left untreated all patients will develop CRC (Fearon 2011). FAP is responsible for 0.5 % of all CRC patients and interestingly the location of the mutation in *APC* appears to effect the severity, this will be discussed in section 2.5 (Fearon 2011). Mutations in *APC* also occur in Turcots syndrome and Gardener syndrome (Fearon 2011). HNPCC predisposes individuals to multiple cancer types, predominantly CRC and accounts for up to 5 % of CRC patients (Fearon 2011). These patients have germline mutations in

the DNA mismatch repair genes (*mutL homolog 1* (*MLH1), MutS protein homolog 2 (MSH2), mutS homolog 6 (MSH6), PMS1 homolog 2 (PMS2)*) causing MSI, 70 % of mutations in HNPCC occur in *MLH1* and *MSH2* (Fearon 2011). In sporadic CRC mutations in the *APC* gene frequently occur in up to 80 % of all CRC patients. Mutations in the DNA mismatch repair genes are less common in sporadic cancers, instead hypermethylation of the *MLH1* promoter is more frequent (accounting for 12 % of all CRC patients) and results in reduced MLH1 expression causing MSI (Fearon 2011; Boland & Goel 2010).

1.5 Treatment options for colorectal cancer

The treatment available for CRC depends on the stage of the tumour, of which there are four (Damin & Lazzaron 2014). Stage I is when the cancer has grown into the inner lining or muscle wall of the bowel. In Stage II, the cancer has grown to the outer covering of the bowel and may have spread to local tissues, but there is no sign of cancer cells in the lymph nodes. Stage III is when cancer cells have spread to nearby lymph nodes and stage IV is when the cancer has metastasised to other parts of the body (Damin & Lazzaron 2014). The standard treatment involves a combination of surgery, chemotherapy and radiation. Often stage I can be treated with surgery alone, whereas stages II upwards include courses of chemotherapy and radiation often before surgery, to try to shrink the tumour (Damin & Lazzaron 2014). Chemotherapy drugs can be used alone or in combination and include; 5-fluorouracil (5-FU), folinic acid (FA), oxaliplatin and irinotecan (Chee & Sinicrope 2010). Newly developed targeted agents against the EGFR and vascular endothelial growth factor (VEGF) pathway have been approved for use in stage IV CRC and are either used in combination with chemotherapy or as single agents (Chee & Sinicrope 2010).

Targeted agents against the EGFR pathway include cetuximab and panitumumab. The EGFR pathway is important in CRC and research has shown higher EGFR expression is associated with poorer prognosis (Rego et al. 2010). Cetuximab and panitumumab are monoclonal antibodies, binding to the extracellular domain of the EGFR, preventing receptor phosphorylation and dimerisation when a ligand binds, reducing the level of EGFR pathway activation (Pabla 2015). Cetuximab is approved for use alone or in combination, whilst panitumumab is approved as a single agent (Chee & Sinicrope 2010). There are well validated biomarkers to predict response to EGFR inhibitors. *KRAS* and *BRAF* status are assessed before considering EGFR inhibitors because patients with a mutation in *KRAS* codon 12, 13 or 61 or mutations in *BRAF* do not respond to EGFR inhibitors, because these mutations cause the pathway to be hyperactive and unresponsive to signals from EGFR (Figure 2) (Walther et al. 2009).

Despite this marker, only 35 % patients with wildtype *KRAS* respond and ultimately even those that do initially respond will develop resistance, highlighting the problem of targeted therapy (Linnekamp et al. 2015). Mechanisms of resistance include emergence of *KRAS* or *BRAF* mutations in previously wildtype cancer populations and the upregulation of RTK pathways including C-Met and Erb-B2 receptor tyrosine kinase 2 (ERBB2) (Morkel et al. 2015; Pabla 2015).

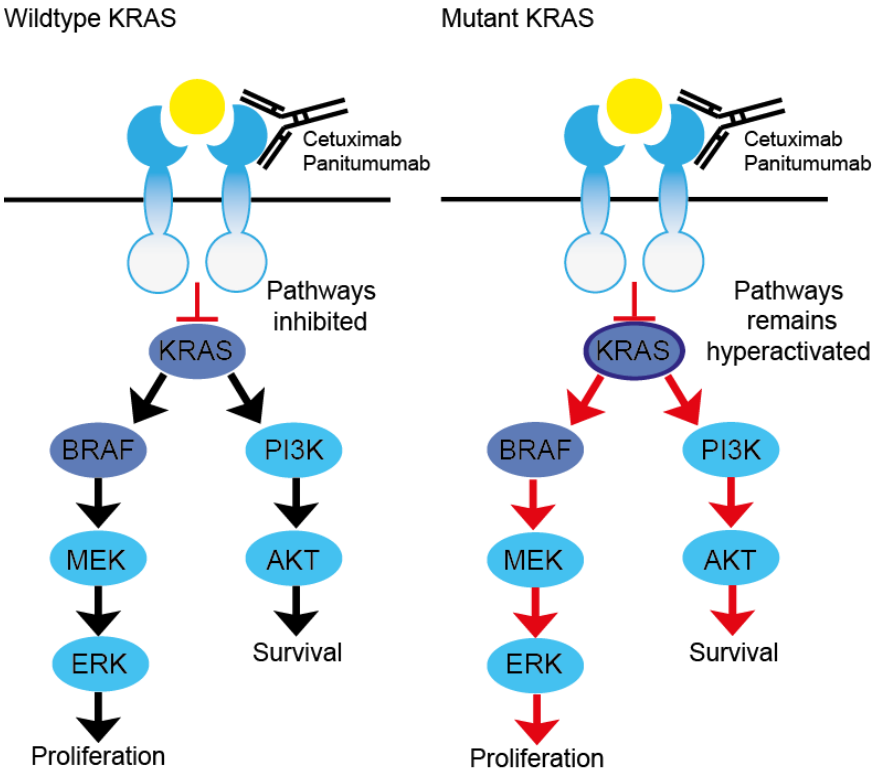

Figure 2 EGFR inhibitors in KRAS wt and mutant tumours

In KRAS wildtype cells EGFR inhibitors (eg cetuximab and panitumumab) bind to the extracellular domain of EGFR and prevent activation of KRAS, inhibiting proliferation and survival. In KRAS mutant cells the EGFR pathway is constantly activated and therefore the cells do not respond to EGFR inhibitors.

Additionally targeted agents have been developed and approved to target angiogenesis which is required for tumour growth and to promote metastasis. Bevacizumab is approved for use in combination with chemotherapy because it has been shown to increase the efficiency of chemotherapy (Chee & Sinicrope 2010). The reason for this is tumour vessels are leaky and poorly organised, inhibiting angiogenesis leads to the normalisation of vessels, which increases delivery of therapeutics (Mulcahy 2008). Bevacizumab is a monoclonal antibody which binds vascular endothelial growth factor A (VEGF-A), preventing this ligand from binding its receptor, reducing pathway activation and levels of angiogenesis (Chee & Sinicrope 2010). Unlike EGFR inhibitors there are no markers to predict patient response to

bevacizumab and the protein level of VEGF does not correlate with response (Chee & Sinicrope 2010). Interestingly a recent paper suggests patients with *KRAS* mutations also have a poorer outcome in comparison to patients with wildtype *KRAS* to bevacizumab (Fiala et al. 2015). As with EGFR therapy patients have innate resistance or develop resistance, although the mechanisms of resistance are poorly understood. Suggested mechanisms include the increase in autocrine VEGF signalling to promote angiogenesis (Mésange et al. 2014).

Recently a new targeted therapy has been approved for the treatment of metastatic MSI CRC, known as pembrolizumab (Marginean & Melosky 2018). Pembrolizumab is a programmed cell death protein 1 (PD1) inhibitor and is broadly known as an immune checkpoint inhibitor. Other immune checkpoint inhibitors are directed against programmed death ligand 1 (PD-L1) and cytotoxic T-lymphocyte associated protein 4 (CTLA4) (Viale et al. 2017). There has been growing interest into the potential of immune checkpoint inhibitors to re-activate the immune system, helping to eliminate the tumour cells. Responses to these drugs have not been as substantial as hoped. Therefore, the identification of biomarkers is essential to enable the treatment to be given to patients who could benefit, MSI has been recently shown to be a good biomarker (Marginean & Melosky 2018). The theory behind this is MSI tumours have a higher mutational load, leading to an increase in neoantigens, this upregulates immune checkpoint molecules resulting in immune suppression. Inhibiting the immune checkpoint molecules reverses the immune suppression (Marginean & Melosky 2018). Currently there are no targeted therapies to treat patients with stage I – III CRC, although many avenues are being explored.

2 Adenomatous polyposis coli

2.1 Discovery

Studying FAP, an inherited condition predisposing to CRC development played an important role in the discovery of the *APC* gene. FAP was first described and linked to cancer in the early 20th century and advances in technology lead to the discovery of the disease-causing gene, *APC* (Thomson 1990). In 1986 studying the banding pattern of chromosomes in a patient with FAP gave the first clue to the location of the *APC* gene, because a segment of DNA was missing from the long arm of chromosome 5 (Herrera et al. 1986). Next two groups narrowed down this region of chromosome 5 to the segment 5q21, one group studied FAP patients and the other group studied sporadic cases of CRC (Bodmer et al. 1987; Solomon et al. 1987). This research supported

Knudsons theory that genes causing inherited forms of cancer can also be responsible for sporadic cases of cancer (Knudson 1971). Over 10 years later, from searching over 8000 kilobases (kb) of DNA researchers identified two candidate genes. Mutations found just in FAP patients were identified in just one of the candidate genes and this is now known to be *APC* (Kinzler et al. 1991; Groden et al. 1991). Since its discovery the *APC* gene has been shown to play a key role as a tumour suppressor in CRC.

2.2 Structure of APC

The *APC* gene covers 8535 base pairs (bp) and contains at least 21 exons, 17 are coding exons and 4 are non coding (Figure 3) (De Rosa et al. 2007). The most studied APC transcripts listed on NCBI include transcript 1 NM_001127511.2, transcript 2 NM_001127510.2 and transcript 3 NM_000038.5 (Gene Id 324) and are shown in figure 4. Transcript 1 contains 14 exons and encodes protein isoform A (2825 amino acids (aa), 310 kilodaltons (kDa)). This transcript lacks exon 6 and uses promoter 1B (Rohlin et al. 2011). Transcript 2 and 3 both contain 15 coding exons (the transcripts differ in the number of non coding exons), use promoter 1A and encode protein isoform B (2843 aa, 312 kDa), the most abundant full length APC product (Fearnhead et al. 2001). Promoter 1A is believed to play the larger role in the regulation of APC, though emerging evidence is suggesting promoter 1B might contribute more than once thought (Rohlin et al. 2011). An interesting feature of APC is that exon 15 is the longest exon and encodes over 75 % of the coding sequence of APC (Fearnhead et al. 2001). Alongside the two APC protein isoforms listed on NCBI there are 11 newer APC protein isoforms, which range from 281 kDa to 315 kDa.

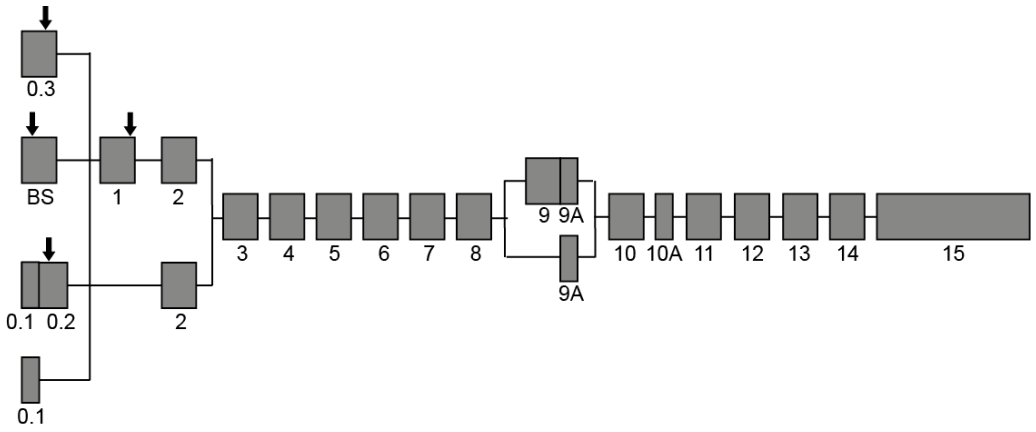

Figure 3 The exon structure of the *APC* gene.

The arrows indicate initiation codons which are inframe with exon 2. Adapted from (Santoro & Groden 1997).

In addition research suggests there are shorter APC transcripts translating into proteins 90 kDa and larger. The following exons have been suggested to be alternatively spliced; 0.1, 0.2, 0.3, BS, 1, 2, 3, 4, 7, 9, 10A, 11, 12, 13 and 14 (De Rosa et al. 2007; Santoro & Groden 1997). Some APC splice variants may be tissue specific (Horii et al. 1993; Santoro & Groden 1997). For example, APC splice variants lacking exon 1 are generally less common apart from in the brain, heart and skeletal muscle tissues where higher levels without exon 1 have been found (Santoro & Groden 1997). Without exon 1 APC is unable to homodimerize suggesting this function is less important in terminally differentiated cells (Santoro & Groden 1997). The role of the different splice variants of APC is unclear and under investigation, some may have no function and others could be degraded by non-sense mediated decay (NMD) (De Rosa et al. 2007).

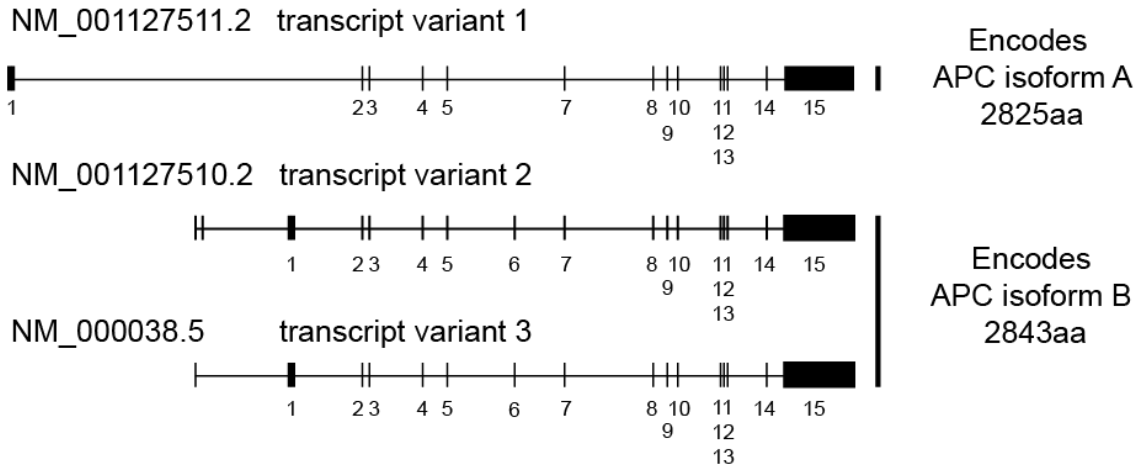

Figure 4 The most studied full length APC transcripts

Transcripts encoded by the genomic sequence NG_008481.4. Schematic shows the exons included in the transcripts and the resulting protein isoform they encode. We refer to protein isoform B and transcript variant 3 NM_000038.5 throughout the thesis.

Full length APC contains an oligomerization domain, armadillo region, 15 amino acid repeats (15aa), 20 amino acid repeats (20aa), SAMP repeats, basic domain, end-binding protein 1 (EB1) binding domain and discs large (DLG) binding domain (Figure 5). The oligomerization domain consists of heptad repeats through which APC forms homodimers or heterodimers. For example, homodimers form if two full length APC proteins dimerize and heterodimers form if full length APC binds truncated forms of APC (Fearnhead et al. 2001). The armadillo region contains seven repeats and is named because the region shares homology with β-catenin and the drosophila homologue armadillo (Fearnhead et al. 2001). The proteins APC-stimulated guanine nucleotide exchange factor 1 and 2 (ASEF1/ASEF2) and protein phosphatase 2A

(PP2A) interact with the armadillo region (Fearnhead et al. 2001; Aoki & Taketo 2007). The 15aa repeats consist of three repeats and are β-catenin binding sites. The seven 20aa repeats also bind β-catenin, glycogen synthase kinase 3β (GSK3β) uses the SXXXS consensus site as a substrate for phosphorylation, enabling β-catenin to bind and APC regulates its levels (M. Sieber et al. 2000). Only the first repeat is required for β-catenin binding, the regulation of β-catenin degradation requires three or more 20aa repeats. The SAMP repeats enable APC to interact with Axin (Fearnhead et al. 2001). The basic domain has a high percentage of arginine, lysine and proline amino acids and EB1 binding domain is where the protein EB1 interacts with APC (Fearnhead et al. 2001). The DLG binding domain interacts with proteins containing the PDZ domain including Dlg (Näthke 2006). The various domains of APC allow the interaction with a wide range of proteins and result in APC playing a role in a wide range of functions.

2.3 Localisation of APC

The majority of APC is found in the cytoplasm and can be found at various sites (Brocardo et al. 2005). APC can shuttle between the nucleus and cytoplasm, nuclear import requires sequences, known as a nuclear localisation sequence (NLS), found at the N-terminal. Nuclear export occurs through CRM1 export receptors and requires a nuclear export signal (NES) also found in the N-terminus (Brocardo & Henderson 2008). Truncated APC has been shown to shuttle between the nucleus and the cytoplasm more efficiently, this could be due to alterations in its functions in the cytoplasm which are discussed later in section 2.5 (Brocardo & Henderson 2008).

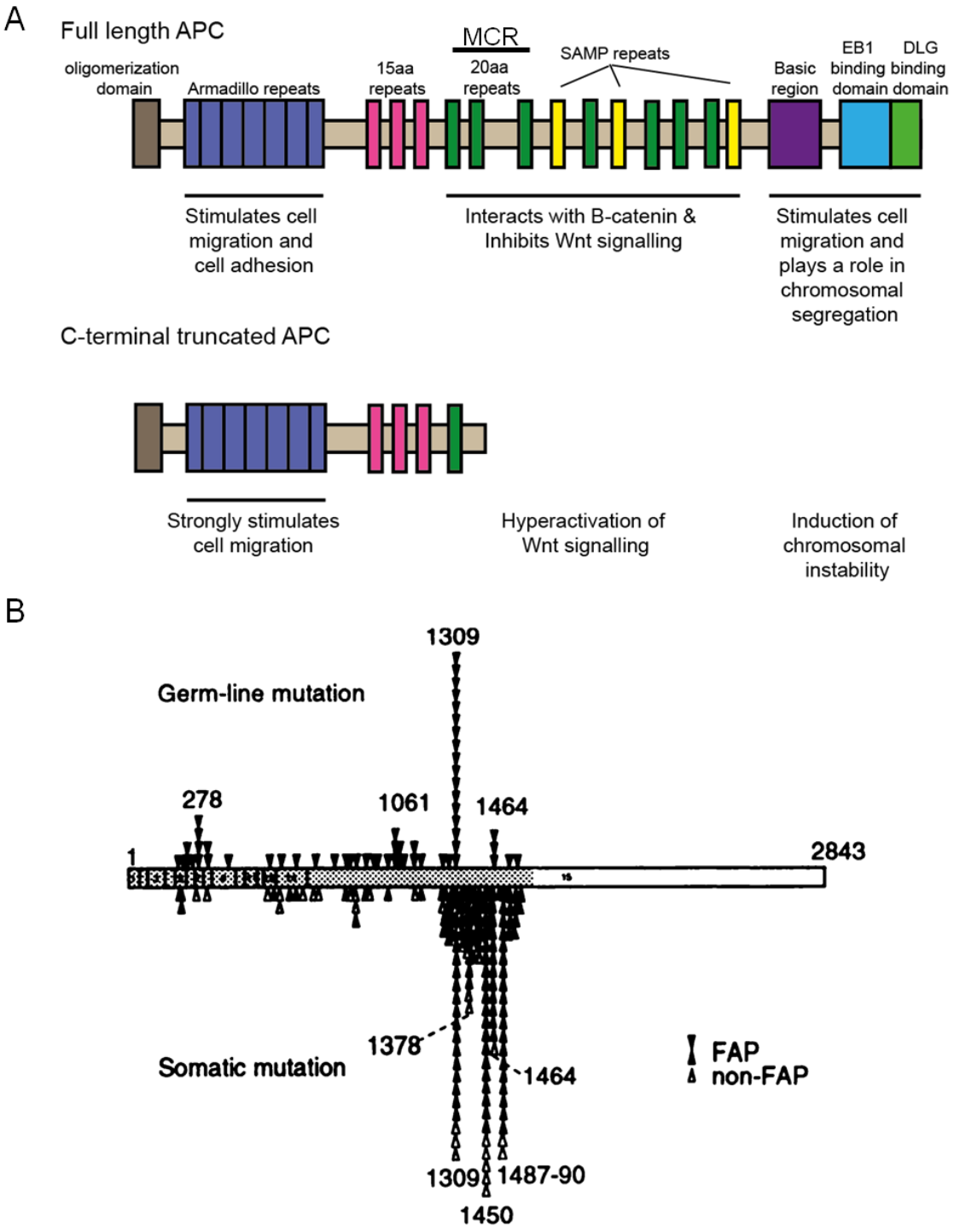

Figure 5 Structure of APC and the common mutation sites

A) Full length APC contains eight different domains and APC interacts with different proteins through these domains. The most common mutations in APC occur in the MCR region where APC interacts with β-catenin, resulting in a C-terminal truncated APC product with less domains and therefore different functions. Adapted from (Aoki & Taketo 2007). B) Image from (Miyaki et al. 1994), the APC gene was characterised in 309 tumours from FAP and non-FAP patients (sequencing covered the first 60 % of the coding region of APC). The mutation frequencies are shown along APC and are separated into germline and somatic mutations. The distribution of mutations along APC is different between germline and somatic mutations. The majority of somatic mutations occur in the MCR region.

2.4 Role of APC in the cell

2.4.1 Wnt signalling

The Wnt signalling pathways play an important role in cell proliferation, cell polarity and cell fate determination during embryogenesis and tissue homeostasis (MacDonald et al. 2009). Typically, Wnt pathways are divided into the canonical pathway (involves β-catenin) and the non-canonical pathways (independent of β-catenin). APC is involved in the canonical Wnt signalling pathway and this is one of the best characterised roles of APC (Figure 6). APC forms part of the β-catenin destruction complex along with Axin, GSK3β and casein kinase 1α (CK1α) to negatively regulate levels of β-catenin. The pathway is switched off when Wnt ligands are absent from the frizzled receptor. APC and Axin act as scaffold proteins interacting with β-catenin and recruiting CK1α and GSK3β to the complex to phosphorylate the N-terminal of β-catenin (Burgess et al. 2011; Klaus & Birchmeier 2008; Voloshanenko et al. 2013). An E3 ubiquitin ligase known as β-transducing repeat containing protein (βTrCP) then ubiquitinates β-catenin leading to its degradation (Klaus & Birchmeier 2008). As β-catenin is degraded, the transcription factors T cell factor/ lymphoid enhancer factor (TCF/LEF) remain bound to the co-repressor Groucho (Klaus & Birchmeier 2008). The pathway is activated when a Wnt ligand binds to the frizzled receptor, dishevelled is recruited to the membrane to interact with frizzled whilst CK1α and GSK3β phosphorylate low density lipoprotein receptor related proteins 5 and 6 (LRP5 and LRP6), Axin is recruited to the membrane through its interaction with phosphorylated LRP5/6 and dishevelled. This results in the dissociation of the β-catenin destruction complex, whereby β-catenin is not phosphorylated by CK1α/GSK3β and is free to translocate to the nucleus and form a transcriptionally active complex with TCF/LEF, leading to the transcription of Wnt target genes. Wnt target genes include; *Axin2*, *Cyclin D*, *c-myc* and *Cyclooxygenase 2* (*COX2)* (Burgess et al. 2011; Lesko et al. 2014; Davidson & Niehrs 2010). APC additionally prevents transcription of Wnt target genes through its ability to bind to β-catenin, blocking β-catenin binding to TCF/LEF and APC has been shown to promote β-catenin export from the nucleus (Aoki & Taketo 2007).

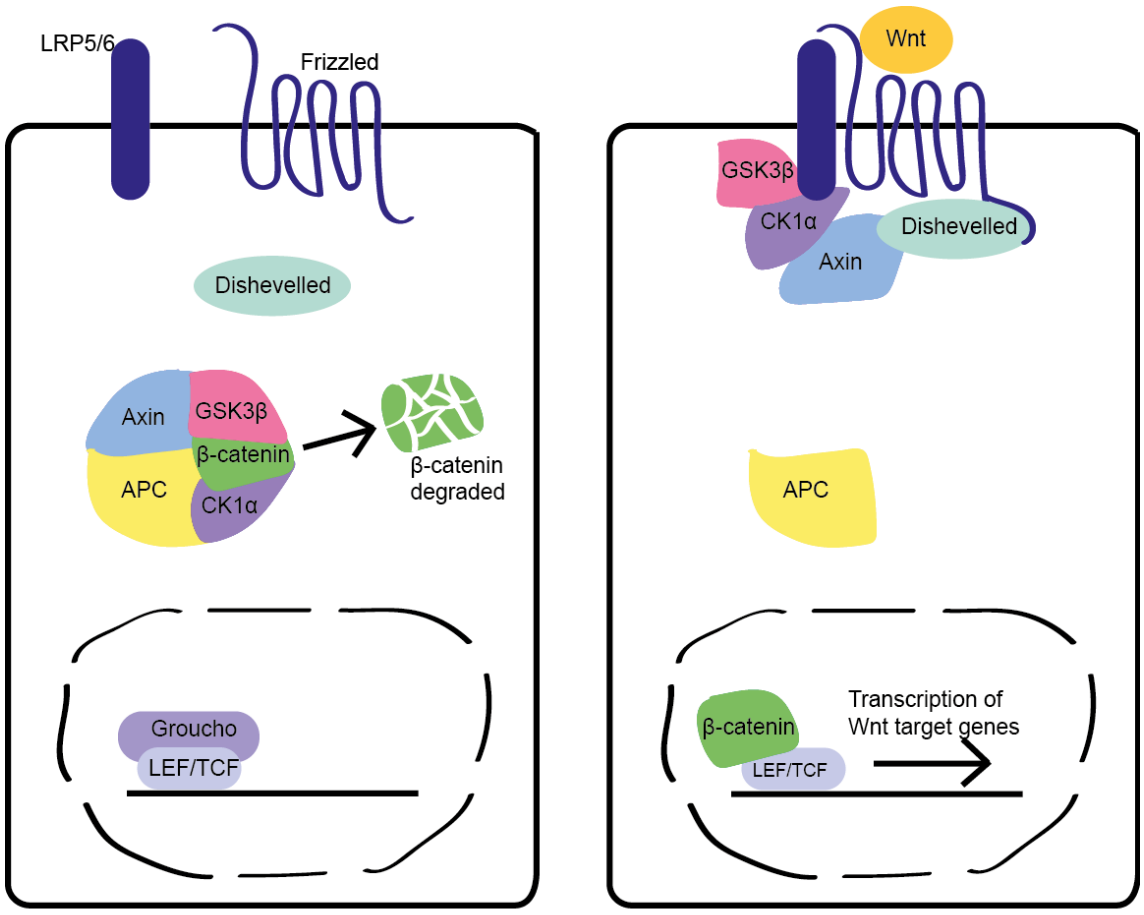

Figure 6 The canonical Wnt signalling pathway

When no Wnt ligand is bound to frizzled the β-catenin destruction complex forms (APC-Axin-GSK3β-CK1α) and this phosphorylates β-catenin for degradation. When a Wnt ligand binds to frizzled the β-catenin destruction complex does not form so β-catenin is free to translocate to the nucleus and activate Wnt target genes.

2.4.2 Cell adhesion and polarity

To maintain tissue organisation it is important that each cell maintains contact with neighbouring cells and maintains its own apical-basal polarity, loss of this organisation has been linked to more aggressive tumours (Lesko et al. 2014). APC is believed to associate through the homologous proteins β-catenin and plakoglobin at two cell-cell contacts; desmosomes (provide tissue strength) and adheren junctions (Zhurinsky et al. 2000; Harris & Tepass 2010). β-catenin and plakoglobin (also known as y-catenin) share some functions for example both are found at adheren junctions, whilst other functions are unique, only plakoglobin forms part of desmosomes (Zhurinsky et al. 2000). We will focus on β-catenin because of its clear role in Wnt signalling (discussed in section 2.4.1) and the resulting interplay with cell adhesion. Adheren junctions link the actin cytoskeleton between neighbouring cells (Harris & Tepass 2010). It is thought that β-catenin is either bound to APC or β-catenin is bound to the actin cytoskeleton

through E-cadherin (Prosperi & Goss 2011). Therefore APC regulates adhesion by controlling the amount of β-catenin available by directly binding to β-catenin or by negativity regulating its level through Wnt signalling, additionally E-cadherin is a Wnt target gene providing an additional level of regulation (Prosperi & Goss 2011).

APC may associate with polarity complexes which control cell polarity (Prosperi & Goss 2011). There are three main polarity complexes; PAR (cdc42-PAR3-PAR6-aPKC) and Crumbs (Crb-PALS-PATJ) controlling apical polarity whilst Scribble (Scrib-Dlg-LG1) controls the basolateral polarity in epithelial cells (Bryant & Mostov 2008). APC may act as a scaffold for the Scribble complex because the three proteins do not interact together and APC has been shown to bind both Scrib and Dlg (Prosperi & Goss 2011). APC might play a role in the formation of the PAR complex because APC can interact with PAR3 to enable the transport of APC along microtubules (Prosperi & Goss 2011). The potential role of APC in polarity is summarised in figure 7A.

2.4.3 Interaction with the cytoskeleton network

The cytoskeleton has three main functions, it organises the contents of the cell, it connects the cell to the outside environment and generates forces to enable the cell to change shape and migrate (Fletcher & Mullins 2010). Key components of the cytoskeleton network are actin filaments, microtubules and intermediate filaments (Fletcher & Mullins 2010). APC binds directly and indirectly to both actin filaments and microtubules. The actin cytoskeleton plays an important role in cell migration and maintaining cell morphology (Lesko et al. 2014; Näthke 2006). APC works alongside diaphanous-related formin-1 (mDia) to promote nucleation. APC is thought to recruit actin monomers and directly binds through the armadillo region and/or the basic region (Lesko et al. 2014). APC also indirectly influences the actin cytoskeleton through directly binding IQ motif containing GTPase activating protein 1 (IQGAP1), ASEF1 and ASEF2. Both proteins activate cell division cycle 42 (Cdc42) and Rac family small GTPase 1 (Rac1) (Aoki & Taketo 2007). Cdc42 and Rac1 are Rho GTPases involved in regulating the actin cytoskeleton, when activated they promote actin polymerisation (Spiering & Hodgson 2011).

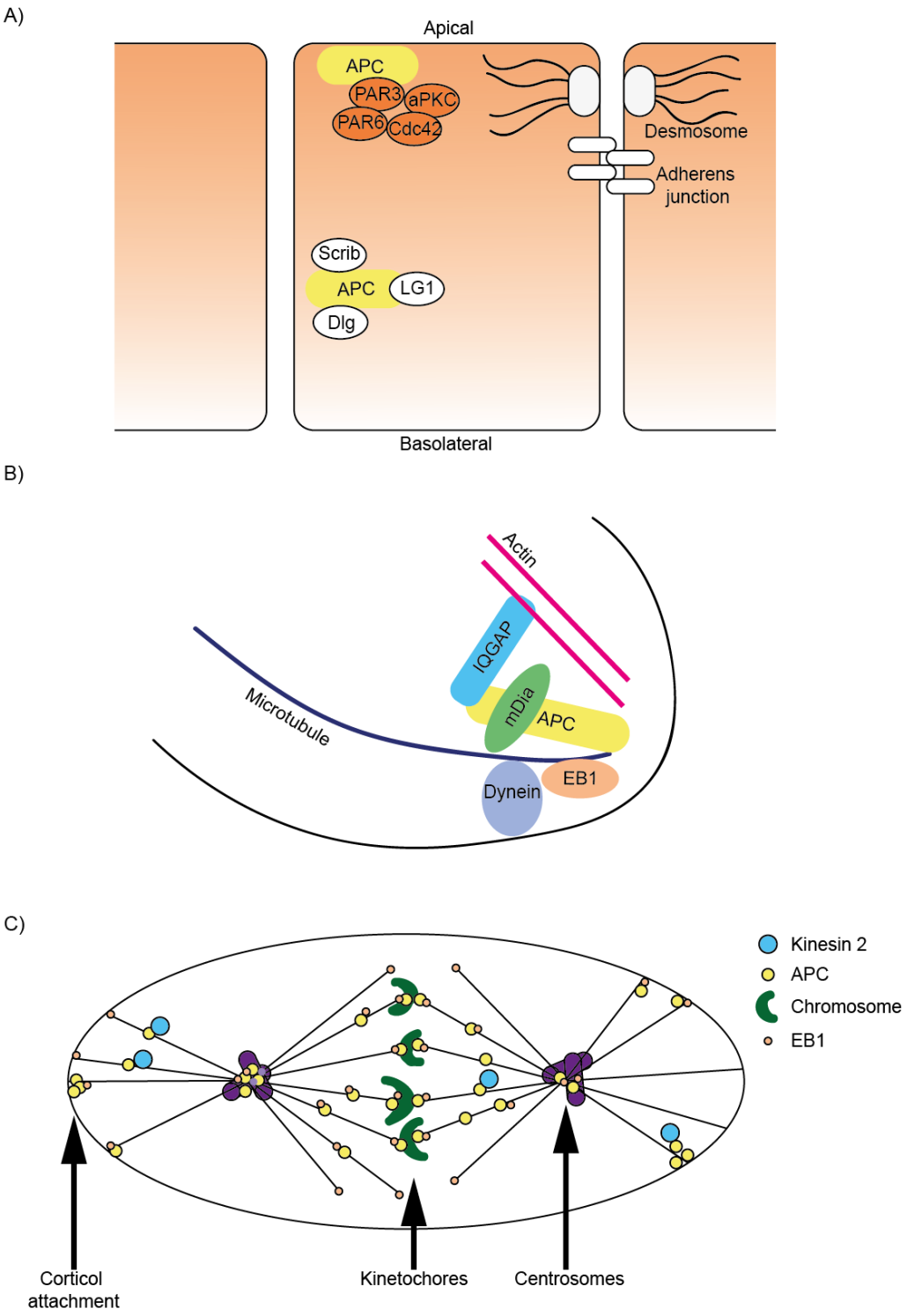

Figure 7 Roles independent of Wnt signalling

A) Schematic showing mechanisms to maintain apical-basal polarity in cells. Cell to cell contacts through desmosomes and adherens are important alongside polarity complexes. APC interacts with PAR3 and may play a role in the formation of the PAR complex (cdc42-PAR3-PAR6-aPKC) which controls apical polarity. APC may act as a scaffold for the Scribble complex which controls basolateral polarity. APC has been shown to interact with both Scrib and Dlg and the three proteins in the complex do not interact together. B) APC interacts with a variety of proteins, actin and microtubules at migrating cellular protrusions. C) APC localisation alongside kinesin 2 and EB1 at corticol attachments, kinetochores and centrosomes. B) C) are adapted from (McCartney & Näthke 2008).

Microtubules are part of the cytoskeleton and play a role in maintaining cell structure, cell migration, intracellular transport, meiosis and mitosis (Fletcher & Mullins 2010; Aoki & Taketo 2007). APC can directly bind microtubules through the basic region and indirectly through the EB1 and mDia to promote microtubule polymerisation at the distal end (Lesko et al. 2014). Interestingly if APC is bound to EB1 and microtubules, the C-terminus of APC cannot interact with the actin cytoskeleton (Aoki & Taketo 2007). A polarity protein mentioned earlier Dlg promotes the accumulation of APC at microtubule tips and the attachment with the plasma membrane (Prosperi & Goss 2011). Through APC interacting with EB1, Dynein (which binds EB1) contributes to the microtubule attachment at the plasma membrane (McCartney & Näthke 2008). APC is transported along microtubules through its interaction with kinesin associated protein 3 (Kap3) and kinesin superfamily protein 3 (Kif3) forming kinesin 2. Typically APC is directed towards the microtubule clusters at cell protrusions and to the leading edge of migrating cells (Lesko et al. 2014). A summary of some of the interactions between APC and the cytoskeleton are shown in figure 7B and 7C.

2.4.4 Cell cycle

APC is expressed and phosphorylated throughout the cell cycle. APC becomes hyperphosphorylated during mitosis. During mitosis, APC localises at the cell cortex, centrosomes and kinetochores (Figure 7C) (Prosperi & Goss 2011). APC associates with cyclinA-cdk2 in G2/M and phosphorylates APC to control the attachment of the spindle to the cell cortex during mitosis (Prosperi & Goss 2011). Additionally at G2/M, data suggests APC interacts with topoisomerase IIα (topo IIα) and proliferating cell nuclear antigen (PCNA), which both participate in DNA replication (Prosperi & Goss 2011; Wang et al. 2008). During mitosis APC co-localises with cyclinB-cdk1 which phosphorylates the C-terminus allowing EB1 to bind, EB1 is an important link between APC and the cytoskeleton. The APC/EB1 complex is joined by Bub1 and Bub3 which phosphorylates APC creating stable kinetochore attachment for proper chromosome alignment (Prosperi & Goss 2011). Currently the exact role of APC in chromosome segregation is controversial, some research suggests APC is important because loss of APC causes cells to suffer severe chromosomal and mitotic spindle defects (Lesko et al. 2014). Localisation of APC at the centrosomes occurs without microtubules and APC may play a role in the mitotic spindle checkpoint (Lui et al. 2012). Interestingly β-catenin is also found at the centrosomes during interphase and mitosis, therefore APC may function through β-catenin (Bahmanyar et al. 2009). APC also negatively regulates the cell cycle through its role in the Wnt signalling pathway which activates many genes

involved in the cell cycle including *c-myc* and *Cyclin D,* which are both involved in the G1/S checkpoint (Davidson & Niehrs 2010).

2.4.5 Other less defined roles of APC

There is evidence suggesting APC plays opposing roles in DNA repair. Upon DNA double strand breaks, APC is recruited to the site of damage and promotes repair by stimulating the marker of DNA damage, histone H2AX phosphorylation and by interacting with DNA dependent protein kinase catalytic subunit (DNA-Pkcs) (Prosperi & Goss 2011). APC is also thought to interact with 14-4-3σ which is involved in the DNA damage response (Prosperi & Goss 2011). APC inhibits the base excision repair (BER) pathway through its interaction with polymerase β (Pol-β) and flap endonuclease 1 (Fen-1) (Prosperi & Goss 2011).

APC can regulate apoptosis through multiple mechanisms. Firstly APC indirectly affects apoptosis through negative regulation of the Wnt target gene *baculoviral IAP repeat containing 5 (BIRC5),* which encodes a anti-apoptotic protein known as survivin (Prosperi & Goss 2011). APC may also bind and regulate B-cell lymphoma 2 (Bcl-2), an anti-apoptotic factor. Research suggests truncated APC binds Bcl-2 and may shuttle it to the mitochondria to increase survival (Lui et al. 2012). Additionally APC is cleaved by caspase 3 and the 90 kDa cleaved fragment binds to hTID1 and modulates apoptosis (Prosperi & Goss 2011).

In addition to roles in DNA repair and apoptosis researchers have suggested over 100 proteins bind to APC, resulting in potential new roles in nuclear transporting, membrane trafficking and metabolism (Nelson & Näthke 2013).

2.5 APC in colorectal cancer

APC mutations typically occur in both alleles as a result of nonsense mutations, frameshifts and allelic loss. The majority of mutations occur between residues 1263 and 1589 which is also known as the mutation cluster region (MCR) (Kohler et al. 2008). This region is where APC interacts with β-catenin, negatively regulating levels of the Wnt signalling pathway. Mutations in this region lead to a truncated protein which cannot regulate β-catenin levels to the same degree as full length, resulting in hyperactivation of the pathway (Figure 5).

Understanding the inherited syndrome FAP has helped develop our understanding of *APC* mutations because the precise location of the germline *APC* mutation affects the

severity of the syndrome (Zeineldin & Neufeld 2013; Nieuwenhuis & Vasen 2007). Germline mutations in the MCR leads to the most severe phenotype, then mutations either side of the MCR display an intermediate phenotype and mutations after residue 1595 or before 157 yield a mild phenotype often referred to as attenuated familial adenomatous polyposis (AFAP). Complete deletion of *APC* can occur and leads to an intermediate phenotype (Zeineldin & Neufeld 2013). Explanations for this observation is that different APC truncations promote different levels of Wnt signalling activation, too low or high reduces proliferation. Mutations around the MCR appear to produce the right level of Wnt signalling for optimal proliferation and this idea has been developed into the 'just right' signalling model (Zeineldin & Neufeld 2013).

In support of the 'just right' signalling model, studying FAP has developed the idea that APC is not a typical tumour suppressor (Figure 8). The Knudsons two hit hypothesis states that independent mutations occur on both copies of the tumour suppressor, however the 2nd mutation in *APC* in CRC seems to be dependent on the location of the first (Albuquerque et al. 2002). Albuquerque et al. (2002) showed in FAP patients the different scenarios; 1) If the germline mutation occurs leaving no 20aa repeats, then the second mutation will be after the first or second 20aa repeats. 2) If the germline mutation occurs after one 20aa then the 2nd hit is often allelic loss or a mutation before the 20aa repeats. 3) If the germline mutation is after two 20aa, the 2nd hit is most commonly before the 20aa repeats or less often allelic loss. This selection for retention of some ability of APC to regulate β-catenin levels supports the idea of a specific activation of Wnt signalling being required to promote tumourigenesis.

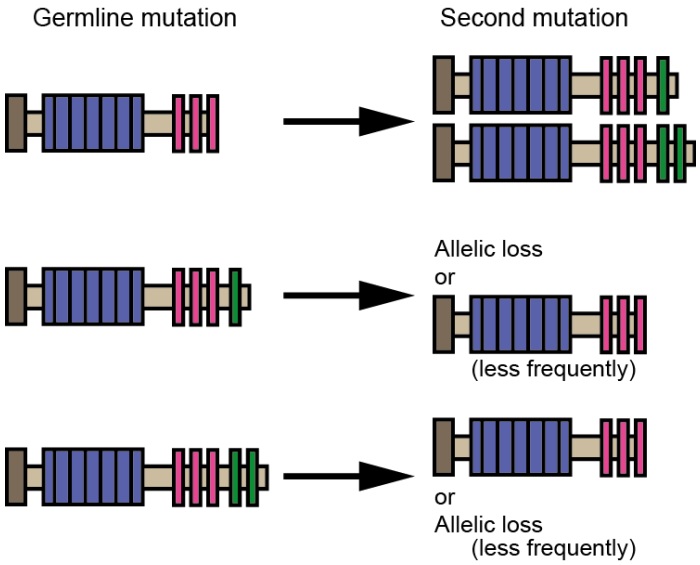

Figure 8 Knudsons two hit hypothesis in FAP

The location of the germline mutation affects the location of the second mutation. This is also applicable to patients with sporadic CRC. 15aa repeats are pink, 20aa repeats are green. Adapted from (Albuquerque et al. 2002).

Hyperactivation of the Wnt pathway plays an important role in CRC development due to the role of this pathway in colonic homeostasis (Burgess et al. 2011). Wnt signalling hyperactivation causes transcriptional changes of Wnt regulated genes and peripheral changes causing disrupted crypt architecture and formation of aberrant crypt foci (Burgess et al. 2011). *APC* mutations cause hyperactivation of the pathway leaving it unresponsive to Wnt ligands, however researchers have suggested cells remain responsive to Wnt ligands but the threshold for pathway activation is lowered (Voloshanenko et al. 2013).

Promoting hyperactivation of the Wnt signalling pathway is just one consequence of C-terminal truncated APC, other consequences are increased cell migration, changes in cell adhesion and induction of CIN (Rao and Yamada 2013; Aoki and Taketo 2007). C-terminally truncated APC binds more strongly to ASEF, enhancing its guanine nucleotide exchange factor (GEF) activity, promoting increased cell migration (Aoki & Taketo 2007). Loss of APC is thought to not be sufficient for promoting an invasive phenotype as additional mutations are required (Aoki & Taketo 2007). Constitutively active ASEF also alters cell adhesion because it decreases the amount of E-cadherin and β-catenin at the junctions (Akiyama & Kawasaki 2006). This might explain why the armadillo repeats remain in truncated forms of APC. Hyperactivation of Wnt signalling further reduces the pool of β-catenin at the junctions, weakening cell adhesion. Without the N-terminus of APC, the region which binds microtubules through mDia and EB1 is lost, leading to spindle dysfunction and CIN (Aoki & Taketo 2007).

2.6 Current models of APC loss in colorectal cancer

2.6.1 *In vitro* models

There are a wide range of human cell lines which have been established from patients with CRC and they represent the range of different combinations of mutations seen in CRC making them useful to study. Cell lines are cheap and easy to work with, however, because they are grown in 2D, any 3D interactions are lost (Young et al. 2013).

2.6.2 *In vivo* models

One of the disadvantages of human cell lines is that you can't investigate the interaction between the tumour cells and the tissue microenvironment. The use of *in vivo* models such as xenografts and genetically engineered mice help to extend work shown *in vitro*. Xenografts involve implanting murine or human tumour cells into an

immunocompromised mouse (nude or severely compromised immunodeficient (SCID)) to prevent the host immune system from rejecting the cells. The disadvantage of xenografts as models is you miss the interaction between the tumour cells and the host immune system, additionally the cells may undergo changes in the time from harvesting to implanting (Young et al. 2013).

Another type of *in vivo* models is genetically engineered mice harbouring different germline mutations in *APC.* As occurs in FAP, the *APC* mutant mice must develop a mutation in the second copy of *APC* for polyps to develop (Zeineldin & Neufeld 2013). The location of the mutation appears to effect the severity of the phenotype, another commonality with FAP patients (Heyer et al. 1999). A significant difference between patients and the *APC* mutated mice models is adenomas generally develop more in the small intestine than the colon and are often benign. It is thought this could be due to the short lifespan of mice and the additional mutations required for the adenomas to progress to a carcinoma do not have a chance to occur (Young et al. 2013).

There are a number of mice generated with *APC* mutations and these are shown in figure 9. APC^{14} expresses a very short APC product containing part of the ASEF binding domain. These mice develop around 65 polyps mostly in the colon and in older mice some invasion has been reported (Young et al. 2013). APC^{580} has a conditional mutation in *APC* at codon 580 and when deleted it leads to adenomas in the colon within 4 weeks (Heyer et al. 1999). APC^{716} expresses an APC truncated product containing the ASEF binding domain and these mice develop around 300 polyps in the small intestine. APC^{min} has a mutation at codon 850 causing a truncated APC product which is slightly longer than seen in the APC^{716} mice. These mice develop approximately 30 polyps in the small intestine. APC^{1309} contains APC with a truncation in the MCR and contains the first 20aa repeat, these mice develop around 35 polyps in the colon and small intestine. These mice have a shorter lifespan than APC^{min} mice which correlates with FAP patients who harbor this mutation and develop CRC earlier (Young et al. 2013). APC^{1638N} produce an unstable APC and develop under 10 polyps in the small intestine but research has shown increased tumour invasion (Young et al. 2013). APC^{1638T} produces a stable 182 kDa protein with the first two 20aa repeats. Interestingly this leads to a normal phenotype and this model is not embryonic lethal in the homozygous state (Heyer et al. 1999). $APC^{neoF/R}$ doesn't harbor a specific mutation, instead APC has reduced expression to 10-20 % in the mice and surprisingly this results in less than one polyp developing by 15 months (Young et al. 2013; Zeineldin & Neufeld 2013).

All the mice models discussed above support the evidence that a mutation in *APC* alone is not sufficient to promote tumourigenesis. In support of this, additional mice models have been generated with additional mutations in genes found later in the adenoma - carcinoma sequence, for example $APC^{716(+/-)}$ $DPC4^{(+/-)}$ mice with an *APC* mutation and a *SMAD4* mutation (encoded by *DPC4*) (Young et al. 2013). SMAD4 is part of the TGF-β pathway and although there were no changes in size or number of adenomas compared to APC^{716} mice the adenomas did show signs of invasion (Young et al. 2013). This supports evidence that TGF-β pathway disruption is required for later stages of the adenoma - carcinoma pathway and not initiation. In comparison a mutation in EPH Receptor B4 (*EphB4)* combined with APC^{min} mice, $APC^{min+/-}$ $EphB4^{+/-}$ leads to a larger number of polyps in the colon and more invasion (Young et al. 2013). The genetically engineered mice modelling different *APC* mutations develop varying phenotypes as seen in FAP patients and helped to develop the theory that *APC* mutations are not mutually exclusive as discussed in section 2.5.

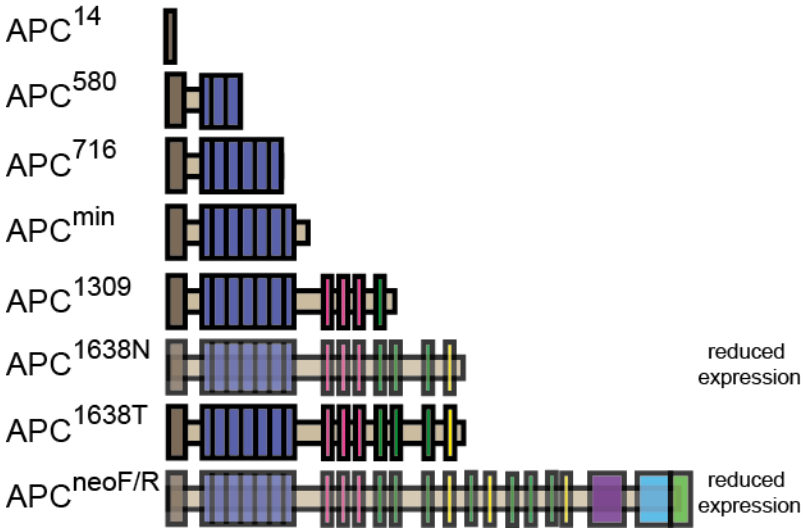

Figure 9 *In vivo* models of APC mutated mice

Schematic shows the location of the *APC* mutations in the mice and the resulting effect on the APC protein product.

3 Targeting APC in colorectal cancer

Targeting the tumour suppressor APC is one avenue being explored and has the potential to benefit up to 80 % of CRC patients. Unfortunately because a significant proportion of the APC protein is lost in the cell it is hard to directly target.

3.1 Restore wildtype APC

One approach being explored is correcting the faulty expression of *APC*, this could help to reverse the consequences of mutant APC. If APC is still driving tumour development then tumour growth could be inhibited and even reversed. An early approach investigated was the use of gene therapy to reintroduce wildtype *APC* in APC^{min} mice. The APC^{min} mice were treated every 72 hours for two months with liposomes containing a plasmid expressing full length APC. This approach restored levels of APC without toxic side effects, but they did not see a large therapeutic difference in the control and treated groups (Arenas et al. 1996). Lee et al. (2004) used a similar approach in APC^{min} mice and found 25 % less polyps developed in the mice treated with liposomes containing full length APC. Research into this approach has not been focused on, however, a recent paper emphasises the striking impact of re-expressing full length APC *in vivo* (Dow et al. 2015). The group developed a mouse model with doxycycline inducible short hairpin RNA (shRNA) against APC, treating the mice with doxycycline lead to tumour development in the small and large intestine, representing clinical disease in humans. Removal of doxycycline treatment lead to re-expression of APC, tumour regression, re-establishment of colon crypt homeostatsis and after 30 days there was no relapse in disease (Dow et al. 2015). This study suggests APC is involved in tumour maintenance and therefore restoring wildtype APC could be an effective therapeutic strategy.

Another approach to correct the faulty expression of *APC* is to use aminoglysides and macrolides to read through the premature stop codon resulting in the expression of full length APC (Floquet et al. 2011; Zilberberg et al. 2010). Zilberberg et al. (2010) successfully showed the effectiveness of the approach in the APC^{min} mouse model and xenograft experiments using the HT29 cell line, both experiments demonstrated restoring full length APC expression reduced the tumourigeneic phenotype. However, there were concerns over this approach because aminoglysides and macrolides are not specific to just the APC premature stop codon, other genes would also be affected causing a high risk of toxicity problems (Lesko et al. 2014).

3.2 mTOR inhibitors

Another approach is to indirectly target the APC mutation by targeting another pathway. The mammalian target of rapamycin (mTOR) pathway lies downstream of many of the key deregulated pathways in CRC including, Wnt signalling, PI3K/AKT pathway, EGFR and p53 (Wang & Zhang 2014). Details of the mTOR pathway are discussed later in section 6. The potential of mTOR inhibitors in CRC has not often been specifically linked to the APC mutation. Researchers have suggested mTOR inhibitors could be used in early tumour development to selectivity kill APC mutated cells (Faller et al. 2014). The *in vivo* study showed that intestinal lining cells from APC deficient mice displayed increased Wnt activation and therefore expression of the Wnt target gene c-myc. This in turn was required for mammalian target of rapamycin complex 1 (mTORC1) mediated inhibition of eukaryotic elongation factor 2 kinase (eEF2K), resulting in activation of translation elongation and subsequent cell proliferation (Faller et al. 2014). The group showed the use of mTOR inhibitors such as rapamycin inhibited proliferation of adenomas in APC deficient mice. This suggests existing mTOR inhibitors could be used for prevention of CRC or for early stage disease. In support of this, research into the chemopreventative effects of aspirin and 5-aminosalicyclic acid (5-ASA) suggests both drugs inhibit the mTOR pathway through different mechanisms (Din et al. 2012; Baan et al. 2012). Aspirin was shown to activate AMP-activated protein kinase (AMPK) resulting in decreased ribosomal protein S6 kinase beta-1 (S6K1), ribosomal protein s6 (S6) and eukaryotic translation initiation factor 4E-binding protein 1 (4E-BP1), causing autophagy (Din et al. 2012). Whereas, 5-ASA was shown to inhibit phospholipase D (PLD) dependent generation of phosphatidic acid (PA), inhibiting mTOR and resulting in cell cycle arrest (for background to mTOR pathway see section 6) (Baan et al. 2012).

3.3 Targeting the Wnt pathway

A key consequence of the APC mutation is the resulting hyperactivation of the Wnt signalling pathway. Targeting components of the pathway downstream of APC are being explored as potential therapeutic strategies for targeting APC. These are depicted in figure 10.

3.3.1 Targeting β-catenin

To reduce Wnt signalling mediated transcription, researchers have investigated the potential of two approaches; 1) reducing β-catenin expression and 2) reducing the interaction between β-catenin and transcription factors or transcriptional co-activators. Antisense oligonucleotides designed to specifically target β-catenin mRNA can be used

to reduce β-catenin expression. Antisense oligonucleotides bind to complementary mRNA and cause mRNA degradation mediated by the nuclease RNaseH. Roh et al. (2001) used antisense oligonucleotides against β-catenin in CRC cell lines and in xenograft models. The research was promising because the treatment inhibited tumour growth in both models and some tumours in the xenograft models completely shrank. Similar results were also shown in the APC^{min} mouse model, those treated with antisense oligonucleotides developed less intestinal adenomas (Foley et al. 2008). However, this approach lowers all β-catenin levels in the cell and could be quite toxic, because β-catenin also has roles in cell adhesion (Lesko et al. 2014).

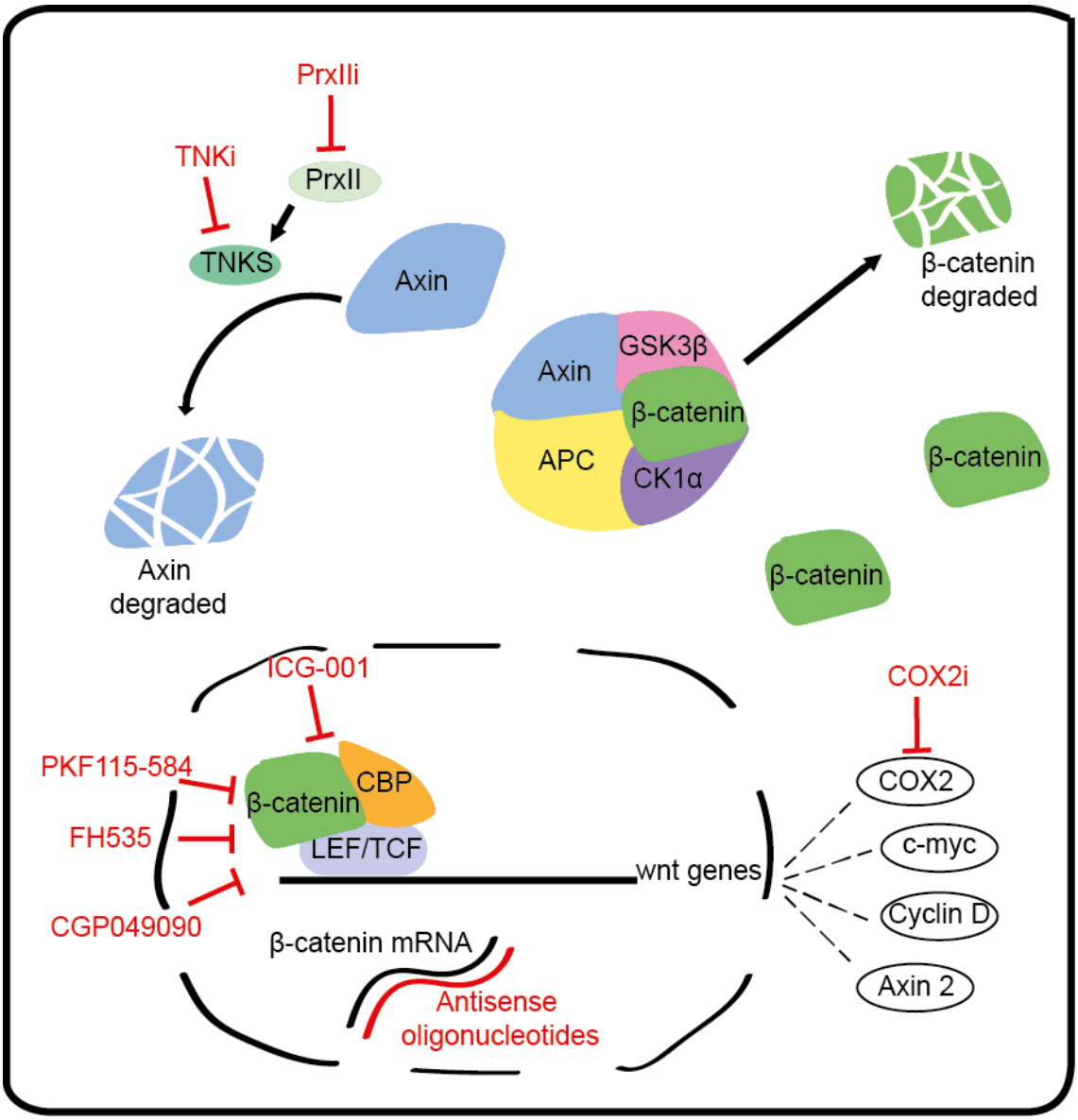

Figure 10 Targeting the Wnt pathway

Schematic showing a number of approaches discussed to lower Wnt signalling by targeting β-catenin, TNKS and COX2.

Small molecule inhibitors can interfere with the interaction of β-catenin to transcription factors and transcriptional co-activators. FH535, PKF115-584 and CGP049090 all reduce the transcriptional activity of β-catenin and TCF/LEF complexes *in vitro* (Handeli & Simon 2008; Lepourcelet et al. 2004). Another small molecule inhibitor ICG-001 has been shown to prevent β-catenin binding to the transcriptional co-activator CREB binding protein (CBP). In CRC cell lines, treatment with ICG-001 caused a reduction in proliferation (Emami et al. 2004). Additionally ICG-001 treatment in the APC^{min} mouse model resulted in a 42 % reduction in the formation of polyps and in a xenograft model using SW620 cell line ICG-001 treatment resulted in a large reduction in tumour size (Emami et al. 2004). A second generation ICG-001 inhibitor was developed called PRI-724 and was tested in a phase 1 trial. This drug has a lower IC50 of 150 nM (compared to 3 μM for ICG-001) and was tolerated well in the phase 1 clinical trial (Emami et al. 2004; Lenz & Kahn 2014; El-Khoueiry et al. 2013).

3.3.2 Tankyrase inhibition

Tankyrases (TNKS) were first identified to have a role in the Wnt signalling pathway through investigating the mechanism of the compound XAV939 (Huang et al. 2009). TNKS consist of two members tankyrase 1 (TNKS1) and tankyrase 2 (TNKS2) and they are part of the poly (ADP-ribose) polymerase (PARP) superfamily of enzymes (Haikarainen et al. 2014). PARP enzymes add ADP-ribose groups onto proteins, also referred to as PARsylation (Riffell et al. 2012). In addition to TNKS role in Wnt signalling, TNKS also play a role in regulating telomeres, mitosis, vesicle transport and viral replication (Lehtiö et al. 2013). The expression of TNKS has been shown to be altered in many cancers including CRC (Lehtiö et al. 2013). Inhibitors of TNKS are being explored as potential therapeutic agents in cancer.

TNKS PARsylate axin and direct ubiquitination by ring finger protein 146 (RNF146) resulting in Axin degradation. The level of axin is regulated by TNKS and self regulated through the pathway because it is a Wnt target gene (Huang et al. 2009). Axin is tightly regulated and is thought to be the rate limiting step in the formation of the β-catenin destruction complex (Huang et al. 2009). TNKS inhibitors prevent TNKS from signalling axin for degradation, therefore axin is available to form part of the β-catenin destruction complex. Increased formation of the β-catenin destruction complex increases the degradation of β-catenin and decreases the activation of Wnt target genes. The first inhibitors identified were XAV939 and IWR-1 and now there are many published inhibitors including WIK14, JW55, JW67, JW74, G007-LK and G244-LM (Lehtiö et al. 2013; Waaler et al. 2011; Waaler et al. 2012; Lau et al. 2013). TNKS inhibitors are

being investigated in CRC to lower the hyperactivation of the Wnt signalling pathway commonly seen in CRC. Sensitivity to TNKS inhibitors in a range of CRC cell lines has been variable and not all APC mutant lines are sensitive. For example, Lau et al. (2013) tested 11 APC mutant CRC cell lines and found only six showed a decrease in Wnt signalling when treated with G007-LK or G244-LM. SW480 was one of the cell lines, which did not respond to G007-LK/G244-LM. However, treatment with JW74 in SW480 reduced cell line growth and tumour growth in an xenograft model suggesting differences in sensitivities between different TNKS inhibitors (Lau et al. 2013; Waaler et al. 2011). Recently a group suggested the location of the APC mutation explained why not all APC mutant cell lines respond to TNKS inhibitors. Cell lines with APC mutations lacking all seven 20aa repeats were sensitive and those with two or more 20aa repeats were resistant to TNKS inhibitors (Tanaka et al. 2017). The group further validated this model in patient samples and therefore this finding has the potential to be used as a biomarker for patients who would benefit from TNKS inhibitors (Tanaka et al. 2017). Further research will be required to see if this is applicable to all TNKS inhibitors developed and in development. Another reason some cell lines may be less responsive is if they have become less dependent on Wnt signalling for proliferation. A recent study investigated drug resistance to the TNKS inhibitor IWR-1 and found the mTOR pathway was upregulated in colo-320DM cells made resistant to IWR-1 (Mashima et al. 2017). Interestingly TNKS mRNA has been reported to be lower in more advanced CRC and this could suggest TNKS inhibitors may be more effective at early stages (Gelmini et al. 2006). TNKS inhibitors have the potential to treat CRC, however findings ways to minimise the toxicity effects on normal cells in the intestine is essential for this treatment to reach the clinic (Zhong et al. 2016; Lau et al. 2013).

A recent paper has uncovered a new way to potentially target TNKS which is specific to APC mutated cells and therefore may be better tolerated as a treatment. Mammalian 2-Cys peroxiredoxin type II (PrxII) has been shown to regulate TNKS in APC mutant CRC (Kang et al. 2017). PrxII binds directly to TNKS and protects the zinc binding domain on TNKS from oxidative inactivation by H_2O_2, the zinc binding domain is essential for TNKS to PARsylate axin and signal its degradation, promoting Wnt signalling. It is believed the mechanism is specific to APC mutated cells because the APC mutation seems to increase levels of H_2O_2 in the cell and causes a change to both PrxII and TNKS allowing them to bind. Inhibiting PrxII prevents TNKS from destabilising axin resulting in reduced Wnt signalling and inhibition of growth in APC mutant CRC cell lines and xenograft experiments (Kang et al. 2017). Interestingly PrxII is overexpressed in CRC regardless of APC status (Kang et al. 2017). Currently, the only

available compound to specifically inhibit PrxII is conoidin A and therefore there is an opportunity to develop more compounds (Kang et al. 2017).

3.4 COX2 inhibitors

COX2 is one of two cycloxygenase isozymes which catalyze the conversion of arachidonic acid to prostaglandin H_2 (Oshima et al. 1996). COX2 has been identified as a Wnt target gene and APC mutant cells show increased expression of COX2 (Lesko et al. 2014). Therefore, targeting COX2 has the potential to be a therapeutic strategy for APC mutant CRC. Loss of *prostaglandin-endoperoxide synthase 2 (Ptgs2)* which encodes COX2 in the APC^{716} mice resulted in a decrease in the number of polyps and size (Oshima et al. 1996). Additionally treating APC^{716} mice with MF-tricyclic (COX2 specific inhibitor) and the non-steroidal anti-inflammatory drug (NSAID) sulindac (COX1 and COX2 inhibitor) resulted in a reduction in polyp formation. MF-tricyclic was shown to be more effective than sulindac (Oshima et al. 1996).

COX2 inhibitors have been tested in combination with other drugs, for example EGFR inhibitors. Research showed combining celecoxib (COX2 inhibitor) with erlotinib (EGFR inhibitor) resulted in less polyps in the APC^{min} mouse model and reduced tumour volume in CRC xenografts (Buchanan et al. 2007). Unfortunately, a phase 2 clinical trial on recurrent metastatic CRC suggested the combined inhibition of COX2 and EGFR does not increase the benefit of treating with the EGFR inhibitor alone (Chan et al. 2011). Another clinical trial explored the potential of COX2 inhibitors and EGFR inhibitors in preventing tumourigenesis. The randomised trial combined sulindac and erlotinib (EGFR inhibitor) to treat FAP patients who develop many polyps which are precursors to tumourigensis. This combination decreased the duodenal polyp burden, however at the doses used there were concerns over toxicity and this may limit its potential (Samadder et al. 2016). More research is needed into this field to see if inhibiting COX2 could benefit patients with APC mutations.

3.5 TASIN-1

A recent paper has identified truncated APC selective inhibitor-1 (TASIN-1) as a compound which induces apoptotic cell death in APC mutant CRC (Zhang et al. 2016). The compound was originally identified from a screen against 200,000 compounds using isogenic immortilised human colonic epithelial cell lines (HCEC) derived from ICT. Both cell lines expressed KRAS G12V, TP53 shRNA, APC shRNA and one of the lines additionally ectopically expressed APC1309 truncation. This resulted in two cell

lines known as ICTRPA and ICTRPA A1309 which differed just in the presence of truncated APC (Zhang et al. 2016). TASIN-1 was then shown to be effective in other models including commonly used APC mutant CRC cell lines, xenograft models (using APC mutant HT29 and DLD1 cell lines) and the mouse model APC^{580}.TASIN-1 was identified to potentially target emopamil-binding protein (EBP) which is part of the cholesterol synthesis pathway (downstream of 3-hydroxyl-3-methylglutaryl coenzyme A reductase (HMGCR)). In APC mutant cell lines cholesterol synthesis decreases upon TASIN-1 treatment and these cell lines are unable to respond to this decrease because they are unable to upregulate sterol regulatory element-binding protein 2 (SREBP2) and SREBP2 target genes (Zhang et al. 2016). This study shows promise in developing a targeted therapy specific for patients with APC mutations.

4 Using RNAi to identify synthetic lethal interactions

4.1 Silencing genes using RNAi

4.1.1 Discovery of RNAi

By the early 1990's evidence was developing to suggest gene expression was not only mediated before transcription by protein transcription factors but also occurred post transcription (Fellmann & Lowe 2014). One example was the discovery of the *lin4* gene in *Caenorhabditis elegans (C.elegans)* which encodes a pair of small RNA responsible for regulating the levels of the protein LIN-14 (Fellmann & Lowe 2014). By the late 1990's researchers had discovered a mechanism of double stranded RNA (dsRNA) mediated sequence specific gene silencing in *C.elegans*, similar mechanisms were also identified in eukaryotic organisms, enabling the mechanism to be exploited as a scientific tool by the early 21st century (Fellmann & Lowe 2014).

4.1.2 Mechanism

The endogenous system in mammalian cells is mediated by micro RNA (miRNA) which is transcribed from the genome as long primary miRNA (pri-miRNA) and are processed into precursor miRNA (pre-miRNA). Exportin 5 exports pre-miRNA from the nucleus to the cytoplasm (Fellmann & Lowe 2014). In the cytoplasm Dicer cleaves the pre-miRNA into small RNA duplexes (approximately 22 nucleotides (nt)), these duplexes are loaded onto the RNA-induced silencing complex (RISC) complex and one strand is selected as the guide strand. The guide strand binds complementary mRNA

sequences, perfect matching results in cleavage and degradation whilst partial matching leads to translational repression (Fellmann & Lowe 2014).

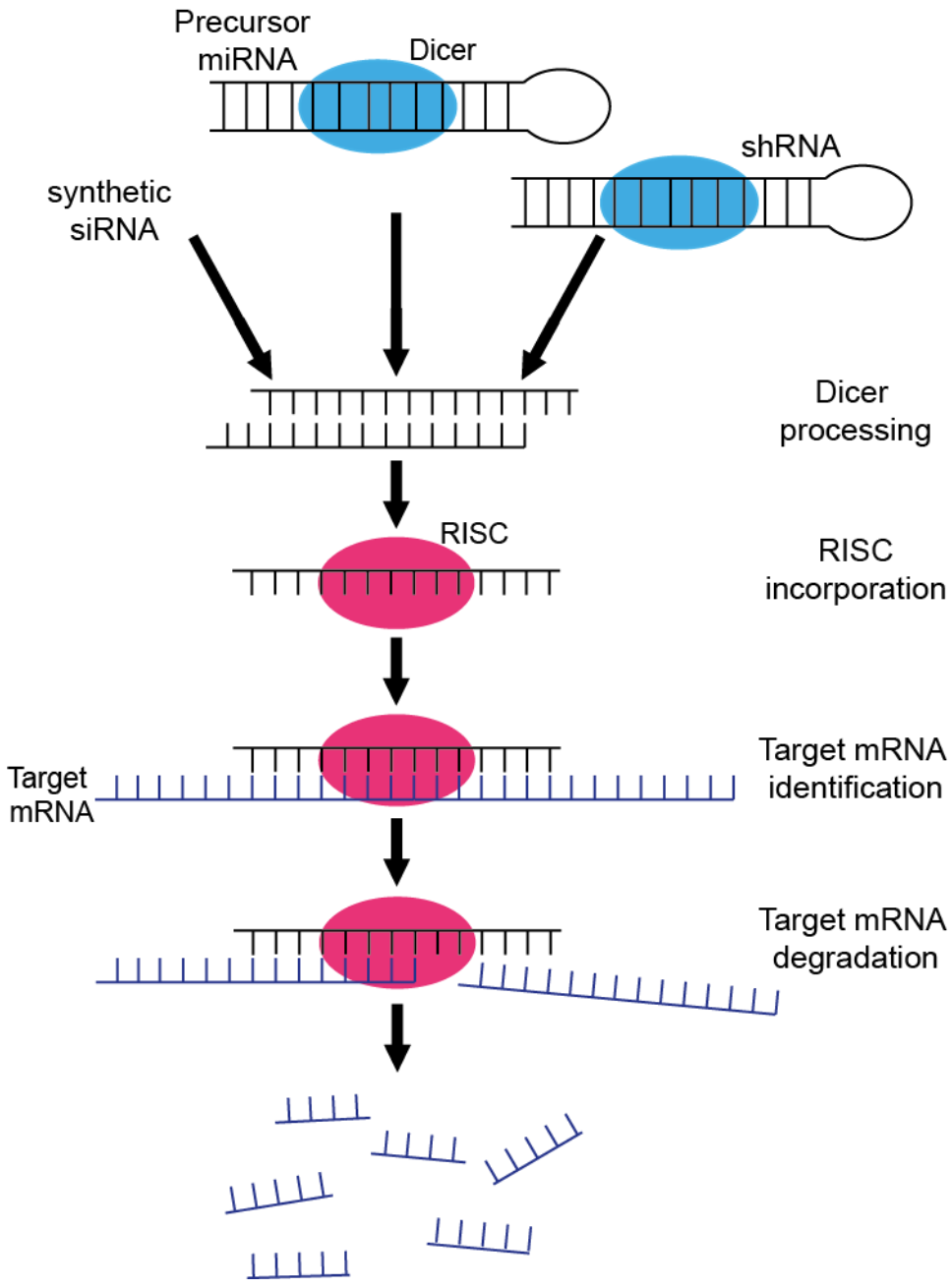

Figure 11 Experimentally exploiting RNAi to silence genes

Introducing siRNA, shRNA or miRNA into cells and these are processed by the RNAi machinery. The guide strand is incorporated into a RISC complex and this binds to the target mRNA and results in the degradation of the target mRNA. Adapted from (Wittrup & Lieberman 2015).

To experimentally exploit the system, exogenous triggers can be introduced directly, for mammalian cells short interfering RNA (siRNA), plasmids expressing shRNA or miRNA are commonly introduced into cells (Figure 11) (Lord et al. 2009). Synthetic siRNA is loaded directly into the RISC complex whilst both shRNA and miRNA undergo processing first, shRNA mimic the pre-miRNA. Synthetic siRNA can be used for short term gene silencing whilst shRNA is used for stable gene silencing because the sequence is incorporated into the host genome (Lord et al. 2009). This technology has become a very useful and widespread tool for loss of function studies. It is a great counterpart to small molecule inhibitors and enables undruggable targets to be targeted (Fellmann & Lowe 2014). The use of this technology for high throughput screens utilises the advantage of this tool and can be used to investigate gene function, understand mechanisms of drug resistance and search for synthetic lethal interactions on a genome wide scale to name a few.

4.2 Synthetic lethality

4.2.1 Discovery

Originally described in bacteria and yeast synthetic lethality was suggested as a new approach to identify new targets in cancer therapy (Canaani 2014; Hartwell 1997). Synthetic lethality is the concept that when gene A or gene B alone are inactive the cell survives, but if both gene A and gene B are inactive together the cell dies. In cancer cells, gene A could be a mutation and gene B becomes a potential therapeutic target. Targeting gene B would be a cancer cell specific target because normal cells would have a normal non-mutated form of gene A, therefore survive the targeted treatment. Genes identified to be in a synthetic lethal relationship could be in the same complex, same pathway, parallel pathways, divergent pathways or even in unrelated pathways (Chan & Giaccia 2011).

There are numerous benefits to this approach, firstly it enables the treatment to specifically target just the cancer cells, enhancing the therapeutic index and reducing chemotherapy associated side effects. Secondly the approach is ideal for targeting tumour suppressor genes which are hard to target because unlike oncogenes there is often no protein to inhibit. Finally the therapy could be used as a monotherapy or in combination with conventional treatments, enhancing the effect of radiotherapy or chemotherapy enabling lower doses to be given and reducing side effects (Chan & Giaccia 2011).

4.2.2 High throughput screens to identify synthetic lethal interactions

After the initial idea of applying synthetic lethality to cancer therapeutics, genetic screens to investigate the theory were performed in model genetic systems using classical genetics including *Saccharomyces cerevisiae (S.cerevisiae)*, *C.elegans* and *Drosophila melanogaster* (*D.melanogaster)*. For example, *S.cerevisiae* mutants where screened with 50 FDA chemotherapeutics to increase understanding of these agents and one of the findings was that yeast strains defective in post replicative repair were more sensitive to cisplatin (Hartwell 1997). These early screens provided proof of concept and with the development of RNA interference (RNAi) it became possible to perform data rich high throughput screens, identifying synthetic lethal interactions directly in human cancer cell lines.

As described earlier siRNA and shRNA can be used in mammalian cells to post transcriptionally repress gene expression of specific genes and this technology enables large scale loss of function screens to be performed. The choice of siRNA or shRNA depends on the cell line and experimental design because siRNA is transiently transfected into cells using lipid and peptide based transfection or electroporation, whereas shRNA is stably delivered using a viral based vector. shRNA is preferred for longer term silencing and cell lines which are hard to transfect (Echeverri & Perrimon 2006). Screens can involve different sized RNAi libraries targeting the whole genome or specific groups of proteins including kinases, DNA repair or tumour suppressors. The benefit of looking for synthetic lethal interactions with kinases is that these genes are easier to target with drugs, with many existing compounds already available.

There are two main screening approaches, target each gene individually (systematic) or target multiple genes in a pool (pooled). Systematic approaches typically use an arrayed format, this approach can be expensive but has the advantage that it provides information on each gene in the library individually. A pooled approach delivers a whole library to a population of cells and a phenotype is selected (for example resistance to a drug) to identify genes of interest. DNA is then extracted from the cells, amplified and sequenced to identify the gene the shRNA targeted (Lord et al. 2009). There are many screen read out options for example; cellular viability, cell morphology, reporter assays and functional assays (Falschlehner et al. 2010). To obtain these read outs a variety of technologies are used including; fluorescence, microscopy, microfluidics and flow cytometry (Janzen 2014). Screens collecting multiple measurements are known as high content screens (Lord et al. 2009).

In addition to using RNAi to identify synthetic lethal interactions, small molecule libraries and CRISPR-cas9 (discussed in section 5) can also be used. The advantage

of screening with small molecule libraries is any findings can be quickly translated into the clinic because an inhibitor is already available and may just need to be modified to increase efficiency (Chan & Giaccia 2011).

4.2.3 Examples in cancer therapy

Numerous synthetic lethal interactions have already been identified using RNAi in a range of cancers, offering a wide range of potential new therapeutic strategies. In CRC deficiencies in the mismatch repair pathway have been shown to be synthetically lethal with DNA Polymerases. More specifically MSH2 loss was synthetically lethal with Pol-β inhibition and MLH1 loss was synthetically lethal with DNA Polymerase γ (Pol-γ). Both relationships lead to an increase in 8-Oxoguanine (8-oxo G) levels resulting in lethal DNA breaks due to the inability to repair the damage caused by 8-oxo G (Martin et al. 2010). More potent inhibitors of both DNA polymerase β and γ are required for clinical trials.

An example in non-small cell lung cancer (NSCLC) is the identification of a synthetic lethal relationship between *cdk4* and $KRAS^{G12V}$. The synthetic lethal interaction was not shared with cdk2 or cdk6, highlighting why broad cdk inhibitors may have limited efficiency in this mutational background (Chan & Giaccia 2011). In support of this work Mao et al. (2014) showed it was possible to deliver siRNA targeting *CDK4* in micellar nanoparticles (MNP) into A549 mice xenografts, resulting in the inhibition of tumour growth.

A well known synthetic lethal interaction which has now reached the clinic occurs between breast and ovarian cancer patients with breast cancer 1 or 2 (BRCA1 or BRCA2) mutations and inhibition of PARP. These cancers are sensitive to PARP inhibition because homologous recombination (HR) is compromised upon BRCA1/2 loss and PARP inhibition halts single stranded repair, so any unrepaired single strand breaks become double stranded and prove lethal for the cells (Canaani 2014). After years of clinical trials PARP inhibitors have recently been approved for use in BRCA deficient patients (Bose & Basu 2015). This demonstrates identifying synthetic lethal relationships using high throughput screens can deliver new treatments for cancer patients.

5 CRISPR-cas9 to edit genes

5.1 Discovery

The CRISPR-cas9 story started back in 1987 with the identification of unusual repetitive elements in *Escherichia coli* (*E.coli)*, instead of forming tandem repeats the 29 nt repeats were interspaced by five intervening 32 nt non-repetitive sequences. As the number of genome sequences increased, this type of repetitive element was also identified in over 40 % of bacteria sequenced and 90 % of archaea. In 2002 these repetitive elements became known as clustered regularly interspaced short palindromic repeats (CRISPR). Further characterisation of these regions lead to the discovery of well conserved regions located alongside CRISPR. These CRISPR associated genes translate into CRISPR associated proteins (cas). Continued research lead to the classification of three microbial CRISPR systems; type I, type II and type III (Hsu et al. 2014). The systems were found to be adaptable immune mechanisms used to provide protection from foreign nucleic acids (Sander & Joung 2014). The big revelation arrived when researchers demonstrated the ability to utilise this naturally occurring mechanism to perform genome editing in eukaryotic cells (Hsu et al. 2014).

5.2 Mechanism

For genome editing the type II system from *Streptococcus pyogenes* (*S.pyogenes)* has been most commonly utilised, other type II systems from other species have also been used (Sander & Joung 2014). There are three essential components; cas9, guide RNA (gRNA) and the protospacer adjacent motif (PAM). Cas9 is an endonuclease which can cleave DNA 3-4 nt upstream of the PAM sequence (Sander & Joung 2014). This enzyme undergoes large conformational changes when it binds to the gRNA and again when it binds to the target site in the DNA (Doudna & Charpentier 2014). The 20 nt at the 5' of gRNA directs cas9 to the specific DNA site for editing (Sander & Joung 2014). The PAM sequence is critical for DNA binding and the sequence is specific for the species cas9 is derived from, for example *S.pyogenes* requires a PAM sequence of 5' NGG (Sander & Joung 2014). Once cas9 is at the correct site it cleaves the DNA causing a DNA break which is repaired by non-homologous end joining (NHEJ) or homology directed repair (HDR). This results in either a truncated protein or a complete knockout due to NMD (Figure 12) (Barrangou et al. 2015).

The cas9 is encoded by a plasmid and some plasmids also express the gRNA. To select the cells which have received the cas9 plasmid, the plasmid also contains an antibiotic resistance gene or a fluorescent protein such as mKate2. The gRNA can be

encoded by a plasmid or can be delivered as synthetic RNA. The cas9 and gRNA can be delivered using a range of methods including electroporation, nucleofection, lipofectamine or viral-mediated (Sander & Joung 2014). Transient methods have been shown to be sufficient for editing and have the advantage that the expression of the components is only temporary, reducing off target effects from cas9. Constitutive expression of components using viral delivery methods is ideal for hard to transfect cells and could lead to higher efficiencies (Sander & Joung 2014).

A potential problem with CRISPR-cas9 is the potential for off target effects. Cas9 has been shown to tolerate sequence mismatches and bulges between the target DNA and the gRNA, suggesting off target effects are a problem (Sander & Joung 2014). Many ways have been suggested to minimise off target effects including; using minimal reagents, careful design of gRNAs or using paired nickases to generate adjacent off set nicks in the DNA (Sander & Joung 2014).

5.3 Applications

CRISPR-cas9 has been developed into a powerful tool in genome engineering to facilitate studies into gene function, perform genome wide screens, developing disease models and potentially as new therapeutic agents (Barrangou et al. 2015). CRISPR-cas9 can be used to completely knock out a protein, insert epitope tags or fluorescent proteins to gene products and to specifically alter a gene sequence. Any alteration occurs at the DNA level and is therefore inherited to daughter cells.

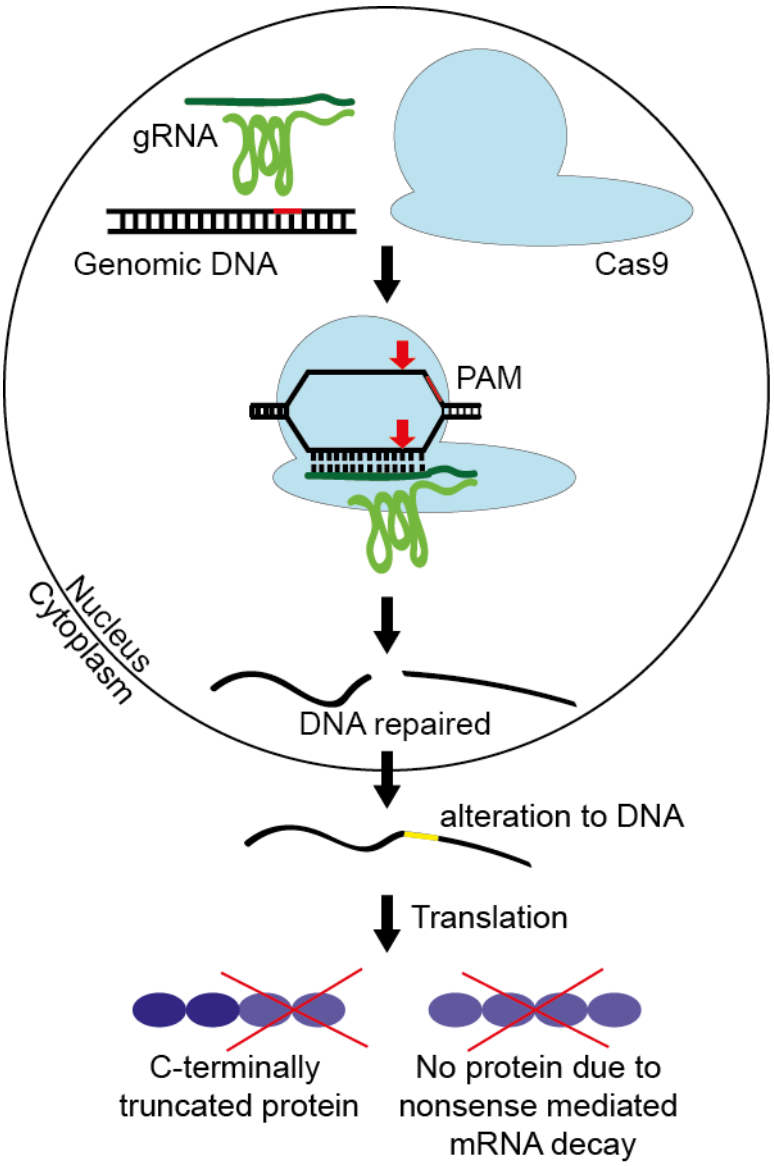

Figure 12 CRISPR-cas9 mechanism

The gRNA directs the cas9 to the correct site in the genome to cleave the DNA. The DNA break is then repaired and could result in an alteration to the DNA sequence which either causes the expression of a C-terminally truncated protein or no protein. Adapted from (Barrangou et al. 2015).

6 mTOR and colorectal cancer

6.1 mTOR pathway

The mTOR pathway is a central regulator of key cellular processes and consists of two main signalling hubs called mTORC1 and mammalian target of rapamycin complex 2 (mTORC2). The main protein in both complexes is a serine threonine kinase called mTOR, it forms part of the PI3K family (Laplante & Sabatini 2009). Both complexes contain the mTOR inhibitor proline-rich akt substrate of 40kDa (pras40), the scaffold proteins tti1 and tel2, and protein mammalian lethal with SEC13 protein 8 (mLST8) whose function is unclear (Laplante & Sabatini 2012). The mTORC1 complex additionally consists of the scaffold protein raptor and the mTORC2 complex is joined by protein observed with rictor 1/2 (protor 1/2) and the scaffold protein mammalian stress-activated map kinase-interacting protein 1 (msin1) (Laplante & Sabatini 2012).

The mTOR pathway integrates intracellular and extracellular signals including; oxygen, amino acids, stress, energy levels and growth factors (Laplante & Sabatini 2012). Therefore many signalling pathways feed into this pathway (eg Wnt pathway, MAPK pathway and PI3K pathway) resulting in a wide range of changes downstream of mTORC1 and mTORC2 (Figure 13).

6.2 Roles of the mTOR pathway

The mTOR pathway has a wide range of functions in the cell including activating macromolecule synthesis, cell cycle progression, growth, metabolism, cytoskeletal organisation, cell survival and the inhibition of autophagy (Laplante & Sabatini 2012). mTORC1 is responsible for the majority of these roles and will be discussed first.

Firstly the activation/inhibition of mTORC1 relies on signals from growth factors, energy levels, oxygen, amino acids and stress. Some of these signals feed through a sensor known as tuberous sclerosis complex (TSC), this is a heterodimer consisting of tuberous sclerosis 1 (TSC1) and tuberous sclerosis 2 (TSC2) which are GTPase-activating proteins (GAP) for ras homolog enriched in brain (Rheb) causing guanosine triphosphate (GTP) bound to Rheb to hydrolyse to guanosine diphosphate (GDP). Rheb interacts with mTOR and when bound GDP it inhibits the mTORC1 complex (Laplante & Sabatini 2012). For example, growth factors activate key signalling proteins including AKT, ERK1/2 and S6K1, resulting in the phosphorylation of TSC2 and subsequent activation of mTORC1. If energy is high or adequate oxygen is available, AMPK remains inactive, TSC2 is inactive and this results in mTORC1 remaining active.

When AMPK is activated due to low energy or hypoxia the inhibition of mTORC1 can occur through TSC2 or independently through raptor (Laplante & Sabatini 2012).

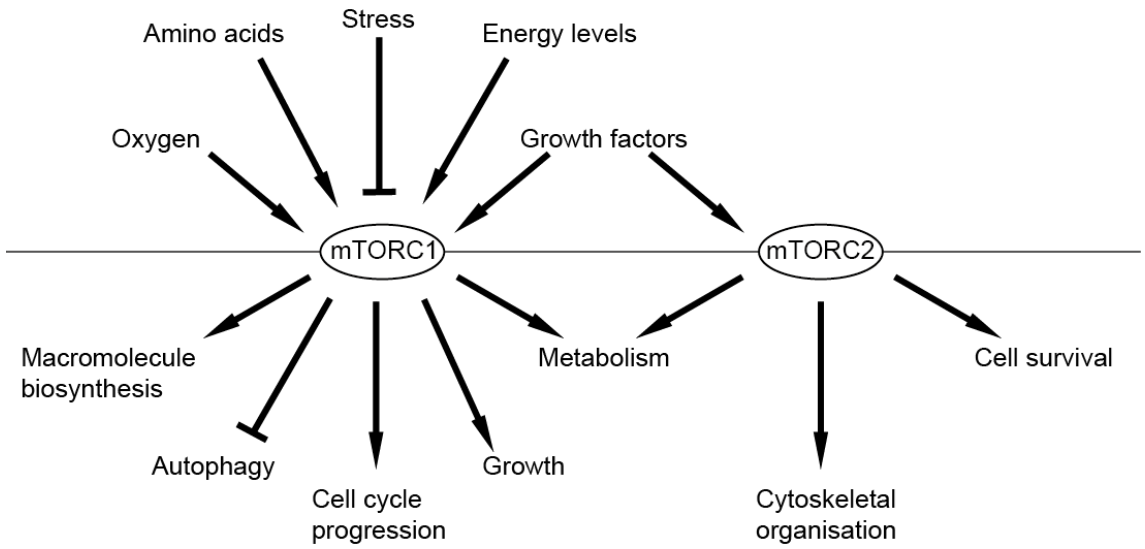

Figure 13 Summary of the mTOR pathway

Schematic showing the inputs and outputs of the two main signalling complexes in mTOR signalling. Adapted from (Laplante & Sabatini 2012).

Once mTORC1 is activated it leads to the activation of protein synthesis, lipid synthesis, mitochondrial metabolism and inhibition of autophagy. mTORC1 directly activates protein synthesis through the phosphorylation of 4E-BP1, S6K1 and PP2A (Laplante & Sabatini 2009). The phosphorylation of 4E-BP1 prevents binding and inhibition of eukaryotic translation initiation factor 4E (eIF4E), enabling eIF4E to promote cap-dependent translation. Phosphorylated S6K1 activates mRNA biogenesis, cap dependent translation, elongation and translation of ribosomal proteins. The phosphorylation of PP2A inhibits this protein, resulting in the transcription of ribosomal RNA, the machinery required for protein synthesis. Lipid synthesis occurs through mTORC1 direct activation of transcription factors sterol regulatory element-binding transcription factor 1 (SREBP1) and peroxisome proliferator-activated receptor gamma (PPARγ). mTORC1 activates mitochondrial metabolism and biogenesis through altering peroxisome proliferator-activated receptor gamma coactivator 1 alpha (PGC1α) interaction with another transcription factor ying yang 1 (YY1). Under normal conditions mTORC1 represses autophagy, which can be used to provide biological material when nutrient sources are low. This occurs through mTORC1 phosphorylation and repression of uridine kinase-like protein 1 (UKL1), autophagy related 13 (ATG13) and FAK family kinase-interacting protein of 200 kDa (FIP200) (Laplante & Sabatini 2009).

The less well known mTOR complex is mTORC2 and it plays a role in cell survival, metabolism and regulation of the cytoskeleton. mTORC2 is required for the full activation of AKT and this prevents the activation of transcription factors forkhead box O1 (Fox01) and forkhead box O3a (Fox03a). When activated Fox01/03a activate transcription of genes involved in stress resistance, metabolism, cell cycle arrest and apoptosis (Laplante & Sabatini 2009). mTORC2 acts on the cytoskeleton through phosphorylating protein kinase C alpha (PKCα) (Laplante & Sabatini 2009).

6.3 Deregulation in cancer

Many of the pathways feeding into the mTOR pathway are commonly mutated in cancers leading to deregulation of the pathway, additionally familial syndromes arise from mutations in genes upstream of mTOR (Laplante & Sabatini 2012). In CRC mutations in Ras, p53, Wnt pathway and PI3K/PTEN/AKT pathways are common resulting in hyperactivation of the mTOR pathway (Wang & Zhang 2014). It is thought that the increase in protein synthesis through phosphorylation of 4E-BP1 is the main contributor to tumour development through hyperactivation of the mTOR pathway because this provides the cell with proteins required for cell survival, cell cycle progression, angiogenesis, energy metabolism and metastasis. Therefore it is believed the ability of mTOR inhibitors to inhibit this particular part of the mTOR pathway is key to the success of inhibiting this pathway (Laplante & Sabatini 2012).

Rapamycin was the first mTOR inhibitor discovered and was found to inhibit mTORC1 with a high specificity, but is thought to only partially phosphorylate 4E-BP1. Limitations in solubility and pharmokinetic properties lead to the development of improved versions known as rapalogs and included; temsirolimus, everolimus and ridaforolimus (Zaytseva et al. 2012). Rapamycin and the rapalogs appear to inhibit mTORC2 complex to some extent but this depends on the cell line and impacts on the ability to induce apoptosis (Zaytseva et al. 2012). The next generation of mTOR inhibitors were designed on the importance of inhibiting both mTORC1 and mTORC2, therefore the kinase activity of the protein mTOR was targeted. mTOR kinase inhibitors are more potent than rapamycin and rapalogs, they completely inhibit phosphorylation of 4E-BP1 and are currently being tested in the clinic (Laplante & Sabatini 2012). The broader inhibition of mTOR has increased the toxicity to normal tissues and there has been limited success in KRAS driven tumours (Zaytseva et al. 2012). Another approach is dual inhibitors of PI3K and mTOR, due to the similarity of the catalytic domains, these show higher potency in clinical trials, however, the toxicity to normal tissues is higher (Laplante & Sabatini 2012).

A wide range of mTOR inhibitors have been trialled and are ongoing, results are varying. Some have received food and drug administration (FDA) approval for example temisirolimus is approved for advanced stage renal cell carcinoma (Laplante & Sabatini 2012). In general the response to mTOR inhibitors is not as anticipated, it is a complex pathway and potentially the number of feedback loops poses limitations to the inhibition of this pathway. Despite this responses are seen in some tumours, therefore a greater understanding and clear biomarkers are required to identify patients who could benefit the most from this therapeutic strategy (Laplante & Sabatini 2012).

7 Statins

7.1 Introduction to statins

In 1987 the first statin was approved by the FDA for the prevention of cardiovascular disease (CVD). Statins are a family of drugs which are small molecule inhibitors of HMGCR in the mevalonate pathway. HMGCR catalyses the conversion of 3-hydroxyl-3-methylglutaryl coenzyme A (HMG-CoA) to mevalonate and this is the rate limiting step in the pathway resulting in cholesterol production (Figure 14) (Bardou et al. 2010). Inhibition of HMGCR results in the reduction of plasma cholesterol levels and there is strong evidence showing that this reduces your risk and this reduction in risk continues over treatment time (Collins et al. 2016). In recent years it has been suggested that the use of statins could be broadened to a wide range of additional conditions including; multiple sclerosis, IBD, rheumatoid arthritis, systemic lupus erythematosus, chronic obstructive pulmonary disease, cancer, strokes, HIV, parkinsons and alzheimers (Davies et al. 2016). This is due to statins also modulating immune responses, enhancing anti-inflammatory processes and altering signalling pathways (Davies et al. 2016).

7.2 Mechanism of action

7.2.1 HMGCR dependent

Cholesterol is made in hepatocytes and statins compete with HMG-CoA to bind HMGCR in hepatocytes. Cholesterol is mostly transported by low density lipoprotein (LDL) and is then referred to as LDL-C (‘Bad’ cholesterol). Cholesterol bound to high density lipoprotein (HDL) is destined for recycling and excretion at the liver and often called ‘good’ cholesterol. When statins bind to HMGCR, cholesterol production is reduced and intracellular levels decrease, causing LDL-C to be transported into the cell

to restore intracellular levels. This in turn results in a reduction in levels of LDL-C in the plasma (Davies et al. 2016).

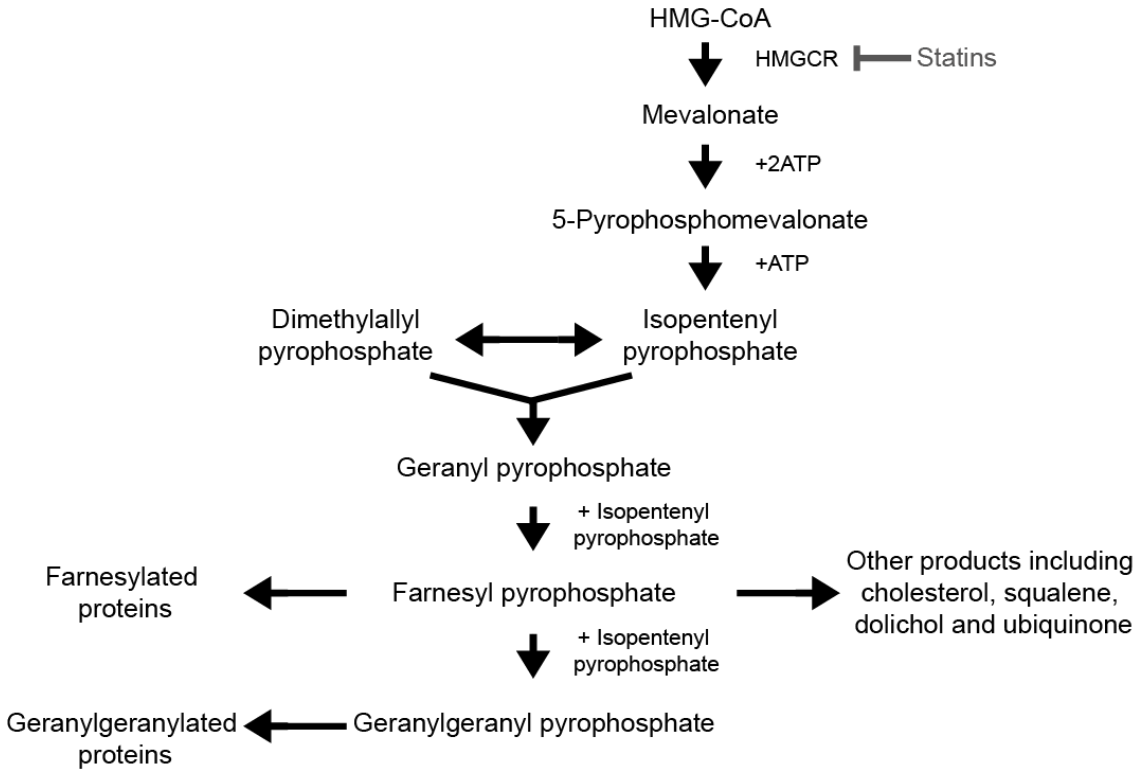

Figure 14 Mevalonate pathway

The Mevalonate pathway synthesises cholesterol, squalene, dolichol, ubiquinone and isoprenoids. Statins compete with HMG-CoA to bind HMGCR which is the first step in the Mevalonate pathway, resulting in a reduction in all Mevalonate pathway products. Adapted from (Demierre et al. 2005).

Another impact of the inhibition of HMGCR is the reduction in isoprenoids including farnesyl pyrophosphate (FPP) and geranylgeranyl pyrophosphate (GGPP) (Figure 14). Isoprenoids are added to certain proteins as a post translational modification, known as prenylation. Prenylation adds long hydrophobic molecules to proteins enabling proteins to anchor to cell membranes. Prenylation is mediated by either farnesyl transferase (FTase) or geranylgeranyl transferase (GGTase) and occurs at a CAAX, CXC or CC sequence (Figure 15) (Greenwood et al. 2006). The Ras superfamily commonly undergoes prenylation and alongside other post translational modifications determines the correct localisation and functioning of these proteins (discussed later in section 9) (Demierre et al. 2005; Roberts et al. 2008). Ras, Rac and Rho are commonly deregulated in cancers and reducing isoprenoids effects the function of these proteins and is potentially how statins exert their pro-apoptotic, anti-proliferative, angiogenic and inflammatory effects on cancer cells (Lochhead & Chan 2013; Demierre et al. 2005).

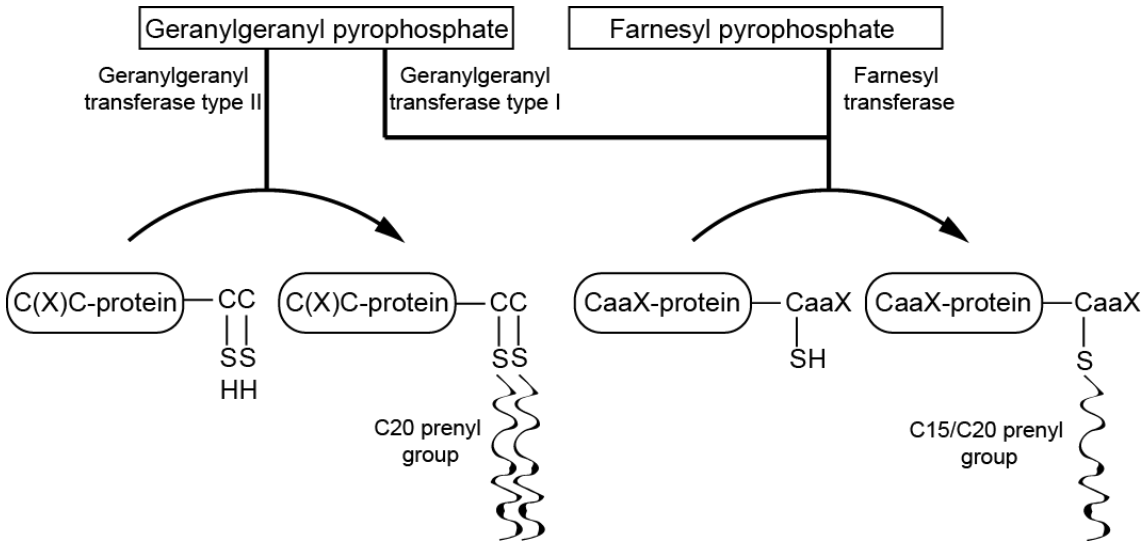

Figure 15 Protein prenylation

Prenylation adds a hydrophobic molecule to proteins. Proteins containing CaaX sequence can be prenylated by either FTase of GGTase resulting in the addition of either FPP or GGPP. Proteins containing the CXC sequence are only prenylated by GGTase resulting in the addition of GGPP. Adapted from (Greenwood et al. 2006).

7.2.2 HMGCR independent

Statins also function independently of HMGCR causing a range of additional changes in the body. Statins inhibit the lymphocyte functions-associated antigen 1 (LFA1) integrin which modulates leukocyte trafficking and T cell activation and intercellular adhesion molecule 1 (ICAM1) which sustains leukocyte adhesion and facilitates migration (Davies et al. 2016). A range of signal transduction molecules are inhibited including AKT, ERK/MAPK, JAK/STAT resulting in changes in cell proliferation, apoptosis and the immune system. Statins inhibit transcription factors involved in pro-inflammatory responses (including NF-kappaB (NF-kB), activator protein 1 (AP1), histone deacetylases (HDAC) and STAT1/3/4) and activate transcription factors with an anti-inflammatory role (including Kruppel like factor 2 (KLF2) and peroxisome proliferator-activated receptor alpha/beta (pPARα/β)) (Davies et al. 2016). Statins further modulate the immune system through the following inflammatory mediators cluster of differentiation 40 (CD40), interleukin1 beta (IL-1B), interleukin 6 (IL6), tumour necrosis factor alpha (TNFα), major histocompatibility class II (MHC-II), T-helper 1 and 2 cytokines and c-reactive protein (CRP) (Demierre et al. 2005). Statins also influence angiogenesis, it is thought that statins may be pro-angiogenic at low doses and anti-angiogenic at high doses (Demierre et al. 2005). Given all the HMGCR independent roles of statins these drugs induce a wide range of changes resulting in altering antioxidant activity, cell adhesion, inflammation, immunomodulation, angiogenesis, cell apoptosis and proliferation (Lochhead & Chan 2013).

7.3 Concerns for statin use

Statins have proven benefits in patients at risk of CVD, unfortunately there are concerns over safety. Some concerns are genuine, whilst others are a result of misleading data from observational studies which includes case-control cohort studies and retrospective cohort studies. The cholesterol treatment trialists (CTT) collaboration recently published a paper discussing results of a meta-analysis of all randomised controlled trials (with over 2 years statin treatment in over 1,000 patients) and highlighted the facts from the fiction (Collins et al. 2016).

The use of statins has three proven adverse effects; myopathy, diabetes mellitus and haemorrhagic stroke. Myopathy is described as muscle pain, tendernesss or weakness and is associated with increased blood creatine kinase concentration. The risk is relatively low with one case for every 10,000 patients treated with statins and the myopathy normally resolves when treatment is stopped (Collins et al. 2016). The risk of diabetes is more pronounced, on standard doses the risk increases by 10 %, whilst on stronger doses the risk increases to 20 %. The risk of haemorrhagic stroke increases with reduction in LDL-C levels but this risk is thought to be outweighed by the decreased risk of ischaemic stroke (Collins et al. 2016). Other adverse effects with no proven link to the use of statins include memory problems, cataracts and kidney related problems. Unfortunately it is believed that statin uptake is severely affected because of misleading information on the adverse effects.

A potential adverse effect suggested years ago was the link of statin use and cancer seen in some observational studies and early laboratory data. Since the original observations there is now mounting evidence that statins either have no impact on cancer development or may have a protective effect (Collins et al. 2016). Data from observational studies taken from cohorts and health care databases are often misleading due to inherent biases in the data and design (Collins et al. 2016). Additionally many of the studies available have been designed to test the safety and efficacy of preventing CVD with statins. Resulting in insufficient data to interpret due to limited information and a short follow up period, cancer takes years to develop so a long follow up is essential. Additionally the trial population is often biased to those at high risk of CVD, who are often also at higher risk of cancer due to low physical exercise and poor diet (Lochhead & Chan 2013).

7.4 Statins in colorectal cancer

7.4.1 The protective role of statins

There is growing evidence of statins preventing CRC and this is supported by both population studies and laboratory data. Case-control studies have shown varying levels of effect, for example, a case control study with over 4,000 people in Israel found a 47 % decreased risk in CRC whilst a case control study in US veterans with diabetes showed a 9 % decreased CRC risk (Poynter et al. 2005; Hachem et al. 2009). Many other case-control studies across the globe have shown no significant associations (Lochhead & Chan 2013). Retrospective cohort studies show a similar pattern too, a study of 37,000 US veterans using statins identified a 35 % reduction in CRC risk whilst a number of other studies have shown no effect (Farwell et al. 2008; Lochhead & Chan 2013). Many of the randomised controlled trials, which are more reliable than observational studies suggest statins do not increase the risk of CRC (Lochhead & Chan 2013). Most importantly these studies may not strongly support a protective effect, but they highlight that statins do not appear to cause CRC.

Laboratory data is more supportive for the protective effect of statins against CRC. A key step in the development of CRC is the development of polyps in the colon or rectum, reducing the number of polyps reduces your risk of developing CRC. In the APC^{min} mice statins alone have been shown to reduce the number of polyps by a third (Teraoka et al. 2011; Swamy et al. 2006). A study in F344 rats chemically induced to develop CRC, showed treatment with prevastatin significantly reduced the development of tumours (Narisawa et al. 1996). Similar effects have also been seen in a colitis associated colon cancer model (CAC) where tumours were chemically induced in C57/BL6 mice, the development of tumours was reduced in the mice treated with simvastatin (Cho et al. 2008). This is an important model because patients with ulcerative colitis have a high risk of developing bowel cancer.

NSAIDs have protective effects against CRC and many studies are investigating combining statins and NSAIDs. The advantage of using both together is the use of lower doses of both drugs, reducing concerns over side effects. Various statins and NSAIDs have been trialled *in vitro* and *in vivo*. Combining lovastatin with the NSAID sulindac increased apoptosis up to five times more in HCT116, SW480 and LOVO cell lines (Agarwal, Rao, et al. 1999). The same combination of lovastatin and sulindac showed similar results *in vivo* in the Azomethane rat model, showing a reduction in decreased tumour growth by 30 % (Agarwal, Rao, et al. 1999). Other combinations have been trailed including atrovastatin and the NSAID celecoxib in APC^{min} mice,

tumour growth was suppressed by over 86 % and levels of apoptosis increased by 2/3 times (Swamy et al. 2006).

7.4.2 Statins alone to treat colorectal cancer

There is promising data suggesting the potential of statins to be used to treat CRC. Numerous studies show statins cause tumour cell death *in vivo* and *in vitro*. *In vitro* data have shown statins cause varying levels of apoptosis in the following CRC cell lines HT29, HCT116, SW480, LS180, LOVO, colo205 (Chang et al. 2013; Cho et al. 2008; Kaneko et al. 2007; Agarwal, Bhendwal, et al. 1999; Agarwal, Rao, et al. 1999). There are a range of mechanisms suggested for statin induced apoptosis. Some studies suggest apoptosis occurs through the inhibition of the anti-apoptotic protein survivin. Inhibition of survivin has been reported to occur by different mechanisms, activation of p38MAPK-p53 (HCT116 cells treated with simvastatin) and through the inhibition of Ras induced PI3K (SW480 cells treated with lovastatin) (Chang et al. 2013; Kaneko et al. 2007). Other studies suggest statin induced apoptosis occurs through the activation of NF-kB pathway or the bone morphogenic protein (BMP) pathway (Cho et al. 2008; Kodach et al. 2007). Furthermore Kodach et al. (2007) suggests sensitivity to statin treatment is related to the expression of SMAD4 which is part of the BMP pathway, this work helps to identify the patients who may benefit the most. More *in vitro* research is needed to understand the different mechanisms leading to this activation of apoptosis and understanding whether it is due to different types of statins, doses or mutational backgrounds. Research *in vivo* also shows promising results for the use of statins as a cancer treatment. For example, an xenograft model in mice injected with colo205 cell line and treated with simvastatin had smaller tumour volumes, larger necrotic areas, less angiogensis and more apoptosis compared to the mice treated without simvastatin (Cho et al. 2008).

Understanding why normal cells are less sensitive to statins is an important avenue to explore. Research suggests tumours cells are more sensitive to HMGCR inhibition because tumour cells upregulate HMGCR due to abnormal feedback, increasing isopenoid levels, which are required for the Ras superfamily, in turn promoting tumourigensis (Demierre et al. 2005; Hentosh et al. 2001). A concern for using statins alone to treat CRC is the dose required in many of the *in vivo* and *in vitro* studies (1-200 μM) is higher than currently used for treating CVD (10-200 nM). Statins may not be safe to give at the higher doses showing anti-tumour effects, however by understanding the mechanisms of effects seen this may lead to the identification or development of a drug which inhibits the target more effectively (Demierre et al. 2005).

7.4.3 Other uses in colorectal cancer treatment

Researchers are investigating combining statins with chemotherapy to enhance the effect of the chemotherapeutics. A study pretreating SW480, HCT116, LOVO and HT29 with lovastatin before 5-FU or cisplatin treatment showed increased levels of apoptosis (Agarwal, Bhendwal, et al. 1999). Recently a phase III trial was completed where simvastatin was combined with chemotherapy in patients with metastatic colorectal disease. Unfortunately there was no improvement in progression free survival, however this may be because statins may be more effective against early stage disease (Lim et al. 2015).

An interesting avenue of research is using statins to sensitise cells resistant to EGFR therapy, normally KRAS mutant cancers are not treated with EGFR therapy. *In vitro* data showed combining simvastatin with cetuximab reduced cell proliferation in KRAS mutant cell lines and tumour growth in a xenograft model (Lee et al. 2011). However, the same effect was not seen in a phase 2 clinical trial using this concept (Baas et al. 2015).

8 Survivin

8.1 Roles of survivin

Survivin (encoded by the gene *BIRC5*) is one of eight members of the inhibitor of apoptosis (IAP) family, the family also includes cellular inhibitor of apoptosis protein 1 (cIAP1), cellular inhibitor of apoptosis protein 2 (cIAP2) and x-linked inhibitor of apoptosis (XIAP) (Chen et al. 2016). Survivin contributes to two major cellular processes, apoptosis and the cell cycle. Survivin prevents apoptosis by interacting and inhibiting caspase 9 and the effector caspases 3 and 7, causing the inhibition of both intrinsic (via mitochondria) and extrinsic (via death receptor) apoptosis (Figure 16) (Chen et al. 2016). This inhibition of effector caspases prevents the cleavage of cellular substrates and therefore prevents apoptosis. Research also suggests survivin enables cancer cells to avoid apoptosis induced by immune cells by increasing the expression of FasL on the cancer cell surface, resulting in the apoptosis of immune cells via extrinsic apoptosis (Asanuma et al. 2004).

Survivin is carefully regulated during the cell cycle and it is thought to be part of the chromosomal passenger complex (CPC) (Lens et al. 2006). The expression of survivin peaks in G2/M phase then reduces in G1 (Chen et al. 2016). At G2 survivin accumulates at the centromeres, during prophase and metaphase survivin becomes diffuse along the chromosome arms and remains concentrated at the centromere. As

the cell enters anaphase survivin dissociates from the centromere and localises to the central spindle. Then during cytokinesis survivin moves to the midbody before removal from the cell (Lens et al. 2006). This localisation pattern during the cell cycle supports a role for survivin in the CPC, additionally survivin interacts with other members of the complex including INCENP, aurora B and borealin (Lens et al. 2006). Survivin has also been shown to be phosphorylated by cyclin dependent kinase 1 (CDK1) during mitosis resulting in the stabilisation of survivin (Chen et al. 2016). This evidence supports a role for survivin in the cell cycle.

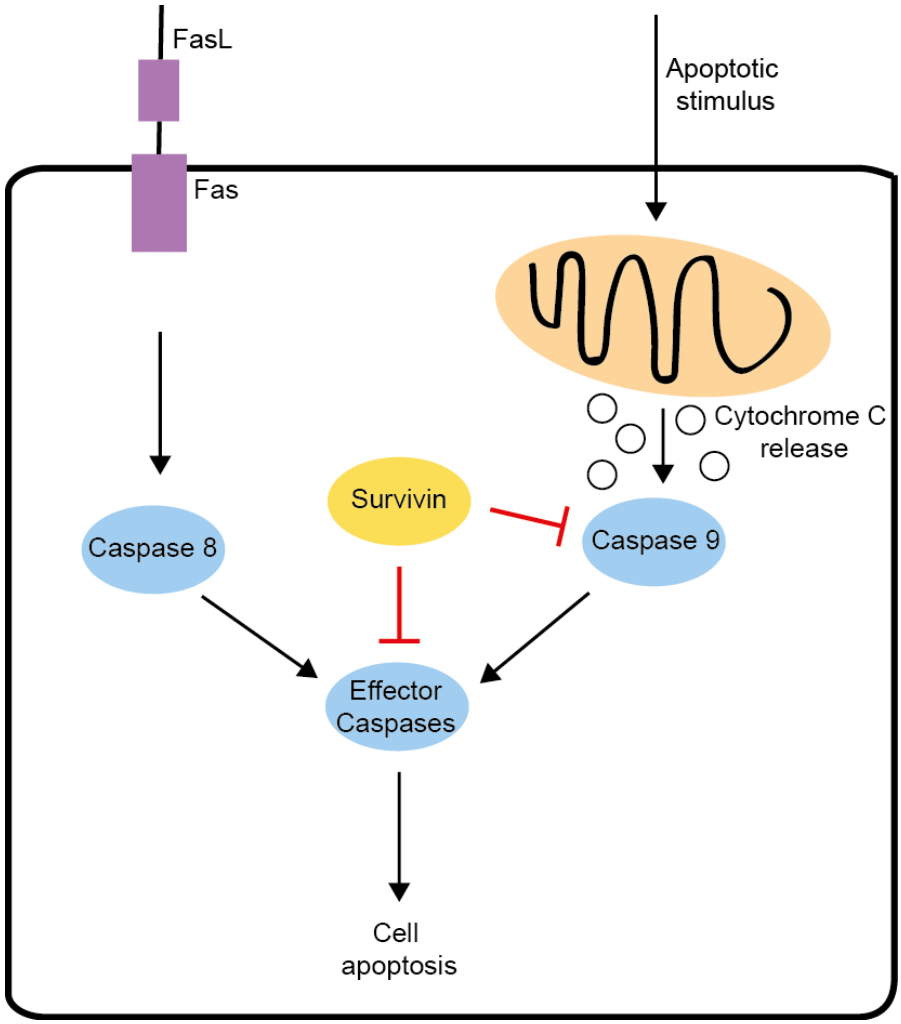

Figure 16 Survivin and apoptosis

Survivin inhibits caspase 9 and effector caspases resulting in the inhibition of both intrinsic (via mitochondria) and extrinsic apoptosis (via death receptor). Adapted from (Chen et al. 2016).

Research has also suggested survivin may enhance levels of telomerase, which is responsible for the maintenance of the telomeres, preventing DNA damage and cell death (Endoh et al. 2005). The paper suggests survivin enhances the transcription of human telomerase reverse transcriptase (hTERT) leading to enhanced telomerase activity (Endoh et al. 2005). The emerging roles of survivin support a key role for this protein in tumourigenesis and indicate treatment strategies which lower levels of this protein could be successful.

8.2 Survivin transcripts

The *BIRC5* gene is composed of six exons and is transcribed into at least six different transcripts. The wildtype transcript is 142 aa and this translates into a 16 kDa protein and has been widely studied. Alternatively spliced variants include survivin 2B (18 kDa), survivin ΔEx3 (15 kDa), survivin 2α (8 kDa), survivin 3α (7 kDa) and survivin 3B (13 kDa) (Necochea-Campion et al. 2013). The resulting proteins arising from the different isoforms all share the same N-terminus (preserving the region known to interact with the apoptotic pathway) but differ in the C-terminus (Necochea-Campion et al. 2013). The alternative splice variants survivin 2B and survivin ΔEx3 were discovered earlier and therefore have been investigated more frequently than the other variants (Necochea-Campion et al. 2013).

8.3 Survivin expression

Survivin localises to the cytosol, mitochondria, nucleus and the mitotic apparatus (Altieri 2008). Normally survivin is highly expressed in embryonic and fetal organs, whilst in adult normal cells it is mostly undetectable. The following adult normal cells do express survivin; thymocytes, CD34+ bone marrow derived stem cells and basal colonic epithelial cells (Altieri 2008). The regulation of survivin expression is controlled by a wide range of pathways including; microRNA, RTK, PI3K/AKT, MEK/MAPK, NF-kB, mTOR, STAT3, p53, Wnt, hypoxia, TGF and Notch (Chen et al. 2016).

8.4 Survivin and cancer

In contrast to the majority of adult normal tissues survivin expression is high in tumourigenesis and this has been shown in the following cancers; colorectal, lung, breast, oesophagus, stomach, pancreas, liver, uterus, ovaries, leukemia, lymphoma, neuroblastoma, phaechromocytoma, sarcomas, gliomas and melanoma (Kaneko et al.

2007; Altieri 2003). Survivin overexpression is believed to be caused by transcriptional deregulation and would confer cells with a growth and survival advantage. Many deregulated pathways in cancer are involved in the transcriptional regulation of survivin and these pathways could be responsible for the overexpression of survivin in cancer. For example *TP53* mutations are common in cancers and only wildtype p53 can negatively regulate survivin expression (Chen et al. 2016). Research has shown patients with tumours expressing survivin is linked to poor survival, higher risk of recurrence and resistance to treatments (Altieri 2003). Therefore targeting survivin is a potential therapeutic strategy being investigated (Chen et al. 2016).

8.5 Survivin in normal colon cells and colorectal cancer

In CRC it is hypothesised that levels of survivin are high because it is a Wnt target gene and the majority of CRC display hyperactivation of the Wnt signalling pathway (Altieri 2003). Other pathways could equally be responsible but the Wnt pathway is likely to play a large role in CRC. Several papers have linked high survivin expression to poor prognosis in CRC (Kawasaki et al. 1998; Sarela et al. 2000). There is some controversy over survivin levels in normal colon cells. Kawasaki et al. (1998) reported survivin is not expressed in normal cells. Sarela et al. (2000) suggested expression is lower than in tumourigenic cells. Gianani et al. (2001) found survivin expression was restricted to the crypt. The differences reported from these studies could be down to the technique used to detect survivin expression and the methodology. Many studies indicate survivin is expressed in basal colonic epithelial cells and it has been suggested that APC and survivin are important regulators of colon homeostasis, Zhang et al. (2001) showed survivin levels are highest at the lower crypt, protecting the stem cells which are essential for the colon renewal process. APC is thought to negatively regulate survivin levels at the crypt through the Wnt signalling pathway. APC expression is highest at the top of the crypt. Therefore when APC is mutated survivin expression is no longer regulated resulting in constitutive expression, promoting cell survival and growth (Zhang et al. 2001). This highlights the importance in CRC between APC, Wnt signalling and survivin.

9 Rho protein family

9.1 Roles and regulation

The Rho family is part of the Ras superfamily of small GTPases and consists of at least 20 proteins in eight subgroups (Wennerberg & Der 2004; Hodge & Ridley 2016). The majority of our understanding of this family comes from the study of classical members; ras homolog gene family member A (RhoA), Rac1 and Cdc42 (Roberts et al. 2008). Rho proteins have roles in regulating cytoskeletal rearrangements, cell motility, cell polarity, axon guidance, vesicle trafficking and the cell cycle (Hodge & Ridley 2016). As GTPases Rho proteins alternate between an inactive (GDP bound) and active (GTP bound) state and this process is regulated by GEF, GAP and guanine nucleotide dissociation inhibitors (GDI). GEF exchange GDP for GTP therefore converting Rho proteins into the active state. GAP increase the rate of GTP hydrolysis, resulting in the inactivation of Rho proteins. GDI bind prenylated inactive Rho proteins (bound GDP), inhibit the dissociation of GDP and inhibit GTP hydrolysis, therefore preventing the activation of Rho protein effectors (Figure 17) (DerMardirossian & Bokoch 2005). GDI play a role in the cycling of Rho proteins between the cytosol and membranes. The isoprenoid added by prenylation hide in a pocket on the GDI, therefore the GDI must be displaced to allow the Rho protein to associate with the membrane and activate downstream effectors. To end the signal propagation GDI rebind to Rho proteins causing dissociation from the membrane (DerMardirossian & Bokoch 2005).

Spatiotemporal regulation is very important for GTPases to ensure the correct downstream signalling pathways are activated. The pathway activated depends on the stimulus and cell type (Hodge & Ridley 2016). Multiple post translational modifications play an important role in this regulation. Lipid modifications including prenylation (see section 7.2.1) and s-palmitoylation make the proteins more hydrophobic, helping to determine localisation to specific membrane compartments. A factor independent of lipid modifications which also controls localisation is the presence of polybasic residues near the C-terminus. Additionally, if phosphorylation occurs near the lipid modification then this can also influence the localisation. Phosphorylation also regulates the activity of Rho proteins, if the phosphorylation occurs within the GTPase domain then this either affects the cycling between GTP and GDP or the interaction with downstream effectors. Ubiquitination and sumoylation regulates the turnover of Rho proteins (Hodge & Ridley 2016). All these post translational modifications play an important role in regulating the proper activation of Rho proteins and initiating the appropriate downstream signalling pathways.

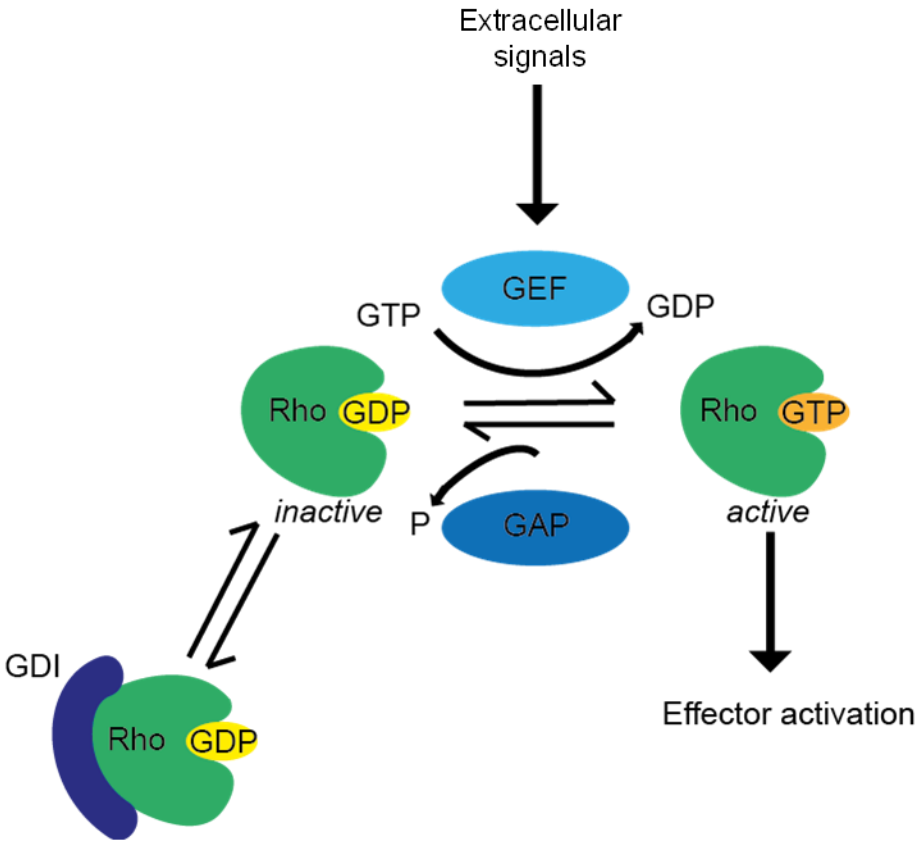

Figure 17 The Rho family are GTPases

The main proteins involved in altering the cycling of Rho proteins between inactive and active state.

9.2 Localisation of Rho proteins

Rho proteins can be found in many cellular compartments including; cytosol, endoplasmic reticulum (ER), plasma membrane, golgi, endosomes, nuclear envelope, endomembranes, mitochondria and vesicles (Roberts et al. 2008). Each Rho protein localises differently, for example Rac1 is localised to the plasma membrane and cytosol, in comparison Cdc42 is localised to the plasma membrane, golgi, ER and nuclear envelope (Roberts et al. 2008). The localisation to specific compartments is essential to the downstream functions of each Rho protein and is influenced by different factors. Currently the factors are not completely understood for all Rho proteins. For localisation to membranes prenylation is the first and essential step, it provides proteins with a hydrophobic C-terminal, enabling the protein to associate with membranes (Seabra 1998; Wang & Casey 2016). Mutation of the -CAAX in Rac1 (site required for prenylation), results in reduced activation of the Rac1 effector p21 activated kinase 1 (Pak1), due to Rac1 mislocalisation (del Pozo et al. 2000).

Prenylated proteins have a high affinity to the ER, Rho proteins localising to the ER do not require further modification eg Cdc42 (Michaelson et al. 2005). Further modification after prenylation involves the cleavage of -AAX amino acids by the endoprotease Ras-converting enzyme 1 (Rce1), this enables the addition of a methyl group to the prenylated cysteine residue by isoprenylcysteine-O-carboxyl methyltransferase (Icm1) (Roberts et al. 2008). Some Rho proteins will then be further modified by the attachment of palmitate groups on cysteine residues, which promotes localisation to the plasma membrane (Bustelo et al. 2007; Michaelson et al. 2005). There is currently debate whether the steps mediated by Rce1 and Icm1 are essential for membrane localisation for all Rho proteins, this is due to conflicting data on the effects of mutating Rce1 and Icm1 on Rho protein localisation (Michaelson et al. 2005; Roberts et al. 2008). Other factors influencing the localisation of Rho proteins include the presence of additional structural determinants and the activation of upstream signalling (discussed in 9.3.3).

9.3 Rac1

Rac1 is part of the Rac subgroup of the Rho family and plays a role in regulating intracellular adhesion, membrane ruffling, cell migration and proliferation (Jamieson et al. 2015).

9.3.1 Rac1 and tumourigenesis

Evidence suggests Rac1 is commonly overexpressed in tumours and is considered to be a driver of tumourigenesis. The importance of Rac1 in CRC has been shown in various studies. In intestinal stem cells, Rac1 activation has been shown to be upregulated after APC loss and the upregulation of active Rac1 triggers ROS production and NF-kB activation, promoting tumour initiation (Myant et al. 2013). Rac1 may also play a role at later stages of CRC too. The SW620 cell line (lymph node metastasis from a colorectal adenocarcinoma) was altered to overexpress Rac1 or lack Rac1 and these cell lines were orthotopically injected into the cecal wall of athymic nude mice. The overexpression of Rac1 accelerated tumourigenesis whilst the suppression of Rac1 expression inhibited tumour formation (Espina et al. 2008). This research supports a key role for Rac1 in promoting CRC tumourigenesis.

9.3.2 Rac1 and Wnt signalling

The Wnt signalling pathway is particularly important in CRC and Rac1 is proposed to have a role in the canonical Wnt signalling pathway, but the exact mechanism is currently disputed. The first potential mechanism involves active Rac1 activating c-jun n-terminal kinase 2 (JNK2), JNK2 then phosphorylates β-catenin at ser191 and ser605. The phosphorylation of β-catenin at these residues is required for β-catenin to translocate to the nucleus (Wu et al. 2008). The second mechanism also involves Rac1 activating JNK2 and JNK2 phosphorylating β-catenin at the same residues, however the phosphorylation of β-catenin is thought to enhance β-catenin binding to TCF/LEF and not the transport of β-catenin into the nucleus (Jamieson et al. 2015).

9.3.3 Rac1 and localisation

Rac1 is found in the cytosol and at the plasma membrane, the majority of Rac1 is in the cytosol (Das et al. 2015). In addition to prenylation many factors contribute to Rac1 localising at the plasma membrane, Rac1 does not undergo palmitoylation, this modification helps other proteins to localise to the plasma membrane (Roberts et al. 2008). Rac1 does contain a specific polybasic amino acid sequence upstream of the CAAX sequence and this contributes towards Rac1 localisation at the plasma membrane. Mutation of this sequence causes less Rac1 to accumulate at the plasma membrane (Del Pozo et al. 2002). Interestingly, a slight variation in this sequence contributes to Rac2 localising to the endosome (Bustelo et al. 2007). The signalling mechanisms contributing to Rac1 localisation are still under investigation and here are some of the current ideas. Research suggests integrins potentially increase the affinity of membranes to Rac, promoting Rac dissociation from GDI and activation of downstream effectors (Del Pozo et al. 2002). This would enable activation at specific sites, which is essential for Rac processes such as the formation of lamellipodia (Del Pozo et al. 2002). Another suggested mechanism involves GTPase ADP-ribosylation factor 6 (ARF6) (part of the endocytosis pathway) which is thought to play a role in transporting Rac1 from the endosomes to the plasma membrane (Symons 2000; Palamidessi et al. 2008). Additionally, a recent paper suggests phospholipids play a role in localising Rac1 to the plasma membrane (Das et al. 2015). At the moment it is not clear whether these are distinct or overlapping mechanisms enabling Rac1 to localise at the plasma membrane.

Due to the importance of APC in the development of CRC we investigated ways to target APC using the concept of synthetic lethality. We created an *in vitro* model using CRISPR-cas9 to mutate APC, resulting in the following; control cell lines (APC WT) and APC mutant cell lines (APC Lys736fs). We used this model to perform siRNA and compound screens to identify synthetic lethal relationships with mutated APC. We investigated a potential synthetic lethal relationship between APC and the mTOR pathway in our *in vitro* model. Our research focused on investigating the synthetic lethal relationship between statins and mutant APC in our *in vitro* model. Statins have been shown to have an impact on Rho proteins (including Rac1) and Rac1 plays a key role in CRC, therefore we focused on analysing if Rac1 was involved in the mechanism. We also analysed the involvement of the anti-apoptotic protein survivin in the mechanism. This enabled us to suggest a potential mechanism explaining the synthetic lethal relationship we see between the APC mutation and statins.

Aims

The tumour suppressor gene *Adenomatous polyposis coli* (*APC)* is commonly mutated in over 80 % of patients with colorectal cancer (CRC) (Fearon 2011). Designing therapies against the loss of APC has the potential to treat a large number of patients. The development of targeted therapies against EGFR, VEGF and PD-1 has resulted in new options for CRC (Chee & Sinicrope 2010; Marginean & Melosky 2018). Our aim was to uncover new therapeutic strategies specific for CRC patients with *APC* mutations by using the concept of synthetic lethality. This strategy is ideal for tumour suppressor genes because you can indirectly target APC by targeting another gene, resulting in cell death specific to the cells with the *APC* mutation (Figure 18).

1) Create an *in vitro* model of APC mutation in a wildtype APC CRC cell line

2) Identify synthetic lethal interactions with the APC mutation using an siRNA kinome screen and FDA-approved compound screen

3) Investigate the mechanism of synthetic lethality identified from the screens

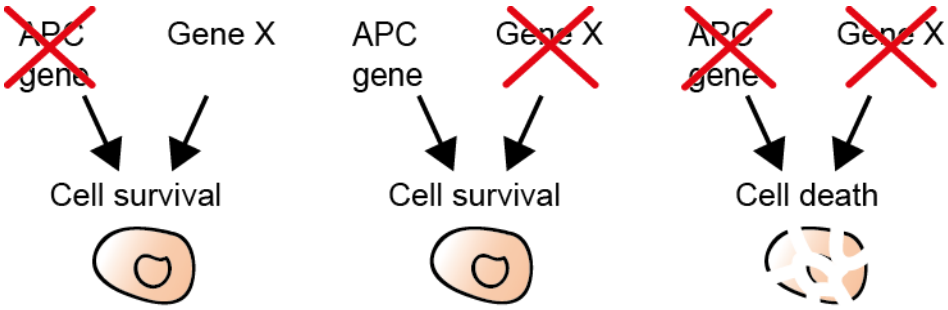

Figure 18 The synthetic lethality approach

Materials and Methods

1 Cell culture

1.1 Cell lines and reagents

The human colorectal cancer cell lines DLD1, HCT116, HT29, RKO, SW48, SW620 were obtained from ATCC and the human embryonic kidney cell line HEK293T was a kind gift from the Sharp lab, Barts Cancer Institute (BCI). HCT116, HEK293T, HT29, RKO, SW48 and SW620 were all grown in Dulbecco's Modified Eagles medium (DMEM) supplemented with heat inactivated fetal bovine serum (FBS) (10 % v/v) and penicillin-streptomycin (1 % v/v). DLD1 were grown in Roswell Park Memorial Institute (RPMI) supplemented with FBS (10 % v/v) and penicillin-streptomycin (1 % v/v). FBS was from Gibco and the following reagents were purchased from Sigma; DMEM, trypsin-EDTA, penicillin-streptomycin.

1.2 Growing and seeding conditions

All cells were routinely grown in T75 flasks and maintained at 37 °C, 5 % CO_2. Stocks were kept frozen in FBS supplemented with 10 % dimethyl sulfoxide (DMSO) in -80 °C and liquid nitrogen. Depending on the cell line, cells were passaged every 2-4 days when 70-90 % confluent and grown for 10 passages. Cells were routinely visually checked, tested for mycoplasma and STR profiled. To passage the cells the media was removed and the cells were washed with 1x phosphate buffered saline (PBS), then 3 mLs 1x trypsin was added to the flasks and incubated for 5 mins at 37 °C or until cells detached. Next the 1x trypsin was neutralised with 7 mLs media and spun down at 1200 rpm for 3 mins to pellet the cells. Finally the media was removed and the cells resuspended in fresh media and a proportion of the cells were transferred to a new flask depending on the experiments planned.

To seed cells the same protocol was followed as described for passaging, up until fresh media was added. Next after seeding a new flask the cells were counted, for this 10 µL cell suspension was added to the dual chamber cell counter slides (Bio-rad)/countess cell counting chamber slides (Invitrogen) and counted using the TC20 cell counter (Bio-rad)/Countess II automated cell counter (Life technologies). Next depending on the size and setup of the experiment the appropriate number of cells were added to media and plated.

1.3 Proliferation assay

Cells were plated at a density of 1000 cells/well in five 96 well plates and labelled day 0, day 1, day 2, day 3 and day 4. Cell viability was measured using CellTiter-glo (CTG) and the luminescence setting on the Perkin Elmer 1420 multilabel counter victor 3 plate reader (Section 7). The day 0 plate was read six hours after plating to account for differences in the starting number. Subsequent plates were read every 24 hours. The fold difference was calculated by dividing every value by the average day 0 value for the cell line. The fold difference was plotted on a graph. The doubling time was then calculated, using just the time period representing linear growth. For example we saw this between day 2 and day 4. We then used the fold change values to calculate doubling time (T_d) (Uzbekov 2004).

$$T_d = t / \log_2 (N_1/N_0)$$

t=time between two time points, N_0 = cell number at start, N_1 = cell number at end

2 CRISPR-cas9

2.1 Designing the gRNA

To design APC targeted gRNA, we used the gRNA design tool from DNA2.0 (now renamed to Atum), see table 1 for the sequences and target locations.

https://www.atum.bio/eCommerce/cas9/input

Name	gRNA sequence	Exon targeted
gRNA APC #2	TTGGCATCCTTGTACTTCGC	15
gRNA APC #3	GCATGTTAGTTTTACACCGG	15
gRNA APC #4	AGCATGTTAGTTTTACACCG	15
gRNA APC #5	TTTTATGGGCTAGGTCGGCT	15
gRNA APC #6	CCTATTATCATCATGTCGAT	15
gRNA APC #8	GATTTATTAGAGCGTCTTAA	2
gRNA APC #9	GATGAAGCTATGGCTTCTTC	2

Table 1 The gRNA used to target APC

2.2 Dharmacon Edit-R approach

We ordered custom Edit-R crRNA from Dharmacon, see table 1 for sequences. On day 1 60,000 cells/well were plated into a 24 well plate. On day 2 cells were transfected with Edit-R cas9 expression plasmid with puromycin resistance, Edit-R synthetic tracrRNA and Edit-R crRNA targeting APC, using DharmaFECT Duo transfection reagent (Dharmacon). Per well we added 3 µL DharmaconDuo reagent, 10 µL cas9 plasmid, 2.5 µL tracrRNA, 2.5 µL crRNA (either one or combination of two) and made the volume up to 100 µL with optimen. We had two controls; 1) received the cas9 plasmid containing puromycin resistance without crRNA, 2) received the cas9 plasmid containing mKate2 (instead of puromycin resistance). After 20 mins incubation the transfection mixes were added to the cells. After 24 hours we checked for mKate2 expression using the fluorescence microscope to check transfection efficiency. On day 4 0.5 µg/mL puromycin was added to the cells and cells were removed from selection on day 8. Single colony selection was started as described in section 2.4.

2.3 Lentivirus approach

2.3.1 Site directed mutagenesis

The lentiCRISPRv2 plasmid encoding cas9 and the gRNA were a kind gift from the Sharp lab (BCI) and were developed by F.Zhang (Sanjana et al. 2014). We designed primers (Table 2) to alter the gRNA sequence in the lentiCRISPRv2 plasmid using the Q5 site directed mutagenesis kit (New England Biolabs) with some modifications. Per reaction, 12.5 µL of 2x phusion hot start master mix, 1.25 µL 10 µM forward and reverse primers, 1 µL of 10 ng template DNA, 0.7 µL DMSO and 8.3 µL water. Samples then underwent the following thermocycling conditions; 98 °C for 30 sec, 25 cycles of 98 °C 10 sec, 61 °C for 20 sec, 72 °C for 3 mins, after the 25 cycles 72 °C for 5 mins.

The next step was the kinase, ligase and dpn1 (KLD) reaction involving 1 µL PCR product, 1x KLD reaction buffer, 1x KLD enzyme mix and water up to 10 µL, this reaction was left to incubate for 5 mins at room temp. The KLD product was then transformed into *E.coli* competent cells (NEB C2987), 2.5 µL KLD product was added to 25 µL competent cells and incubated on ice for 30 mins. Next the cells were heatshocked for 30 sec at 42 °C, then incubated on ice for 2 mins. Then 500 µL SOC media was added and cells were left at 37 °C for 1 hour, then 150 µL was spread onto an agar plate and incubated overnight at 37 °C. Colonies were picked and grown up for DNA extraction in LB broth using the Qiagen DNA mini prep kit (see section 5.1). After

extraction DNA was sequenced to check whether the site directed mutagenesis had been successful.

We sent 1 µg of DNA in 10 µL water and 3.2 pmol/µL primers to Source Bioscience for sanger sequencing. LentiCRISPRv2 hU6-F was used to check whether the site directed mutagenesis of the gRNA site had been successful (see table 2 for sequence).

Name	Primers (5'-3')
gRNA APC #2 F	TGTACTTCGCGTTTTAGAGCTAGAAATAGCAAG
gRNA APC #2 R	AGGATGCCAACGGTGTTTCGTCCTTTCC
gRNA APC #3 F	TTTACACCGGGTTTTAGAGCTAGAAATAGCAAG
gRNA APC #3 R	ACTAACATGCCGGTGTTTCGTCCTTTCC
gRNA APC #4 F	TTTTACACCGGTTTTAGAGCTAGAAATAGCAAG
gRNA APC #4 R	CTAACATGCTCGGTGTTTCGTCCTTTCC
gRNA APC #5 F	TAGGTCGGCTGTTTTAGAGCTAGAAATAGCAAG
gRNA APC #5 R	GCCCATAAAACGGTGTTTCGTCCTTTCC
gRNA APC #6 F	TCATGTCGATGTTTTAGAGCTAGAAATAGCAAG
gRNA APC #6 R	TGATAATAGGCGGTGTTTCGTCCTTTCC
LentiCRISPRv2 hU6-F	GAGGGCCTATTTCCCATGATT

Table 2 Primers used in the lentiviral CRISPR-cas9 approach

2.3.2 Virus production

The plasmids required were a kind gift from the Sharp lab (BCI) and were developed by L.Naldini (Naldini et al. 1996). The lentiCRISPRv2 plasmids designed to target APC were each individually packaged into lentivirus before infecting RKO cells. On day 1, HEK293T cells were plated in 6 well plates. On day 2 fugene (Promega) was used to transfect HEK293T cells with 1.5 µg lentiCRISPRv2 along with 0.6 µg pCMV (packaging) and 1.1 µg pMDG2 (envelope). On day 4 the lentivirus containing media from the HEK293T cells was removed and filtered and added to the RKO cell line plated in a 6 well plate. Positive cells were then selected for, using 0.5 µg/mL puromycin for 10 days. After puromycin selection, cells were single colony selected as described in section 2.4.

2.4 Single colony selection

After puromycin selection, single colony selection was started and we used two different approaches. Method one involved plating 200 cells in a 15 cm dish and leaving for 14 days. Then individual colonies were picked using filter paper soaked in trypsin and transferred to a 96 well plate. The next day the filter paper was removed

and the colonies were expanded. Method two involved seeding 0.8 cells per well in a 96 well plate, then identifying which wells contained a single cell and expanding these colonies.

2.5 Topocloning

Firstly we extracted DNA from cell pellets, see section 5.2. Next we amplified the region around the target site gRNA #2 using the primers gRNA 2F and gRNA 2R (Table 3 shows the primer sequences). We amplified 250 ng of DNA, per reaction we added 10 µL 5x PCR buffer, 1 µL 10 mM dNTP, 1 µL of both forward and reverse primers at 10 µM, 0.25 µL One Taq hot start DNA polymerase and water up to 50 µL. The thermocycling reaction was as follows; 94 °C for 30 sec, 30 cycles of 94 °C 20 sec, 59 °C 30 sec, 68 °C 60 sec then 68 °C for 20-30 mins. After amplification we ran the PCR products on a 1 % TBE agarose gel to check for a single band of the correct size as described in section 5.3.

Next we used the pcDNA4/HisMax TOPO TA Expression kit (Thermofisher). To perform the topocloning reaction we used 4 µL of the PCR product from the amplification and combined it with 1 µL salt solution and 1 µL TOPO vector and left this to incubate for 5-20 mins at room temperature. After the incubation the reaction was then stored on ice. Next 2 µL of the topocloning reaction was transformed into 25 µL chemically competent *E.coli* and incubated on ice for 30 mins. After the incubation the cells were heat shocked for 30 sec at 42 °C, then 250 µL SOC medium was added. Then the cells were left to shake at 37 °C for an hour and spread on agar plates to grow overnight. The next day clones were then picked to grow overnight in 4 mL LB with amplicillin at 100 µg/mL, DNA was extracted as in section 5.1 using the DNA mini kit. Samples were sent for sequencing with GATC, the DNA at 50 ng/µL and 10 µM Xpress™ forward primer (Table 3 for primer sequence).

Primer	Sequence 5'-3'
Xpress™ forward	TATGGCTAGCATGACTGGT
gRNA 2F	CCCCCTGCAAATGTTTTAAGCTA
gRNA 2R	GGAGATCTGCAAACCTCGCT

Table 3 Primers used in topocloning to sequence the alterations to the APC gene

3 Protein expression analysis

3.1 Extraction

All steps were performed on ice. Firstly cells were washed with PBS twice and then lysed with 100-200 µL NP-40 buffer (20 mM tris (pH 8.0), 200 mM NaCl, 0.5 % NP-40, 10 % glycerol, 1 mM EDTA) with protease inhibitor (Roche) and incubated for 10 mins. Cells lysed from plates were scraped and transferred to tubes and incubated for a further 15 mins. After incubation the lysates were centrifuged for 20 mins at 4 °C for 12,000 rpm. The supernatent was transferred to a new tube and stored at -80 °C. The protein concentration was measured using the bradford reagent along with bovine serum albumin (BSA) to create a standard curve (both Sigma).

3.2 Western blotting

For western blotting, 10-90 µg of lysate was combined with 10 % dithiothreitol (DTT) and 4x NuPage LDS samples buffer (Invitrogen) to a maximum final volume of 37 µL. After preparation lysates were denatured by incubation for 5 mins at 95 °C and electrophorised on Novex precast gels (Invitrogen) 3-8 % tris acetate, 4-12 % tris glycine or 10% bis tris using either 20x NuPAGE tris acetate SDS running buffer, 20x NuPAGE MOPS SDS running buffer or 20x NuPAGE MES SDS running buffer respectively. The gels were run for 1 hour 30 mins to 2 hours at 120 V, the protein was then transferred onto nitrocellulose membrane (Thermoscientific) using a wet transfer system for 2 hours at 25 V.

The membrane was blocked in 5 % milk/0.1 % tween/1x TBS for an hour and immunoblotted in primary antibody (Table 4), typically in 5 % milk/0.1 % tween/1x TBS overnight at 4 °C. Next the membranes were washed three times for 5-10 mins in 0.1 % tween/1x TBS. After washing, the membranes were incubated in either anti-rabbit or anti-mouse secondary anti-IgG-horseradish peroxidase (Invitrogen/Dako), for one hour at room temperature. After incubation in secondary antibody the membranes were washed as before and chemiluminescence was added to allow detection of the protein of interest (SuperSignal West Pico Chemiluminescent Substrate, Pierce). Immunoblotting for β-actin or β-tubulin was used as a loading control. The signal was developed either onto x-ray films or using the Amersham Imager 600.

For quantification of western blots we used the image analysis software ImageQuant TL 8.1 (GE healthcare). The intensity of the band was measured by drawing a box around the first band, this same box was copied and placed around the remaining

bands on the blot. Background was subtracted by drawing a box above or below every band to account for differences in background across the blot. The software subtracts the background then calculates the percentage density for each band highlighted on the blot relative to one another.

Antibody name	Company and code	Standard dilution
APC ALi 12-28	Abcam ab58	1:1000
APC 2504	Cell signaling 2504	1:250
APC C28.9	Santa Cruz sc-53166	1:250 - 1:500
β-actin-HRP	Cell signaling 5125	1:1000 - 1:20,000
β-catenin unphosphorylated ser33/ser37/thr41	Cell signaling 4270	1:5000
β-catenin total	Abcam ab32572	1:10,000
HMGCR	Abcam ab174830	1:1000
mTOR phosphorylated ser2448	Cell signaling 2971	1:1000
mTOR total	Cell signaling 2972	1:1000
Pak1 phosphorylated ser144	Cell signaling 2606	1:1000
Pak1 total	Cell signaling 2602	1:1000
Rac1 total	From Rac1 pull down kit (Thermoscientific #16118)	1:1000
Rho total	From Rho pull down kit (Thermoscientific #16116)	1:650
SMAD4	Cell signaling 9515	1:1000
Survivin	Abcam ab76424	1:1000
β-tubulin	Sigma T8328	1:10,000 - 1:20,000
Secondary mouse	Invitrogen 62-6520	1:5000
Secondary mouse	Dako P0260	1:5000
Secondary rabbit	Invitrogen 62-6120	1:5000
Secondary rabbit	Dako P0448	1:5000

Table 4 Antibodies used for western blotting

4 RNA expression analysis

4.1 Extraction

The Qiagen RNeasy mini kit was used to extract RNA from either pelleted cells or cells grown as a monolayer in a 6 well plate. After trypsinisation, $2x10^6$ cells were pelleted at 300 g for 5 mins and the media was removed leaving the pellet. Next lysis buffer RLT was added to the cell pellet and mixed by pipetting up and down to homogenise the sample. Alternatively cells were grown as a monolayer on a 6 well plate, next the media was removed and lysis buffer RLT was added. After addition of buffer RLT the cells were scrapped and the resulting mixture was transferred to a 1.5 mL tube. After lysis with RLT buffer, 70 % ethanol was added to the sample and the sample was

transferred to an RNeasy spin column. The column was then spun for 15 sec at 8000 g and the flow through discarded. Next the wash buffer RW1 was added, the column spun and the flow through discarded. The wash steps were repeated twice with the wash buffer RPE, initially 15 sec spin at 8000 g followed by a second wash for 2 mins at 8000 g. After washing, the spin column was placed in a new collection tube and centrifuged for 1 min without any buffer. Finally the RNA was eluted by adding RNase free water to the centre of the column and then centrifugated for 1 min at 8000 g. The RNA concentration and purity was measured using a nanodrop (ND-1000/ND-2000 Thermofisher).

4.2 RT-PCR

Firstly cDNA was generated using the Qiagen Omniscript reverse transcription kit. Water was added to 1 µg RNA to bring the volume up to 12 µL, next 8 µL mastermix was added which contained a final concentration of 1x RT buffer, 0.5 mM each dNTP, 1 µM Oligo-dt primer, 10 units of RNase inhibitor, 4 units of omniscript reverse transcriptase. Tubes were then incubated at 37 °C for 60 mins to generate cDNA.

For RT-PCR the ddCT method was used, for each sample we ran reactions containing taqman probes for housekeeping genes (GAPDH Vic-Tamra probe #4310884E, Applied Biosystems or β-actin Vic-Tamra probe #4310881E) and probes for the gene of interest (APC FAM-MGB probe hs01568269.m1, Applied Biosystems #4331182) in triplicate. We made a mastermix per probe containing; 10 µL TaqMan universal PCR master mix (Applied Biosystems #4304437), 8 µL H_2O and 1 µL probe. To each well 19 µL mastermix was added to the MicroAmp optical 96 well PCR plate (Applied Biosystems #N8010560). Next we added 1 µL of the appropriate cDNA to the PCR plate and added water to the no template control (NTC). The RT-PCR was run using the 7500 real time PCR system (Applied Biosystems)/Quantstudio5 real time PCR system (Thermofisher). To calculate the ddCT firstly the means were calculated for each cDNA reaction with either housekeeping or the probe of interest. Then the mean ct of the housekeeping is subtracted from the mean ct of probe of interest and this gives you the dCT. To calculate the ddCT you subtract the dCT of the cDNA you wish to normalise to. Finally the 2^(ddCT) is calculated and this is the value plotted on the graphs.

5 DNA extraction and analysis

5.1 Extraction from bacteria

Extracting small amounts of DNA using the DNA mini prep kit (Qiagen) involved picking bacterial colonies to grow overnight in 5 mL of lysogeny broth (LB) (with antibiotic) and incubated overnight at 37 °C. The bacterial cells were then harvested by centrifugation at 8000 rpm for 3 mins. The supernatant was removed and 250 µL resuspension buffer P1 was added to the bacterial cell pellet. Next 250 µL lysis buffer P2 was added and the tube was inverted six times. Next 350 µL neutralisation buffer N3 was added and the tube was inverted six times. The tube was then centrifuged for 10 mins at 13,000 rpm, the supernatant was kept and then transferred to a QIAprep spin column. The column was centrifuged for 1 min and the flow through was discarded. Next 500 µL wash buffer PB was added and centrifuged for 1 min. After centrifugation the flow through was discarded and 750 µL wash buffer PE was added and the column was centrifuged for 1 min. The final flow through was discarded and the column was spun again for 1 min. Finally the DNA was eluted with water by adding water to the column and spinning the column to elute the DNA from the membrane. DNA concentration and purity was measured using a nanodrop (ND-1000/ND-2000 Thermofisher).

5.2 Extraction from cell pellet

DNA was extracted from a cell pellet using the DNeasy blood and tissue kit (Qiagen). Firstly $2x10^6$ - $4x10^6$ cells were pelleted by centrifugation for 5 mins at 300 g. The media was removed and the pellet was resuspended in 200 µL PBS, then 20 µL proteinase K and 200 µL lysis buffer AL was added, vortexed and the mixture was incubated at 56 °C for 10 mins. After the incubation 200 µL 100 % ethanol was added and the sample was vortexed thoroughly and added to a DNeasy mini spin column, then centrifuged at 6000 g for 1 min. The flow through was discarded and the spin column was placed in a new collection tube. Next 500 µL wash buffer AW1 was added, the column spun as before, flow through discarded and then placed in a new collection tube. Next 500 µL wash buffer AW2 was added and the column was centrifuged for 3 mins at 20,000 g to dry the membrane in the column. The DNeasy spin column was then placed in a new 1.5 mL tube and 200 µL elution buffer AE was added, incubated for 1 min before centrifugation for 1 min at 6,000 g to elute the DNA. DNA concentration and purity was measured using a nanodrop (ND-1000/ND-2000 Thermofisher).

5.3 Agarose gels

Agarose gels (1%) were made by melting agarose in 1x TBE in a microwave, once fully dissolved and cooled to hand touch, the agarose was poured into a mould and a comb was added. Once set the gel was placed in the agarose gel apparatus and topped up with 1x TBE. To the first well 1 µL Thermo Scientific GeneRuler 1 kb plus DNA ladder (SM1333) was added and the remaining wells contained 1 µL sample mixed with 2 µL 2 x loading dye (diluted from Biolabs gel loading dye purple 6x (B7024S)). The gel was run at 100 W for 1 hour and visualised with the G Box.

6 TCF/LEF Reporter Assay

For this assay reporter constructs were obtained from the Cignal TCF/LEF reporter assay kit; positive, negative and reporter (Qiagen). The luciferase signal was read using the dual luciferase reporter assay (Promega).

6.1 Reporter constructs transfection

We transfected 1 µL reporter constructs per well using either lipofectamine 2000 (Invitrogen) or fugene. When lipofectamine 2000 was used the standard siRNA protocol was followed (Section 9.2). If fugene was used we made a mastermix of optimen, reporter construct and fugene, per well this contained 24.75 µL optimen, 1 uL reporter construct and 0.25 µL fugene. The mastermix was incubated for 10-15 mins and then 25 µL was added to a well containing 75 µL of media. On day 5 the plates were read using the dual luciferase reporter assay (Section 6.4).

6.2 siRNA and reporter constructs transfection

To transfect both siRNA and the reporter constructs into the cells, two methods were used. Method one involved plating cells on day 1 in a 96 well plate and on day 2 cells were transfected using the standard siRNA protocol (Section 9.2) with both 2.5 µL 2 µM siRNA and 1 µL reporter constructs. The assay was read on day 5 using the dual luciferase reporter assay (Section 6.4).

Method two involved plating cells on day 1 in a 96 well plate then the siRNA was transfected on day 2 (Section 9.2) and reporter constructs on day 3 using fugene (Section 6.1 describes fugene protocol). The plates were read on day 6 using the dual luciferase reporter assay (Section 6.4).

6.3 Reporter constructs transfection and compound treatment

To transfect the constructs and follow with compound treatment, the cells were plated on day 1, then 1 µL reporter constructs were transfected with fugene on day 2 (Section 6.1 describes fugene protocol). The cells were then drugged on day 3 and the plates were read on day 6 using the dual luciferase reporter assay.

6.4 Dual luciferase reporter assay

Media was removed from cell culture plates and the plates were firstly washed with PBS, next 20-30 µL of 1x passive lysis buffer (PLB) was added to each well. Then the plates were shaken for 15 mins at room temperature. After the incubation the cell lysates was transferred to a white bottom plate and 100 µL luciferase assay reagent II (LARII) substrate was added to the wells and the luminescence read immediately on the plate reader. After the first measurement 100 µL stop and glow reagent was added to the same wells and the luminescence was read again. To analyse the LARII values were divided by the stop and glow values, then values were normalised to the control condition negative control. When different cell lines were run in the same assay the data was first normalised to the cell lines average positive control before normalising to the average control cell line negative control.

7 CellTitre-glo luminescent cell viability assay

The CTG was diluted 1:4 with PBS, then the cell culture media in the 96 well plate was removed and 100 µL diluted CTG was added to each well. The plate was shaken for 2 mins at a low speed, then left at room temperature covered from the light for 10 mins. After incubation the plate was read on the plate reader using the luminescence setting.

8 High through-put screens

8.1 siRNA kinase screen

8.1.1 Initial screen

The Dharmacon human siGENOME siRNA protein kinase library targets protein kinases and kinase-related genes and was used at a concentration of 50 nM. The library was aliquoted over 9 x 96 well plates, each plate contained 5 µL of 2 µM siRNA and this was enough to transfect two cell line culture plates. The first and last column were left empty to add four wells per control; media alone (no transfection mix), mock (water with transfection mix), non-targeting control siRNA (siCON) and polo like kinase 1 (PLK1) targeting siRNA (siPLK1).

On day 1 1000-2000 cells were plated per well in a 96 well plate. On day 2 50 µL transfection mix was added to the kinome library after a 5 minute incubation containing 49.5 µL optimen and 0.5 µL lipofectamine RNAimax transfection reagent (Invitrogen) per well. The plates were then incubated for 20 mins, after the incubation 160 µL media was added to each kinome plate. The media was then removed from two cell culture plates and 100 µL transfection mix/media was added from the kinome plate to each cell culture plate. After 4-5 hours the media was changed and plates were read using CTG on day 5 or 6 depending on the cell confluency (Section 7).

To analyse the screen data the luminescence readings from each well were firstly log transformed, then normalised to the median signal on each plate. The data was then standardised to Z scores using the medium absolute deviation (MAD), this assumes a normal distribution of cell viability.

$$\text{Z score} = X - \frac{\text{median (sample)}}{\text{MAD (sample)}} \qquad \text{MAD(sample)} = \text{median}_i\,(|X_i - \text{median}_j\,(X_j)|)$$

Z scores enable us to see the effect of individual siRNA compared to the rest of the screen. We compared two cells lines and used Z scores to calculate the ΔZ score

$$\Delta Z \text{ score} = Z \text{ score (RKO APC}^{mut}) - Z \text{ score (RKO APC}^{wt})$$

Any siRNA responsible for a ΔZ score <-1.5 potentially targets a gene which is synthetically lethal with the APC mutation.

8.1.2 Validation

Seven hit genes were selected for validation from the siRNA kinome screen. A personalised 96 well plate (GE Healthcare) was ordered with the siRNA SMARTpool and four individual siRNA (deconvoluted from the SMARTpool siRNA) for each hit gene (Table 5 shows siRNA details). This library was aliquoted like the original screen into 96 well plates, each plate contained enough for two cell lines (5 µL of 2 µM siRNA). Controls were added; siCON and siPLK1 to access the transfection efficiency. The protocol was the same as the siRNA screen (Section 8.1.1). The only difference was the way the data was analysed, for the validation experiments survival fractions were calculated from the CTG readings by normalising to the average value from the siCON wells.

Name siRNA	Manufacturer	Code
NAGK (Pool)	Dharmacon	M-006750-01
NAGK *1	Dharmacon	D-006750-01
NAGK *3	Dharmacon	D-006750-03
NAGK *4	Dharmacon	D-006750-04
NAGK *7	Dharmacon	D-006750-17
DYRK2 (Pool)	Dharmacon	M-004730-03
DYRK2*1	Dharmacon	D-004730-01
DYRK2*2	Dharmacon	D-004730-02
DYRK2*3	Dharmacon	D-004730-03
DYRK2*5	Dharmacon	D-004730-05
FN3KRP (Pool)	Dharmacon	M-006817-00
FN3KRP*1	Dharmacon	D-006817-01
FN3KRP*2	Dharmacon	D-006817-02
FN3KRP*3	Dharmacon	D-006817-03
FN3KRP*4	Dharmacon	D-006817-04
MAP3K15 (Pool)	Dharmacon	M-004847-02
MAP3K15*	Dharmacon	D-004847-01
MAP3K15	Dharmacon	D-004847-02
MAP3K15	Dharmacon	D-004847-03
MAP3K15	Dharmacon	D-004847-04
N4BP2 (Pool)	Dharmacon	M-019063-01
N4BP2*1	Dharmacon	D-019063-01
N4BP2*2	Dharmacon	D-019063-02
N4BP2*3	Dharmacon	D-019063-03
N4BP2*17	Dharmacon	D-019063-17
SMG1 (Pool)	Dharmacon	M-005033-01
SMG1*1	Dharmacon	D-005033-01
SMG1*2	Dharmacon	D-005033-02
SMG1*3	Dharmacon	D-005033-03
SMG1*4	Dharmacon	D-005033-04
PIM2 (Pool)	Dharmacon	M-005359-00
PIM2*1	Dharmacon	D-005359-01
PIM2*2	Dharmacon	D-005359-02
PIM2*3	Dharmacon	D-005359-03
PIM2*4	Dharmacon	D-005359-04

Table 5 siRNA on the validation plate

8.2 FDA compound screen

8.2.1 Initial screen

The FDA compound library contains 1120 FDA-approved compounds and was purchased from Selleck Chemicals. The library was across 14 x 96 well plates and at a concentration of 10 mM. The final column contained no drugs to enable controls to be added; media only and DMSO (2 µL added per well). The library was diluted to 200 µM before use. On day 1 2000 cells/well were plated in 96 well plates. The next day cells were treated with 10 µM of each drug, 5 µL of the 200 µM stock was added to 95 µL media per well. Cells were re-drugged on day 4 then the cell viability was measured on day 6 using CTG (Section 7).

The analysis followed the same methodology as the siRNA screen, the luminescence readings were log transformed and normalised to the median signal on each plate. The Z score was calculated to standardise the values and indicated drugs which showed a greater loss in cell viability in the RKO APC mutant lines compared to the RKO control cells. Any compounds responsible for a Z score <-1.5 in the RKO APC mutant lines and not the control cells potentially target a gene which is synthetically lethal with APC mutations.

8.2.2 Validation

Promising compounds were selected for validation and are listed alongside other compounds in table 6. On day 1 2000 cells/well were plated, on day 2 doses of each drug from 0.5 µM to 200 µM were added to the cells to enable a drug dose response curve to be made from the data. The plates were drugged again on day 4 and cell viability was measured on day 6 using CTG (Section 7). Next survival fractions were calculated, by normalising the treated cell viability values to the average vehicle (received no drug) cell viability values for each cell line. The survival fractions were plotted, and enabled the drug dose response in each cell line to be compared.

Drug name	Company and code	Stock concentration
Desonide	MedChemexpress LLC B0248	20 mM DMSO
Diclofenac potassium	APExBIO B1929	20 mM DMSO
EHT1864	Sigma E1657	1 mM DMSO
FTI-277	Santa Cruz sc215058	5 mM water
GDP	From Thermoscientific pull down kit	100 mM
GGTI-298	Calbiochem 345883	5 mM DMSO
GTPyS	From Thermoscientific pull down kit	10 mM
Harmine	Santa Cruz sc202644	20 mM DMSO
Losartan potassium	Santa Cruz sc204796	20 mM DMSO
Lovastatin	Sigma PHR1285	20 mM DMSO
Mesalamine	Sigma PHR1060	20 mM DMSO
Mevalonic acid	Sigma 79849	20 mM water
Mevastatin	Sigma M2537	20 mM DMSO
Moxifloxacin HCL	Abmole M3514	20 mM DMSO
3-O-Methyl-N-acetyl-D-glucosamine	Abcam (ab144671)	10 mM DMSO
Rapamycin	Cambridge Bioscience SM83-25	10 mM DMSO
Ridaforolimus	ApexBio B1639	10 mM DMSO
Saxagliptin	Biovision 9528-50	20 mM DMSO
Simvastatin	Sigma S6196	20 mM DMSO
Tizanidine HCL	Santa Cruz SC200148	20 mM water
Tolnaftate	Sigma T6638	20 mM DMSO
Troxipide	APExBIO B1892	20 mM DMSO

Table 6 compounds used

Name	Company	Code
ALLSTAR Negative control (siCON)	Qiagen	1027281
PLK1 (Pool)	Qiagen	GS5347
APC*3	Qiagen	S100000588
APC*6	Qiagen	S102757251
DYRK2*1	Dharmacon	D-004730-01
DYRK2*2	Dharmacon	D-004730-02
NAGK*1	Dharmacon	D-006750-01
NAGK*4	Dharmacon	D-006750-04
N4BP2*2	Dharmacon	D-019063-02
N4BP2 (Pool)	Dharmacon	M-019063-01
FLT3 (Pool)	Dharmacon	M-003137-02
mTOR (Pool)	Dharmacon	M-003008-03
HMGCR (Pool)	Dharmacon	M-009811-02
Survivin/BIRC5 (Pool)	Dharmacon	M-003459-03

Table 7 siRNA used

9 siRNA Transfection

Transfections were performed in reduced serum media, optimen (Gibco) and the following transfection reagents were used; lipofectamine 2000 and lipofectamine RNAimax. Table 7 shows the siRNA used.

9.1 siRNA transfection in a 6 well

Cells were plated on day 1 100,000-200,000 cells/well. On day 2 250 µL optimen and 2.5 µL transfection reagent per well were combined and incubated for 5 mins. After the incubation 2.5 µL 20 µM siRNA stocks per well were added and incubated for a further 20 mins. After 20 mins the media was replaced on the 6 well plate and the transfection mix was added drop by drop to each well. After 4-5 hours the media was changed and lysates or RNA were collected on day 5 (Section 3.1 and 4.1 respectively).

9.2 siRNA transfection in a 96 well

Cells were plated on day 1 (1000–5000 cells/well). On day 2 mixtures of 24.75 µL optimen and 0.25 µL transfection reagent per well were combined and incubated for 5 mins. After the incubation 2.5 µL 2 µM siRNA stocks per well were added and incubated for 20 mins. After 20 mins incubation the media was replaced in the 96 well plate and the transfection mix was added. After 4-5 hours the media was changed. CTG was used to analyse the results on day 5 or day 6 depending on the cell confluence (Section 7). Analysis of CTG values involved calculating the survival fraction by normalising to the average of CTG values of cells transfected with siCON.

10 Cell viability upon compound treatment

10.1 Compounds used

See table 6 for the compounds used.

10.2 Cell viability

To look at differences in responses to the compounds in 9.1 a similar approach was used as discussed in the FDA compound screen validation. Briefly on day 1 2000 cell/well were plated, on day 2 (and some re-drugged on day 4 depending on the drug) up to six different doses for each drug were added to the cells. Cell viability was

typically measured on day 6 using CTG (Section 7), some assays were read after 48 hours of drug treatment and involved fewer drug concentrations. The cell viability data was used to calculate survival fractions by normalising to each cell lines average vehicle cell viability (received no drug). The survival fractions were plotted either as bar charts or as drug dose response curves enabling comparison between cell lines.

11 Active Rac1 and Rho pull down and detection

We used the Thermofisher active Rac1 pull down and detection kit (#16118) and the Thermofisher active Rho pull down and detection kit (#16116). We collected at least 500 µg of lysate using the protocol in section 3.1. We performed the *in vitro* GTPyS and GDP treatment to check the assay was working. For this 500 µg of lysate was diluted to 500 µL, 10 µL of 0.5 M EDTA pH 8.0 was added and the sample was vortexed. Next 5 µL of 10 mM GTPyS or 5 µL 100 mM GDP was added and the sample was vortexed. Both reactions were incubated for 15 mins at 30 °C in a heated tube shaker. To stop the reaction the samples were placed on ice and 32 µL of 1 M $MgCl_2$ was added and the sample was vortexed. These samples were then run through the pull down kit columns as described next, in addition samples to test were also run through these columns.

To carry out the pull down reactions firstly a spin cup was placed into a collection tube. Next the bottle of glutathione resin was swirled and 100 µL of the resin was added to the spin cup in the collection tube. Next the tube was centrifuged at 6000 g for 10-30 secs and the flow through was discarded. Next 400 µL of lysis/binding/wash buffer was added to the tube with the resin, then the tube was inverted several times and then centrifuged at 6000 g for 10-30 secs. The flow through was discarded and the GST fusion protein (20 µg of GST-human Pak1-PBD or 400 µg GST-Rhotekin-RBD) was added to the spin cup. Next 500 µg of protein lysate was added to the spin cup and the lid closed for vortexing. Next the cap of the collection tube was sealed with parafilm and the sample was vortexed again. The mixture was then incubated at 4 °C for 1 hour with gentle rocking. After the incubation the tube was then centrifuged at 6000 g for 10-30 secs. Then the spin cup was transferred to a new collection tube. To wash the resin 400 µL of lysis/binding/wash buffer was added and the tube was inverted 3 times then centrifuged at 6000 g for 10-30 secs. We then removed the buffer and repeated the wash step two more times. After the wash steps the spin cup was then transferred to a new collection tube. Next we prepared the reducing sample buffer by adding DTT to 2x SDS sample buffer to a final concentration of 200 mM. We added 50 µL 2x reducing sample buffer to the resin, vortexed and left to incubate for 2 mins at room

temperature. The tube was then centrifuged at 6000 g for 2 mins, after centrifugation the spin cup containing the resin was removed.

The 2x reducing sample buffer was already added to the pull down samples (controls and samples to test), therefore we added this to the 10 µg of input sample. We followed the same western protocol described in section 3.2, except we used the 2x sample buffer from the pull down kit. For loading the westerns we ran 10 µg of input sample, 10 µL of the control samples (treated with GTPyS or GDP) and 40 µL of the test samples. We used the appropriate primary antibody depending on the kit (total Rac1 or total Rho).

12 Immunofluorescence

On day 1 we plated 40,000-100,000 cells/well on top of 12 mm poly-L-lysine coated coverslips (Corning 354085) in 24 well plates. On day 2 we treated the cells with vehicle or drug for 72 hours. On day 5 cells were permeabilised for 1 min in 0.1 % triton in 1x PBS. After permeabilisation the cells were fixed for 15-25 mins in 3.7 % paraformaldehyde (PFA) and 2 % sucrose in 1x PBS. The cells were then washed in 1x PBS three times and stored in the fridge till ready to stain the coverslips.

Primary antibodies were added (Table 8) in 2 % BSA-1x PBS to the coverslips for 40 mins at 37 °C. After incubation in primary antibody the coverslips were washed on the rocker for 5 mins at low speed three times in 1x PBS. Secondary antibody (Invitrogen) was added 1:1000 in 2 % BSA-1x PBS at 37 °C for 30 mins and kept in the dark (Table 8). After secondary antibody incubation the coverslips were washed 3-4 times in 1x PBS for 5 mins on the rocker. Next the cells were stained with DAPI (1:10,000) for 1 min in 1x PBS. The slides were then washed twice with 1x PBS. The slides were then mounted with 5 µL mowiol (Calbiochem) and left in the fridge overnight before imaging. The coverslips were imaged using the confocal LSM 710 microscope (Zeiss), the 63x oil objective was used and at least 4 images were captured per condition using the same settings (to enable us to count 150-300 cells per condition). ImageJ was used to quantify the images and percentages were calculated comparing to the total number of cells (quantified by DAPI staining).

	Company and code	Standard dilution
Alexa 488	Invitrogen A11001	1:1000
Alexa 568	Invitrogen A11036	1:1000
β-catenin total	Abcam ab32572	1:250
Pan-cadherin	Abcam 6529	1:200
Rac1 total	From Rac1 pull down kit (Thermoscientific #16118)	1:1000

Table 8 Antibodies used for immunofluorescence

13 Data analysis and representation

Prism was used to generate all graphs, if multiple repeats were represented in one graph error bars were plotted as standard error of the mean (SEM). If results from one experiment were shown error bars were plotted as standard deviation (SD). Appropriate statistical tests were performed using prism and indicated on the graphs and figure legends including; t-tests, one way anovas and two way anovas. If statistical tests showed significance p value ≤0.05 the levels of significance were indicated by the following * p≤ 0.05, ** p≤ 0.01, *** p≤ 0.001, **** p≤ 0.0001.

Results

Chapter 1 - Generation of an *in vitro* model of APC mutation

Chapter 2 - Searching for synthetic lethal interactions with APC mutation using an siRNA kinome screen

Chapter 3 - A FDA-approved compound screen identified compounds showing synthetic lethality with mutant APC in our *in vitro* model

Chapter 1 - Generation of an *in vitro* model of APC mutation

The *APC* gene is a tumour suppressor gene, mutated in over 80 % of CRC patients (Fearon 2011). The mutation occurs early in the development of CRC and is therefore seen as an ideal target for novel cancer therapeutics. The *APC* gene is difficult to target when mutated in CRC because typically a significant proportion of the protein is not translated, one approach to overcome this is synthetic lethality. To improve our chances of finding a synthetic lethal relationship with APC mutation, we generated a 'clean' isogenic human cell model where the main difference in the cell lines was the alteration in the *APC* gene.

1 Optimisation of APC antibodies and siRNA

Firstly in order to create an *in vitro* model of APC mutation, we needed to test different APC antibodies and optimise each one. The most abundant full length APC protein isoform is 312 kDa (Fearnhead et al. 2001). There are a number of reported shorter transcripts but these are less abundant and their role in CRC is unknown (De Rosa et al. 2007). We tested the following APC specific antibodies; Abcam APC Ali12-28 (ab58), Cell signalling APC (2504), Santa cruz APC C28.9 (Figure 19D shows the different binding sites). Given the large size of APC, we needed to optimise our antibodies and ensure the detected band was APC. To this end, we immunoblotted protein lysates isolated from the APC wildtype CRC cell line RKO, which had been transfected with either siRNA against APC (siAPC*3 or siAPC*6) or a non-targeting siRNA control (siCON). Figure 19A-C shows the three antibodies, we successfully optimised. Figure 19A shows the APC ab58 antibody detects four bands above the 150 kDa size marker in the RKO cell line, the top three bands are more abundant than the lower band of ~170 kDa. The lower band completely disappears when siRNA silences APC, whilst the intensity of the top three bands is significantly reduced. Lysates in figure 19A were electrophorised on a 4-12 % tris glycine gel, the protein size marker is not as accurate for large proteins compared to the 3-8% tris acetate gels used for the lysates in figure 19B/C. Figure 19B shows the bands detected with the APC antibody 2504 and the antibody epitope is in the middle of the N-terminal section of APC. This antibody detects two stronger bands above the 225 kDa marker and a very faint band

just above the 225 kDa marker in the RKO cell line. All three bands are reduced upon transfection with siRNA against APC and therefore represent different APC isoforms. Antibody APC C28.9 (Figure 19C) binds to the C-terminus of APC and the antibody detects one large band above the 225 kDa marker, this band completely disappears when RKO cells are transfected with siRNA targeting APC. This antibody also detects a weaker lower band, this band remains upon siRNA treatment targeting APC and therefore appears to be non specific. This antibody is less likely to detect different APC protein isoforms because the antibody binds to the C-terminus. To confirm the efficiency of our siRNA, we used RT-PCR to analyse the APC transcript levels in the RKO cell line transfected with non-targeting siRNA and siRNA targeted against APC (Figure 19E). APC transcript levels reduced up to 80 % when targeted with two different siRNA against APC.

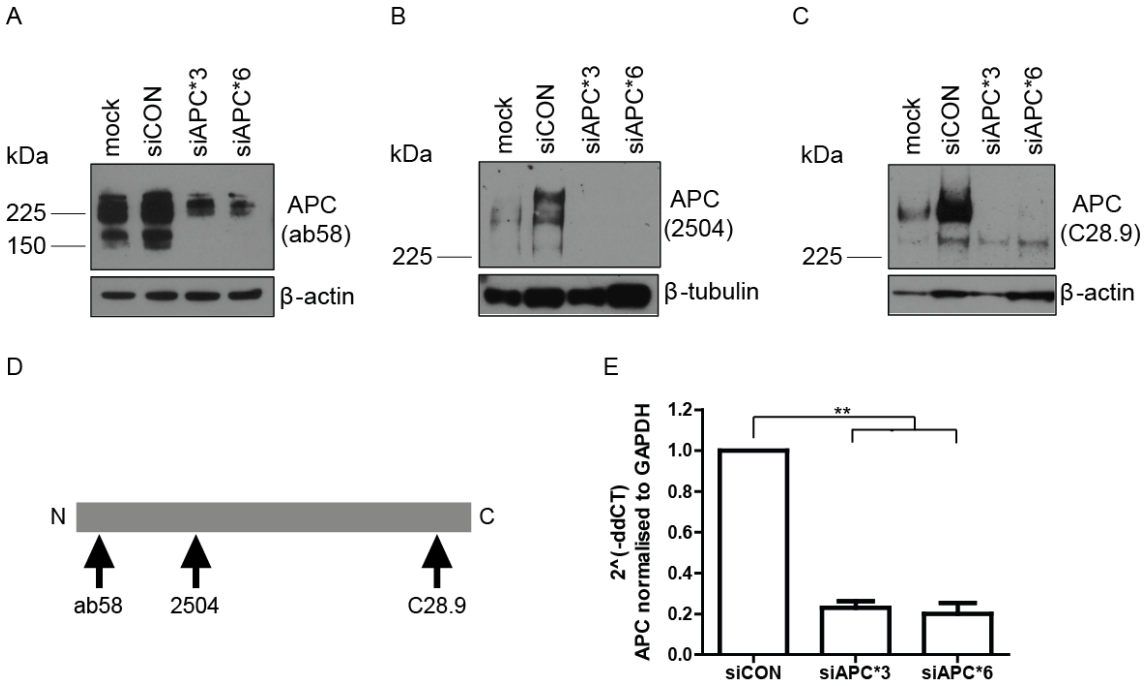

Figure 19 Optimisation of APC antibodies

RKO wildtype cells transfected with water (mock), non-targeting siRNA (siCON) and two siRNA targeting APC (siAPC*3 and siAPC*6) and whole cell lysates collected to help optimise the following antibodies; A) APC ab58 (4-12% tris glycine), B) APC 2504 (3-8% tris acetate), C) APC C28.9 (3-8% tris acetate). D) Schematic showing the binding sites of the three APC antibodies. E) RKO wildtype cells transfected with siCON, siAPC*3 and siAPC*6 and RNA collected for RT-PCR analysis. Levels of APC transcript were measured and normalised to the housekeeping gene GAPDH then siCON. The ddCT method was used. Data from two experiments and error bars are SEM. One way anova (post hoc Tukey) was performed (** p≤ 0.01).

Cell lines	Type[1]	MSI or MSS[1]	APC[2]	CTNNB1 (β-catenin)[3]	KRAS or BRAF[1]	TP53[1]
DLD1	Colorectal adenocarcinoma	MSI	c.4248delC/ LOH p.I1417fs*2	No	KRAS G13D	S241F
HCT116	Colorectal carcinoma - Primary	MSI	WT	Yes	KRAS G13D	WT
HT29	Colorectal adenocarcinoma - Primary	MSS	c.[2557G>T]; [4660_4661insA] p.[E853*];[T1556fs*3]	No	BRAF V600E	R273H
RKO	Colonic carcinoma - Primary	MSI	WT	No	BRAF V600E	WT
SW48	Colorectal adenocarcinoma	MSI	WT	Yes	WT	WT
SW620	Colorectal adenocarcinoma - Lymph node metastasis	MSS	c.4012C>T/LOH p.Q1338*	No	KRAS G12V	R273H;P309S

Table 9 CRC panel mutations

1 information from (Ahmed et al. 2013)

2 information from COSMIC

3 information from (Gayet et al. 2001)

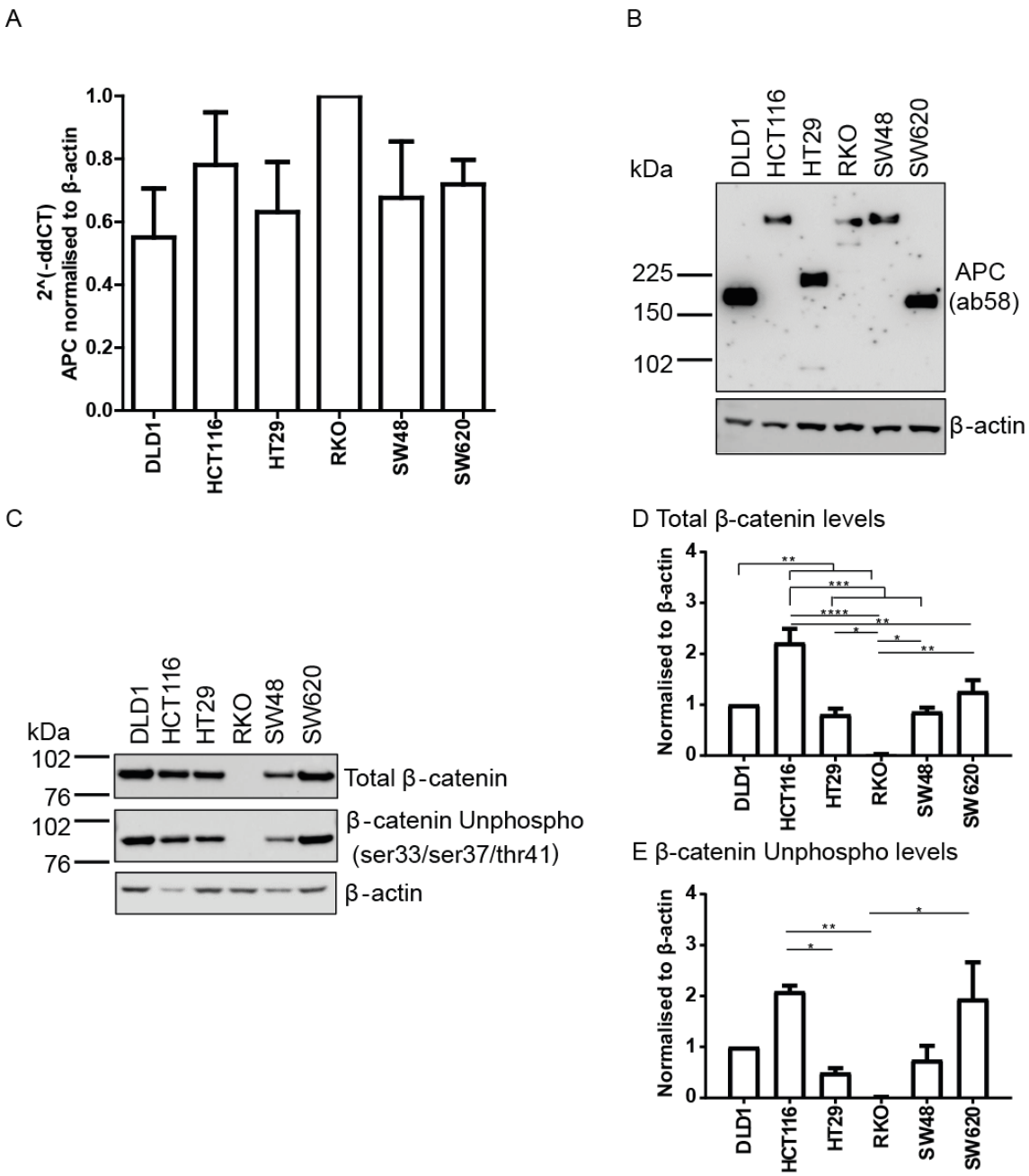

Figure 20 CRC cell line panel express different APC proteins

A) RNA collected from the CRC cell lines and RT-PCR performed. APC transcript levels were normalised to the housekeeping gene β-actin, then RKO and the ddCT method was used. Data shows three repeats, error bars are SEM and a one way anova was non significant (ns). B) Whole cell lysates were analysed on a western blot and probed with APC antibody (ab58). β-actin used as loading control. C) Whole cell lysates were analysed on a western blot and probed with total β-catenin and unphosphorylated β-catenin antibodies. Experiment performed three times, a representative blot is shown, β-actin used as loading control. D) E) β-catenin total and unphosphorylated blots were quantified. Band density measured then a % was calculated and then normalised to % β-actin, then normalised to DLD1. Bar chart shows a combination of three experiments. Error bars are SEM and one way anova (post hoc Tukey) was performed (* p≤ 0.05, ** p≤ 0.01, *** p≤ 0.001, **** p≤ 0.0001).

2 Selecting an appropriate cell line for our *in vitro* model

2.1 CRC cell lines express different APC proteins

To analyse the expression of APC in our panel of CRC cell lines, we compared three APC wildtype cell lines (HCT116, RKO and SW48) against three APC mutant cell lines (DLD1, HT29 and SW620) (Table 9). Firstly we confirmed by RT-PCR all six cell lines express the APC transcript, the probe we used binds between exon 13 and 14 and therefore the mutations in the CRC panel will not interfere with the probes binding. Figure 20A confirms the APC transcript was present in all six cell lines and there was some variation in levels but no significant differences. Next we confirmed the size of APC protein present in all six cell lines (Figure 20B). HCT116, RKO and SW48 express full length APC, ~312 kDa. DLD1 expresses a 155 kDa APC protein which retains the 2nd 20aa repeat. HT29 contain two APC proteins, 93 kDa APC protein (appears quite faint on the western), which retains the armadillo repeats and a 171 kDa APC protein which includes the 3rd 20aa repeat. SW620 expresses a 147 kDa protein which retains the 1st 20aa repeat. Interestingly all three cell lines with truncated APC appear to express more truncated APC product compared to the wildtype APC lines, however this could be a result of large proteins transferring less efficiently in western blotting.

The activation of Wnt signalling is critical to the progression of CRC. To determine the level of Wnt signalling in the cell lines, we analysed the protein levels of β-catenin because activation of the pathway prevents β-catenin from phosphorylation at ser33, ser37 and thr41. This prevents its degradation and results in an increase in unphosphorylated β-catenin levels. Therefore, β-catenin is free to translocate to the nucleus and activate Wnt target genes. We probed for total β-catenin levels and unphosphorylated ser33/ser37/thr41 β-catenin (indicates the proportion of total β-catenin which is active) in whole cell lysates for the whole panel to determine the activation of the pathway (Figure 20C/D/E). The results show when total β-catenin levels are high, unphosphorylated β-catenin is also high. As expected all the lines except RKO have high levels of total and unphosphorylated β-catenin. The APC mutant lines (DLD1, HT29 and SW620) are expected to have increased levels of β-catenin due to the APC mutation and therefore show hyperactivation of the Wnt signalling pathway. The cell lines HCT116 and SW48 are APC wildtype but have β-catenin mutations causing hyperactivation of the Wnt signalling pathway, our results support this. The RKO cell line is reported to have normal levels of Wnt signalling, however one group suggests this cell line has a mutation in the inhibitor of dishevelled called naked cuticle

homolog 1 (NKD1) which could result in activation of the Wnt signalling pathway (Guo et al. 2009). We do not see upregulation of the Wnt signalling pathway in the RKO cell line in comparison to the other five cell lines which show higher levels of both total and unphosphorylated β-catenin.

2.2 The RKO cell line is an appropriate model

There are a limited number of APC wildtype CRC cell lines available. We selected the CRC cell line RKO to create our APC mutated cell lines because it is wildtype for APC and β-catenin and as shown in figure 20C it does not display upregulation of β-catenin expression, which is characteristic of activation of the Wnt signalling pathway. To ensure that the cell line was appropriate and responsive to an APC mutation, we silenced APC using two different siRNA targeting APC and analysed Wnt activation using a TCF/LEF luciferase reporter assay. In the TCF/LEF luciferase reporter assay, the firefly luciferase is under the control of the TCF response element (TRE) which the transcription factors TCF/LEF bind to. The assay contains a positive control with constitutive firefly luciferase activity and a negative control with non-inducible firefly luciferase. As a negative control for our experiment, we performed the same assay in DLD1 cells which already have a mutation in APC therefore they have endogenous hyperactivation of the Wnt pathway.

In the RKO cells, we observed that silencing APC with siRNA resulted in a significant increase in TCF/LEF activation compared to RKO cells transfected with non-targeting siRNA (Figure 21A). The same effect was not seen in the DLD1 cells which have endogenous hyperactivation of the Wnt pathway. In DLD1 cells silencing APC with siRNA resulted in a slight increase in TCF/LEF activation compared to the cells targeted with non-targeting siRNA, this supports the specificity of our assay (Figure 21B). The effect seen in the RKO cell line showed this cell line was suitable for use in our study.

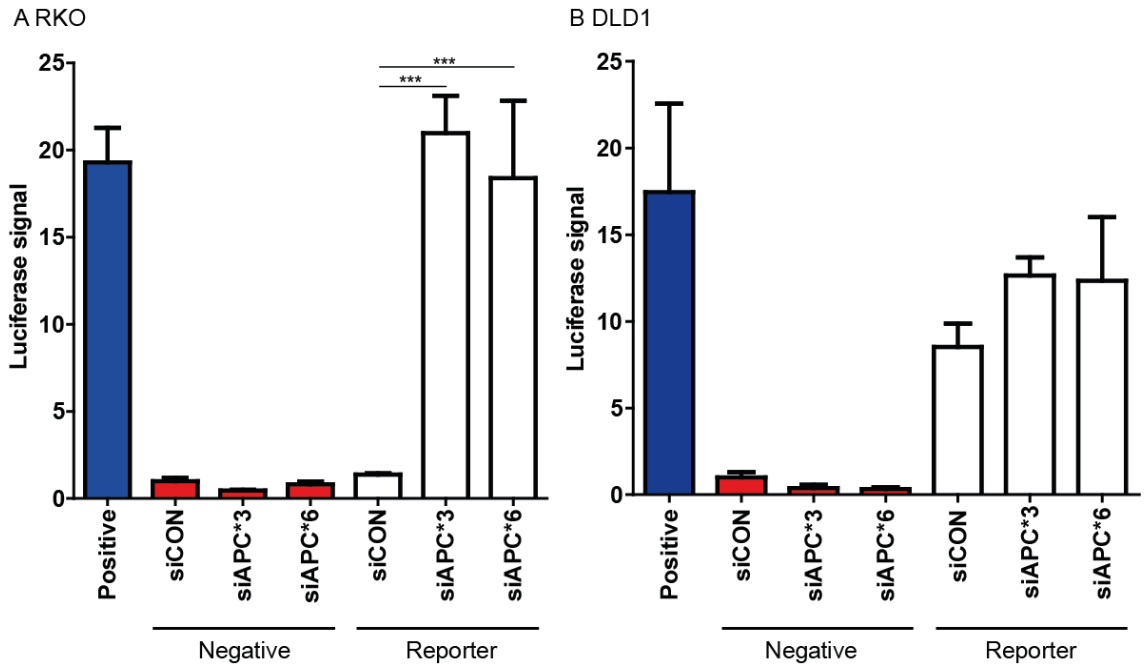

Figure 21 The RKO cell line is an appropriate cell line for the *in vitro* model

TCF/LEF reporter assay performed, cells targeted with siCON, siAPC*3 and siAPC*6. Data is normalised to the negative + siCON. A) RKO cell line, representative shown of three repeats, error bars are SD and a one way anova (post hoc Tukey) was performed (*** p≤ 0.001) B) DLD1 cell line, representative shown of two repeats, error bars are SD and a one way anova was ns.

3 Using the Dharmacon Edit-R CRISPR-cas9 system to alter APC

3.1 Generation of mixed populations

Our aim was to create an *in vitro* model of complete APC loss and to this end, we designed two gRNA to target exon 2 of the *APC* gene using the design tool from dna2.0 (Figure 22A and table 1). We used the Dharmacon Edit-R system which involves transiently transfecting three components; cas9 plasmid containing puromycin resistance, trans-activating crRNA (tracrRNA) and CRISPR RNA (crRNA). The tracrRNA and crRNA bind together to form the gRNA. This approach has the advantage that the cas9 expression is only temporary. We decided to transfect gRNA #8 alone and gRNA #8 and #9 together because co-transfecting two gRNA could increase efficiency but it is of note that co-transfection may also increase levels of off target effects. gRNA #8 had the highest score from the design tool dna2.0 which indicated it was predicted to have the least off target effects. We included two controls which expressed the cas9 plasmid alone and no tracrRNA or crRNA. Control 1 expressed the cas9 plasmid with puromycin resistance. This control would undergo

puromycin selection and then single colony selection. Control 2 expressed the cas9 plasmid with mKATE2 expression (instead of puromycin resistance). mKATE2 is a red fluorescent protein and enabled us to assess the transfection efficiency. After 48 hours post transfection, cells transfected with the cas9 plasmid with puromycin resistance were selected for using 0.5 µg/mL puromycin. After four days in puromycin selection, we had heterogenous populations which expressed the cas9 plasmid and may or may not have also been transfected with the tracrRNA and crRNA. A proportion of cells may have alterations to the APC gene resulting in complete loss of the APC protein. To help decide which mixed population to select single colonies from, we analysed the APC protein levels from the heterogenous populations by western blotting and performed the TCF/LEF reporter assay (Figure 22B/C). Both populations showed a similar reduction in the level of full length APC in comparison to the control population targeted with no gRNA. However, the TCF/LEF reporter assay showed no corresponding increase in Wnt signalling in either mixed populations, this could be due to the remaining level of full length APC being too high to see an effect on Wnt signalling.

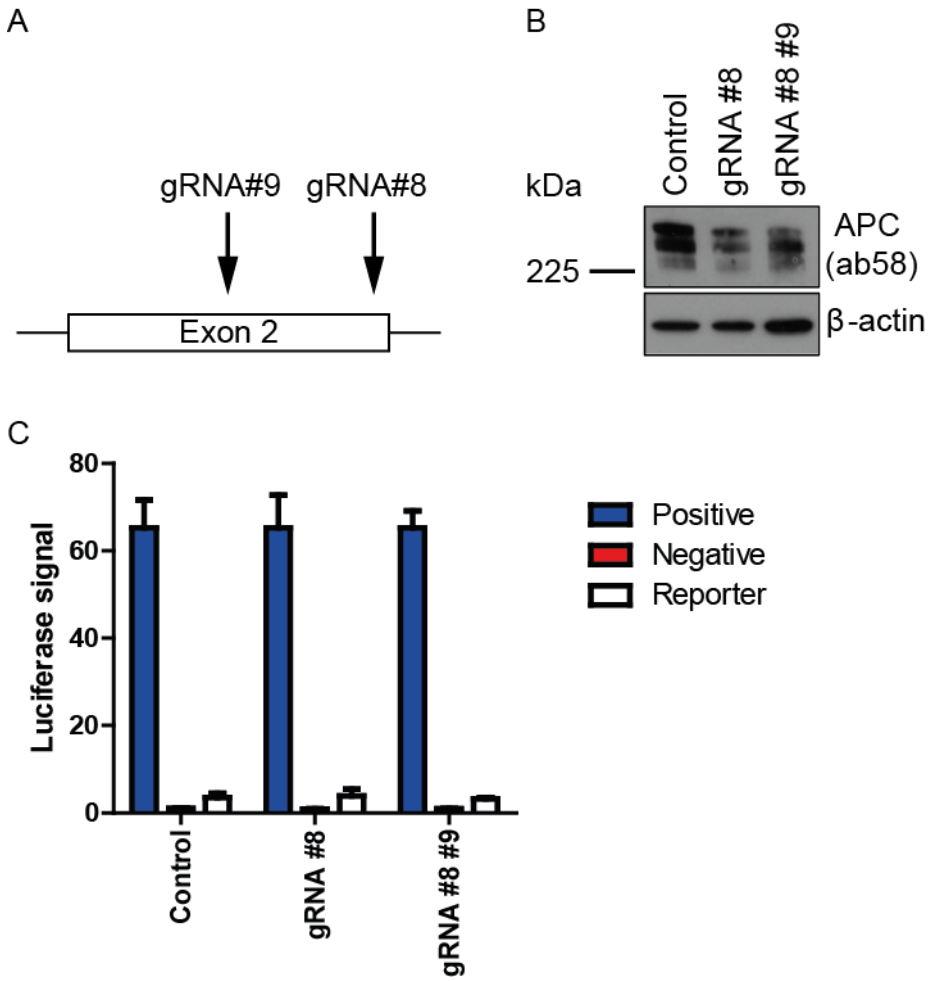

Figure 22 Dharmacon Edit-R CRISPR-cas9 generated mixed populations

A) The target sites of the gRNA in exon 2 of *APC*. B) Whole cell lysates collected from the mixed population and probed for APC on a western blot. β-actin used as a loading control. C) TCF/LEF assay performed on the mixed populations, data was normalised to each positive control then to the control cell line negative control. Error bars are SD, a one way anova was ns.

3.2 Single colony selection

We single colony selected both heterogeneous populations and clones we successfully established from a single colony are shown in figure 23A. In the majority of clones, we could still detect full length APC with the APC antibody Ali 12-28 (ab58). Two clones 8_1 and 8_6 seemed to be absent of any APC protein and were potentially APC knock-outs (Figure 23A). To see if this resulted in activation of the Wnt signalling pathway, we determined levels of total and unphosphorylated β-catenin by western blotting. We observed no increase in β-catenin level (Figure 23B). Additionally, we performed the TCF/LEF reporter assay on these clones and found there was no increase in Wnt signalling, supporting the blot results (Figure 23C). We next analysed APC expression using two different APC antibodies targeting different regions of the protein. Both APC C28.9 and APC 2504 detected full length APC in the RKO 8_1 and RKO 8_6 (Figure 23D). The APC ab58 antibody epitope is in the protein region which is encoded by the same region of DNA where gRNA #8 and #9 target. The gene alteration induced by cas9 in clones 8_1 and 8_6 was inframe and we propose the change altered the structure of the antibody binding site. Unfortunately from targeting exon 2 using the Dharmacon Edit-R system, we did not manage to generate clones with altered APC.

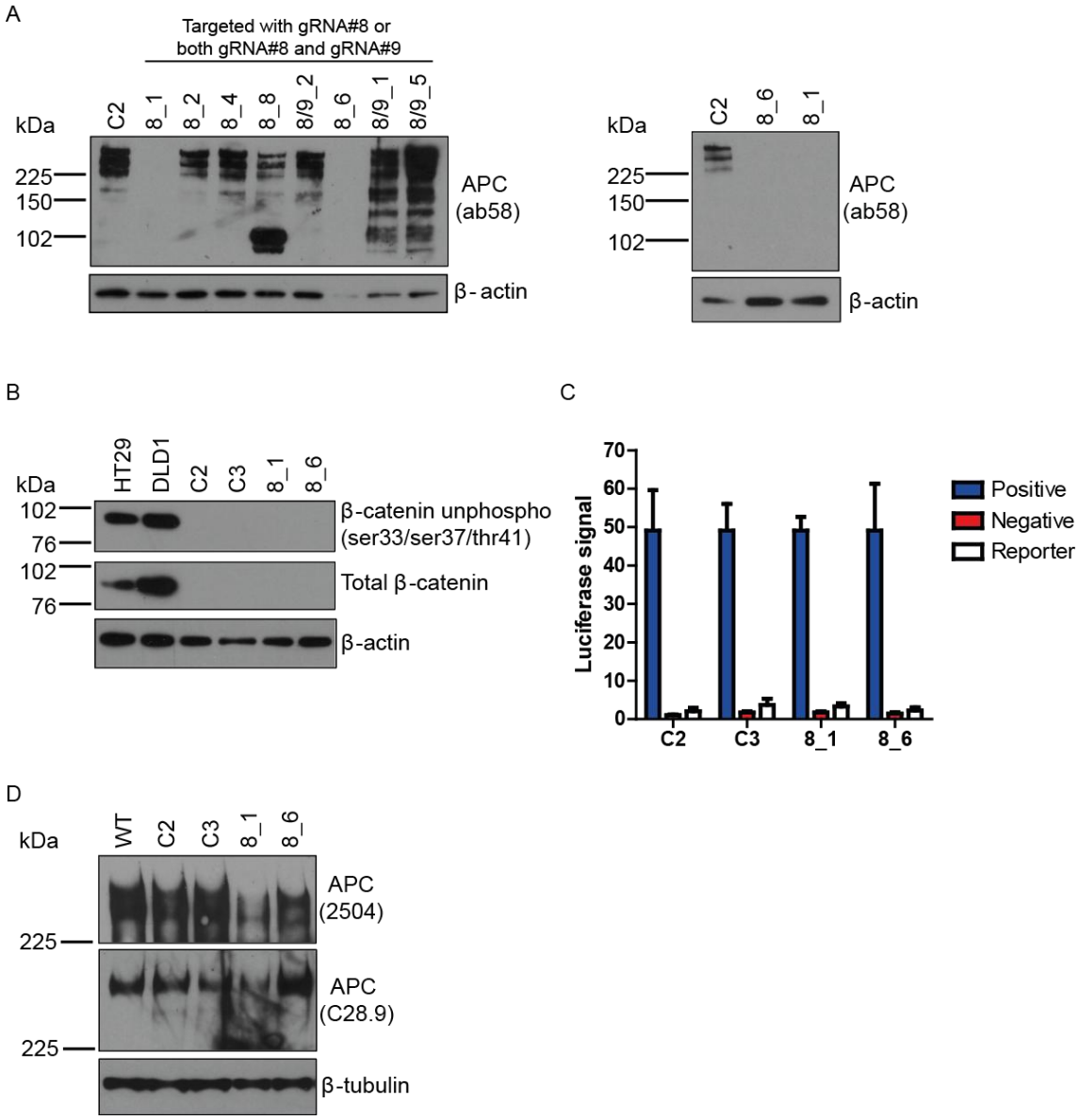

Figure 23 Single colony selection of the Dharmacon Edit-R mixed populations

A) Whole cell lysates collected from the individual clones and probed for APC. β-actin used as a loading control B) Whole cell lysates collected and levels of total and unphosphorylated β-catenin were analysed and compared to HT29 and DLD1 (APC truncated cell lines). β-actin used as a loading control, representative shown, experiment performed three times. C) TCF/LEF assay performed twice, representative shown, one way anova was ns. Data normalised to each positive control then C2 negative control. D) Whole cell lysates collected and probed for APC, β-tubulin used as loading control.

4 CRISPR-cas9 using a lentiviral system to alter APC

4.1 Generation of mixed populations

The Dharmacon Edit-R system relies on the cells receiving the cas9 plasmid, the tracrRNA and the crRNA. Therefore to increase the efficiency of generating an APC mutated cell line, we decided to try a lentiviral approach with all components expressed from one plasmid. We also designed new gRNA using the design tool from dna2.0 targeting exon 15 which contains 80 % of the coding region. gRNA #2, #5 and #6 all target upstream of the MCR and gRNA #3 and #4 target downstream of the MCR (Figure 24A and table 1). Targeting exon 15 increases our chances of generating a truncated APC product, however, there is still a chance of generating an alteration, which causes the transcript to be degraded by NMD generating an APC knock-out.

The lentiCRISPRv2 plasmid encoded cas9, gRNA and puromycin resistance, shown in figure 24B. Site directed mutagenesis was performed to clone the five gRNA sequences into the plasmid. The five plasmids containing gRNA targeting APC and a plasmid containing a non-targeting gRNA (Scr) were transfected into the HEK293T cell line along with the packaging plasmids to produce lentivirus to infect into the RKO cell line. One day after infection, 0.5 µg/mL puromycin was used to select for 'edited cells' for 10 days.

After puromycin selection, the cell population should only contain cells, which received the lentiCRISPRv2 plasmid. However some cells will have received the plasmid but no editing occurred, whilst other cells may have been edited but this change may or may not have altered the APC protein. To help us determine which heterogenous population to single colony select, we collected lysates to analyse APC expression and performed the TCF/LEF reporter assay (Figure 24C and 24D). Figure 24C shows the APC expression in all mixed populations including the non-targeting gRNA control. The mixed populations targeted with gRNA #3, #4 and #6 have resulted in cells expressing full length APC to a similar level of the non-targeting gRNA control. This suggests these gRNA have not been very effective at inducing an alteration to the *APC* gene. In comparison both gRNA #2 and #5 have resulted in mixed populations with truncated forms of APC, ~ 80 kDa and ~ 120 kDa protein respectively. The high level of truncated APC suggests these gRNA have a high efficiency and this increases the likelihood of identifying a single clone with altered APC on both alleles. The TCF/LEF reporter assay on the mixed populations targeted with each gRNA support the findings from the western blot. The cells targeted with gRNA #3, #4 and #6 do not activate Wnt signalling higher than the non-targeting gRNA control. Whereas, the cells targeted with gRNA #2

and #5 show a significant increase in Wnt activation in comparison to the non-targeting gRNA control. The population targeted with gRNA #5 appears to activate Wnt signalling more than twice the level in the population targeted by gRNA #2. This could be a result of the size of the APC truncation or because the population targeted by gRNA #2 still has some expression of full length APC, which could counteract the APC truncation.

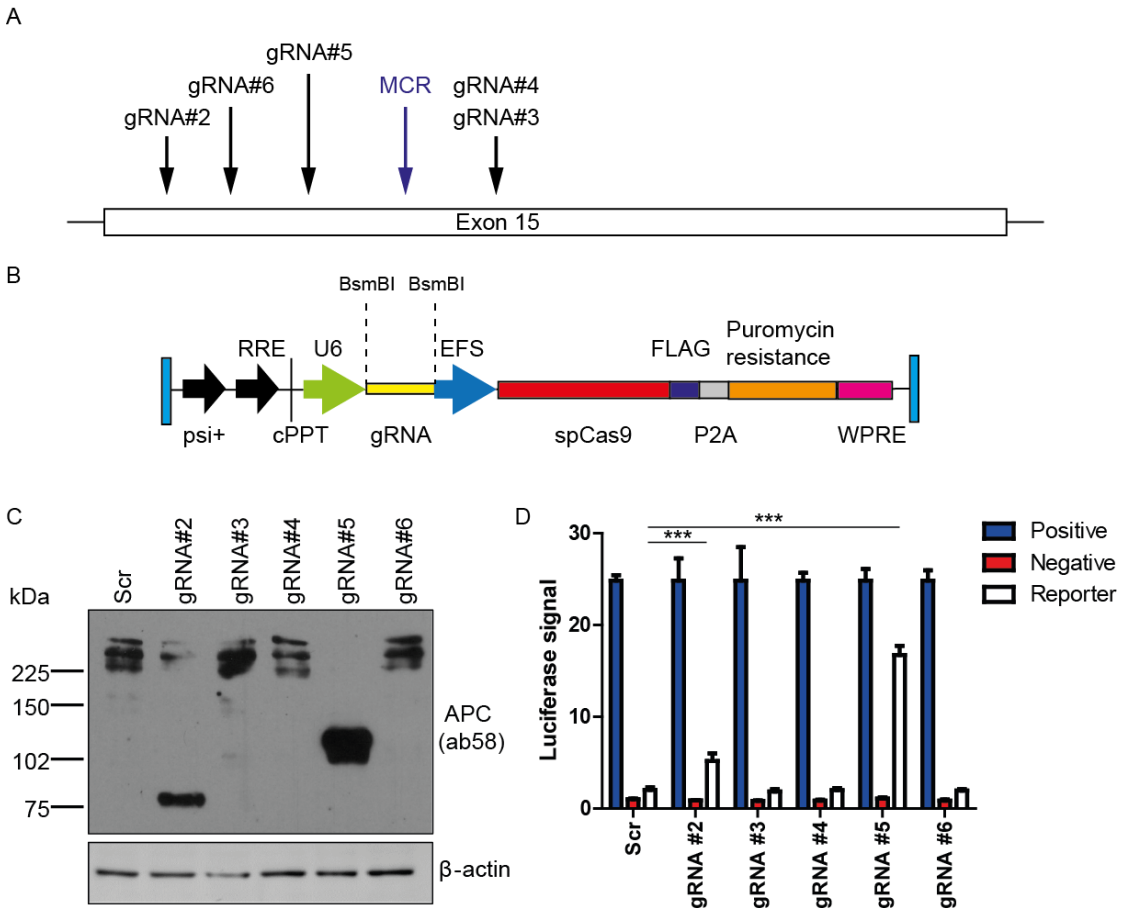

Figure 24 Lentiviral CRISPR-cas9 generated mixed populations

A) The target sites of the gRNA in exon 15 of *APC* in relation to the MCR region. B) Schematic showing the lentiCRISPRv2 plasmid, RRE = Rev response element, cPPT = central polypurine tract, WPRE = WHP post transcriptional regulatory element. C) Whole cell lysates collected from the mixed populations and probed for APC on a western blot. Non-targeting gRNA referred to as scrambled (scr). β-actin used as a loading control. D) TCF/LEF assay performed on the mixed populations, data was normalised to each positive control then to the scrambled negative. Error bars are SD, a one way anova (post hoc Dunnet) was performed (*** $p \leq 0.001$).

4.2 Single colony selection of the mixed populations targeted by gRNA #2 and gRNA #5

4.2.1 Single colony selection of the mixed population targeted by gRNA #5 does not generate an APC mutant

Initially we decided to single colony select the population targeted by gRNA #5, figure 25 shows the clones we successfully expanded. All clones shown in figure 25 express some degree of full length APC, for example clone 5_9 seems to be heterozygous containing both full length APC and a truncated form ~ 120 kDa. We decided not to investigate any of these clones further.

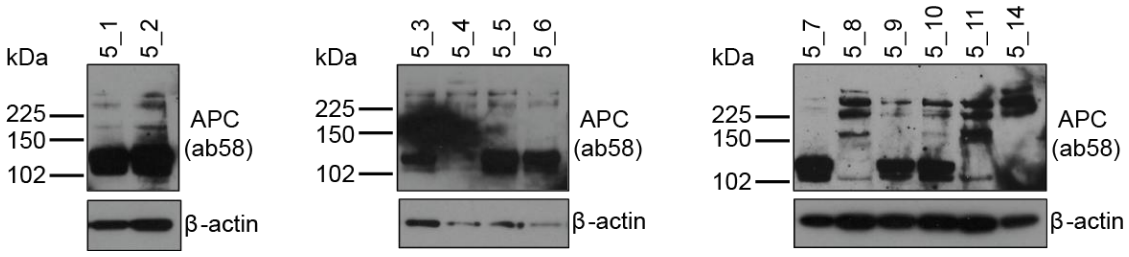

Figure 25 Single colony selection of the population targeted with gRNA #5

Whole cell lysates collected and APC probed for on western blots. β-actin used as a loading control.

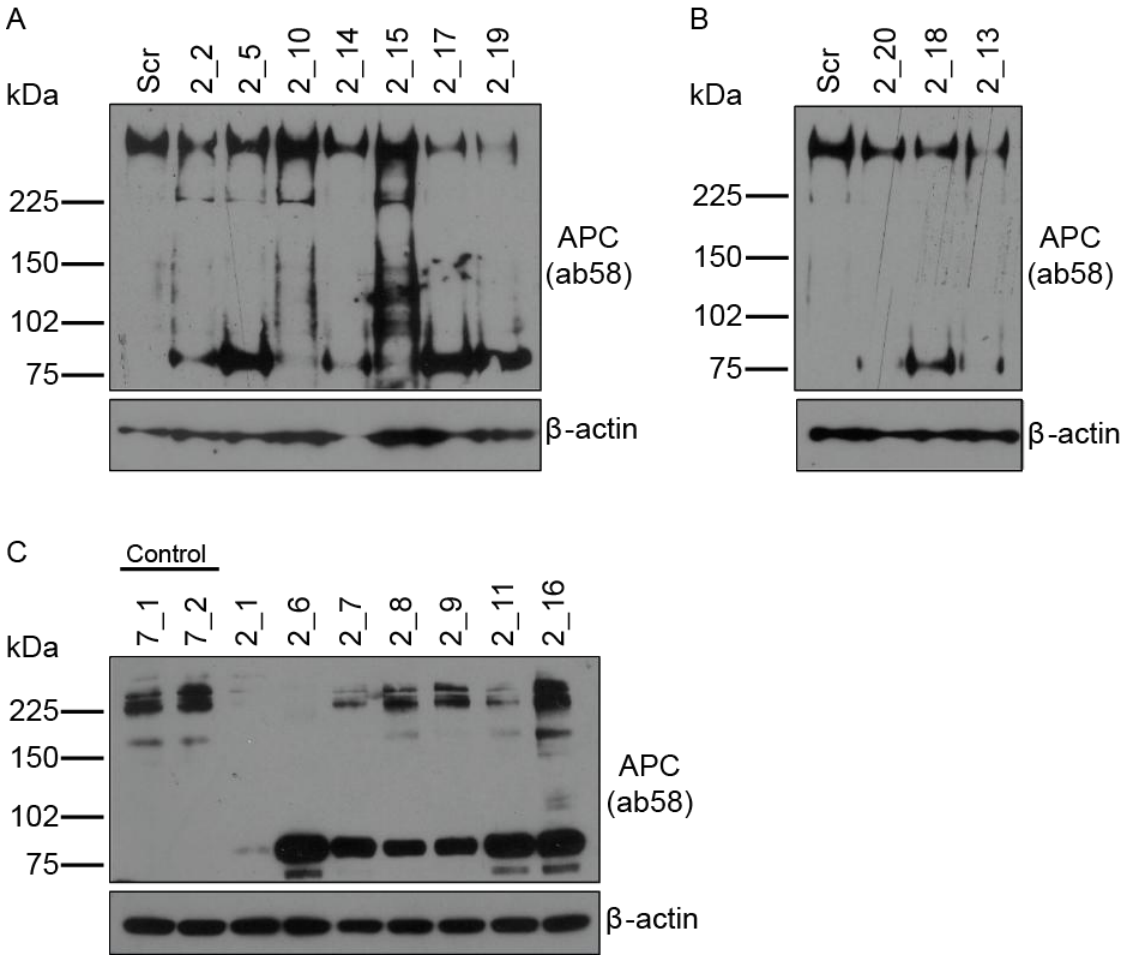

Figure 26 Single colony selection of the population targeted with gRNA #2

A) B) C) Whole cell lysates collected and APC probed for on western blots. β-actin used as a loading control.

4.2.2 Single colony selection of the mixed population targeted by gRNA #2 generates the RKO APC mutated line 2_6

Next we single colony selected the population targeted by gRNA #2 and the successfully expanded clones are shown in figure 26. The blots show single colony selection identified many clones, which were heterozygous for full length APC and an ~ 80 kDa APC truncated protein. The RKO 2_6 clone (Figure 26C) was of particular interest because both copies of APC appear to harbour a truncated protein ~ 80 kDa. We predicted this truncation to have occurred in the 7th armadillo repeat where APC interacts with ASEF1/2, and we later confirmed this by topocloning (Figure 30). RKO 2_1 appears to have low levels of both full length and the truncation which made us hypothesise that this was not a 'clean' single colony population, and therefore, we did not investigate this clone further (Figure 26C). We did not identify a full APC knock-out from this single colony selection. We have identified a clone RKO 2_6 which has an APC truncation and is more representative of the mutations seen in the clinic. In the clinic APC truncations are common and complete loss is rare. However, the RKO 2_6 clone is more dramatically truncated than the typical truncations seen in the clinic. Alongside the single colony selection of the population targeted with gRNA #2, we also single colony selected the scrambled population, this generated two control cell lines with full length APC as shown in figure 26C.

4.2.3 RKO APC mutant line 2_6 activates Wnt signalling

Firstly, we checked the levels of the APC mRNA transcript in RKO 2_6. Figure 27A shows the APC transcript levels are similar to those of both control lines RKO 7_1 and RKO 7_2. Next we analysed levels of Wnt signalling by analysing levels of total and unphosphorylated β-catenin by western blotting and performing the TCF/LEF reporter assay. Figure 27B shows RKO 2_6 had significantly increased levels of both total and unphosphorylated β-catenin in whole cell lysates compared to the controls. This is supported by the TCF/LEF reporter assay which showed RKO 2_6 significantly increased TCF/LEF activation in comparison to the control cell lines (Figure 27C). This finding is supportive of evidence from patients with APC truncations.

To generate our *in vitro* model of APC mutation, we used CRISPR-cas9 to alter APC in the RKO cell line. We attempted to generate an *in vitro* model with complete APC loss, alternatively we have generated an *in vitro* model with approximately 25 % of the N-terminus of APC remaining. This cell line strongly activates Wnt signalling in comparison to the control cell line and is more representative of APC mutational status found in patients. We have three cell lines derived from the same parental APC

wildtype RKO cell line; RKO control cell lines (7_1 and 7_2) and RKO APC truncated (2_6). The main difference between these cell lines is the *APC* mutation (there is potential for off-target effects from the CRISPR-cas9 approach), enabling us to look for genes which are synthetically lethal with a truncated APC protein.

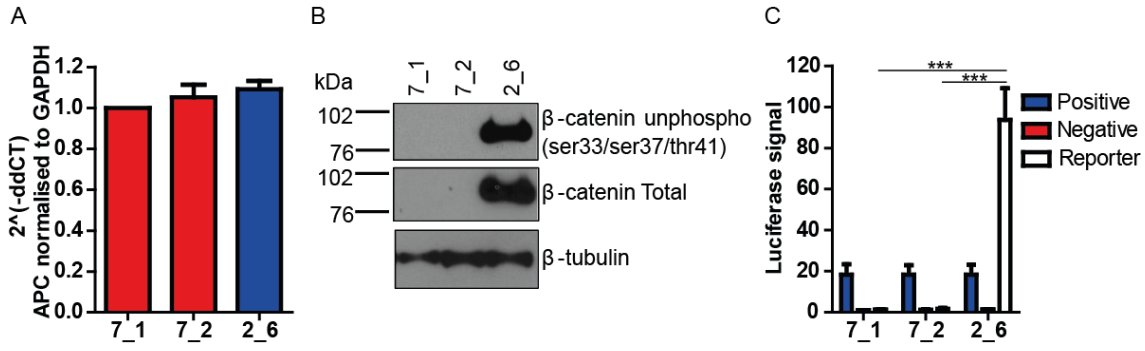

Figure 27 Characterisation of RKO 2_6

A) RNA collected and RT-PCR performed, APC transcript levels normalised to GAPDH then RKO 7_1. Data analysed using ddCT. Data was repeated twice, error bars are SEM and one way anova was ns. B) Whole cell lysates collected and probed for total and unphosphorylated β-catenin, β-tubulin used as loading control. Representative is shown of three experiments. C) TCF/LEF reporter assay performed, data was repeated three times, error bars are SEM and a one way anova (post hoc Tukey) was performed (*** p≤ 0.001). Data normalised to each positive control then 7_1 negative control.

4.3 Re-single colony selection

It became apparent with time, that RKO 2_6 cells expressing a truncated APC also expressed a small level of full length APC, which could be influencing the phenotype observed (Figure 28A). The amount of full length APC is marginal in comparison to wildtype RKO and control clones RKO 7_1 and RKO 7_2, however the full length APC population may expand as the clone is passaged. We did not see any full length APC in our original blots, so we believe this population may have overtime become contaminated from another clone. We decided to undergo single colony selection again and figure 28B shows the clones successfully expanded. Figure 28C shows the clones RKO 2_21, RKO 2_22, RKO 2_30 and RKO 2_36 which do not express any trace of full length APC, as confirmed by immunoblotting with the two antibodies, APC ab58 and APC C28.9.

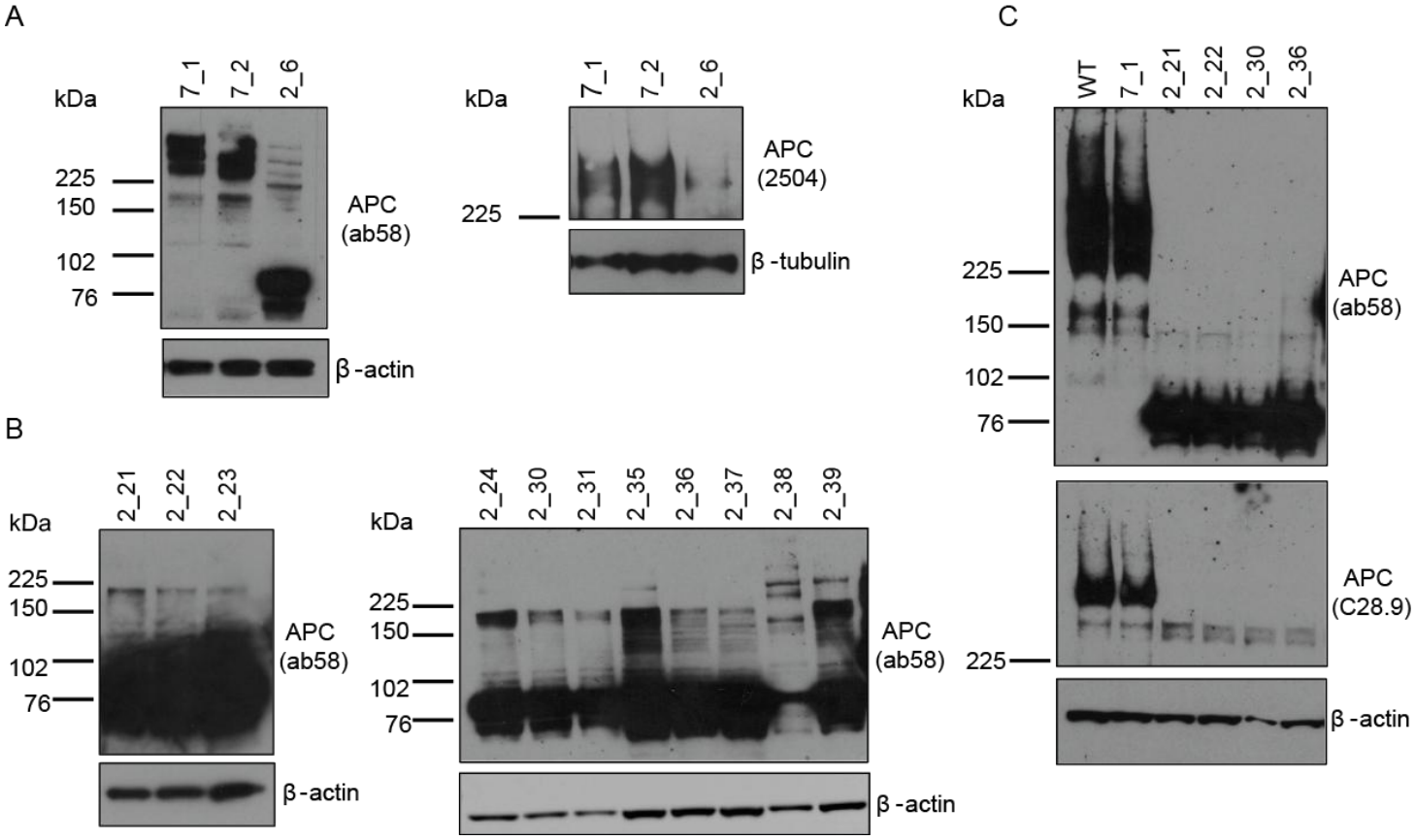

Figure 28 Re-single colony selection of RKO 2_6

All whole cell lysates collected and probed for APC. β-actin or β-tubulin used as loading controls. A) RKO 2_6 contained some full length APC expression B) Clones established from re-single colony selection of RKO 2_6 C) The final clones probed with APC ab58 and APC C28.9. APC ab58 repeated three times, representative shown.

4.4 Characterisation of final RKO APC mutated lines

To confirm the new single colony selected cell lines have similar characteristics to RKO 2_6 we determined the levels of APC transcript and activation of the Wnt signalling pathway. We used RT-PCR to analyse the level of APC transcript in the controls RKO 7_1 and RKO 7_2 in comparison to RKO 2_30 and RKO 2_36. Figure 29A shows the APC mutant line RKO 2_30 has a similar level of APC transcript to the control cell lines, whilst RKO 2_36 has a slightly higher level of APC transcript only when compared to the control RKO 7_1. We analysed the activation of the Wnt signalling pathway by western blotting for β-catenin and performing the TCF/LEF reporter assay. Levels of total and unphosphorylated β-catenin were still significantly upregulated in comparison to the control cell lines (Figure 29B). The TCF/LEF reporter assay showed all the clones upregulate Wnt signalling. RKO 2_21, RKO 2_22 and RKO 2_36 showed a significant increase in Wnt signalling compared to the controls (Figure 29C). Interestingly RKO 2_30 activates Wnt signalling to a lower level, therefore we decided to focus on RKO 2_30 and 2_36.

Additionally we analysed the rates of proliferation between the original RKO wildtype cell line and the *in vitro* model lines generated using CRISPR-cas9 (Figure 29D). We plated the cell lines into 96 well plates and measured cell viability using a ATP-based luminescence assay CellTiter-glo (CTG) daily for five days to enable us to analyse the rate of proliferation in the cell lines. We calculated the fold change in cell viability for each time point by comparing the CTG values (measured every 24 hours) to the average CTG values for time point 0 (measured 6 hours after plating). The fold change values were plotted to show the increase in population size for all the cell lines. The RKO wildtype cell line and RKO controls 7_1 and 7_2 show similar increases in population size throughout the experiment. In comparison, the RKO APC mutant lines appear to slightly increase in population size more over the course of the experiment, which could be explained by the higher level of Wnt signalling in these cell lines. Interestingly RKO 2_36 shows a higher level of Wnt signalling than RKO 2_30 but this is not reflected in a greater increase in population size. We then calculated the population doubling time (PDT), for this we used the fold change values at 48 hours and 96 hours because the population was growing exponentially. Table 10 shows the PDT for each cell line. The PDT for the cell lines varies from 18-20 hours which supports why there are not huge differences in the population sizes over the course of the experiment. Despite seeing slighter bigger increases in population size in the APC mutant cell lines, only RKO 2_30 has a slightly shorter PDT.

We also performed topocloning to determine the alterations on both alleles of the clones RKO 2_21, RKO 2_30 and RKO 2_36. All three RKO APC mutant clones have the same alterations because they are derived from the same original population RKO 2_6. We used the APC transcript 3 (NM_000038.5) which encodes the most common protein isoform to enable us to describe the DNA and resulting protein changes. APC allele no.1 contained a 16 bp deletion causing a frameshift and a premature stop codon. APC allele no.2 contained a 26 bp deletion resulting in a frameshift and a premature stop codon (Figure 30A). The DNA nomenclature is the following in reference to the APC mutant cell lines; NM_000038.5 c.[2206_2221del];[2206_2231del]. The protein nomenclature is the following in reference to the APC mutant cell lines; NP000029.2 p.[K736IfsTer20];[K736SfsTer11] and this can be shorterned to APC Lys736fs. Topocloning enabled us to confirm the RKO APC mutant lines contain APC mutations in the armadillo repeat 7 domain resulting in APC products of 82 kDa and 83 kDa (Figure 30B).

Taken together we have generated a set of cell lines, differing in the APC status; two wildtype APC lines (RKO 7_1 and 7_2) and four APC truncated lines (RKO 2_21, 2_22, 2_30 and 2_36).

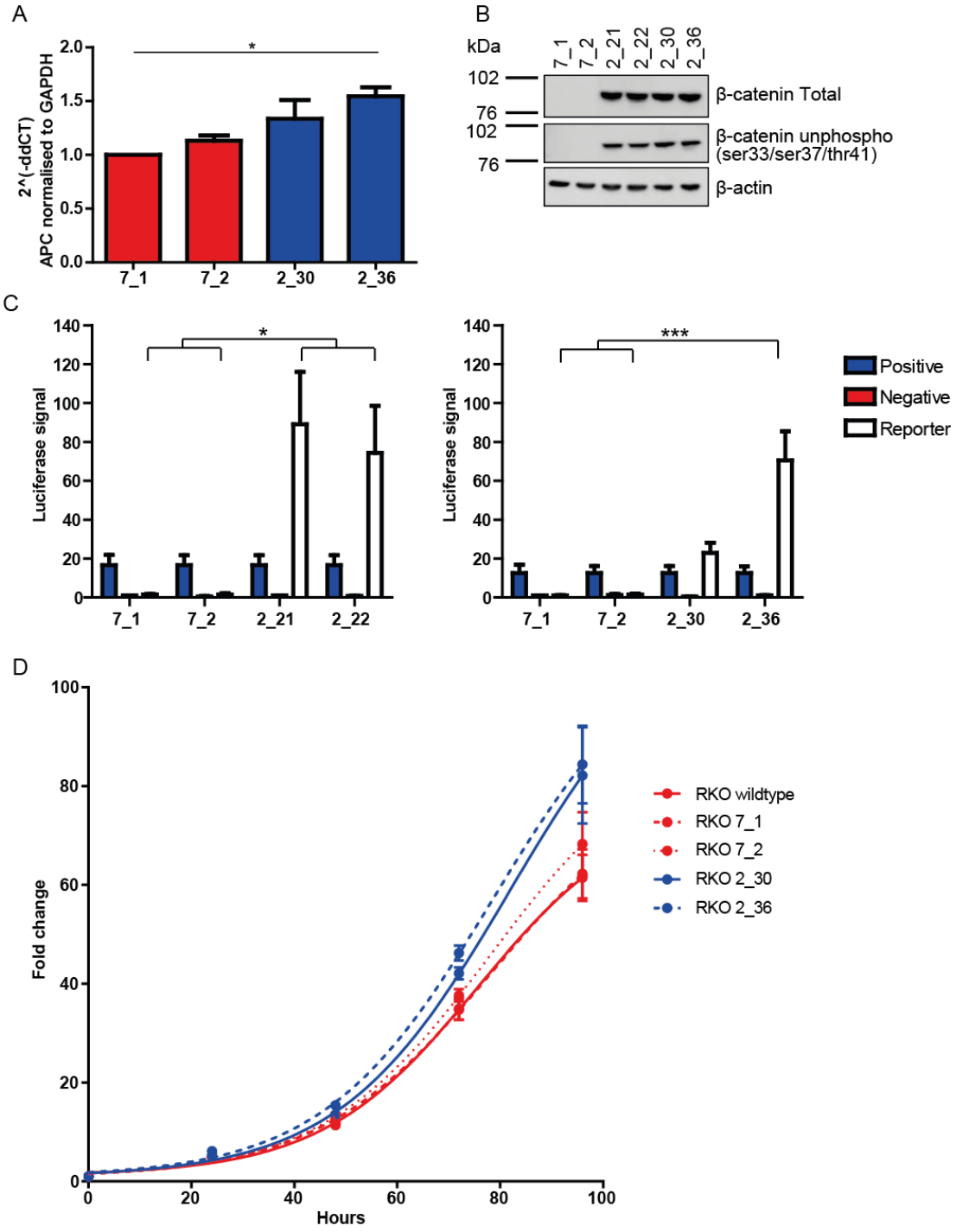

Figure 29 Characterisation of RKO 2_21, 2_22, 2_30 and 2_36

A) RNA collected and RT-PCR performed, APC transcript levels normalised to GAPDH then RKO 7_1. Data analysed using ddCT. Experiment was repeated three times, error bars are SEM and one way anova (post hoc Tukey) was performed (* p≤ 0.01) B) Whole cell lysates collected and total and unphosphorylated β-catenin was probed, β-actin used as loading control. Representative is shown of three experiments. C) TCF/LEF reporter assay performed, data was repeated twice, error bars are SEM and a one way anova (post hoc Tukey) was performed (* p≤ 0.05, *** p≤ 0.001). Data normalised to each positive control then 7_1 negative control D) Measured cell viability every 24 hours over 5 days to determine cell proliferation rates. Fold change calculated using the average of day 0 values for each cell line. Experiment performed twice, error bars are SEM.

Cell line	PDT (hrs)
RKO WT	19.7
RKO 7_1	20.4
RKO 7_2	19.8
RKO 2_30	18.5
RKO 2_36	19.6

Table 10 PDT of cell lines

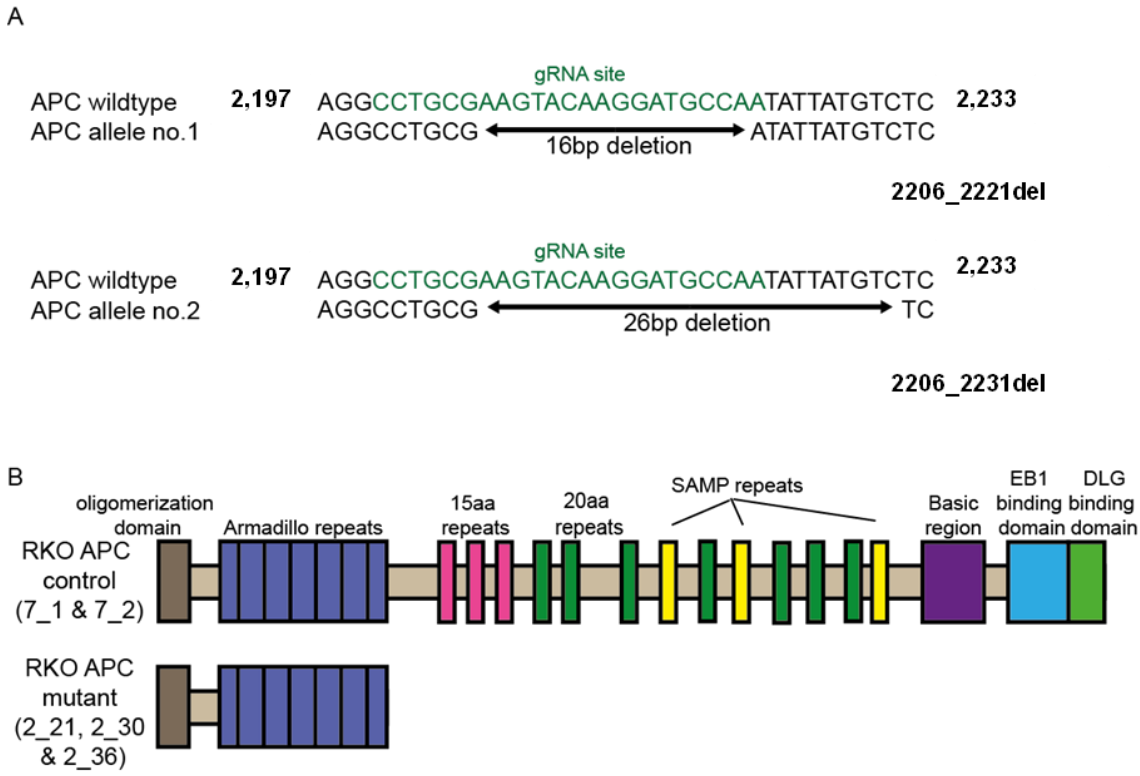

Figure 30 Topocloning identified the exact APC mutations in our *in vitro* model

A) The sequence alterations in our APC mutant cell lines on allele 1 and 2, numbering starts from the start codon and we used the coding DNA ref sequence NM_000038.5. Changes confirmed by at least 2 sequences for each alteration. B) Schematic showing the resulting APC truncation confirmed from the topocloning, with reference to the APC protein sequence NP000029.2 p.[K736IfsTer20];[K736SfsTer11].

Chapter 2 - Searching for synthetic lethal interactions with APC mutation using an siRNA kinome screen

1 Identification of potential hit kinases which are synthetically lethal with APC mutation

1.1 Using an siRNA kinome screen to identify synthetic lethal kinases

To identify synthetic lethal interactions with truncated APC in our *in vitro* model, we designed an siRNA screen targeting 720 kinases and kinase related genes. The same layout was previously used to identify PTEN induced putative kinase 1 (PINK1) as synthetically lethal with MMR deficiency (Martin et al. 2011). The advantage of searching for synthetic lethal relationships with kinases is the potential to use existing compounds to inhibit the target and the ability to design new compounds to interfere with the kinase domain. The siRNA library was aliquoted over 9 x 96 well plates and each well contained one siRNA SMARTpool targeting a specific gene (the pool consists of four deconvoluted siRNAs targeting the same gene). The use of pooled siRNA in a screen has been shown to have a greater phenotypic effect and identify more hits, in comparison to the use of individual siRNA (Parsons et al. 2009). Each plate contained controls in the first and last columns including; media only, mock transfection, non-targeting siRNA (siCON) and siRNA against PLK1 (siPLK1). We use siRNA against polo like kinase 1 (PLK1) as a positive control because PLK1 is part of the G2/M checkpoint in the cell cycle, therefore silencing of PLK1 results in reduced cell viability. Controls enable the transfection efficiency and plate-plate variation to be analysed. We performed the siRNA screen in duplicate in two cell lines, RKO APC wt control 7_1 and RKO APC mutant 2_6.

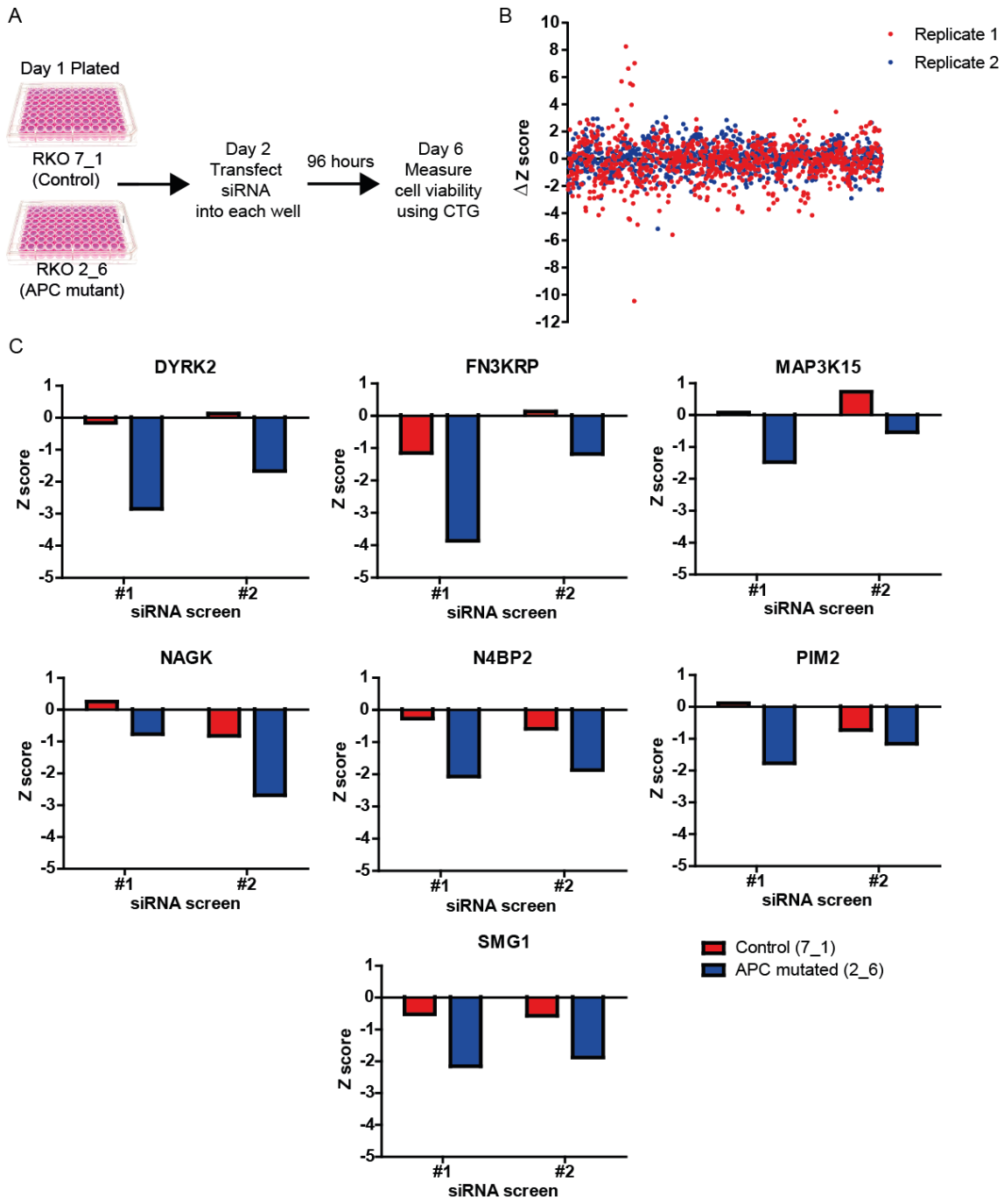

Figure 31 siRNA screen identifies seven potential hit genes

A) Schematic showing the format of the siRNA screen targeting 720 kinases and kinase related genes. B) ΔZ scores for all siRNA in the screen plotted for both screen replicates to illustrate the spread of the data. C) The seven potential hits identified from the siRNA screen. The Z score from both replicate 1 and 2 were plotted for both cell lines. Control cell line RKO 7_1 (red) and APC mutant cell line RKO 2_6 (blue).

Figure 31A shows a schematic of the siRNA screen. On day 1 both cell lines were plated at 2000 cells/well. After 24 hrs the siRNA library was transfected into both cell lines using the transfection reagent RNAimax, the media was changed 4-5 hours later to reduce toxicity from the transfection reagent. On day 6 we used the ATP-based luminescence assay, CellTiter-Glo (CTG) to analyse cell viability. To ensure all the siRNA targeting different genes had time to be effective due to the variation in protein turn over time, we measured cell viability 96 hours post transfection. The luminescence readings were then log transformed and normalised to the median signal per plate. Next the values were standardised by calculating Z scores, this measure tells us how many standard deviations the value is from the mean, this gives a value which enables us to understand the effect of the siRNA compared to the rest of the siRNA in the screen. We used a variation known as robust Z score to reduce sensitivity to outliers, by using the median and median absolute deviation (MAD) instead of mean and standard deviation in the calculation (Birmingham et al. 2009). We then compared the Z scores between the control RKO 7_1 and the APC mutant RKO 2_6 cell lines, by calculating the ΔZ score. To classify an siRNA as a potential hit we excluded any siRNA which resulted in more growth in the controls (using the Z score values) and the siRNA required a ΔZ score of below -1.5.

	ΔZ score	
	#1	#2
DYRK2	-2.6865	-1.7969
FN3KRP	-2.7146	-1.3204
MAP3K12	-1.9726	-0.5550
NAGK	-1.0286	-1.8705
N4BP2	-1.7935	-1.2834
PIM2	-1.8761	-0.4296
SMG1	-1.6225	-1.3109

Table 11 ΔZ score for the potential hit genes identified

shown for each siRNA screen replicate

Figure 31B shows the spread of the ΔZ score for each siRNA in each repeat of the screen performed. We identified seven potential hits with a lower Z score in RKO 2_6 compared to RKO 7_1 (Figure 31C) and table 11 shows the ΔZ score for each replicate. The potential hit genes were dual-specificity tyrosine (y) phosphorylation regulated kinase 2 (DYRK2), fructosamine 3 kinase related protein (FN3KRP), mitogen activated protein kinase kinase kinase 12 (MAP3K12), N-acetylglucosamine kinase (NAGK), NEDD4 binding protein 2 (N4BP2), proviral integrations of moloney virus 2 (PIM2) and suppressor with morphogenetic effect on genitalia (SMG1).

Gene	Function	Reference
DYRK2	Activate apoptosis, controlling cell cycle and inhibit metastasis	(Nihiraa & Yoshidaa 2015; Yan et al. 2016)
FN3KRP	Potential role in metabolism	(Conner et al. 2005)
MAP3K12	Regulator of neuronal degeneration	(Huntwork-Rodriguez et al. 2013)
NAGK	Part of the hexosamine biosynthetic pathway	(Yamamoto & Yamamoto 2015)
N4BP2	Potential role in repair or recombination	(Watanabe et al. 2003)
PIM2	Involved in cell survivial and proliferation	(Zhang et al. 2015)
SMG1	Nonsense- mediated mRNA decay, responding to cellular stress, telomere integrity, apoptosis, responses to hypoxia and regulating the G1/S checkpoint.	(Gubanova et al. 2013)

Table 12 Summary of the potential siRNA hits

The potential hits from the siRNA screen have a range of functions and some have been linked to cancer and more specifically CRC (roles summarised in table 12). DYRK2 is a member of the dual specificity kinase family, phosphorylating both serine/threonine and tyrosine substrates (Yan et al. 2016). DYRK2 has been shown to activate apoptosis, control cell cycle progression through regulating the degradation of c-jun and c-myc and inhibiting metastasis (Nihiraa & Yoshidaa 2015; Yan et al. 2016). It is thought to act as a tumour suppressor in many cancers including CRC, where DYRK2 has been shown to be down regulated in CRC tissues (Yan et al. 2016). FN3KRP has not been previously linked to cancer and is thought to be a housekeeping gene with an important role in metabolism, potentially deglycating enzymes (Conner et al. 2005). MAP3K12 has not been linked to cancer and is thought to be a regulator of neuronal degeneration (Huntwork-Rodriguez et al. 2013). NAGK is a kinase converting N-acetylglucosamine (GlcNAc) to GlcNAc–Phosphate which is either processed to fructose-6-phosphate or to UDP-GlcNAc (Yamamoto & Yamamoto 2015). This forms part of the hexosamine biosynthetic pathway, responsible for processing 2-5 % of glucose into compounds used for glycosylation (most glucose is processed by glycolysis) (Vasconcelos-Dos-Santos et al. 2017). The hexosamine pathway has been linked to CRC with key components being upregulated and aberrant glycosylation has been reported to promote oncogenic transformation (Yamamoto & Yamamoto 2015). The N4BP2 kinase has not been directly linked to CRC. It has been shown to interact with Bcl-3 and p300/CBP and might have a role in DNA repair or recombination

(Watanabe et al. 2003). PIM2 has been implicated in a range of human cancers. It is involved in cell survival and proliferation. PIM2 is mostly increased in hematologic malignancies and prostate cancer (Brault et al. 2010). Recently PIM2 has been shown to be highly expressed in CRC and promotes tumourigenesis by upregulating aerobic glycolysis through mTOR (Zhang et al. 2015). SMG1 has many cellular roles including; NMD, responding to cellular stress, telomere integrity, apoptosis, responses to hypoxia and regulating the G1/S checkpoint. Additionally, SMG1 may play a role as a tumour suppressor in HPV-positive head and neck squamous cell carcinoma and acute myloid leukemia (AML) (Gubanova et al. 2012; Gubanova et al. 2013; Du et al. 2014).

As discussed above the roles of the potential hits are varied and not all are well characterised, interestingly some have already been linked to tumourigenesis. Current understanding of the genes helps to hypothesise potential mechanisms, although the genes could behave differently in different cellular contexts.

1.2 Validation of the potential hit genes from the siRNA kinase screen

1.2.1 Validation of the potential hit genes using a validation plate

To determine whether our potential hit kinases are synthetically lethal in our APC mutated cells, we initially carried out a secondary siRNA screen containing five siRNA against each of the following seven potential hit genes; DYRK2, FN3KRP, MAP3K15, NAGK, N4BP2, PIM2, SMG1. The secondary siRNA screen contained the same SMARTpool siRNA used in the screen and the four deconvoluted siRNA, which make up the SMARTpool. To validate the identified potential hits, we followed the same protocol used in the screen. We plated 2000 cells/well in 96 well plates, transfected the cells with the five different siRNA targeting each kinase and measured cell viability using CTG, 96 hours post transfection. To enable us to assess transfection efficiency we transfected a negative control referred to as non-targeting siRNA (siCON) and a positive control targeting PLK1 (siPLK1). For the potential hit kinases to validate, we required at least two siRNAs to cause a greater level of decreased cell viability in the APC mutated RKO 2_6 in comparison to the control RKO 7_1. The analysis is different to the screen because we do not normalise to the plate median (which is required to calculate Z scores), instead we calculate survival fractions upon siRNA transfection. To calculate the survival fraction, we normalised the siKinase CTG values to the average of the siCON CTG values.

Figure 32 shows the combination of two independent experiments transfecting RKO 7_1 and RKO 2_6 with the siRNA in the validation plate. Silencing three out of the seven genes showed a slight difference in cell viability between RKO 7_1 and RKO 2_6, for two or more of the siRNA targeting each kinase. Two deconvoluted siRNA targeting DYRK2 (siDYRK2*1 and siDYRK2*2) and the SMARTpool decreased survival by 10-20 % in the APC mutant RKO 2_6 cells in comparison to RKO 7_1. Two of the deconvoluted siRNA (siDYRK*3 and siDYRK*5) do not cause a greater decreased cell viability in RKO 2_6 compared to RKO 7_1. Three of the deconvoluted siRNA targeting NAGK (siNAGK*1, siNAGK*4 and siNAGK*17) show a 10-20 % greater decrease in survival in RKO 2_6 compared to RKO 7_1. We do not see an effect with the siNAGK pool, this could be explained by the significant toxicity seen when siNAGK*3 is transfected alone. One of the deconvoluted siRNA (siN4BP2*3) and the pool cause a 5-10 % greater reduction in survival in the RKO 2_6 compared to RKO 7_1. None of the siRNA in the secondary screen, targeting FN3KRP, MAP3K15, PIM2 and SMG1 cause a larger decrease in survival in the RKO 2_6 compared to RKO 7_1. Unfortuanetly the effects seen are not consistant or large enough and therefore this data does not support any of the genes validating as hits.

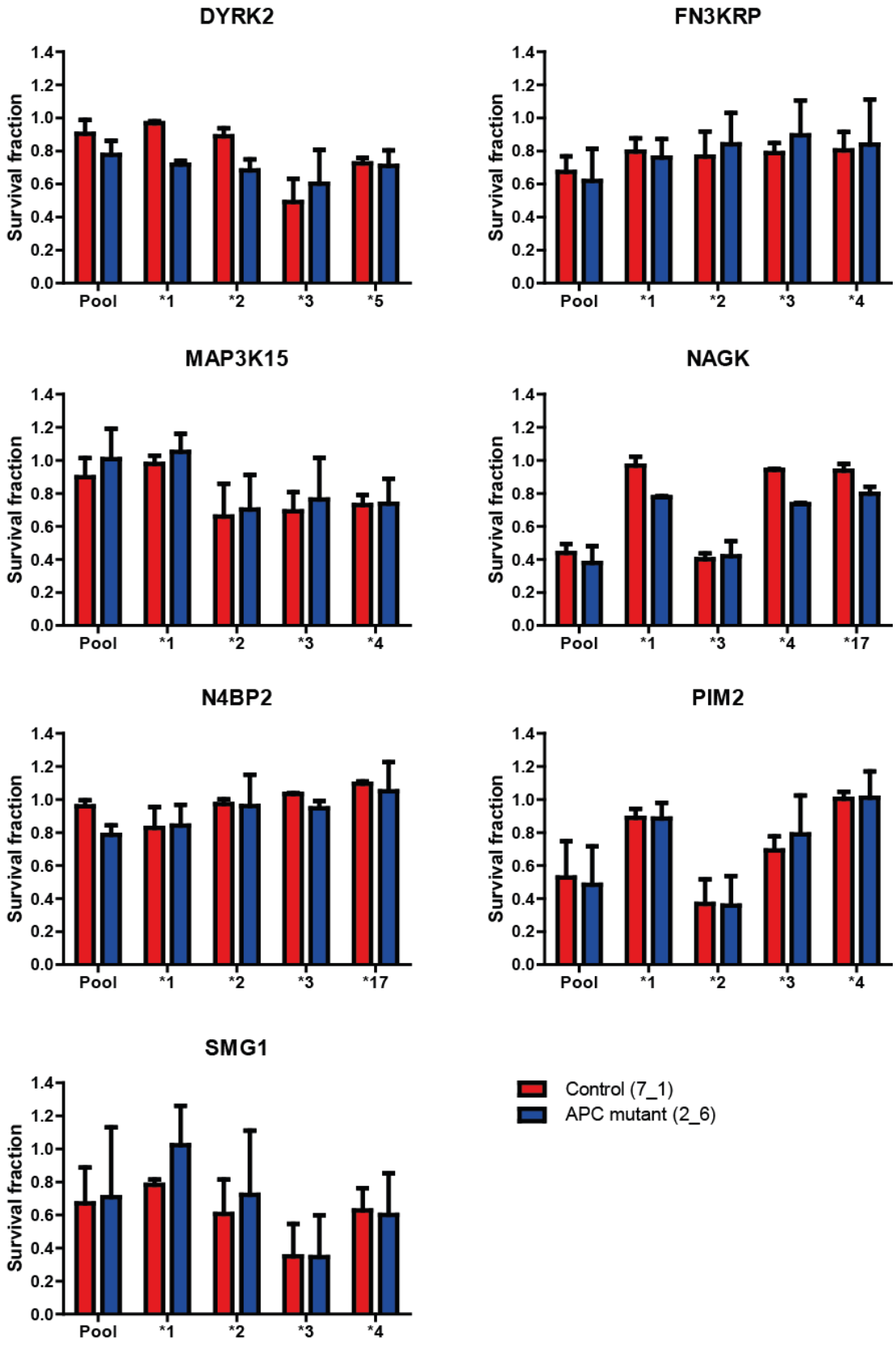

Figure 32 Validation plate in RKO 2_6

Validation of the potential hits identified from the screen using the SMARTpool siRNA (used in the screen) and the four deconvoluted siRNA in 96 well plates. CTG read 96 hours post transfection. Results are from two repeats and error bars show SEM. Control cell line RKO 7_1 (red) and APC mutant cell line RKO 2_6 (blue). Two way anova (post hoc Bonferroni) performed for each and all ns.

1.2.2 Validation in new single colony selected cells

Having identified residual full length APC in the RKO 2_6 cell line (as discussed in results chapter 1, section 4.3), we hypothesised that potentially the residual full length APC may have influenced the results from the secondary siRNA screen. To rule this out, we carried out the secondary screen as above in the new single colony selected cell lines RKO 2_21, RKO 2_22, RKO 2_30 and RKO 2_36 (Figure 33). Upon siRNA transfection, the four APC mutant cell lines show varying sensitivities to the siRNA targeting the seven potential hit kinases. For the siRNA targeting DYRK2 we observed a 5-20 % reduction in survival for both siDYRK2*1 and siDYRK2*2 in both RKO 2_21 and RKO 2_22 in comparison to the APC wt RKO 7_1 and RKO 7_2 cell lines. Upon silencing of NAGK in the new APC mutant cell lines, we observed that siNAGK*1, siNAGK*4 and siNAGK*17 were the most effective in RKO 2_21 and RKO 2_22, causing a 5-20 % reduction in survival compared to the controls RKO 7_1 and RKO 7_2. Silencing N4BP2 is most effective in RKO 2_21 which shows a 5-10 % reduction in survival compared to the controls with four of the siRNA targeting N4BP2 (SMARTPool, siN4BP2*2, siN4BP*3 and siN4BP2*17). siRNA targeting FN3KRP, MAP3K15 and SMG1 do not decrease survival in RKO APC mutant lines compared to RKO 7_1. Previously we did not see an effect in PIM2 however in the clone RKO 2_21 we see a 10-20 % reduction in survival for two of the deconvoluted siRNA (siPIM2*1 and siPIM2*4) compared to the controls RKO 7_1 and RKO 7_2.

The results are similar to the secondary siRNA screen in the original APC mutant RKO 2_6 cell lines. Therefore we concluded that removal of the residual full length APC had not increased the effect on cell viability when silencing the potential hit genes in the APC mutant lines. Taken together upon analysis of the results from the secondary screen performed in all the cell lines we conclude that none of the potential hit genes validated.

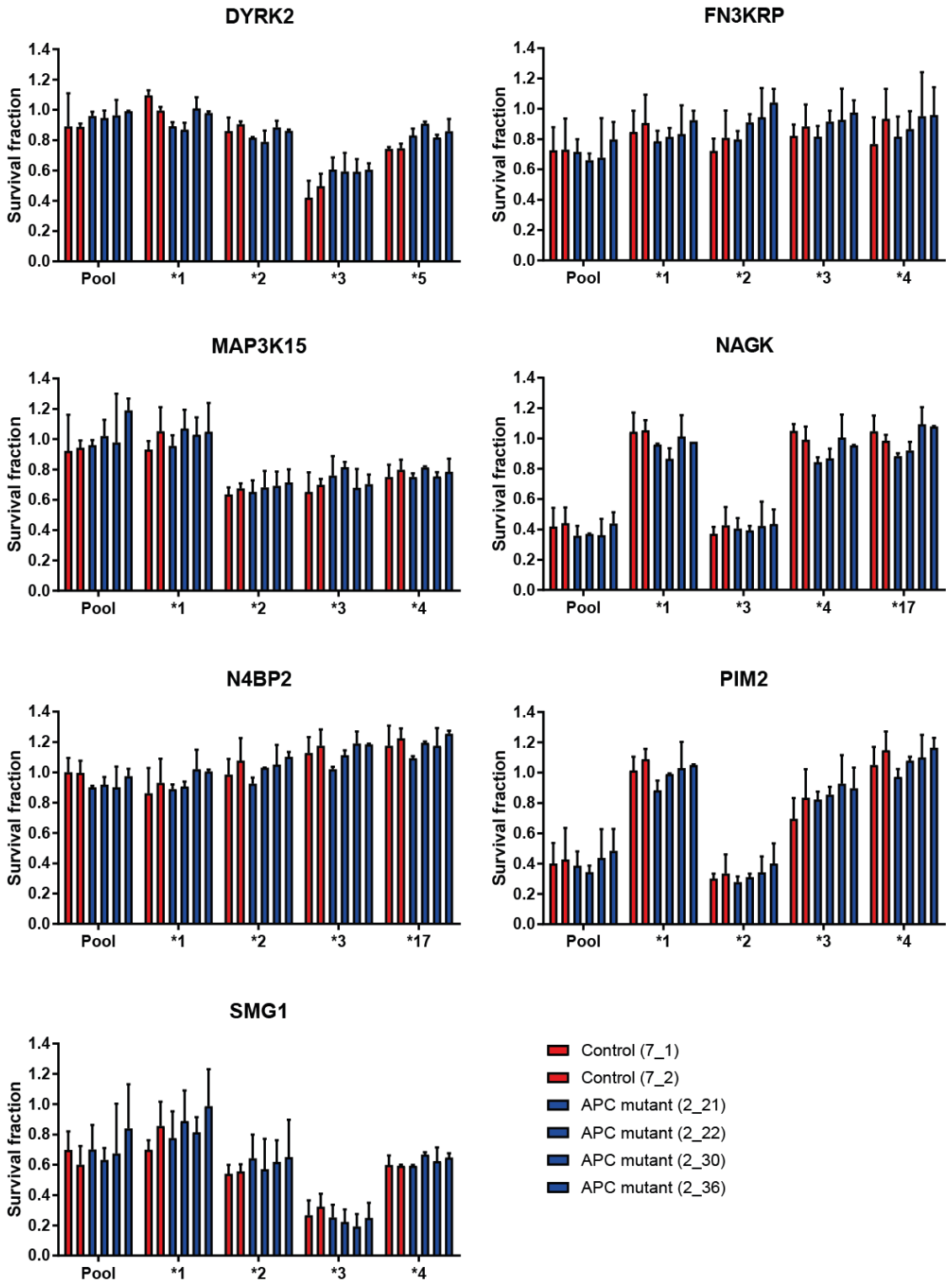

Figure 33 Validation plate in RKO 2_21, RKO 2_22, RKO 2_30 and RKO 2_36

Validation of the hits identified from the screen by transfecting the SMARTpool siRNA (used in the screen) and the four deconvoluted siRNA in the new cell lines, performed in 96 well plates. CTG read 96 hours post transfection. Results are from two repeats and error bars show SEM. Each bar for each siRNA is arranged in the same order as listed in key; Control cell line RKO 7_1 and RKO 7_2 (red) and APC mutant cell lines RKO 2_21, 2_22, 2_30 and 2_36 (blue). Two way anova (post hoc Bonferroni) performed for each and all ns.

1.3 Further investigation into the silencing of DYRK2, NAGK and N4BP2

Upon analysis of both secondary screens performed in all cell lines, the genes DYRK2, NAGK and N4BP2 when silenced with siRNA, cause a slight reduction in survival in our RKO APC mutant lines in comparison to the APC wt control cells. We further investigated this by individually silencing the three genes and measuring cell viability at both 72 hours and 96 hours post transfection using CTG (Figure 34A). This analysis would enable us to determine whether we had missed the synthetic lethal effect when previously validating. The primary and secondary screens were both analysed at 96 hours. Interestingly for all six of the siRNA targeting the three genes we see greater effects at 96 hours (Figure 34A). The two individual siRNA targeting NAGK have different effects on cell viability between the APC wt and APC mutant lines. The deconvoluted siRNA siNAGK*1 has the same effect on cell viability between the APC wt and APC mutant lines, in comparison the second siRNA siNAGK*4 causes a 5-10 % reduction in survival in the APC mutant lines compared to the APC wt at 96 hours post transfection. The deconvoluted siRNA targeting DYRK2 (siDYRK2*1 and siDYRK2*2) do not cause a greater decrease in cell viability in the APC mutant lines compared to the control cell lines at either 72 or 96 hours. Both siN4BP2*2 and N4BP2 SMARTpool cause a 5-10 % reduction in cell viability in the APC mutant lines RKO 2_22, RKO 2_30 and RKO 2_36 compared to the APC wt controls.

Throughout the validation of NAGK, DYRK2 and N4BP2 silencing these genes has inconsistently caused a slight decrease in cell viability in the APC mutant lines, in comparison to the wildtype APC cell lines and therefore these potential hit genes do not validate. Unfortunately to utilise this effect in the clinic the difference in cell viability needs to be consistantly greater because our aim is to selectively cause loss of cell viability only to the APC mutant cells, leaving the APC wt cells unharmed by the treatment. To further understand our results we could analyse the effectiveness of each siRNA to silence the target gene. We would collect lysates 96 hours after transfection with each siRNA and analyse protein levels of the target gene by western blotting. If the level of the protein has not significantly reduced then this could explain the small effects seen on cell viability when using the siRNA.

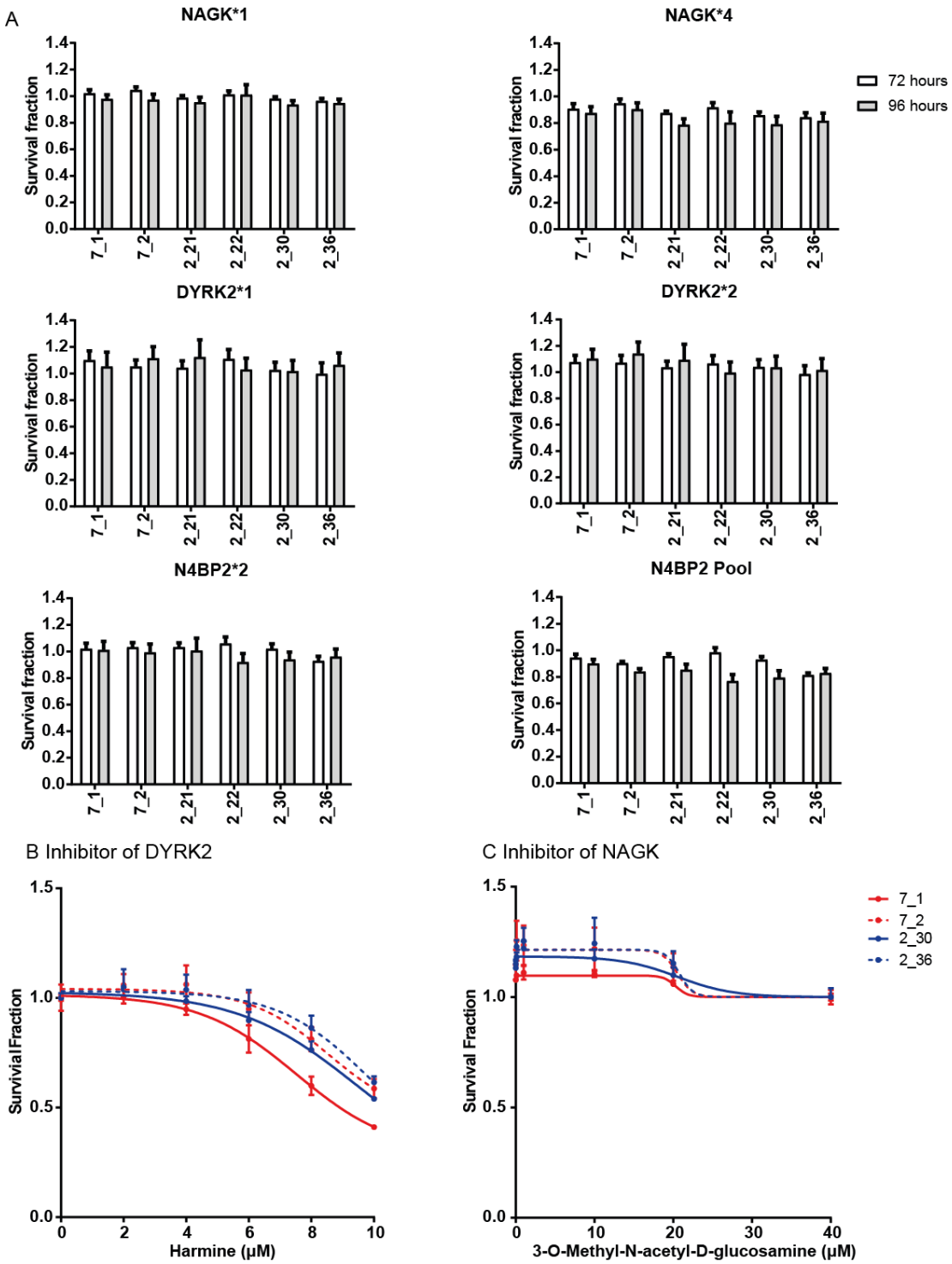

Figure 34 Further investigation into the effect of silencing NAGK, DYRK2 and N4BP2

A) Transfection of two siRNA against each gene and read 72 hours (white bars) and 96 hours (grey bars) post transfection, performed in 96 well plates. Experiments performed twice, error bars are SEM. Two way anova (post hoc Tukey) was performed and all ns. B) Dose response curve for harmine with six doses, experiment performed twice, representative shown, error bars are SD. Drugged twice, total treatment time 96 hours. Control cell line RKO 7_1 and 7_2 (red) and APC mutant cell line RKO 2_30 and RKO 2_36 (blue) C) Dose response curve for 3-O-Methyl-N-acetyl-D-glucosamine with 6 doses, experiment performed twice, representative shown, error bars are SD. Drugged twice, total treatment time 96 hours. Control cell line RKO 7_1 and 7_2 (red) and APC mutant cell line RKO 2_30 and RKO 2_36 (blue).

In addition to validating with siRNA we also tested commercially available inhibitors targeting the hit kinases. We used the DYRK2 inhibitor, harmine and the NAGK inhibitor, 3-O-Methyl-N-acetyl-D-glucosamine. Compounds can be more effective at inhibiting the function of the kinase. siRNA reduces the level of the protein but any residual protein left could be sufficient to fulfill the given role, preventing an effect being seen. We treated our cell lines with increasing doses of harmine and 3-O-Methyl-N-acetyl-D-glucosamine for 96 hours and measured cell viability using CTG. We found no selectivity between our controls (7_1 and 7_2) and APC mutant cell lines (RKO 2_30 and RKO 2_36) (Figure 34B/C). Further work is required to establish if the drugs are efficient at targeting DYRK2 and NAGK in our cell lines. Taken together the validation data shows we did not identify any genes upon silencing to be synthetically lethal with the APC mutation in our *in vitro* model.

2 mTOR is not synthetically lethal in our RKO APCmut lines

2.1 siRNA targeting mTOR and FLT3 do not show selectivity

Upon completion of the siKinome synthetic lethal screening in our APC wt and mutant cell lines, we next attempted to validate the potential hits and unfortunately none of these validated. Therefore in parallel we investigated the literature, to determine whether there were any studies highlighting potential synthetic lethality with mutant APC that we could investigate in our newly generated cell lines. A study in mice suggested mutant APC was synthetically lethal with mTOR pathway inhibition (Faller et al. 2014). Furthermore, our initial analysis of the siKinome screen identified two siRNA targeting components of the mTOR pathway, which showed a small degree of synthetic lethality in our APC mutant cells. These kinases were the fms related tyrosine kinase 3 (FLT3), which is upstream of mTOR and also mTOR itself (Figure 35A). Based on these two findings, we decided to investigate this potential synthetic lethal relationship further. The availability of mTOR inhibitors made this a potential means of therapeutically targeting this pathway in APC mutant CRC patients. Firstly we attempted to validate our findings by silencing FLT3 and mTOR using SMARTpool siRNA in the APC wt control cells (RKO 7_1 and RKO 7_2) and the APC mutant cell lines (RKO 2_30 and RKO 2_36). We measured cell viability using CTG, 96 hours post transfection and calculated survival fractions as described in section 1.2 (Figure 35B). The siRNA targeting FLT3 and mTOR did not cause a greater effect on cell viability in the APC mutant cell lines compared to the controls.

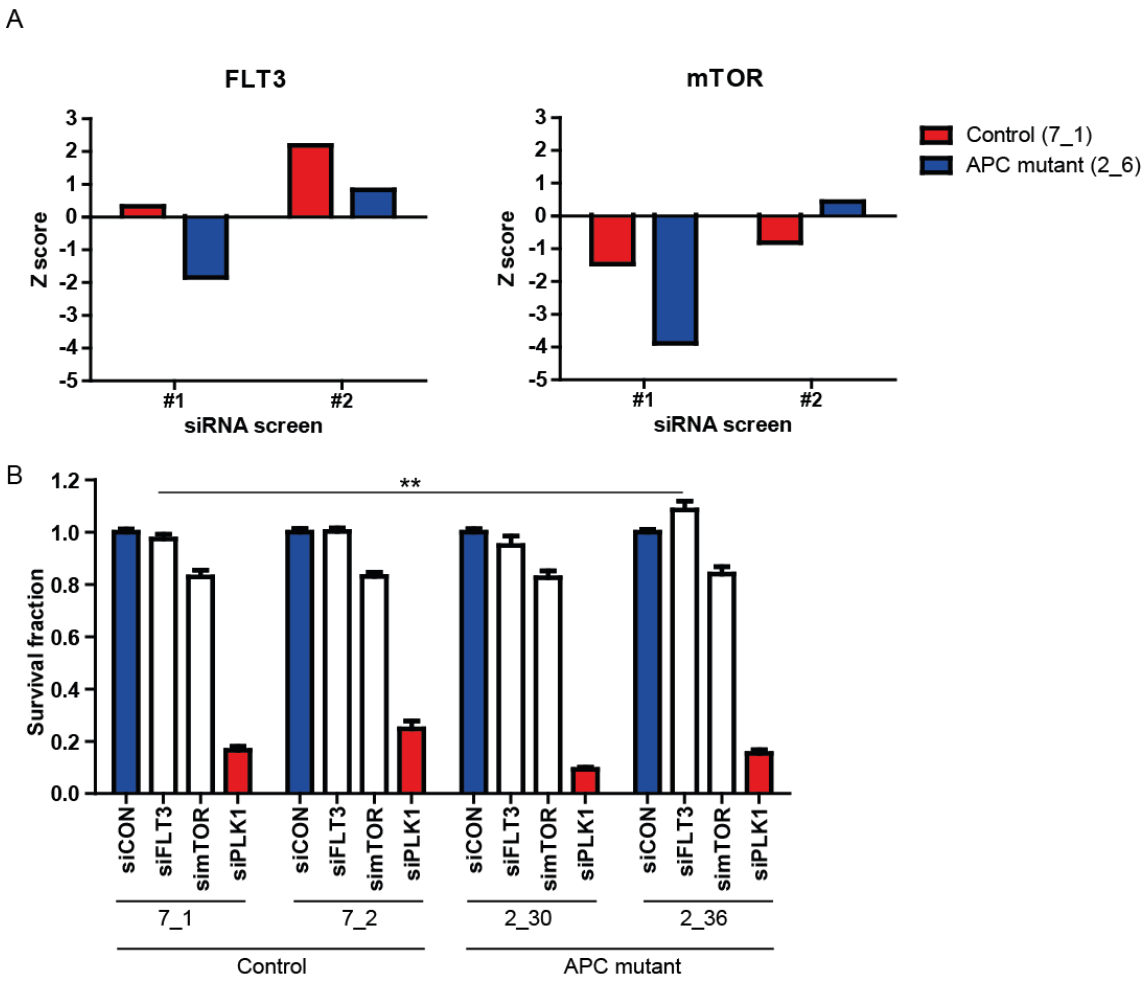

Figure 35 Validation of FLT3 and mTOR

A) Z scores for FLT3 and mTOR from both replicates of the siRNA screen. Control cell line RKO 7_1 (red) and APC mutant cell line RKO 2_6 (blue) B) Survivial fractions shown for siRNA targeting non-targeting control (siCON), FLT3 (siFLT3), mTOR (simTOR) and PLK1 (siPLK1) 96 hours after transfection. siCON is negative control (blue) and siPLK1 is positive control (red). Experiment performed twice, error bars are SEM, 2 way anova (post hoc Bonferroni) performed (** p≤ 0.01).

2.2 mTOR inhibitors do not show selectivity

To further assess the hypothesis that APC mutations are synthetically lethal with mTOR inhibition, we analysed the response of our RKO *in vitro* model cell lines to commonly used inhibitors of mTOR; rapamycin and ridaforolimus. To this end, we treated the APC mutant lines RKO 2_21, RKO 2_22, RKO 2_30 and RKO 2_36 and the APC wt control cells RKO 7_1 and RKO 7_2 with increasing concentrations of either rapamycin or ridaforolimus (Figure 36A). We analysed cell viability after 96 hrs and determined that our APC mutant cells were not more sensitive to rapamycin or ridaforolimus in comparison to the APC wt control cells. To further investigate the effect of mTOR inhibition and APC mutations, we decided to test a panel of CRC cell lines comprising of a range of APC wildtype and APC mutant cell lines. Figure 36B shows dose response curves for rapamycin and ridaforolimus in the following APC wildtype cell lines (HCT116, RKO and SW48) and APC mutant cell lines (DLD1, HT29 and SW620). To highlight the differences in sensitivity to the mTOR inhibitors, figure 36C shows the survival fractions for each cell line at 30 μM. The two most sensitive lines are the APC mutant DLD1 followed by APC wildtype RKO. Upon analysis of our CRC cell line panel, we did not observe any correlation between APC mutation and mTOR inhibitor sensitivity. Taken together, based on our siRNA and inhibitor analysis, our data suggests there is no link between the presence of an APC mutation and response to rapamycin and ridaforolimus in our panel of CRC cell lines.

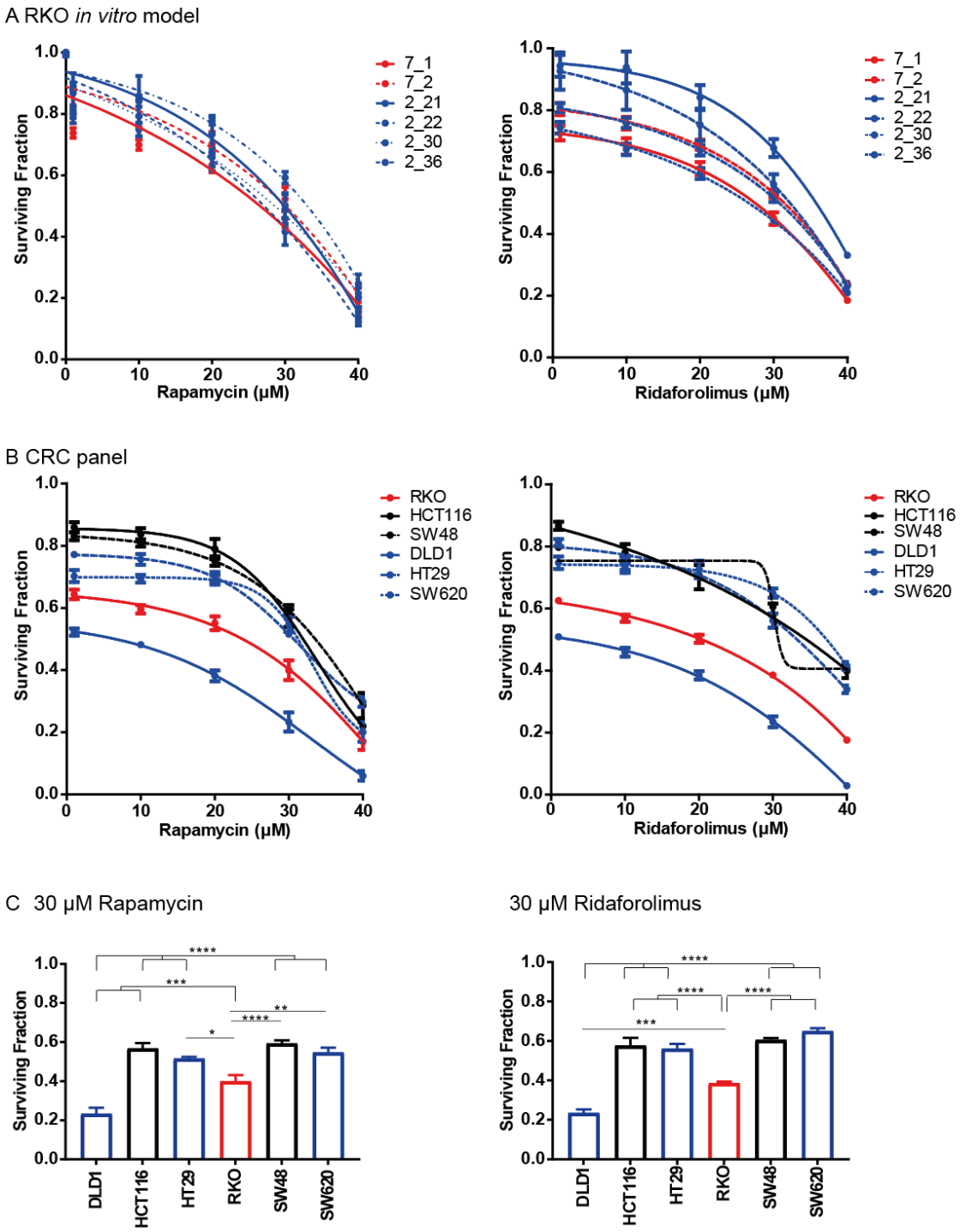

Figure 36 Analysing the sensitivity to rapamycin and ridaforolimus

A) Dose response curves for rapamycin and ridaforolimus in the RKO controls (red) and RKO APC mutant cell lines (blue) 96 hours of treatment in 96 well plate. Experiment performed three times and error bars are SEM. B) Dose response curves for rapamycin and ridaforolimus in the CRC panel 96 hours of treatment in 96 well plate. APC and β-catenin wildtype cell lines (red), APC wildtype, β-catenin mutant cell lines (black) and APC mutant cell lines (blue). Experiment performed three times and error bars are SEM. C) Comparison of the survival fractions after treatment with 30 μM rapamycin and ridaforolimus in the CRC panel. Error bars are SEM and one way anova (post hoc tukey) performed (* p≤ 0.05, ** p≤ 0.01, *** p≤ 0.001, **** p≤ 0.0001).

2.3 Correlation between mTOR protein levels and response to mTOR inhibitors

To determine whether the lack of sensitivity of our APC mutant cell lines to mTOR inhibition was due to different levels of mTOR expression in our panel of cell lines, we next immunoblotted whole cell lysates from our CRC panel and analysed levels of total mTOR and mTOR phosphorylated at serine 2448 (ser2448 p-mTOR). The serine 2448 residue of mTOR is phosphorylated by a protein downstream known as protein S6 kinase (S6K) and this is thought to have a role in regulating mTOR. Research suggests mTOR phosphorylated at ser2448 indicates activation of the mTORC1 complex (Rosner et al. 2010; Copp et al. 2010). Figure 37 shows the levels of total mTOR and ser2448 p-mTOR are generally correlated, such that when total mTOR was highly expressed, mTOR was highly phosphorylated at ser2448 in our CRC panel. HCT116 shows the highest expression level of both total mTOR and ser2448 p-mTOR. The cell lines most sensitive to rapamycin and ridaforolimus DLD1 and RKO have the lowest levels of total mTOR and the most sensitive line DLD1 additionally has the lowest level of ser2448 p-mTOR. Low levels in DLD1 and RKO of the vital pathway mTOR is likely to explain the sensitivity to mTOR inhibitors. The pathway is required for activating macromolecule synthesis, cell cycle progression, growth, metabolism, cytoskeletal organisation, cell survival and the inhibition of autophagy. Potentially reducing all these processes in the cell reduces the level of these functions below a threshold the cells can tolerate inducing cell death. In comparison a cell line highly expressing the mTOR pathway may still function even with a slight decrease in the processes controlled by mTOR. However, other factors must also be involved because the HT29 cell line has a similar level of total mTOR to RKO but is more resistant to rapamycin and ridaforolimus. To further investigate this work it would be interesting to see if the pattern was the same when analysing other phosphorylated forms of mTOR, such as ser2481 which is thought to indicate activation of mTORC2 (Copp et al. 2010).

Our data does not support a synthetic lethal relationship between mTOR inhibition and APC mutation. This may be due to the fact that this synthetic lethality may occur in a small therapeutic window early in the development of CRC. Faller et al. (2014) used two *in vivo* models; Lgr5Cre^{Er}APC$^{fl/fl}$ and APC$^{min/+}$. Lgr5Cre^{Er}APC$^{fl/fl}$ develop APC mutations just in Lgr5 positive stem cells (specific to colorectal epithelial cells) at codon 580 when induced with Cre recombinase and develop adenomas within four weeks (Shibata et al. 1997; Faller et al. 2014). The APC^{min} mice have an APC mutation at codon 850 and develop ~30 polyps in the small intestine (Young et al. 2013). Firstly the Lgr5Cre^{Er}APC$^{fl/fl}$ mice were treated 10 days after Cre induction with rapamycin for 30

days and this prevented the formation of any adenomas (Faller et al. 2014). Next both the Lgr5Cre^{Er}APC$^{fl/fl}$ and APC$^{min/+}$ were left to establish adenomas before treatment with rapamycin for 30 days began, rapamycin treatment resulted in a loss of clinical symptoms of disease and increased the lifespan of the mice compared to the control mice (Faller et al. 2014). Both *in vivo* models represent early stage disease and demonstrate the effectiveness of rapamycin treatment in mice. In comparison our human CRC cell lines are derived from patients with well established tumours and therefore, the selectivity may either only be effective in mice or at early stage disease. Further research would be needed to understand if this is the reason why we did not observe any synthetic lethal effect.

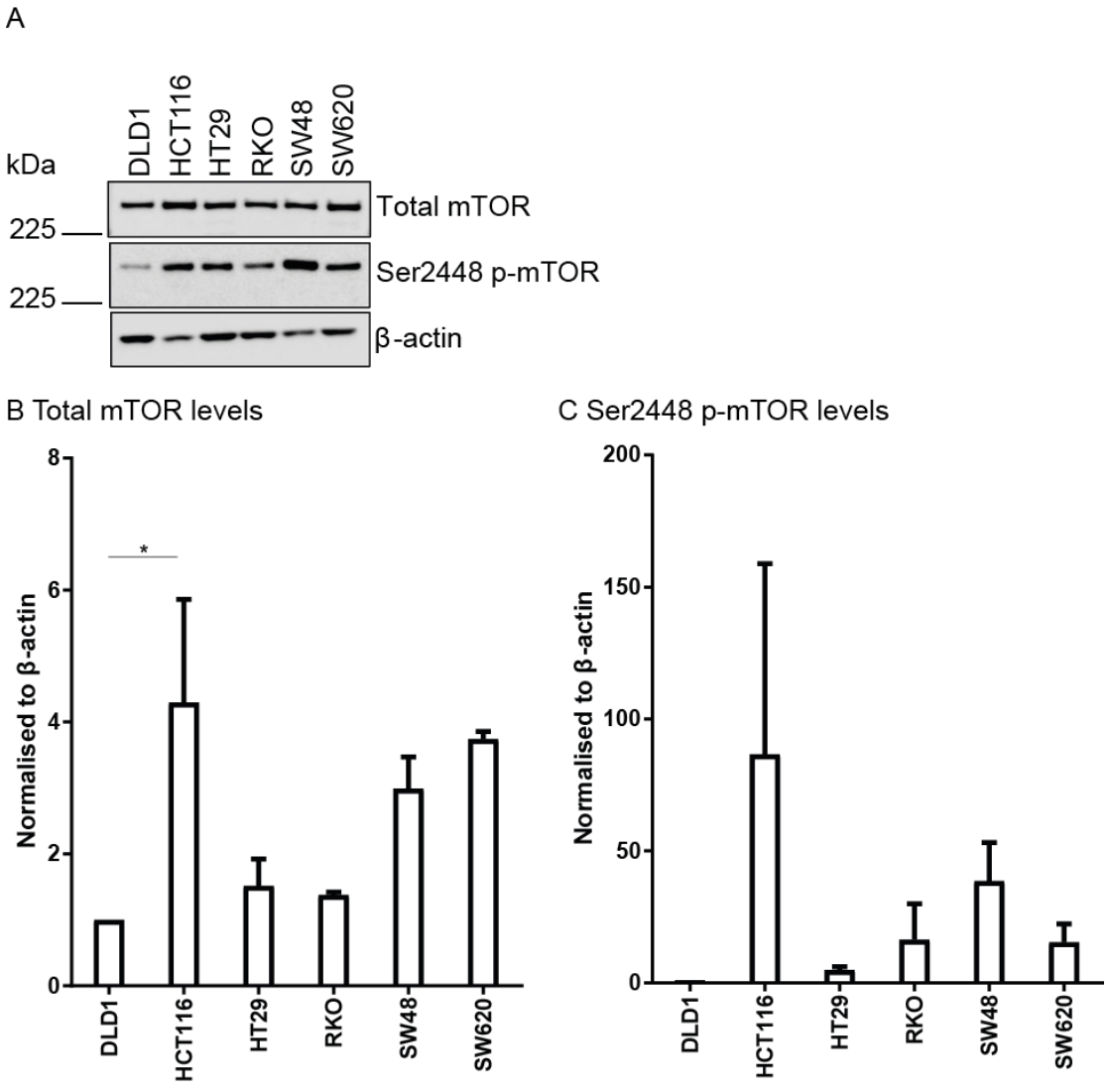

Figure 37 Protein levels of mTOR in the CRC panel

A) Whole cell lysates from the CRC panel were immunoblotted for total mTOR and ser2448 p-mTOR, β-actin used as a loading control. Three repeats were conducted, a representative is shown. B) C) show quantification from westerns in A) Density of bands was quantified and a % was calculated which was then normalised to % β-actin then DLD1. One way anova (post hoc Tukey) performed (* $p \leq 0.05$).

We have used our *in vitro* model of APC mutation to perform a siRNA screen for kinases and kinase related genes to identify genes synthetically lethal with the APC mutation. From the primary screen, we identified seven potential hit kinases, some with roles in cellular processes such as DNA recombination, cell proliferation, cell survival and metabolism. Some had interesting links with tumourigenesis, such as PIM2 which has been linked to many cancers including CRC. For the secondary screen we used the SMARTpool siRNA from the screen alongside the deconvoluted siRNA for each potential hit gene. From the validation none of the seven potential hits validated.

Two mTOR pathway components were potential hits in one of the siRNA screen replicates and researchers have suggested mTOR inhibition may be selectively lethal with APC mutation (Faller et al. 2014). Therefore, we decided to investigate this further and we found silencing mTOR and FLT3 with siRNA did not cause a greater decrease in cell viability in the APC mutant lines compared to the APC wt controls (RKO *in vitro* model). Additionally when performing dose response curves with the mTOR inhibitors rapamycin and ridaforolimus we did not see any discrimination between the APC mutant and APC wt lines (RKO *in vitro* model and CRC panel). The sensitivity to mTOR inhibitors in the CRC panel seemed to correlate with low mTOR levels and not *APC* status. We hypothesised that perhaps the use of mTOR inhibitors in APC mutant cancers has a small therapeutic window and this could be restricted to early tumour development.

We have explored a number of avenues from the siRNA screen against kinases in our RKO *in vitro* model. We did not identify any kinase genes synthetically lethal with the APC mutation.

Chapter 3 - A FDA-approved compound screen identified compounds showing synthetic lethality with mutant APC in our *in vitro* model

1 An FDA-approved compound screen identified compounds causing synthetic lethality with mutant APC in our *in vitro* model

1.1 Conducting the FDA-approved compound screen

To identify drugs causing synthetic lethal relationships with truncated APC in our *in vitro* model, we performed a compound screen testing 1120 FDA-approved drugs. The same setup was used in a study which identified Triamterene to be selectively lethal with DNA mismatch repair (MMR) deficiency in a range of tumour cells (Guillotin et al. 2017). Screening FDA-approved compounds is advantageous because the findings can be translated into the clinic more quickly because the safety profiles are already characterised. The FDA-approved compounds were aliquoted over 14 x 96 well plates and each plate contained controls including; media only and DMSO (<0.01 %). We performed the FDA-approved compound screen in triplicate in two cell lines, control APC wt RKO 7_1 and APC mutant RKO 2_36. On day 1 both cell lines were plated at 2000 cells/well and the following day the cells were drugged with the compound library. The cells were then re-drugged on day 4, and on day 6 cell viability was analysed using CellTiter-glo (CTG) (Figure 38A). The luminescence readings from the CTG were log transformed and normalised to the median signal per plate. Next Z scores were calculated to standardise the values. Z scores show how many standard deviations the value varies compared to the mean, indicating the effect of the compound on the cells in comparison to the rest of the data. In a compound screen most Z scores will be close to 0 indicating the effect of the compound on survival does not differ much from the mean, any outliers are likely to be potential hits (Figure 38B). We compared the Z scores between the control APC wt RKO 7_1 and APC mutant RKO 2_36 cell lines and compounds were selected as potential hits if the Z score was <-1.5 only in the APC

mutant RKO 2_36 cell line and in the APC wt RKO 7_1 cell line the Z score was close to 0.

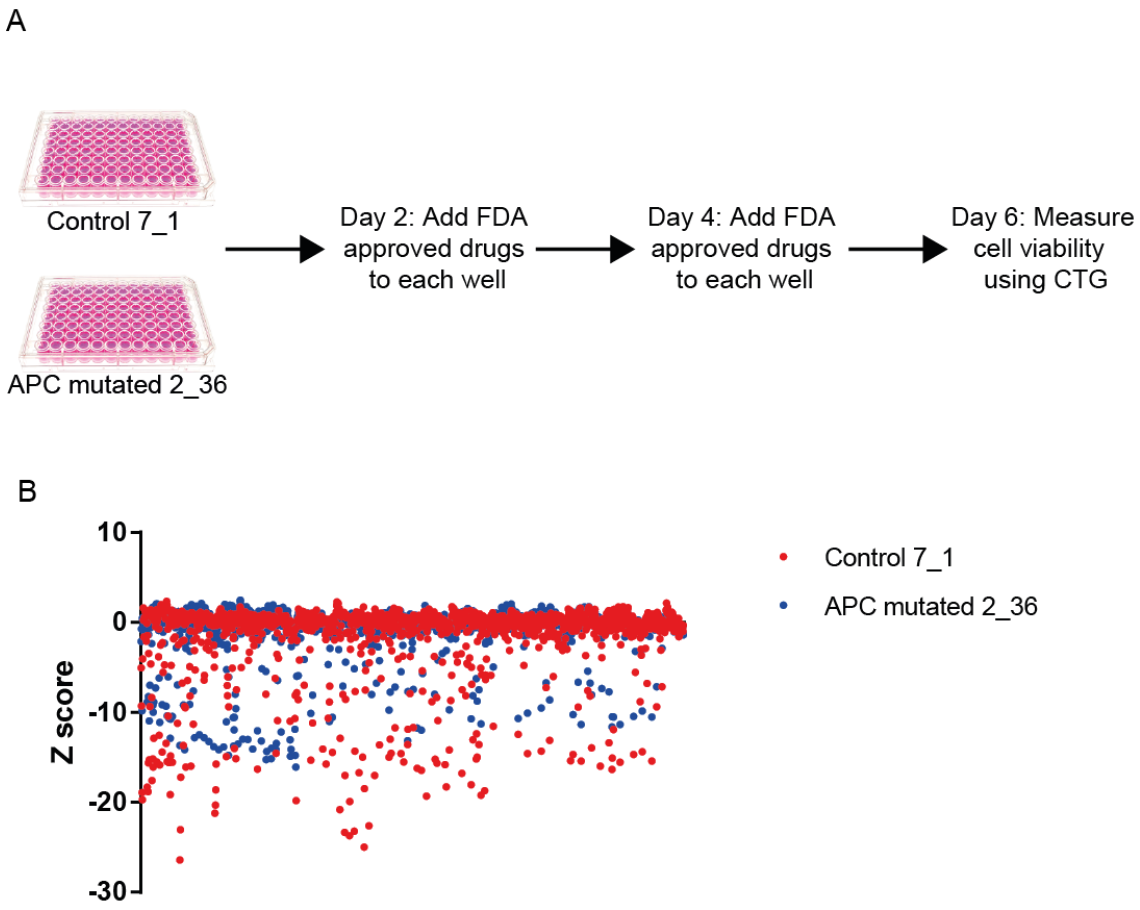

Figure 38 FDA-approved compound screen

A) Schematic showing the screen layout. The library was aliquoted over 14 x 96 well plates. On day 1 cells were plated, followed by drug treatment on day 2 and day 4. Then on day 6 cell viability was measured using CTG. B) The Z score values were plotted for each compound in the screen for both cell lines to illustrate the spread of data, results are from replicate 1. Control 7_1 shown in red and APC mutant 2_36 shown in blue.

1.2 Statins are synthetically lethal with mutated APC

From the FDA-approved compound screen we identified 11 potential hit compounds. A compound was identified as a potential hit if the Z score in the APC mutant 2_36 was <-1.5 and ideally the Z score in the APC wt 7_1 cell line was close to 0. The following drugs were selected as potential hits because they resulted in a lower Z score in the APC mutated RKO 2_36 cell line compared to the control cell line in the majority of repeats; tizanidine HCL, tolnaftate, troxipide and diclofenac potassium (Figure 39). We also chose the following compounds as potential hits because these drugs were very effective at causing greater loss of cell viability in the RKO 2_36 cell line compared to the control RKO 7_1 in the first repeat only, we hypothesised that the drugs may have degraded over the course of the repeats; losartan potassium, moxifloxacin hydrochloride, saxagliptin, mesalamine and desonide (Figure 39). Additionally, we selected two compounds from a family of drugs known as statins; lovastatin and mevastatin. Both compounds caused loss of cell viability in both the control and APC mutant cell lines, however the effect was greater in the APC mutant RKO 2_36 (Figure 39). We hypothesised that we could identify concentrations lower than the 10 μM used in the screen which would have less impact on the viability of the control cells, whilst significantly reducing the viability of the APC mutant lines.

The compounds identified as potential hits have a broad range of action, interestingly some of the compounds have been suggested to have chemopreventive effects. Tizanidine HCL is a α_2-adrenoceptor agonist and is used to treat muscle spasticity (Henney & Runyan 2008). Tolnaftate is an anti-fungal agent (Munguia & Daniel 2008). Troxipide is an anti-ulcer compound used to treat gastric ulcers or gastritis (Kusugami et al. 2000). Diclofenac potassium is an NSAID and NSAIDs are suggested to have chemopreventive effects (McNeely & Goa 1999; Rao & Reddy 2004). Losartan potassium is an angiotension II receptor antagonist and is used to treat hypertension and heart failure (Al-Majed et al. 2015). Moxifloxacin hydrochloride is an antibiotic (Keating & Scott 2004). Saxagliptin is a peptidase-4 inhibitor used to treat type 2 diabetes (Dhillon 2015). Mesalamine (also known as 5-ASA) is used to treat ulcerative colitis and crohns disease, mesalamine has also been suggested to have a chemoprotective effect (Criscuoli et al. 2013; Rousseaux et al. 2013). Desonide is a corticosteroid (Kahanek et al. 2008). Lovastatin and mevastatin are members of the statin compound family, commonly used to lower cholesterol in patients with cardiovascular disease or at high risk (Alberts 1990).

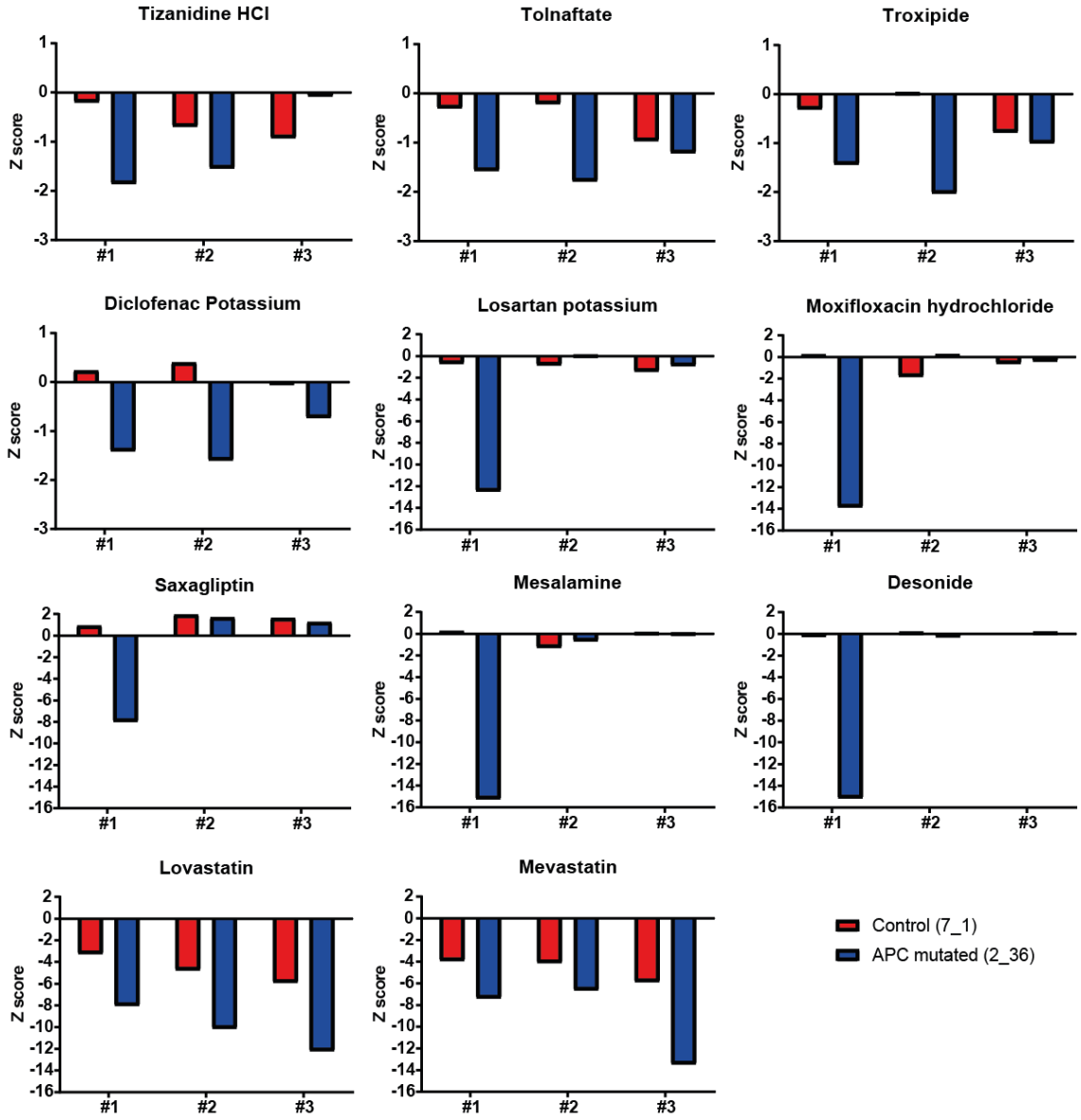

Figure 39 The 11 compounds selected as potential hits from the screen to validate

The Z scores for each potential hit compound are plotted for each cell line and each replicate of the screen. The control RKO 7_1 is shown in red and the APC mutant RKO 2_36 is shown in blue.

To validate the compounds as selectively lethal in APC mutant cells, we performed dose response curves in 96 well plates with a range of concentrations in our APC wt controls RKO 7_1, RKO 7_2 and APC mutant RKO 2_30 and RKO 2_36. We performed the validation using a similar treatment approach to the compound screen. We drugged the control and APC mutant cells on day 2 and day 4 and analysed cell viability using CTG after a total drug treatment of 96 hours. Nine of the eleven compounds did not show greater sensitivity in the APC mutant RKO 2_30 and RKO 2_36 compared to the control APC wt RKO 7_1 and 7_2 (Figure 40 and 41). Lovastatin and mevastatin validated as hits in our *in vitro* model, such that the APC mutant RKO 2_30 and RKO 2_36 were more sensitive to lovastatin and mevastatin than the APC wt control cells (Figure 42A). Additionally we identified concentrations lower than the concentration (10 μM) used in the screen which caused minimal loss of cell viability in the control cell lines, whilst still causing significant loss of cell viability in the APC mutant lines. Lovastatin was less potent than mevastatin. At a concentration of 4 μM lovastatin, the APC mutant lines were 40 % viable and controls were 100 %. At 4 μM mevastatin, the APC mutant cells were just 20 % viable whilst the controls were 80 %.

Additionally we performed dose response curves with another statin compound, simvastatin which is modified from lovastatin and known to show higher potencies (Alberts 1990). We altered the concentration range for the dose response curves and found the same sensitivity in the APC mutant cell lines (Figure 42B). With simvastatin treatment, we observed a significant difference between the APC wt and APC mutant cell lines at lower concentrations, such that at 2 μM we saw 20 % viability in the APC mutant lines and 90 % in the controls. From the FDA-approved compound screen testing 1120 compounds we have shown lovastatin and mevastatin validate, showing a synthetic lethal relationship with the APC mutation in our *in vitro* model. This synthetic lethal relationship also extends to a more potent statin, known as simvastatin.

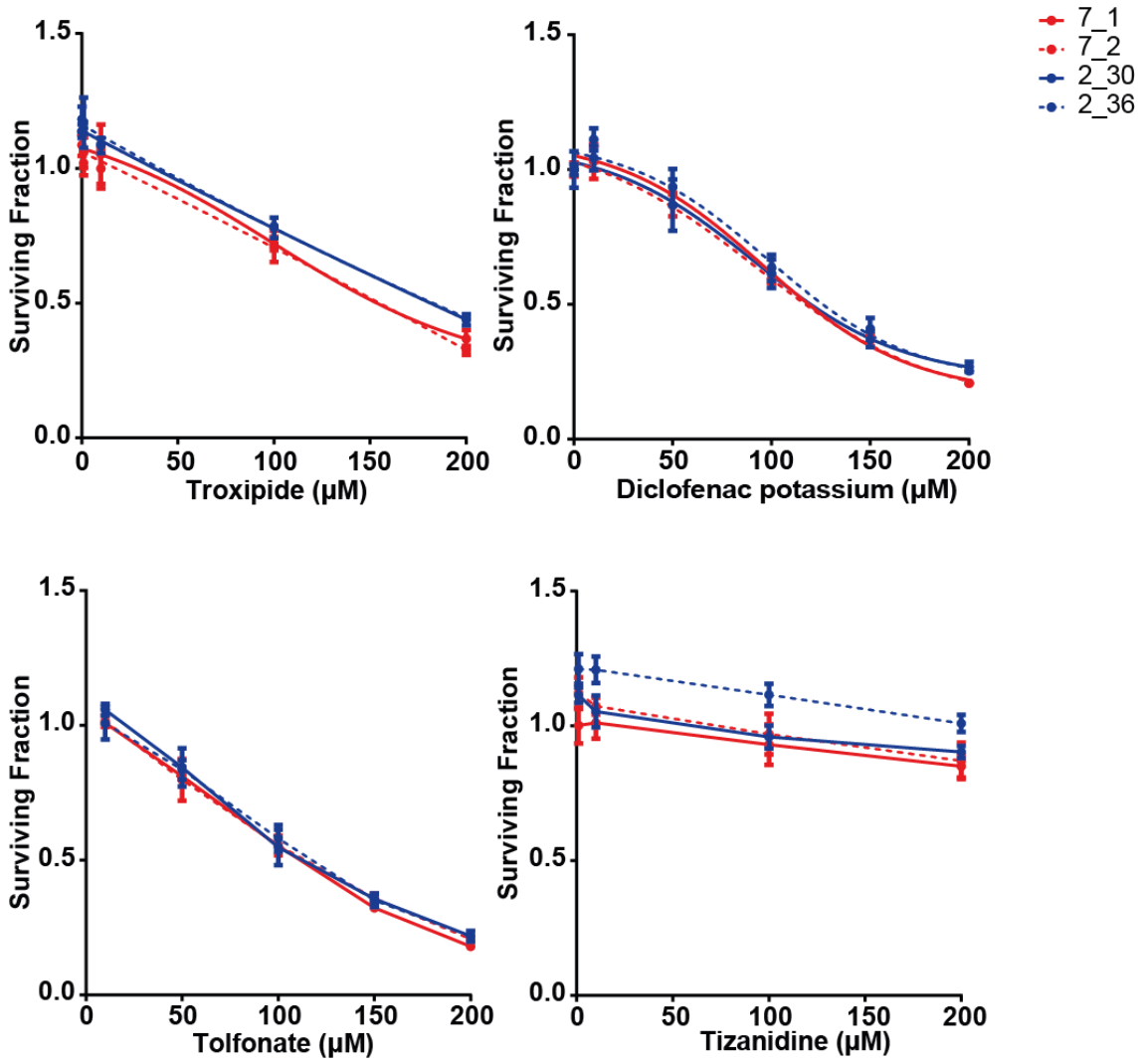

Figure 40 Validation of troxipide, diclofenac potassium, tolfonate and tizanidine

Drug dose response curves for troxipide, diclofenac potassium, tolfonate and tizanidine. Cells were plated in 96 well plates and treated with drug on day 2 and 4. After 96 hours of drug treatment CTG was used to measure cell viability. Survival fractions were calculated and plotted. The controls RKO 7_1 and RKO 7_2 are shown in red and the APC mutant RKO 2_30 and RKO 2_36 are shown in blue. Performed twice, a representative is shown, error bars are SD.

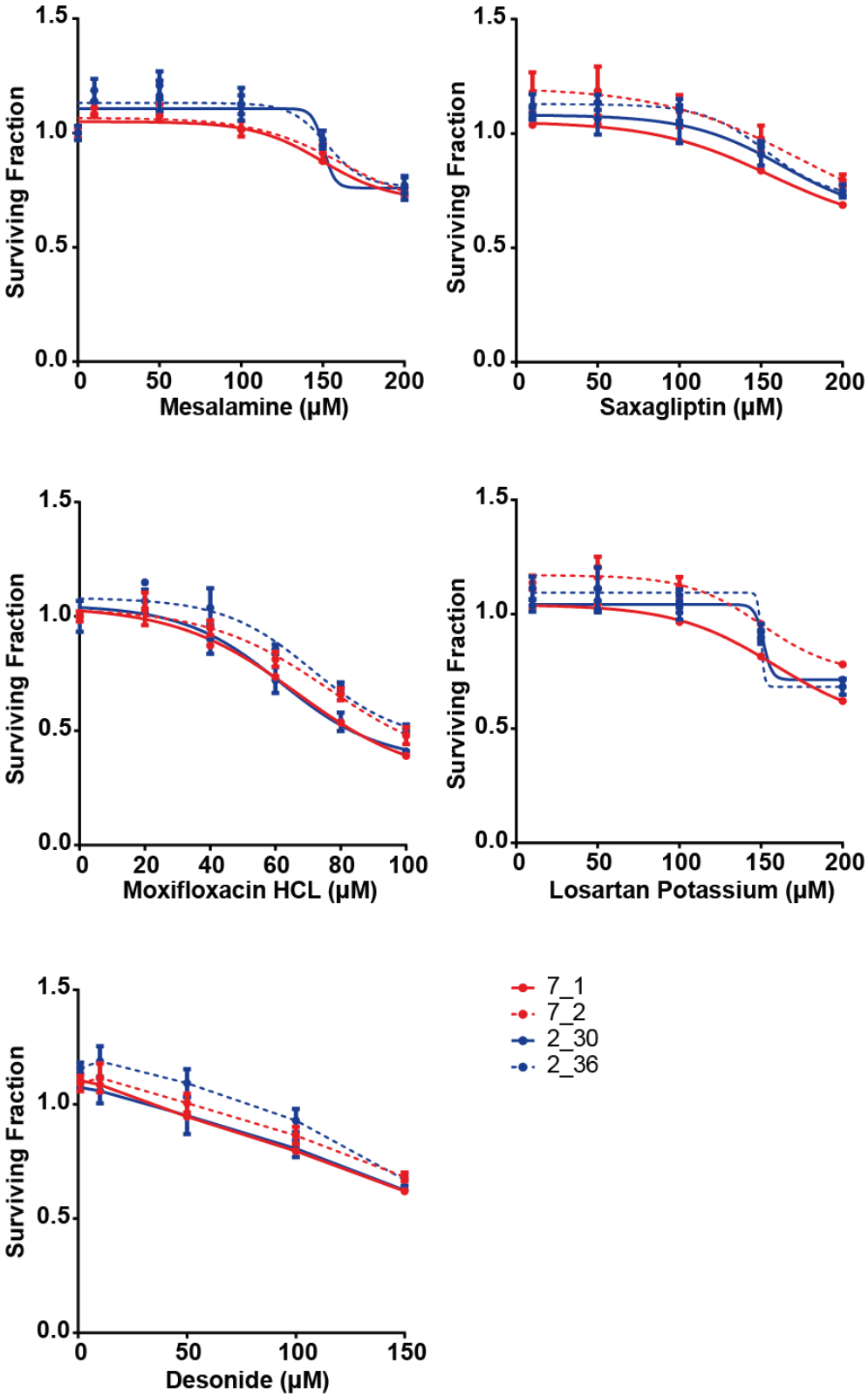

Figure 41 Validation of mesalamine, saxagliptin, moxifloxacin HCL, losartan potassium and desonide

Drug dose response curves for mesalamine, saxagliptin, moxifloxacin HCL, losartan potassium and desonide. Cells were plated in 96 well plates and treated with drug on day 2 and 4. After 96 hours of drug treatment CTG was used to measure cell viability. Survival fractions were calculated and plotted. The controls RKO 7_1 and RKO 7_2 are shown in red and the APC mutant RKO 2_30 and RKO 2_36 are shown in blue. Performed twice, a representative is shown, error bars are SD.

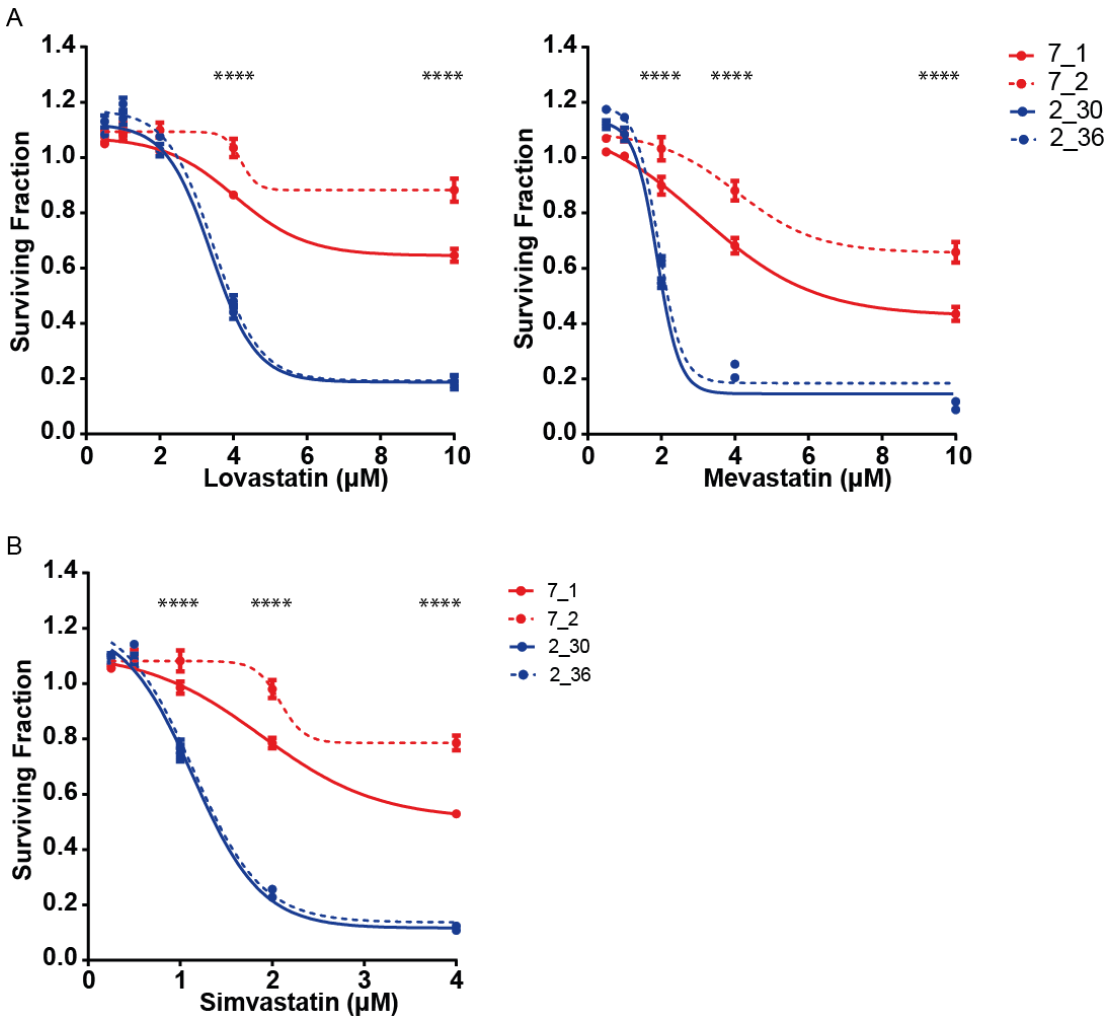

Figure 42 Validation of statins as synthetically lethal with the APC mutation

Dose response curves for three statins. Cells were plated in 96 well plates and treated with drug once, total drug treatment was for 96 hours. Cell viability was measured with CTG and survival fractions were calculated and plotted. Controls RKO 7_1 and RKO 7_2 shown in red, APC mutant RKO 2_30 and RKO 2_36 shown in blue. Graphs represent three experiments and error bars are SEM. Two way anova (post hoc Tukey) was performed (**** p≤ 0.0001) A) Graphs show lovastatin and mevastatin B) Graph shows simvastatin.

2 Statins cause a reduction in Wnt signalling in the APC mutant lines

Having identified statins as a drug family, causing a synthetic lethal relationship with the APC mutation in our *in vitro* model, we next investigated the mechanism of selectivity. A significant difference between our RKO control APC wt and RKO APC mutated lines was the level of Wnt signalling activation. Therefore, we began our mechanistic investigations by analysing whether statin treatment alters levels of Wnt signalling.

Firstly we analysed protein levels of total β-catenin and unphosphorylated β-catenin (unphosphorylated at ser33, ser37 and thr41) after statin treatment to investigate if levels of the Wnt pathway was altered. β-catenin is a key protein in the Wnt signalling pathway and the level indicates activation of the pathway. When the pathway is inactive, β-catenin is phosphorylated at ser33, ser37 and thr41 and this signals β-catenin to be degraded, resulting in significantly reduced levels. When the pathway is active, β-catenin is unphosphorylated at ser33, ser37 and thr41 and this enables β-catenin to accumulate in the nucleus and activate Wnt target genes. To investigate protein levels of β-catenin, we treated the controls APC wt RKO 7_1, RKO 7_2, and the APC mutant RKO 2_30 and RKO 2_36 in 6 well plates for 72 hours with vehicle, 2 μM lovastatin and 4 μM lovastatin or vehicle, 0.5 μM simvastatin and 1 μM simvastatin. After 72 hours of statin treatment, we collected whole cell lysates and immunoblotted for total β-catenin and unphosphorylated β-catenin (unphosphorylated at ser33, ser37 and thr41). The westerns suggest a slight decrease in both total and unphosphorylated β-catenin (Figures 43A/C, figure 44A/C), however upon quantification of three repeats, we found there was no significant difference between the vehicle and either the lovastatin or simvastatin treated at the protein level (Figure 43B/D, figure 44B/D).

To further our analysis of the Wnt signalling pathway, we performed the TCF/LEF luciferase assay, this uses a reporter to measure the level of TCF/LEF binding to TRE and is an indicator of the activation of the Wnt signalling pathway. We treated the cells in a 96 well plate for 72 hours with vehicle or 2 μM lovastatin and then performed the assay. The results shown in figure 43E show the level of Wnt activation remains low upon statin treatment in the two controls APC wt RKO 7_1 and RKO 7_2. In comparison the APC mutant RKO 2_30 and RKO 2_36 show a decrease in Wnt activation after 72 hours of treatment with lovastatin, however the decrease in activation is small and not significant.

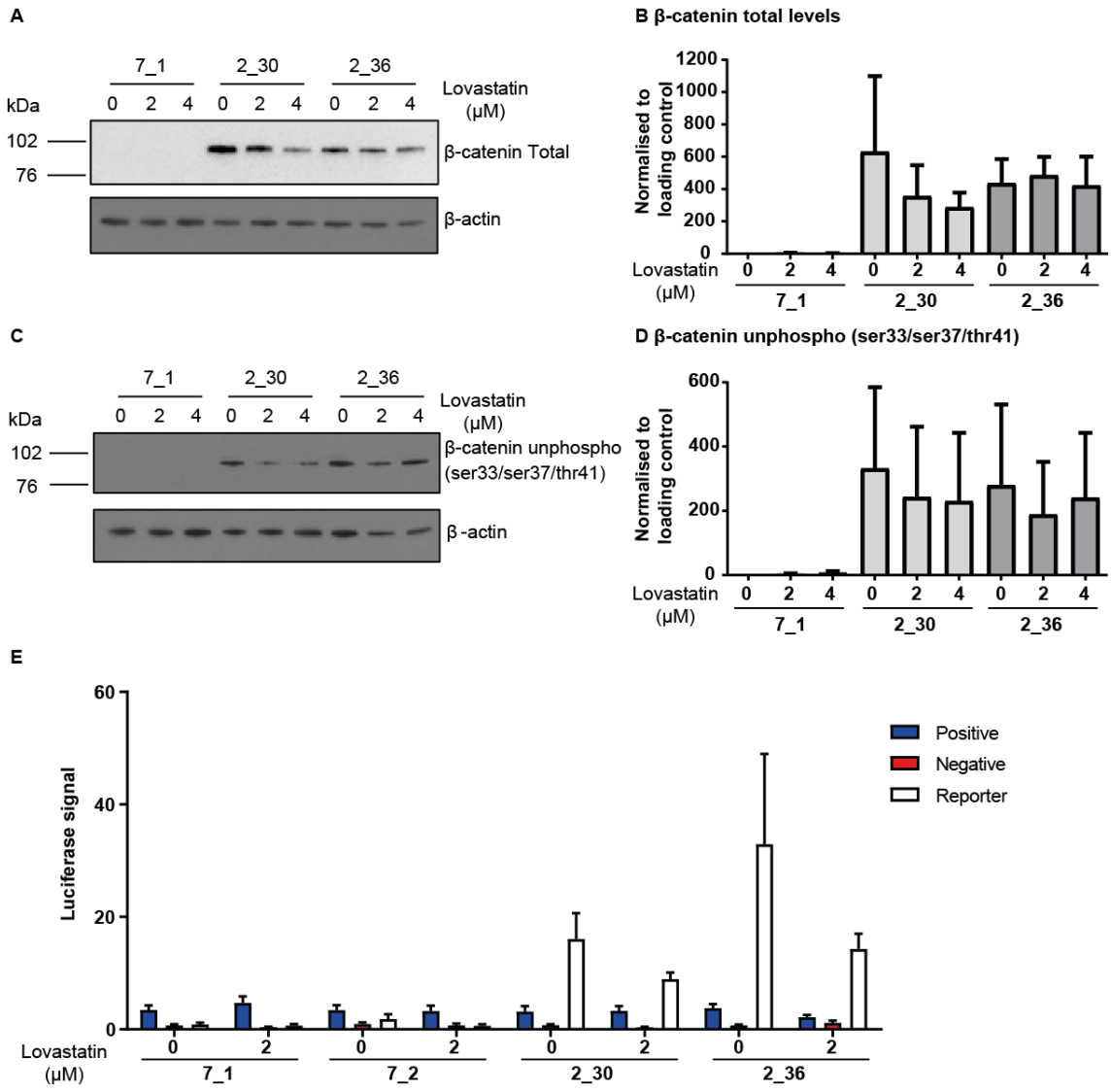

Figure 43 Lovastatin treatment causes a slight reduction in Wnt signalling

A) C) Cells were treated with 0 μM, 2 μM and 4 μM lovastatin for 72 hours and whole cell lysates were collected. Lysates immunoblotted and probed for total and unphosphorylated β-catenin. β-actin or β-tubulin used as loading control. Blots performed three times, representative blot shown. B) D) Quantification of three westerns detecting levels of total β-catenin or unphosphorylated β-catenin. Normalised to loading control. Error bars are SEM and one way anova (post hoc Tukey) was ns E) TCF/LEF Wnt assay performed on cells treated with 0 μM or 2 μM lovastatin for 72 hours in a 96 well plate. Normalised to the untreated negative control of each cell line then normalised to untreated 7_1 negative control. Three experiments combined, error bars are SEM and a one way anova (post hoc Tukey) was ns.

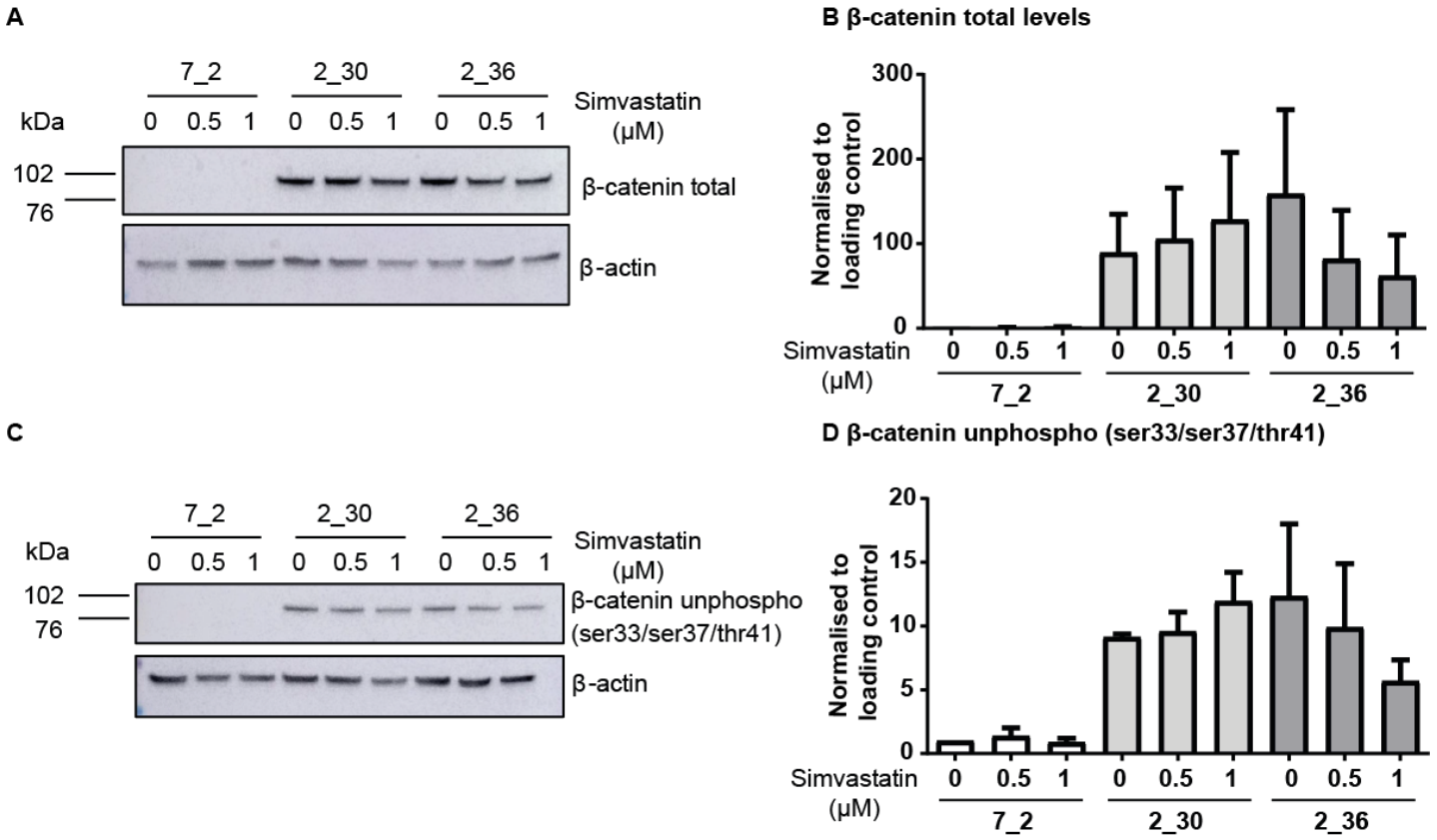

Figure 44 β-catenin levels after simvastatin treatment

A) C) Cells were treated with 0 μM, 0.5 μM and 1 μM simvastatin for 72 hours and whole cell lysates were collected. Lysates were electrophorised and levels of total and unphosphorylated β-catenin were detected. Westerns were performed twice and a representative is shown. β-actin was used as a loading control. B) D) Quantification of two westerns detecting levels of total β-catenin or unphosphorylated β-catenin, normalised to β-actin. Error bars are SEM and one way anova (Tukey post hoc) was ns.

Overall investigating the levels of the protein β-catenin and performing the TCF/LEF luciferase assay has suggested statins cause a slight reduction in the level of the Wnt signalling pathway.

3 The Wnt signalling target gene survivin decreases upon statin treatment

3.1 Statin treatment causes a greater decrease in survivin levels in the APC mutant lines compared to the APC wt controls

We decided to investigate proteins which had previously been linked to statin induced apoptosis in CRC and we began by analysing protein levels of SMAD4 and survivin upon statin treatment (Kodach et al. 2007; Chang et al. 2013; Kaneko et al. 2007). Firstly we analysed SMAD4 levels, SMAD4 expression had previously been linked to cell lines sensitive to statins and no SMAD4 expression was associated with cell lines more resistant to statins (Kodach et al. 2007). We hypothesised the APC wt control cell lines may be absent of SMAD4 or have very low levels, whilst the APC mutant cell lines would highly express SMAD4. To analyse SMAD4 levels we plated the controls APC wt RKO 7_1 and RKO 7_2 and the APC mutant RKO 2_30 and RKO 2_36 in 6 well plates and treated with vehicle or 1 μM or 2 μM lovastatin for 72 hours. After treatment we collected whole cell lysates, immunoblotted the samples and probed for SMAD4. Figure 45 shows SMAD4 protein levels are similar across the cell lines with and without lovastatin treatment, suggesting SMAD4 is not part of the mechanism of the synthetic lethality between statins and the APC mutation in our *in vitro* model.

Another avenue we explored was levels of the Wnt target gene called survivin. The downregulation of survivin has previously been linked to the mechanism of statin induced apoptosis in CRC (Chang et al. 2013; Kaneko et al. 2007). Survivin is an anti-apoptotic protein and its downregulation results in apoptosis. To investigate the role of survivin in sensitivity to statins, we analysed the protein levels of survivin after statin treatment. We plated the controls APC wt RKO 7_1 and RKO 7_2 and the APC mutant RKO 2_30 and RKO 2_36 in 6 well plates and treated with either vehicle, 1 μM or 2 μM lovastatin or vehicle, 0.5 μM or 1 μM simvastatin for 72 hours. After 72 hours of statin treatment we collected whole cell lysates and immunoblotted for survivin levels. We found that statin treatment caused a greater decrease in survivin levels in the APC mutant lines compared to the APC wt cell lines (Figure 46A/C). The westerns were quantified and the results are shown in figure 46B/D. At 1 μM lovastatin the level of survivin is over 80 % lower in RKO 2_30 and RKO 2_36 compared to RKO 7_1. Whilst

at 2 μM lovastatin the difference remains similar in RKO 2_30, this cell line shows a 80 % lower level of survivin compared to RKO 7_1. In the APC mutant RKO 2_36 cells, the survivin level is 40 % lower than RKO 7_1. Simvastatin is more potent and therefore the decrease in survivin occurs at lower concentrations. At 0.5 μM simvastatin RKO 2_30 is 90 % lower and RKO 2_36 is 70 % lower. Whilst at 1 μM simvastatin the level of survivin has decreased to a low level in the control line too so there is little difference between the three cell lines.

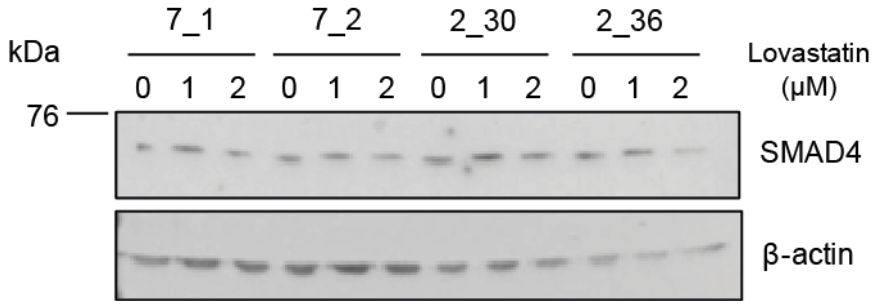

Figure 45 SMAD4 levels after lovastatin treatment

Cells were treated with 0 μM, 1 μM and 2 μM lovastatin for 72 hours and whole cell lysates were collected. Lysates were immunoblotted and probed for SMAD4. β-actin used as loading control.

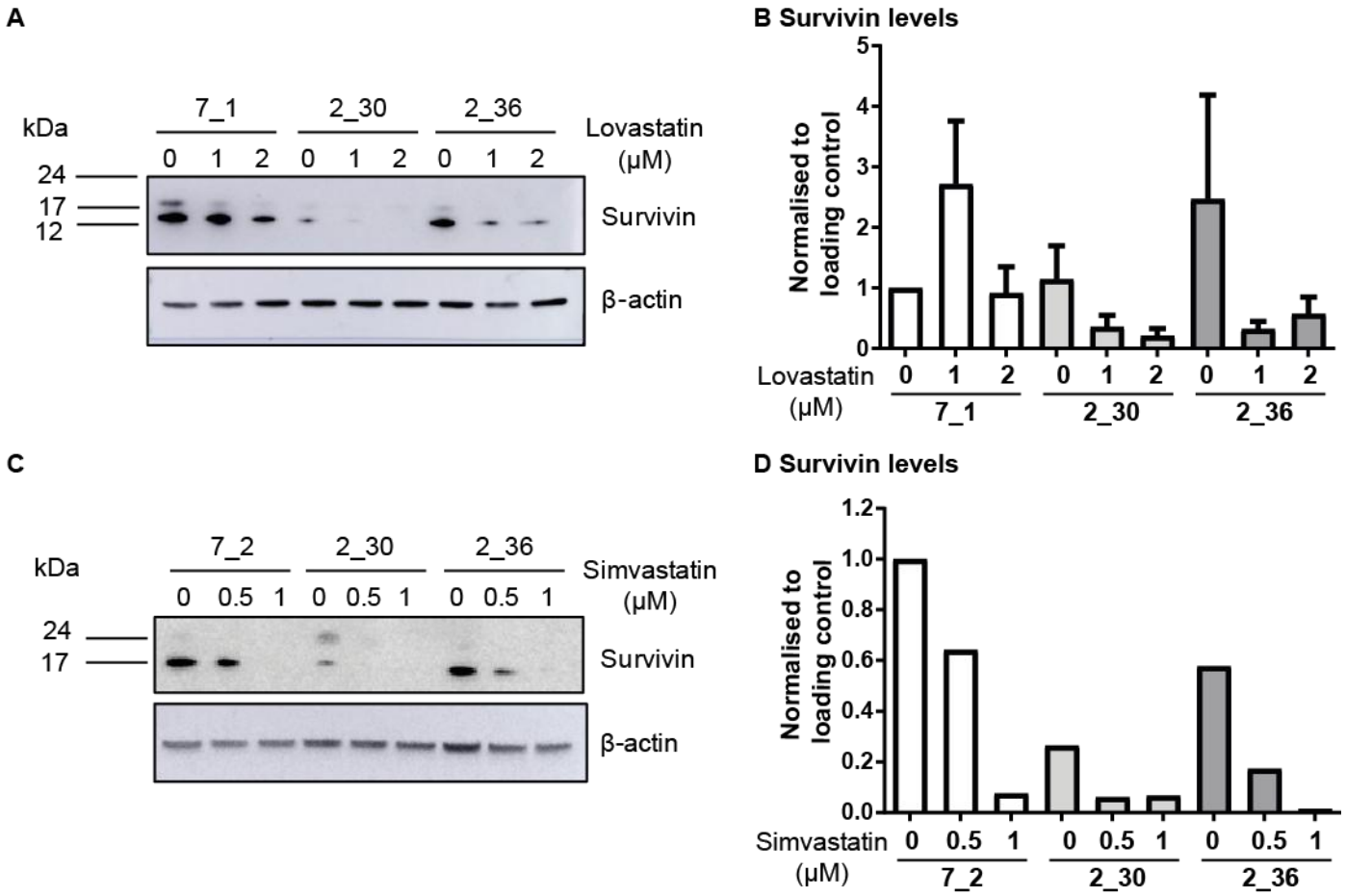

Figure 46 Survivin levels after lovastatin or simvastatin treatment

A) Cells were treated with 0 μM, 1 μM and 2 μM lovastatin for 72 hours and whole cell lysates were collected. Lysates were immunoblotted and probed for survivin. Performed in triplicate, representative shown. β-actin or β-tubulin used as loading control B) Quantification of three westerns detecting levels of survivin (both bands) and normalised to loading control. Error bars are SEM and one way anova (post hoc Tukey) was ns C) Cells were treated with 0 μM, 0.5 μM and 1 μM simvastatin for 72 hours and whole cell lysates were collected. Lysates were immunoblotted and probed for survivin and β-actin used as loading control D) Quantification of survivin levels (both bands) normalised to β-actin.

From our analysis of the survivin protein levels with and without statin treatment, we found the level decreases more in the APC mutant cell lines compared to the APC wt cell lines in our *in vitro* model. We hypothesise because the level of the anti-apoptotic protein survivin is lower in the APC mutant lines RKO 2_30 and 2_36 in comparison to the control lines, the statin induced reduction in survivin may reduce its level beyond a survival threshold resulting in apoptosis at lower concentrations of statins than seen in the controls. As we have seen a slight decrease in the Wnt signalling pathway upon statin treatment and survivin is a Wnt target gene we propose the decrease in Wnt signalling is responsible for the decrease in survivin. However, the decrease in survivin levels could also be due to alterations in other pathways responsible for regulating survivin transcription including; microRNA, RTK, PI3K/Akt, MEK/MAPK, mTOR, STAT3, p53, hypoxia, TGF and Notch (Chen et al. 2016). Further experiments would be required to confirm if the decrease in survivin levels is as a result of the statin induced decrease in Wnt signalling.

3.2 Does survivin influence levels of β-catenin?

We have shown levels of survivin decrease upon statin treatment and β-catenin levels slightly decrease upon statin treatment. A striking difference upon the effect of statin treatment on survivin and β-catenin protein levels is the concentration required to see a change, survivin decreases at lower statin concentrations compared to levels of total and unphosphorylated β-catenin. This could imply that rather than β-catenin being upstream of survivin in the mechanism that perhaps β-catenin is downstream of the reduced survivin levels. Therefore the reduction in β-catenin could be an effect of reduced survivin, for example, cells switching on apoptosis (due to a decrease in survivin) would also reduce pathways promoting proliferation such as Wnt signalling resulting in reduced levels of total and unphosphorylated β-catenin. To investigate a direct link of survivin on β-catenin levels, we decided to investigate the effect of silencing survivin using siRNA on β-catenin levels. In 6 well plates we transfected a non-targeting control (siCON), siRNA against survivin and siRNA against PLK1 in the APC wt RKO 7_1 and RKO 7_2 and the APC mutant RKO 2_30 and RKO 2_36. Ninety-six hours post transfection, we collected whole cell lysates and immunoblotted the samples for survivin and β-catenin levels. Probing the westerns for survivin levels enabled us to determine the efficiency of the siRNA transfection. Strikingly this experiment emphasises the differences in survivin levels without statin treatment, RKO 7_1, RKO 7_2 and RKO 2_36 have higher levels compared to RKO 2_30. Using siRNA against survivin, reduces survivin protein levels in all four cell lines to a similar level (figure 47A/B). We probed for total and unphosphorylated β-catenin levels to determine

if silencing survivin effects the levels of β-catenin and we found silencing survivin had no effect on the levels of β-catenin (Figure 47A/D). Quantification of the westerns further confirmed this (Figure 47C/E). Based on this result it is unlikely that survivin acts upstream of Wnt signalling, resulting in altered β-catenin levels.

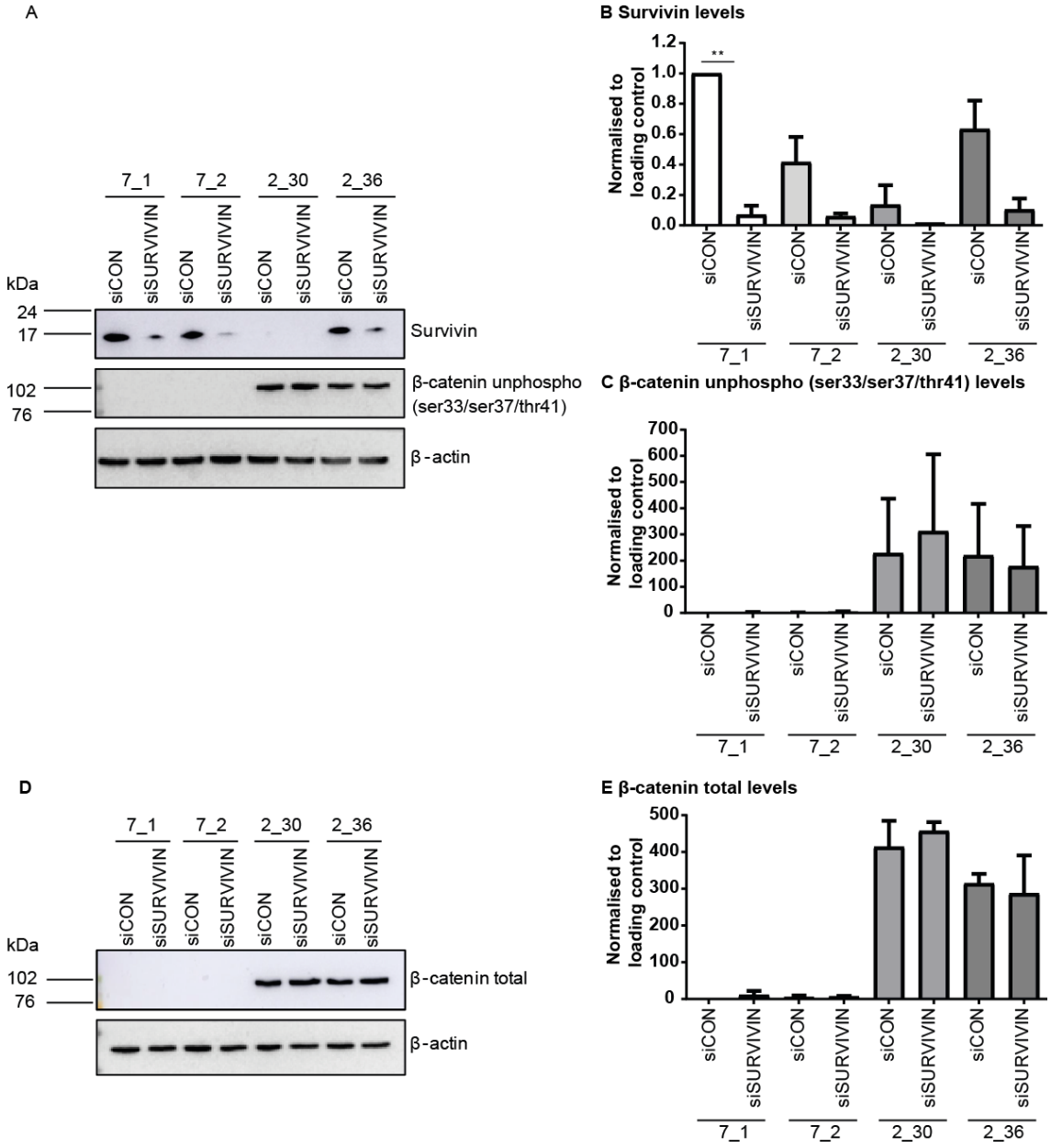

Figure 47 The effect of silencing survivin with siRNA on levels of β-catenin

A) D) Cells were transfected with siRNA against siCON and siSURVIVIN. After 96 hrs whole cell lysates were collected. Lysates were immunoblotted and levels of survivin, unphosphorylated β-catenin and total β-catenin were detected. β-actin used as a loading control. Two experiments performed and a representative blot is shown. B) C) E) Quantification of two westerns, normalised to β-actin. Error bars all SEM. One way anova (post hoc Tukey) was performed (** p≤ 0.01).

3.3 Silencing levels of survivin in the wildtype RKO cell line increases statin sensitivity

To test our hypothesis that survivin levels are important in the sensitivity to statins, we investigated if silencing survivin in the wildtype RKO cell line altered the cell lines sensitivity to statins. We transfected the wildtype RKO cell line with siRNA targeting survivin, siCON and siPLK1. After 24 hours, we treated both the cells transfected with siSURVIVIN and siCON with increasing doses of Lovastatin (0.5-10 μM) for 72 hours. We measured cell viability using CTG and plotted dose response curves (Figure 48A). Upon depletion of survivin, cells treated with 1 μM lovastatin were significantly more sensitive to lovastatin than the siCON transfected RKO cells. Upon 4 μM lovastatin the cells transfected with siSURVIVIN showed a 60 % decrease in survival whilst the cells transfected with siCON only showed a 15 % decrease in survival. This experiment shows silencing survivin in the wildtype RKO cell line increases the cell lines sensitivity to lovastatin. To confirm the siRNA targeting siSURVIVIN caused a decrease in protein levels of survivin, we collected whole cell lysates 72 hours after transfection with siRNA against survivin and immunoblotted the samples. Upon detection of survivin levels and quantification of the westerns we found the levels of survivin were 70 % lower when transfected with siSURVIVIN compared to siCON (Figure 48B/C). This data supports a role of survivin levels in the response to statins.

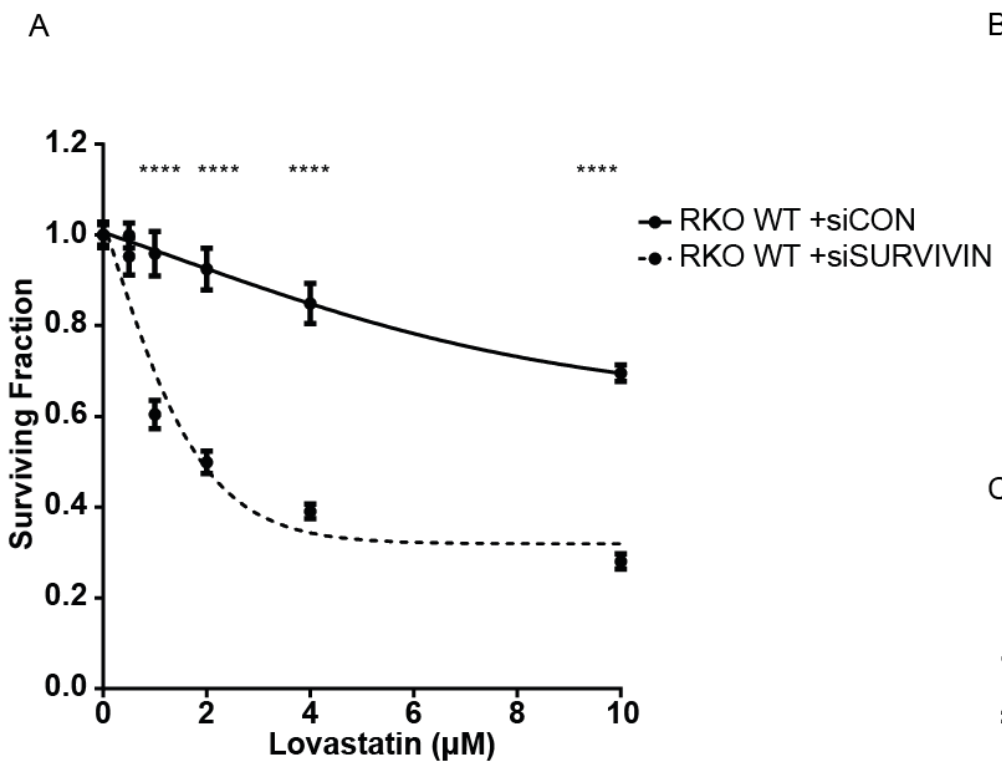

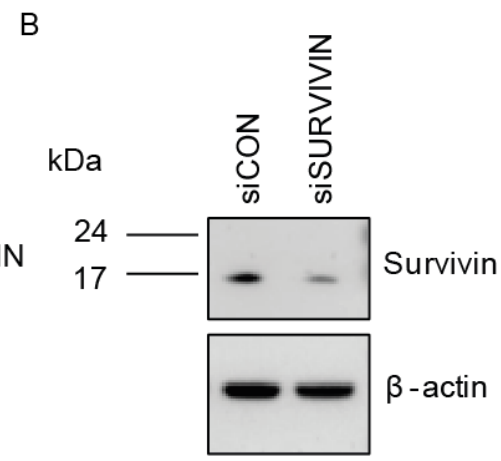

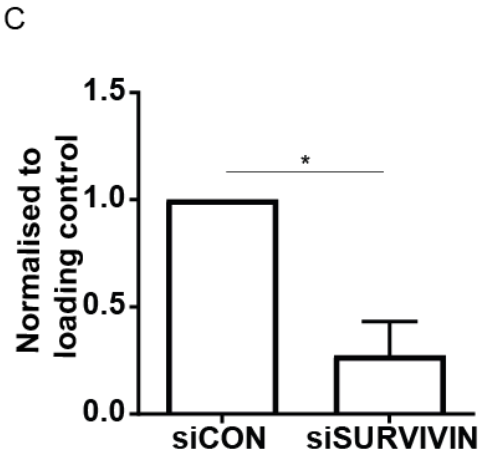

Figure 48 In RKO WT cells silencing survivin sensitises cells to lovastatin

A) In a 96 well plate RKO WT cells were transfected with siCON or siSURVIVIN, the following day cells were drugged with increasing doses of lovastatin. After 72 hours of drug treatment cell viability was measured using CTG and survival fractions were calculated. Experiment performed in triplicate, error bars are SEM and a two way anova (post hoc Sidak) was performed (**** p≤ 0.0001). B) In a 6 well plate RKO WT cells were transfected with siCON or siSURVIVIN and 72 hours later whole cell lysates were collected. Samples were immunoblotted and levels of survivin were detected. Two experiments performed, representative shown. C) Quantification of the two blots performed in B) unpaired t-test (* p≤ 0.05).

4 Do statins act through the Mevalonate pathway to cause synthetic lethality with the APC mutation

4.1 Silencing HMGCR was unsuccessful

The known mechanism of action of statins is inhibiting HMGCR therefore we first looked at whether silencing HMGCR would have a similar effect as statin treatment. In the APC wt RKO 7_1, RKO 7_2 and APC mutant RKO 2_30 and RKO 2_36 we performed assays in 96 well plates and transfected a SMARTpool siRNA targeting HMGCR, siCON and siPLK1 to enable us to analyse the impact on survival of HMGCR silencing (Figure 49A). We measured cell viability using CTG 96 hours post transfection and calculated the survival fraction of the cells. We found no difference in survival upon silencing HMGCR in our controls RKO 7_1 and RKO 7_2 compared to the APC mutated cells RKO 2_30 and RKO 2_36. To confirm the siRNA against HMGCR was reducing protein levels we collected whole cell lysates from cells transfected with siHMGCR and siCON. The lysates were then immunoblotted and probed for HMGCR as shown in figure 49B and the quantification results are shown in figure 49C. The results show silencing HMGCR with siRNA has no effect on the protein levels of HMGCR and therefore we cannot determine if silencing HMGCR has the same effect on our *in vitro* model as statins do.

To investigate if the poor transfection was specific to our *in vitro* model we analysed the same transfection into HEK293T cells which are known to transfect efficiently. In 6 well plates we transfected siHMGCR and siCON into HEK293T cells and collected lysates 96 hours after the transfection. We found transfecting siHMGCR caused no change in HMGCR protein levels in HEK293T cells either (figure 49D). HMGCR may have a high turnover and we may have missed the effect of the siRNA. Therefore we would need to look at the effect of HMGCR silencing at earlier time-points such as 24 and 48 hours.

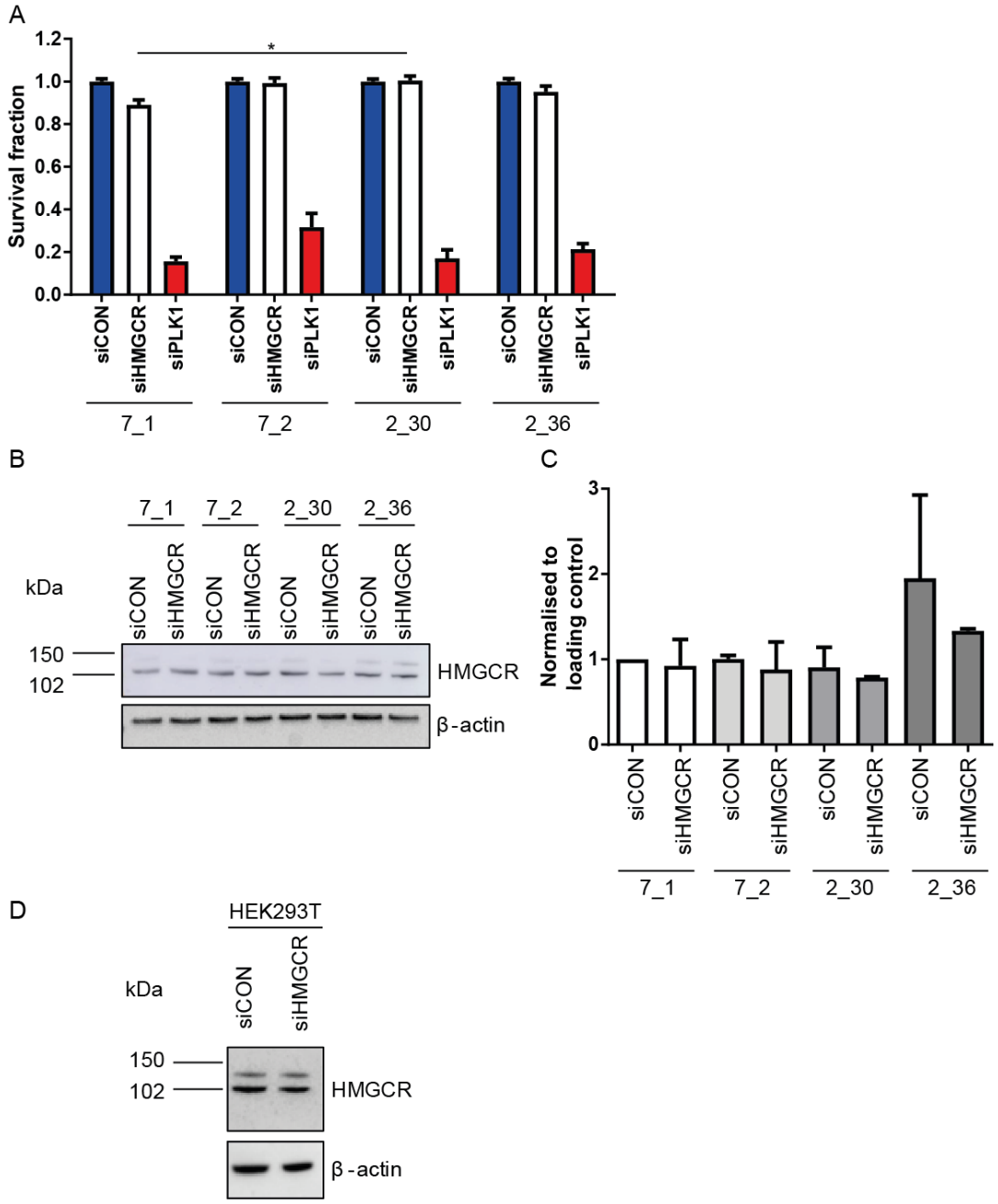

Figure 49 Silencing HMGCR using siRNA

A) Cells transfected in 96 well plate with siCON or siRNA against HMGCR (siHMGCR) or siPlK1 for 96 hours. CTG used to measure cell viability and these values were used to calculate survival fractions. The controls siCON (blue) and siPLK1 (red) indicate transfection efficiency. Experiment performed twice, error bars SEM and two way anova (post hoc Tukey) performed (* p≤ 0.05). B) In a 6 well plate cells were transfected with siHMGCR for 72 hours and whole cell lysates were collected. Lysates were immunoblotted and probed with HMGCR. β-actin was used as a loading control. Performed twice, representative blot shown. C) Quantification of two westerns, normalised to β-actin. Error bars show SEM, one way anova (post hoc Tukey) performed was ns. D) HEK293T cells transfected in a 6 well with either siCON or siHMGCR for 96 hours. Whole cell lysates collected and immunoblotted for HMGCR (lower band at 102 kDa is HMGCR, band above is non specific). β-actin used as a loading control.

4.2 Mevalonic acid does not rescue the effect of statin treatment in the APC mutated cell lines

HMGCR catalyses the conversion of HMG-CoA into Mevalonate, also known as Mevalonic acid (MVA). We investigated if adding MVA rescues the effect of statin treatment in our *in vitro* model because statins reduce the level of MVA in the cell. We plated the APC wt RKO 7_1 and RKO 7_2 and APC mutant RKO 2_30 and RKO 2_36 in 96 well plates, the following day we pre-treated cells for an hour with and without 100 µM MVA, followed by the addition of vehicle or 4 µM or 6 µM lovastatin for 48 hours (Figure 50A). We observed a greater decrease in cell viability in all cell lines when cells were pre-treated with MVA followed by lovastatin treatment for 48 hours. For example, pre-treatment with MVA then 6 µM lovastatin treatment resulted in a further 20-30 % decrease in cell viability in all cell lines compared to no MVA pre-treatment. Pre-treatment with MVA does not rescue the effect of statins in the APC mutant RKO 2_30 and RKO 2_36. This result was unexpected but could help us decipher the mechanism. Cancer cell lines are thought to have lost the negative feedback mechanisms controlling the Mevalonate pathway, whereby downstream products act to negatively regulate the levels of HMGCR (Demierre et al. 2005; Tsai et al. 2012). It is possible that the RKO cell line still has some of these feedback mechanisms and therefore adding MVA further decreases HMGCR levels enhancing the effect of statins and resulting in an increased reduction in cell viability rather than rescuing the effect.

4.3 Treatment with GGTI shows selectivity in the APC mutant cells

To further investigate the role of the Mevalonate pathway in statin sensitivity, we analysed downstream of HMGCR and looked to see if inhibiting GGTase or FTase with geranylgeranyltransferase inhibitor (GGTI) or farnesyltransferase inhibitor (FTI) respectively would show the same pattern of sensitivity as statins in our *in vitro* model. GGTI prevents the formation of GGPP prenylated proteins and FTI prevents the formation of FPP prenylated proteins.

To this end, we tested the sensitivity of GGTI-298 and FTI-277 on our control APC wt RKO 7_1, RKO 7_2 and APC mutated cell lines RKO 2_30 and RKO 2_36. We plated the four cell lines in 96 well plates and treated with 0 µM GGTI-298, 20 µM GGTI-298 or 0 µM FTI-277, 20 µM FTI-277 and 40 µM FTI-277. Additionally, we treated with 0 µM lovastatin, 4 µM lovastatin and 6 µM lovastatin to enable us to compare the effect of the GGTI-298 and FTI-277. We treated the cells with lovastatin, GGTI-298 and FTI-277

for 48 hours and measured cell viability using CTG. We found the APC mutant RKO 2_30 was more sensitive to 20 μM GGTI compared to the controls APC wt, whilst RKO 2_36 was only slightly more sensitive to 20 μM GGTI-298 compared to the controls (Figure 50B). This result suggests statins may mediate their effect through proteins which undergo GGPP prenylation, this includes protein families such as Rac, Rho and Cdc42 (Demierre et al. 2005). In comparison treatment with 20 μM FTI-277 and 40 μM FTI-277 in all the cell lines showed the same sensitivity, such that treatment with 40 μM FTI-277 resulted in 65 % viability in the APC wt and APC mutant lines (Figure 50C). We do not see increased sensitivity to FTI-277 in the APC mutant lines which suggests the mechanism is not through FPP prenylated protein families such as Ras and Rheb (Demierre et al. 2005). To further confirm that GGPP prenylated proteins are important in our mechanism and FPP prenylated proteins are not we would need to investigate if the addition of GGPP or FPP alongside statin treatment rescues the sensitivity to statins in the APC mutant RKO 2_30 and 2_36. However, taken together these experiments do support a role for statins acting through the Mevalonate pathway.

We hypothesised that proteins which undergo GGPP prenylation could have a role in the mechanism of synthetic lethality between statins and the APC mutation. A protein of particular interest was Rac1 because it undergoes GGPP prenylation and has been linked to the Wnt signalling pathway either by transporting β-catenin into the nucleus or by promoting the formation of β-catenin-TCF/LEF complexes (Wu et al. 2008; Jamieson et al. 2015). Hyperactivation of the Wnt signalling pathway is an important consequence of the APC mutation and therefore if statins decrease Rac1 activity through the reduction in isoprenylation, Wnt signalling may also decrease causing a subsequent decrease in the activation of Wnt target genes including survivin.

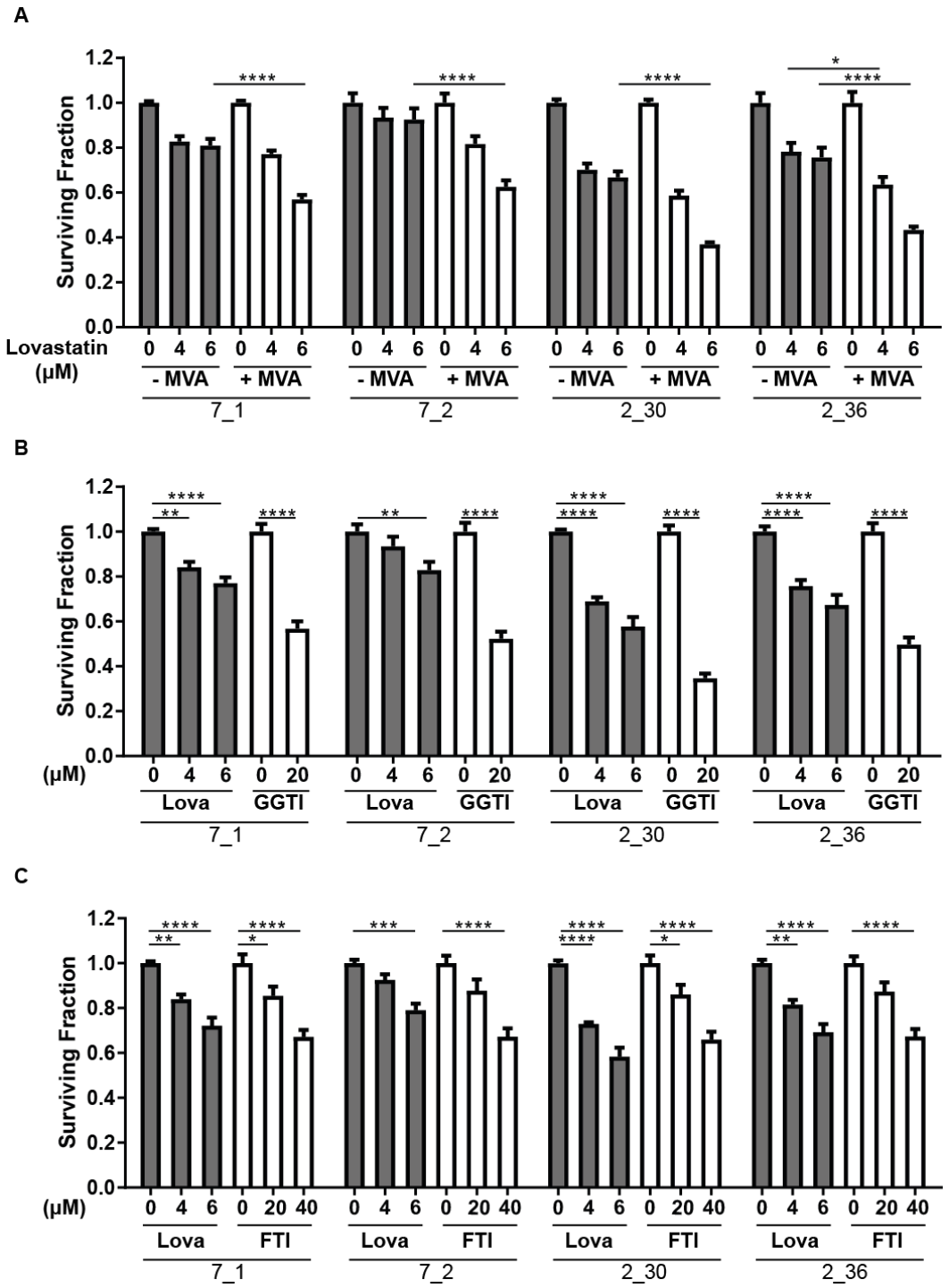

Figure 50 Effect of treating with MVA (followed by statins), GGTI or FTI.

All experiments carried out with controls RKO 7_1, RKO 7_2 and APC mutant RKO 2_30 and 2_36. Two repeats were performed, two way anova (post hoc Tukey) performed (* p≤ 0.05, ** p≤ 0.01, *** p≤ 0.001, **** p≤ 0.0001), error bars are SEM. A) Cells were pre-treated with 0 μM or 100 μM MVA for an hr then treated with either 0 μM, 4 μM and 6 μM lovastatin for 48 hrs in 96 well plates. Measured cell viability using CTG, normalised to each conditions 0 μM lovastatin. B) Cells were treated with 0 μM lovastatin, 4 μM lovastatin, 6 μM lovastatin or 20 μM GGTI-298 for 48 hours in 96 well plates. Cell viability was measured using CTG and survival fractions were calculated. C) Cells were treated with 0 μM lovastatin, 4 μM lovastatin, 6 μM lovastatin, 20 μM FTI-277 or 40 μM FTI-277 for 48 hrs in 96 well plates. Cell viability was measured using CTG and survival fractions were calculated.

5 Is Rac1 involved in the statin induced decrease in survivin levels

5.1 Active Rac1 levels increase upon statin treatment

We hypothesised the statin induced reduction in isoprenylation could result in a decrease in active Rac1 and/or Rho proteins (RhoA, RhoB and RhoC). Rac1 and Rho are GTPase proteins and are active when bound to GTP. To detect levels of Rac1-GTP and Rho-GTP we used specifically designed pull down kits which are commonly used.

For analysis of active Rac1/Rho, we treated the RKO controls 7_1 and 7_2 and the RKO APC mutant 2_30 and 2_36 with and without 2 μM lovastatin for 72 hours and collected whole cell lysates. For analysis of active Rac1/Rho, 500 μg lysate per condition was run through a column containing a resin with a GST-fusion protein. For active Rac1, the GST-fusion protein contained the p21(rac1)-binding domain (PBD) of the Rac1 effector Pak1, where active Rac1 interacts with Pak1. This enables the active Rac1 to be separated from inactive Rac1. For active Rho, the GST-fusion protein contained the Rhotekin-binding domain (RBD) of the Rho effector Rhotekin, which only active Rho binds to. We performed two controls alongside the other reactions, a positive control where lysates were treated with GTPyS (0.1 mM for 15 minutes at 30 °C) or a negative control where lysates were treated with GDP (1 mM for 15 minutes at 30 °C). Upon immunoprecipitation, the control lysates and test lysates were then electrophorised on an SDS-PAGE gel and probed for Rac1 or Rho (RhoA/B/C). This analysis would detect only Rac1/Rho bound to GTP. We also included an input column which detected total Rac1/Rho.

We observed that the APC wt lysates from RKO 7_1 and RKO 7_2 cells had a similar level of active Rac1, before and after lovastatin treatment (Figure 51A/C). Whereas the APC mutant lines RKO 2_30 and RKO 2_36, firstly have a lower level of active Rac1 without lovastatin treatment compared to the controls. However, upon statin treatment, the level of active Rac1 dramatically increases. To determine whether this was due to different levels of total Rac1, we treated cells in 6 wells with 0 μM, 2 μM and 4 μM lovastatin and after 72 hours collected cell lysates. The lysates were then immunoblotted and probed for Rac1 (Figure 51E). The lower basal active Rac1 seen in RKO 2_30 and RKO 2_36 appears to be partly contributed to differences in the total level of Rac1 as these cells have lower levels of total Rac1 without statin treatment in comparison to the control RKO 7_1. The increase in active Rac1 after 2 μM lovastatin treatment in the APC mutant lines does not appear to be due to an increase in total Rac1 because levels of total Rac1 remain similar. Interestingly, the finding that levels of

active Rac1 increase upon statin treatment in the APC mutant lines is the opposite of our original hypothesis, as we thought Rac1 activation might decrease due to a decrease in isoprenoids.

For analysis of active Rho, we detected no change in the level of active Rho upon lovastatin treatment in all four cell lines (Figure 51B/D). We also analysed levels of total Rho in whole cell lysates collected from 6 well plates which had been treated with 0 μM and 2 μM lovastatin for 72 hours (Figure 51F). The level of total Rho upon statin treatment did not appear to change in the four cell lines, however we did observe that the level of total Rho between the cell lines was slightly lower in the APC mutant cell lines. It is interesting we see a change in active Rac1 levels and not active Rho proteins and this suggests Rac1 may be important for the selective effect observed with statin treatment on APC mutant cells.

5.2 Inhibiting the activation of Rac1 does not cause greater loss of cell viability in the APC mutant cell lines compared to the APC wt controls

As we observed a significant activation of Rac1 upon statin treatment in the APC mutant cell line, we next investigated whether Rac1 activation was causing the selectivity in our *in vitro* model. Firstly, we treated our cells with the Rac1 inhibitor EHT1864 which prevents Rac1 binding to GTP and therefore prevents its activation (Onesto et al. 2008). Other Rac1 inhibitors block Rac1 indirectly by inhibiting GAP responsible for activating Rac1 (Onesto et al. 2008). EHT1864 has a Kd value of 40 nM showing it has a high binding affinity for Rac1, therefore we initially performed a dose response curve with doses around this Kd value (Shutes et al. 2007). We performed the dose response curves in 96 well plates in the APC wt RKO 7_1 and RKO 7_2 and the APC mutant RKO 2_30 and RKO 2_36. We drugged for 96 hours and measured cell viability using CTG. Figure 52A shows we did not see a difference in response between the controls (RKO 7_1 and RKO 7_2) and APC mutant cell lines (RKO 2_30 and RKO 2_36). The highest dose 1000 nM (1 μM) did not significantly alter cell viability in the cell lines, and therefore, we next tested a higher dose range up to 15 μM EHT1864. Figure 52B illustrates that we did not see selectivity between the controls and APC mutant cell lines when increasing the dose range to 15 μM EHT1864. These results suggest inhibiting the activation of Rac1 does not have the same impact on the cells as statins.

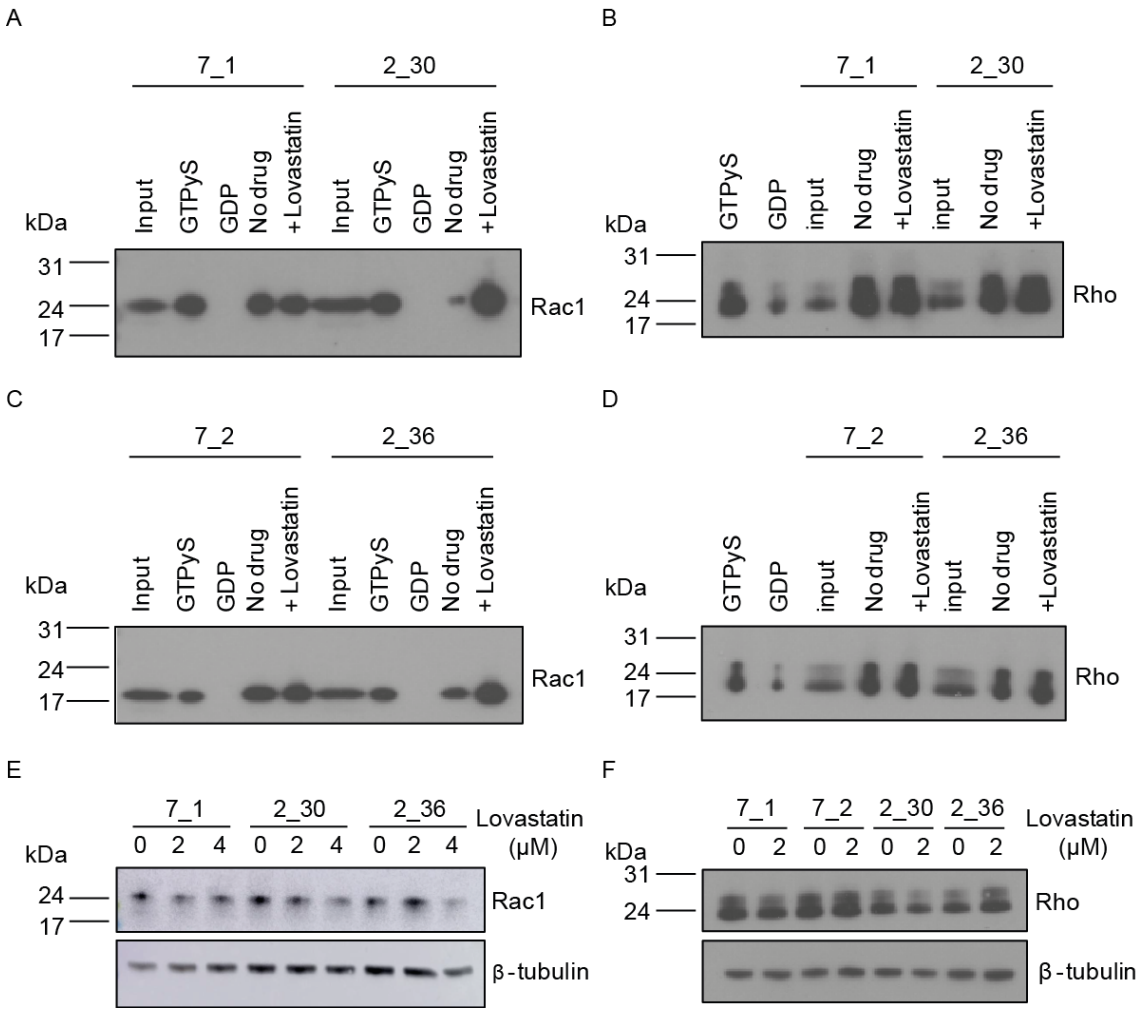

Figure 51 Active Rac1 and active Rho pull down experiments

A) B) C) D) Cells were treated with 0 μM and 2 μM lovastatin for 72 hours. Then whole cell lysates were collected and 500 μg was used for the pull down kits. After the pull down assays were performed, samples were immunoblotted, we loaded 10 μg for input, 10 μL for controls (GTPγS/GDP) and 40 μL for samples. Total Rac1 or total Rho antibody was used for the detection. The input lane shows levels of total Rac1/Rho. All performed twice, representative shown. A) Active Rac1 pull down in 7_1 and 2_30 B) Active Rho pull down in RKO 7_1 and RKO 2_30 C) Active Rac1 pull down in RKO 7_2 and RKO 2_36 D) Active Rho pull down in RKO 7_2 and RKO 2_36 E) Cells were treated with 0 μM, 2 μM and 4 μM lovastatin for 72 hours and whole cell lysates collected. Lysates immunoblotted and levels of total Rac1 detected. β-tubulin used as a loading control. F) Cells were treated with 0 μM and 2 μM lovastatin for 72 hours and whole cell lysates collected. Lysates immunoblotted and levels of total Rho detected. β-tubulin used as a loading control.

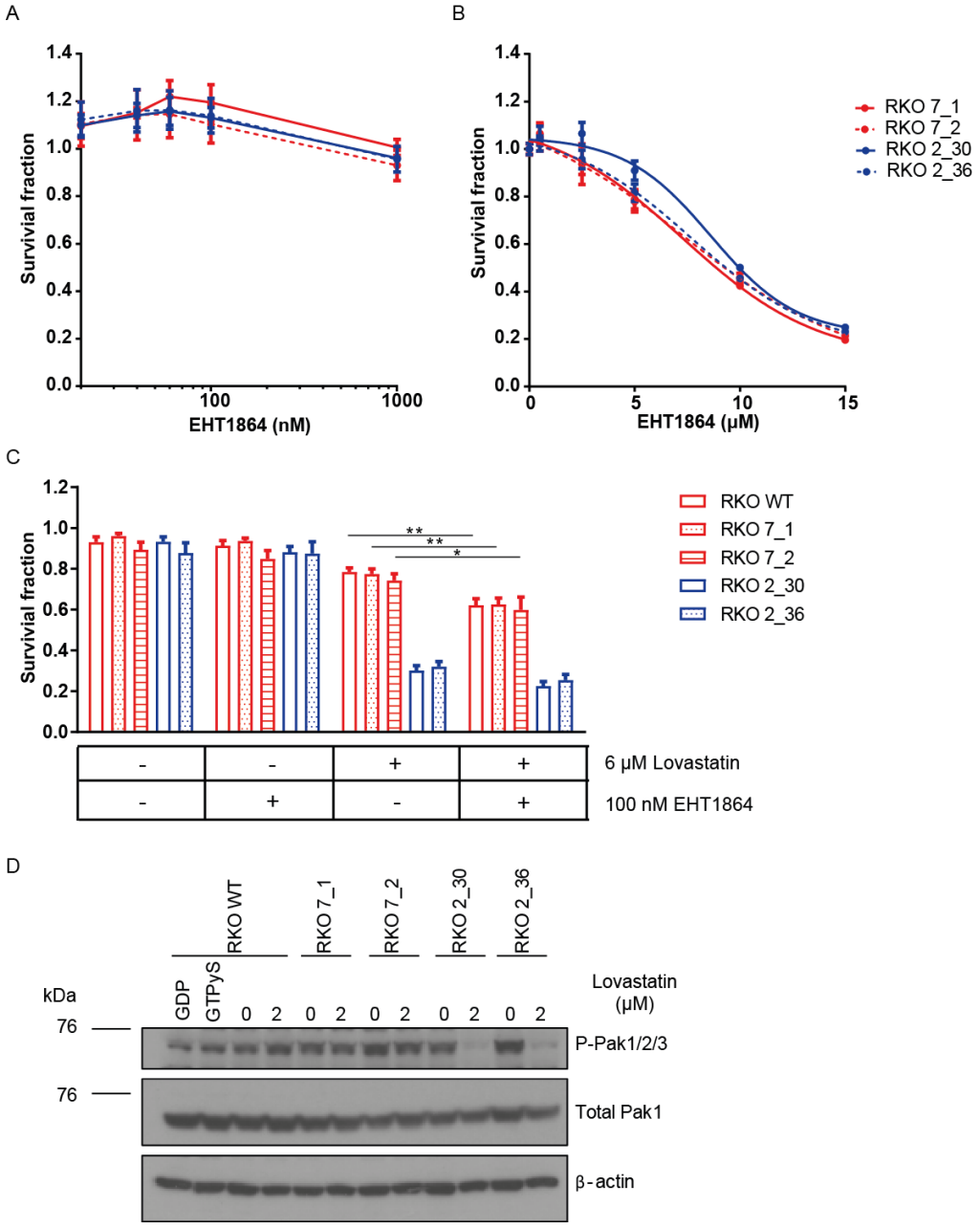

Figure 52 Investigating the potential role of Rac1 in the mechanism

A) B) In 96 well plates dose response curves were performed with two different dose ranges of EHT1864. Cells treated with EHT1864 for 96 hours and cell viability measured with CTG. Control cell lines RKO 7_1 and RKO 7_2 shown in red and APC mutant cell lines RKO 2_30 and RKO 2_36 shown in blue. Error bars are SD. C) In 96 well plates cells were treated twice with either no drug, 100 nM EHT1864, 6 μM lovastatin or 100 nM EHT1864 & 6 μM lovastatin for a total treatment time of 96 hours. Cell viability was analysed with CTG. Control cell lines RKO wt RKO 7_1 and RKO 7_2 shown in red and APC mutant cell lines RKO 2_30 and RKO 2_36 shown in blue. Performed in triplicate, error bars SEM. Two way anova (post hoc Tukey) was performed showing just the results for 6 μM lovastatin vs 100 nM EHT1864 & 6 μM lovastatin (* p≤ 0.05, ** p≤ 0.01). D) Cells were treated with 0 μM or 2 μM lovastatin for 72 hrs and lysates collected. Additionally RKO wt cells were treated for 24 hrs with GDP or GTPγS as controls. Lysates were immunoblotted and probed for pPAK1/2/3 and total PAK1. β-actin used as a loading control, performed twice, representative blot shown.

5.3 Inhibiting Rac1 activation in combination with statin treatment does not rescue the selectivity

Our results suggest that in APC mutated cells, Rac1 is activated upon statin treatment. Therefore to further understand if the increase in active Rac1 upon statin treatment is key to the mechanism of synthetic lethality, we investigated if inhibiting Rac1 activation in combination with statin treatment would rescue the effect in the APC mutant cell lines. To this end, the parental cell line RKO wt, APC wt controls RKO 7_1, RKO 7_2 and the APC mutant RKO 2_30 and RKO 2_36 were plated in 96 well plates. On day 2 and day 4 the cells were treated with the following combinations 1) vehicle 2) 100 nM EHT1864 3) 6 μM lovastatin 4) 6 μM lovastatin and 100 nM EHT1864. Cell viability was measured using CTG, after 96 hours of total drug treatment. Figure 52C shows that addition of EHT1864 did not rescue the effect of lovastatin on the APC mutant cell lines. This suggests the statin induced increase in Rac1 activation is not responsible for the reduced cell viability in the APC mutant cell lines, however, it does not completely rule Rac1 out of the mechanism of synthetic lethality.

5.4 The phosphorylation levels of the Rac1 effector Pak1 at ser144 reduces upon statin treatment

To determine whether the increase in active Rac1 observed is indeed functional in the canonical Rac1 activation pathway, we analysed Pak1 phosphorylation upon statin treatment in the APC wt and APC mutant cell lines. Pak1 is a serine theronine kinase downstream of Rac1 and Pak1 is also activated by PDK1, Pi3K and AKT (Kumar et al. 2006). Pak1 activation by the GTPases Rac1 and Cdc42 is the best characterised mechanism of activation (Kumar et al. 2006). Pak1 activates many pathways and has a role in regulating the cytoskeleton, cell growth and cell survival (Ye & Field 2012). We analysed phosphorylation at ser144 in the kinase inhibitory domain of Pak1 (unique to activation by Rac1 and Cdc42), this results in a conformational change, enabling the kinase domain to autophosphorylate for full Pak1 activation (Chong et al. 2001).

To investigate Pak1 phosphorylation, the parental cell line RKO wt, APC wt controls RKO 7_1, RKO 7_2 and the APC mutant RKO 2_30 and RKO 2_36 were plated into 6 well plates on day 1. On day 2 each cell line was treated with either vehicle or 2 μM lovastatin for 72 hours. Alongside these wells two controls were performed in just the parental RKO wt cell line, on day 4 either 400 μM GDP (inactives Rac1) or 40 μM GTPyS (activates Rac1) was added to the cells for 24 hour treatment. On day 5, protein lysates were collected from all the treated wells and samples were

immunoblotted and probed for total Pak1 and phosphorylated Pak1 at ser144. Due to structural similarity the antibody also detects phosphorylated ser141 of Pak2 and phosphorylated ser139 of Pak3 (Rane & Minden 2018). Our results show levels of total Pak1 are the same for all cell lines regardless of statin treatment and the untreated cells all contain the same level of phosphorylated Pak1/2/3 (Figure 52D). Upon statin treatment only the APC mutated cell lines RKO 2_30 and RKO 2_36 show a substantial decrease in levels of phosphorylated Pak1/2/3, suggesting statins reduce the activation of Pak1. Interestingly in the control wells treated with GDP to inactive Rac1 we do not see a substantial change in the phosphorylation of Pak1/2/3 in comparison to the cells treated with GTPyS to active Rac1. Perhaps treatment with GDP/GTPyS was not sufficient to see an alteration at this part of the pathway. We hypothesise the decrease in phosphorylation of Pak1 despite increased levels of active Rac1 suggests the localisation of the Rac1 could be altered upon statin treatment, preventing the phosphorylation of Pak1 and full activation. Statins decrease levels of prenylation and unprenylated Rac1 would be unable to localise to the plasma membrane. Pak1 is recruited to the membrane for activation and this is where prenylated Rac1 would also locate (Kumar et al. 2006; Wennerberg & Der 2004).

5.5 Rac1 localisation with cadherin upon statin treatment

To further understand the effects of statin treatment on Rac1 in our *in vitro* model, we investigated the localisation of Rac1 in relation to its role in mediating cell-cell adhesion. Cadherins regulate intercellular adhesion through calcium dependent homophilic interactions. Epithelial cadherin (E-cadherin) is a type of cadherin found in epithelial cells (Fukata & Kaibuchi 2001). Rac1 has been shown to co-localise with E-cadherin and this indirectly induces activation of Rac1 through additional proteins (Nakagawa et al. 2001). We performed immunofluorescence in RKO wt cells, RKO 7_1, RKO 7_2, RKO 2_30 and RKO 2_36 to investigate the localisation of both Rac1 and cadherin. For each cell line we plated 100,000 cells/well onto coverslips in 24 well plates and treated with 0 μM lovastatin or 2 μM lovastatin for 72 hours. Additionally we performed two controls in just the RKO wt cells, these cells were treated for just 24 hours with either 80 μM GTPyS (to activate Rac1) or 400 μM GDP (to inactivate Rac1). The cells were then fixed and stained with DAPI, total Rac1 and pan-cadherin (detects all forms of cadherin including E-cadherin) to enable us to understand if statins alter the localisation and activation of Rac1 in relation to its role in cell-cell adhesion.

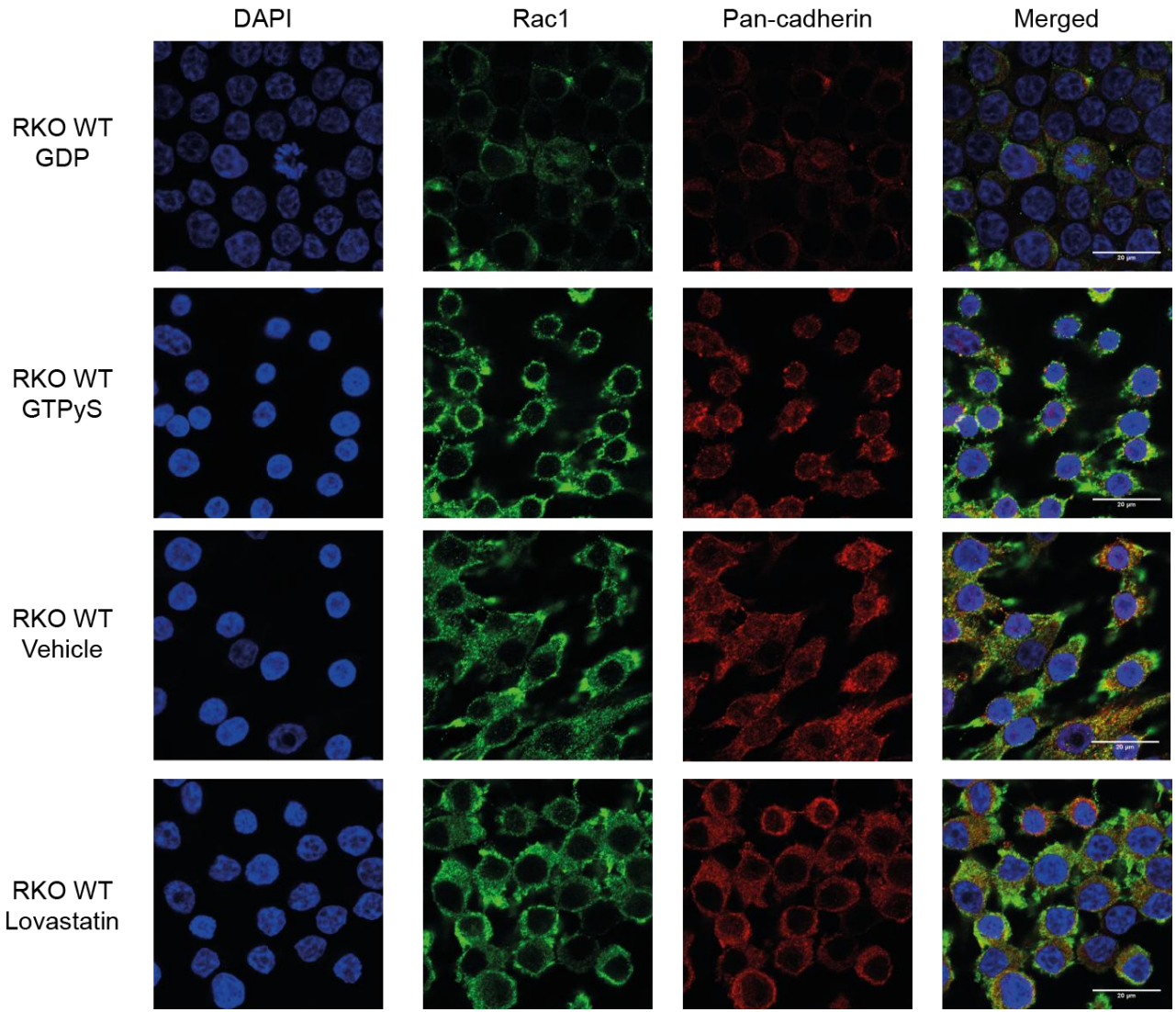

Figure 53 Localisation of Rac1 and cadherin upon statin treatment in RKO WT

For the controls RKO WT cells were treated with 400 μM GDP or 80 μM GTPyS for 24 hours before fixing. The drug treated cells were treated with 0 μM or 2 μM lovastatin for 72 hrs before fixing and preparing for confocal. DAPI staining is in blue, total Rac1 is in green and pan-cadherin is in red. Merged image is a composite of DAPI, total Rac1 and pan-cadherin. Scale bar indicates 20 μM. Representative images shown.

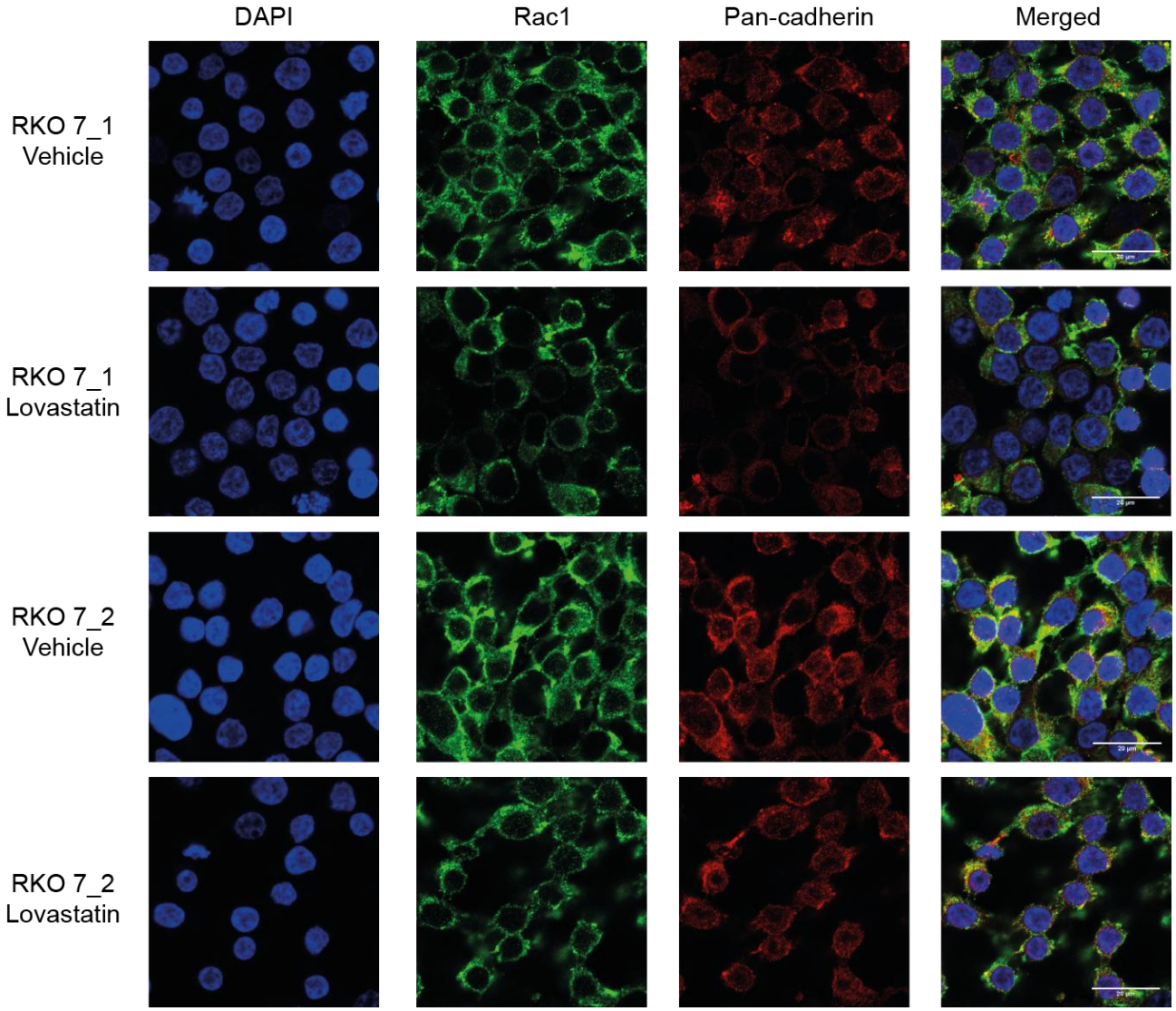

Figure 54 Localisation of Rac1 and cadherin upon statin treatment in RKO 7_1 and 7_2

The drug treated cells were treated with 0 μM or 2 μM lovastatin for 72 hrs before fixing and preparing for confocal. DAPI staining is in blue, total Rac1 is in green and pan-cadherin is in red. Merged image is a composite of DAPI, total Rac1 and pan-cadherin. Scale bar indicates 20 μM. Representative images shown.

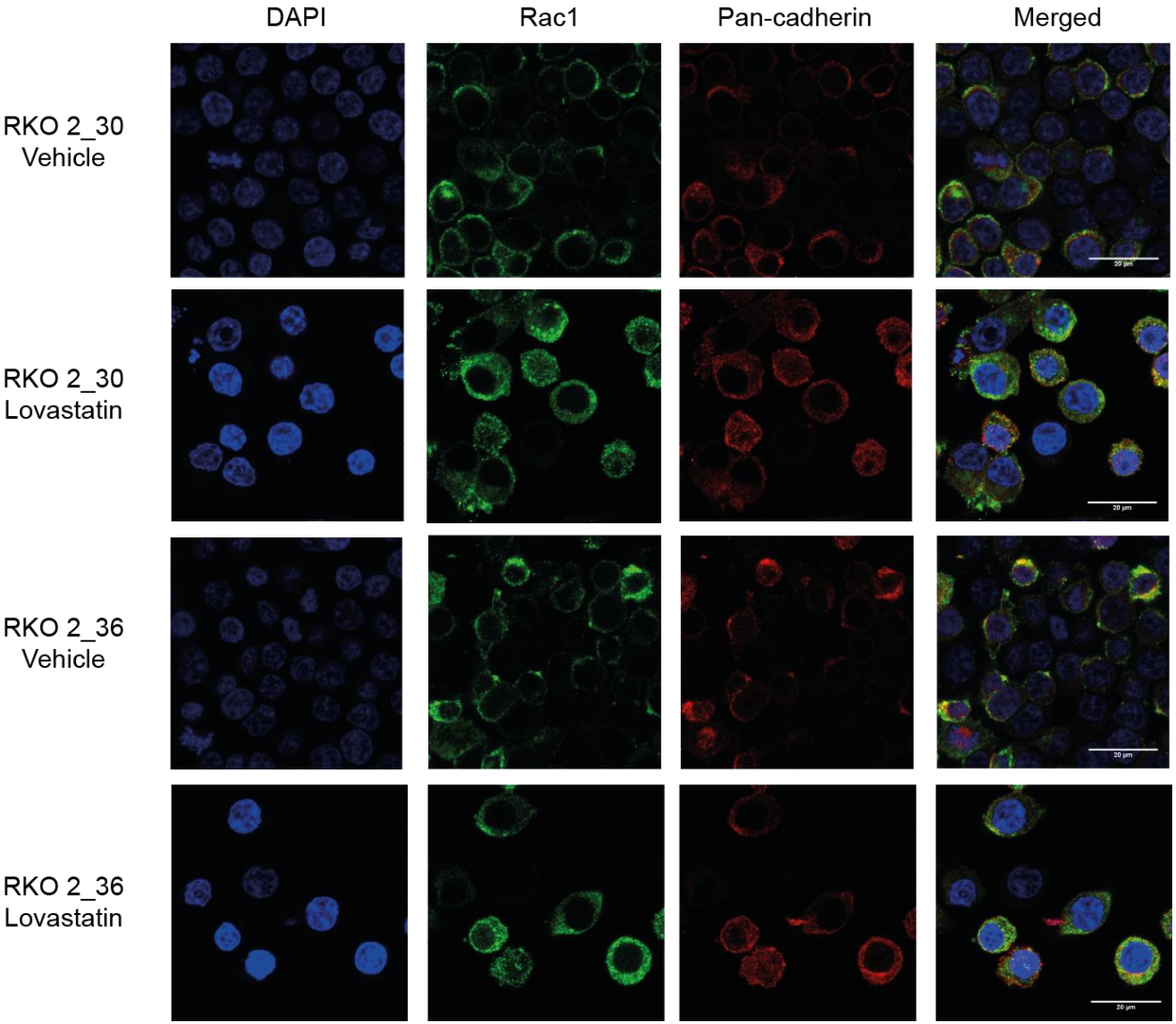

Figure 55 Localisation of Rac1 and cadherin upon statin treatment in RKO 2_30 and 2_36

The drug treated cells were treated with 0 μM or 2 μM lovastatin for 72 hrs before fixing and preparing for confocal. DAPI staining is in blue, total Rac1 is in green and pan-cadherin is in red. Merged image is a composite of DAPI, total Rac1 and pan-cadherin. Scale bar indicates 20 μM. Representative images shown.

Firstly our immunofluorescence images indicate that Rac1 and pan-cadherin do co-localise in the APC wt RKO cell lines (Figures 53-55). It is difficult to draw conclusions from the data because the pan-cadherin staining is not strictly associated with the membrane and this made the images difficult to interpret and quantify. RKO cells are small and the nucleus takes up a large portion of the total cell volume and there is often a small cytoplasm. The staining for both Rac1 and pan-cadherin is throughout the cytoplasm but the strongest staining typically appears to be at the plasma membrane often at sites resembling cell-cell contacts or lamellipodia. Comparison of the images for the controls GDP and GTPyS show the differences between cells with very little active Rac1 (GDP treated) and cells with lots of active Rac1 (GTPyS treated). The RKO WT cells treated with GDP show lower intensity Rac1 staining with fewer foci of intense staining compared to the GTPyS (Figure 53). For the RKO WT, RKO 7_1 and RKO 7_2 the staining is more intense without lovastatin treatment, upon lovastatin treatment we generally see less foci (Figure 53/54). In the untreated RKO APC mutant lines 2_30 and 2_36 the staining looks similar to the GDP control with just light staining. Whereas the treated RKO 2_30 and 2_36 have stronger staining and this appears to be throughout the cytoplasm rather than at specific sites such as cell-cell contacts and lamellipodia (Figure 55). These observations may suggest statins affect Rac1 in both cell lines but the effect is more prominent in the APC mutant cell lines and is suggestive of dysfunctional Rac1 signalling upon statin treatment.

We attempted to quantify the images based on the assumption that a cell positive for active Rac1 showed co-localisation of Rac1 and cadherin at the membrane. This was difficult to score because the pan-cadherin staining was not restricted to the plasma membrane. We compared the number of cells positive for Rac1 and cadherin at the membrane to the total number of cells which were identified by DAPI staining to calculate a percentage of cells containing active Rac1. We counted ~300 cells and used this to quantify the effect of statin treatment on the number of cells showing active Rac1 (Figure 56). The controls RKO wt, RKO 7_1, RKO 7_2 show a similar % of cells displaying active Rac1 upon statin treatment compared to untreated. In comparison the APC mutant RKO 2_30 and RKO 2_36 have a 20 % lower percentage of cells showing active Rac1 without statin treatment. In agreement with the active Rac1 pull down data upon statin treatment we see an increase in the percentage of APC mutant cells showing active Rac1. The effect is more prominent in the RKO 2_30 cell line which is the same as the active Rac1 pull down data (section 5.1). This analysis supports previous data showing the RKO APC mutant cell lines do have lower basal levels of active Rac1 and statin treatment caused an increase in active Rac1. Additionally statin treatment potentially caused the Rac1 staining to be evenly cytoplasmic instead of

stronger at cell-cell contacts and lamellipodia suggesting aberrant Rac1 signalling. Further work is required to fully understand the effect of statins on Rac1 localisation and activation.

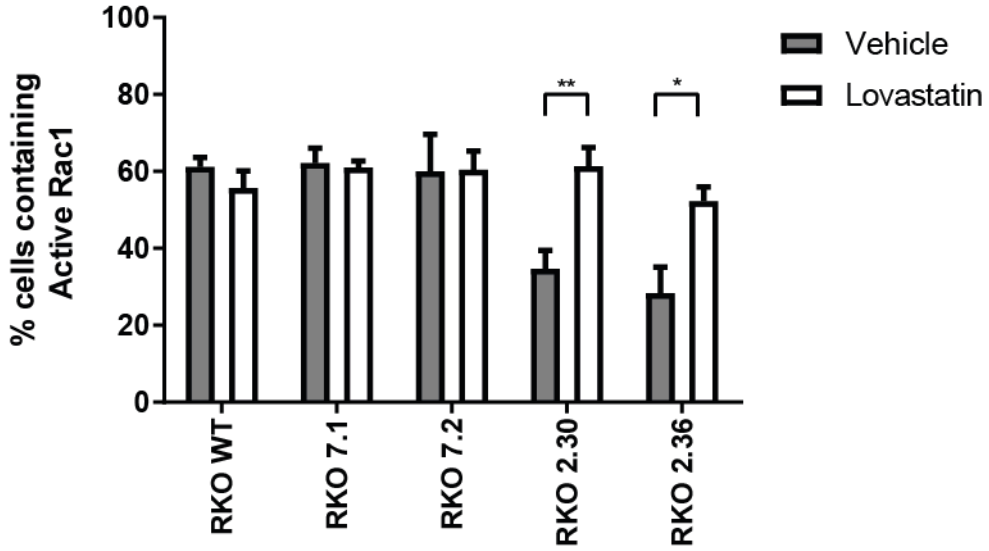

Figure 56 Summary of the % cells containing active Rac1 upon statin treatment

The drug treated cells were treated with 0 µM or 2 µM lovastatin for 72 hrs before fixing and preparing for confocal. Approximately 300 cells were counted per condition per cell line and the % of cells with active Rac1 staining was calculated based on Rac1 and cadherin co-localising at the membrane. Represents results from three experiments and error bars are SEM. Two way anova (post hoc Bonferroni) was performed (* p≤ 0.05, ** p≤ 0.01).

6 The statin induced increase in active Rac1 causes β-catenin to be transported into the nucleus

6.1 Statin treatment increases β-catenin transport into the nucleus

Our data suggested that Wnt signalling and the Wnt target gene survivin decrease upon statin treatment. Therefore we analysed whether statins alter the localisation of β-catenin in our *in vitro* model using immunofluorescence. We plated the control cells RKO 7_1 and RKO 7_2 and the APC mutant RKO 2_30 and RKO 2_36 onto coverslips, using a density of 40,000 cells/well. Next the cells were treated with 0 μM or 4 μM lovastatin for 72 hours. The cells were then fixed and stained with DAPI and total β-catenin to enable us to compare the number of cells with β-catenin in the nucleus and cytoplasm.

Representative images are shown for the control APC wt cells in figure 57 and APC mutant lines in figure 58. As expected without lovastatin, the APC wt RKO 7_1 and RKO 7_2 had low β-catenin staining in the cytoplasm and the nucleus, in comparison to the APC mutant cells RKO 2_30 and RKO 2_36 which showed higher levels of both cytoplasmic and nuclear staining, indicating active Wnt signalling. Approximately 200 cells were analysed for each condition, the percentage of cells with β-catenin staining in the cytoplasm and percentage of cells with β-catenin staining in the nucleus was calculated and the results are illustrated in figure 59. Statin treatment in the APC mutated cells caused a decrease in cells with cytoplasmic β-catenin and an increase in cells with β-catenin in the nucleus. This result is interesting because we would expect an increase in nuclear β-catenin to result in more β-catenin binding to TCF/LEF and activating Wnt target genes. Therefore this result is not in agreement with our previous data, suggesting statins cause a decrease in Wnt signalling. Perhaps β-catenin accumulates in the nucleus but is prevented from activating Wnt target genes, this is further discussed in section 6.2.

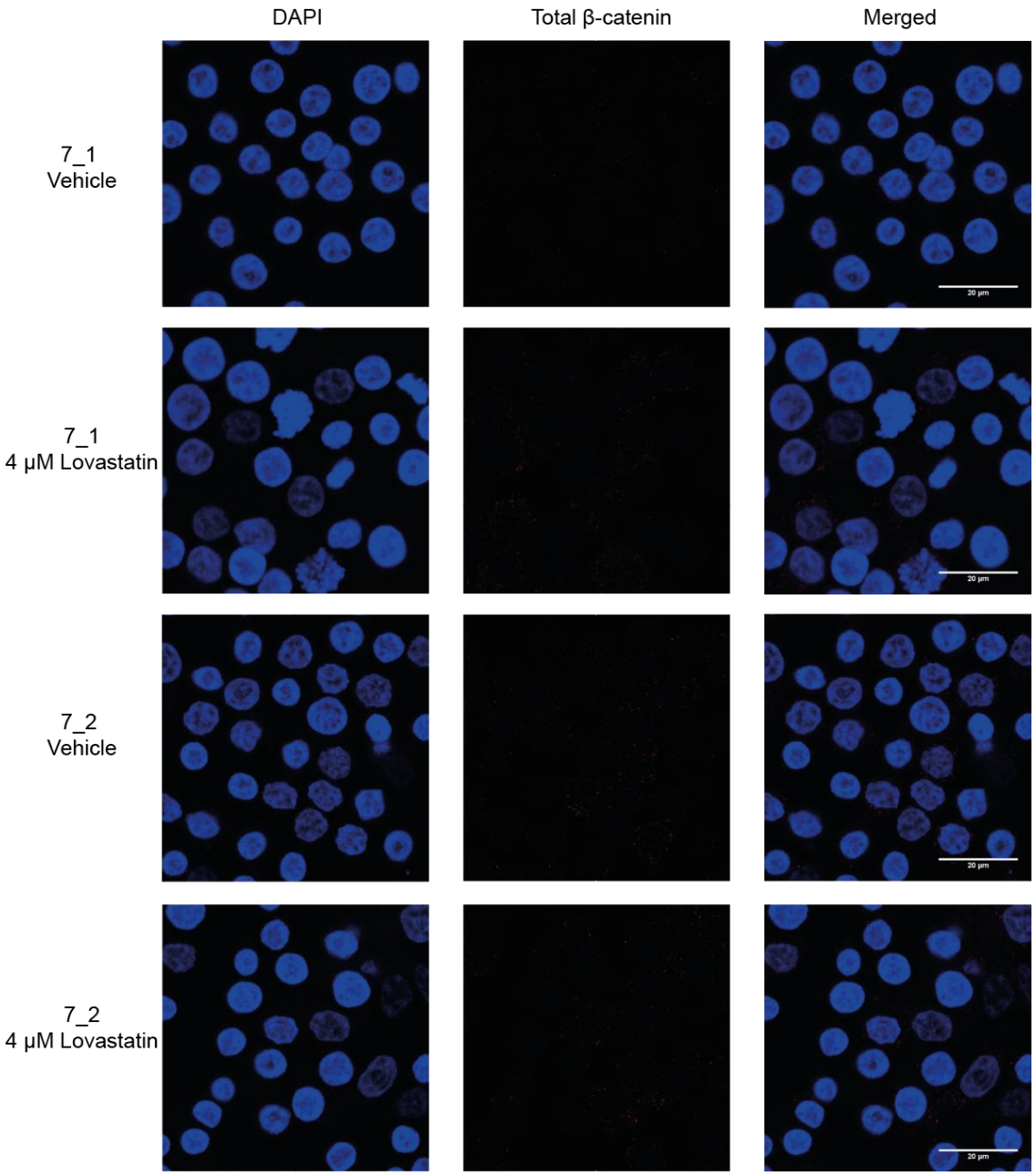

Figure 57 Levels of total β-catenin upon statin treatment in RKO 7_1 and 7_2

Cells were treated with 0 μM or 4 μM lovastatin for 72 hrs before fixing and preparing for confocal. DAPI staining is in blue, total β-catenin is in red. Merged image is a composite of both DAPI and total β-catenin. Scale bar indicates 20 μM. Representative images shown.

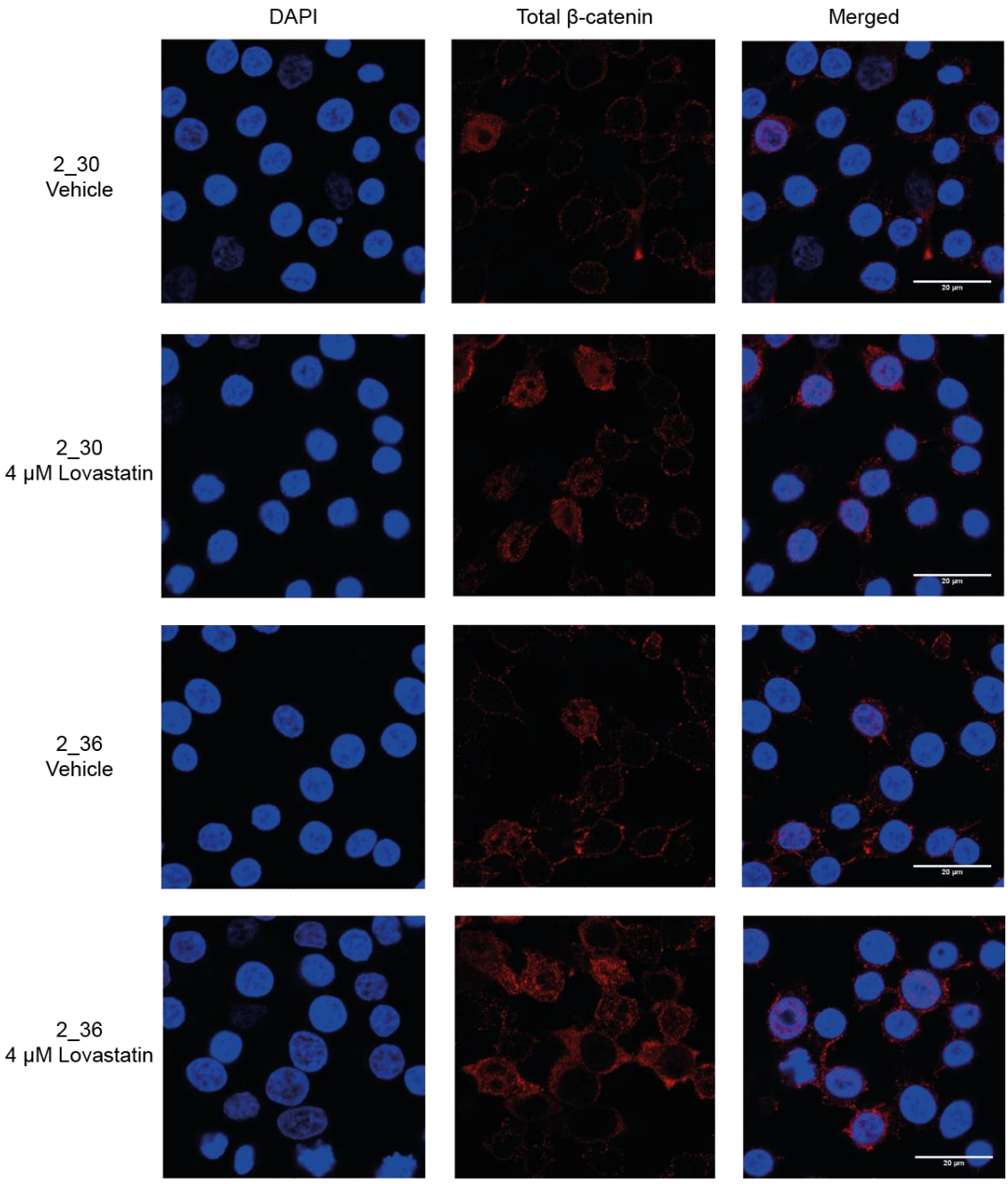

Figure 58 Levels of total β-catenin upon statin treatment in RKO 2_30 and 2_36

Cells were treated with 0 μM or 4 μM lovastatin for 72 hours before fixing and preparing for confocal. DAPI staining is in blue, total β-catenin is in red. Merged image is a composite of both DAPI and total β-catenin. Scale bar indicates 20 μM. Representative images shown.

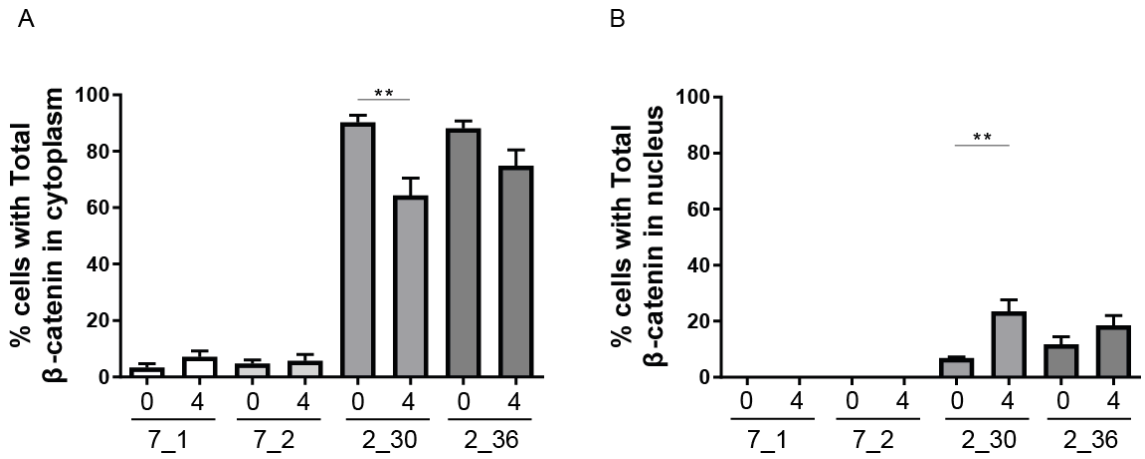

Figure 59 Summary of total β-catenin levels upon statin treatment

Cells were treated with 0 μM or 4 μM lovastatin for 72 hrs before fixing and preparing for confocal. Approximately 200 cells were counted per condition per cell line and the % of cells with A) cytoplasmic staining and % cells with B) nuclear staining was calculated. A) B) Error bars are SEM, one way anova (post hoc Tukey) was performed for both graphs (** p≤ 0.01).

6.2 The Rac1 inhibitor EHT1864 prevents the statin induced transport of β-catenin into the nucleus

Rac1 has previously been shown to play a role in the Wnt signalling pathway through two potential mechanisms. Rac1 may be required for β-catenin to be transported into the nucleus, whereby active Rac1 activates JNK2, which then phosphorylates β-catenin at ser191 and ser605, enabling β-catenin to translocate to the nucleus (Wu et al. 2008). More recent research suggests Rac1 plays a role in enhancing the formation of β-catenin-TCF/LEF complexes (Jamieson et al. 2015). Jamieson et al. (2015) also suggests Rac1 activation mediates the activation of JNK2 and the phosphorylation of β-catenin at ser191 and ser605 by JNK2. The phosphorylation of β-catenin at these residues is believed to enhance its binding to TCF/LEF and not facilitate its transport into the nucleus. Additionally Rac1 has been shown to play a key role in CRC tumourigenesis. Myant et al. (2013) showed the level of active Rac1 is upregulated after APC is mutated and this promotes tumourigensis. Rac1 is suggested to act downstream of Wnt signalling (in contrast to the research mentioned earlier) to promote progenitor cell proliferation and the expansion of LGR5 ISC cells in the colonic crypts (Myant et al. 2013). Espina et al. (2008) demonstrated overexpression of Rac1 in a APC mutant SW620 xenograft model accelerated tumourigenesis, whilst the suppression of Rac1 prevented tumourigenesis. Based on the link of Rac1 with both CRC and Wnt signalling we hypothesised the increase in active Rac1 upon statin

treatment in the APC mutant lines was responsible for the increase in β-catenin being transported from the cytoplasm to the nucleus.

To investigate if Rac1 was involved, we inhibited Rac1 using EHT1864 in combination with lovastatin treatment in the APC wt RKO 7_1 and APC mutant RKO 2_30 and used confocal microscopy to analyse levels of total β-catenin in the cytoplasm and nucleus. We plated RKO 7_1 and RKO 2_30 on coverslips at a density of 40,000 cells/well and treated with 1) vehicle, 2) 4 μM lovastatin, 3) 1 μM EHT1864 or 4) 4 μM lovastatin and 1 μM EHT1864. We treated the cells for 72 hours, then fixed the cells and stained with DAPI and total β-catenin. Representative images for RKO 7_1 are shown in figure 60 and for RKO 2_30 in figure 61. Approximately 150 cells were analysed per condition and the percentage of cells with β-catenin staining in the nucleus and β-catenin staining in the cytoplasm was quantified (Figure 62). The APC wt RKO 7_1 cells show between 10-40 % cells with cytoplasmic total β-catenin staining in the different conditions but all conditions show no cells with nuclear staining. The variation in cytoplasmic staining could be related to these results being from one experiment because previously when treating RKO 7_1 with and without lovastatin we saw less than 10 % cells with cytoplasmic β-catenin staining. The results show no RKO 7_1 cells with nuclear staining and this is because of the low activation of the Wnt signalling pathway in this cell line. Figure 62A shows that lovastatin treatment alone in RKO 2_30 reduces the percentage of cells with total β-catenin in the cytoplasm as seen previously, compared to the levels when treated with EHT1864 alone and vehicle. When lovastatin and EHT1864 are combined the percentage of cells with β-catenin in the cytoplasm is just below the level seen in the vehicle and EHT1864 alone, indicating that Rac1 inhibition using EHT1864 prevented the reduction in β-catenin staining in the cytoplasm upon lovastatin treatment. In agreement with these results the increase in percentage of cells with β-catenin nuclear staining is only seen when the RKO 2_30 cells are treated with lovastatin alone (Figure 62B). When the RKO 2_30 cells are treated with EHT1864 and lovastatin together, the percentage of cells with β-catenin in the nucleus is similar to the vehicle treated. This data supports our hypothesis that the statin driven increase in active Rac1 is causing β-catenin to be transported from the cytoplasm into the nucleus.

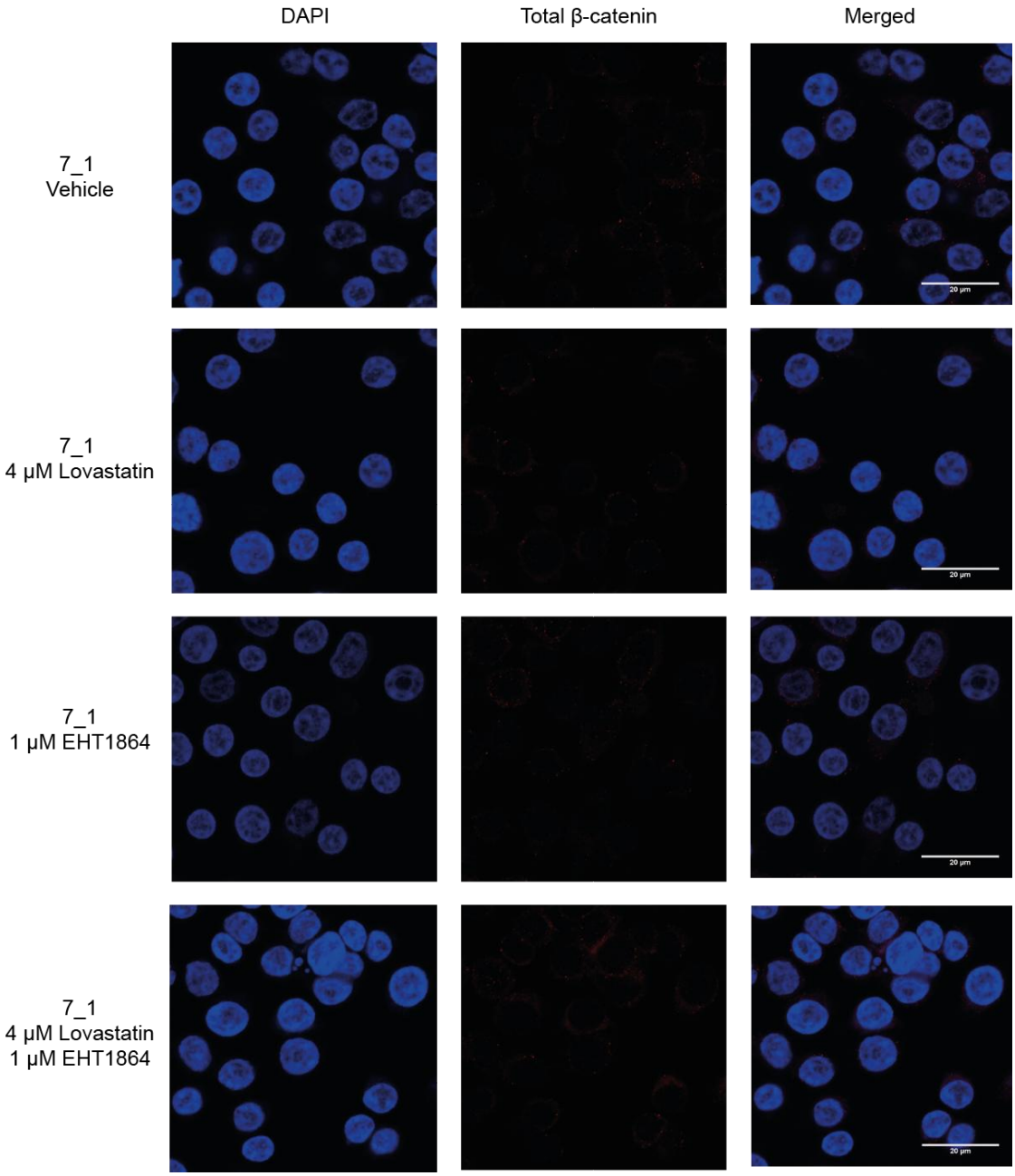

Figure 60 Effect of EHT1864 and statin treatment on β-catenin in RKO 7_1

Control RKO 7_1 were untreated or treated with 4 μM lovastatin or 1 μM EHT1864 or 4 μM lovastatin & 1 μM EHT1864 for 72 hrs before fixing and preparing for confocal. DAPI staining is in blue, total β-catenin is in red. Merged image is a composite of both DAPI and total β-catenin. Representative images shown.

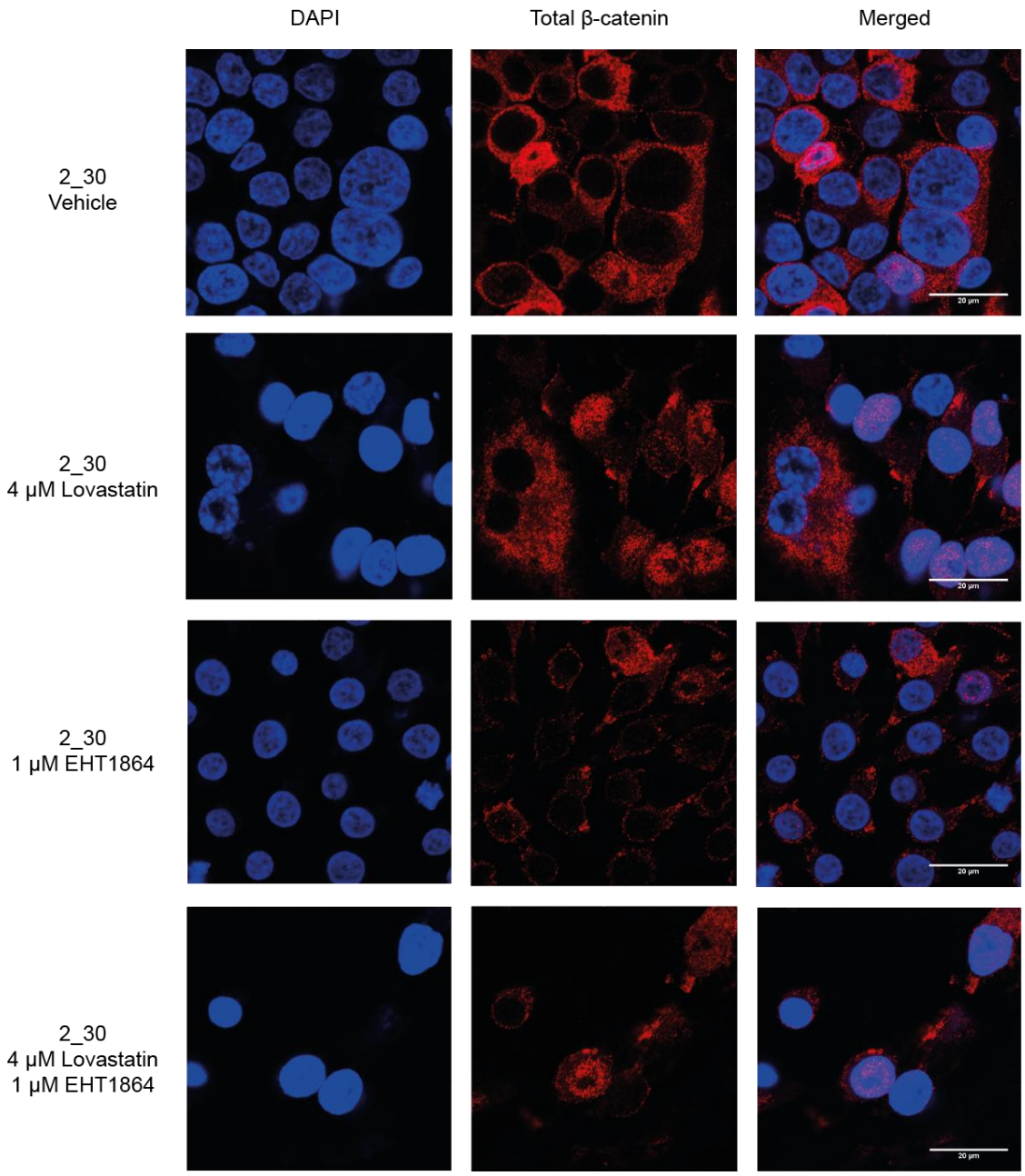

Figure 61 Effect of EHT1864 and statin treatment on β-catenin in RKO 2_30

APC mutant RKO 2_30 were untreated or treated with 4 μM lovastatin or 1 μM EHT1864 or 4 μM lovastatin & 1 μM EHT1864 for 72 hours before fixing and preparing for confocal. DAPI staining is in blue, total β-catenin is in red. Merged image is a composite of both DAPI and total β-catenin. Representative images shown.

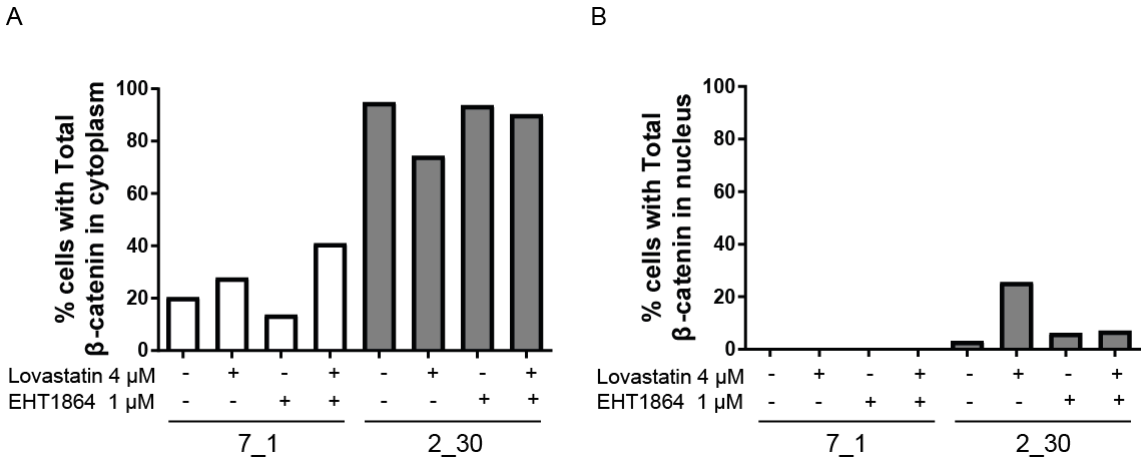

Figure 62 Summary of the effect of EHT1864 and statin treatment on β-catenin

Cells were untreated or treated with 4 μM lovastatin or 1 μM EHT1864 or 4 μM lovastatin & 1 μM EHT1864 for 72 hours before fixing and preparing for confocal. At least 150 cells were counted per condition per cell line and the % of cells with cytoplasmic staining A) and % cells with nuclear staining B) was calculated.

In our *in vitro* model we have shown that statins cause an increase in active Rac1, this increase in active Rac1 is not responsible for the synthetic lethality we see between statins and the APC mutation. The increase in active Rac1 is responsible for an increase in β-catenin being transported from the cytoplasm into the nucleus. Results discussed earlier from immunoblotting both total and unphosphorylated (active) β-catenin (Figure 43/44) and the TCF/LEF reporter assay (Figure 43E) do not demonstrate an increase in Wnt signalling after statin treatment. This implies statins may cause β-catenin to accumulate in the nucleus, but the β-catenin is unable to active Wnt signalling. Our results do not support one of the hypothesised roles of Rac1 in the Wnt signalling pathway, suggesting that Rac1 enhances the formation of β-catenin-TCF/LEF complexes. If this were true, we would expect to observe an increase in transcription of Wnt target genes (measured through the TCF/LEF assay) with the increase in active Rac1, results discussed earlier (section 2 and 3.1) showed a decrease in the TCF/LEF assay and a decrease in expression of the Wnt target gene survivin. The recent data on the phosphorylation of Pak1 may explain this discrepancy in increased nuclear β-catenin and a decrease in TCF/LEF activation. β-catenin has been described as a Pak1 effector, Pak1 has been shown to phosphorylate β-catenin at ser675 and this stabilises β-catenin and enhances transcription of Wnt target genes

(Zhu et al. 2012). We have shown statins prevent the phosphorylation and subsequent activation of Pak1 and we hypothesise this is through the mislocalisation of Rac1, due to the decrease in prenylation. This could be responsible for the reduction in transcription of Wnt target genes regardless of increased levels of nuclear β-catenin. To test this hypothesis we could add active Pak1 to the cells, whilst treating with statins and see if this rescues the synthetic lethality. Additionally, we could test a Pak1 inhibitor and see if this mirrors the synthetic lethal effect seen in the APC mutant cell lines.

7 Silencing APC does not sensitise wildtype RKO cells to statins

We investigated whether silencing APC in the wildtype RKO cell line would cause an increase in statin sensitivity. In 96 well plates, we transfected the wildtype RKO cell line with the two siRNA previously used to target APC (siAPC*3 and siAPC*6; Figure 19 from chapter 1) and then treated with increasing doses of lovastatin. After 72 hours of drug treatment, we measured cell viability using CTG and plotted dose response curves. The results show the transfection of siAPC*3 appears to sensitise the wildtype RKO cell line to statins, whilst the siAPC*6 does not show an increase in sensitivity (Figure 63A). To investigate why we see a difference, we analysed whether both siRNA targeting APC cause a decrease in APC protein and additionally if either siRNA targeting APC alters survivin levels. We collected whole cell lysates from RKO cells transfected with siAPC*3, siAPC*6 and siCON and immunoblotted for APC and survivin levels (Figure 63B/C). We found both siRNA targeting APC reduce full length APC levels, however neither siRNA altered the levels of survivin. Potentially, we did not see an increased sensitivity in wildtype RKO cells when silencing APC because using siRNA is not the same as the mutation we created using CRISPR-cas9, because any full length APC remaining could be enough to fullfill the roles of APC, preventing a decrease in survivin levels and an increase in sensitivity.

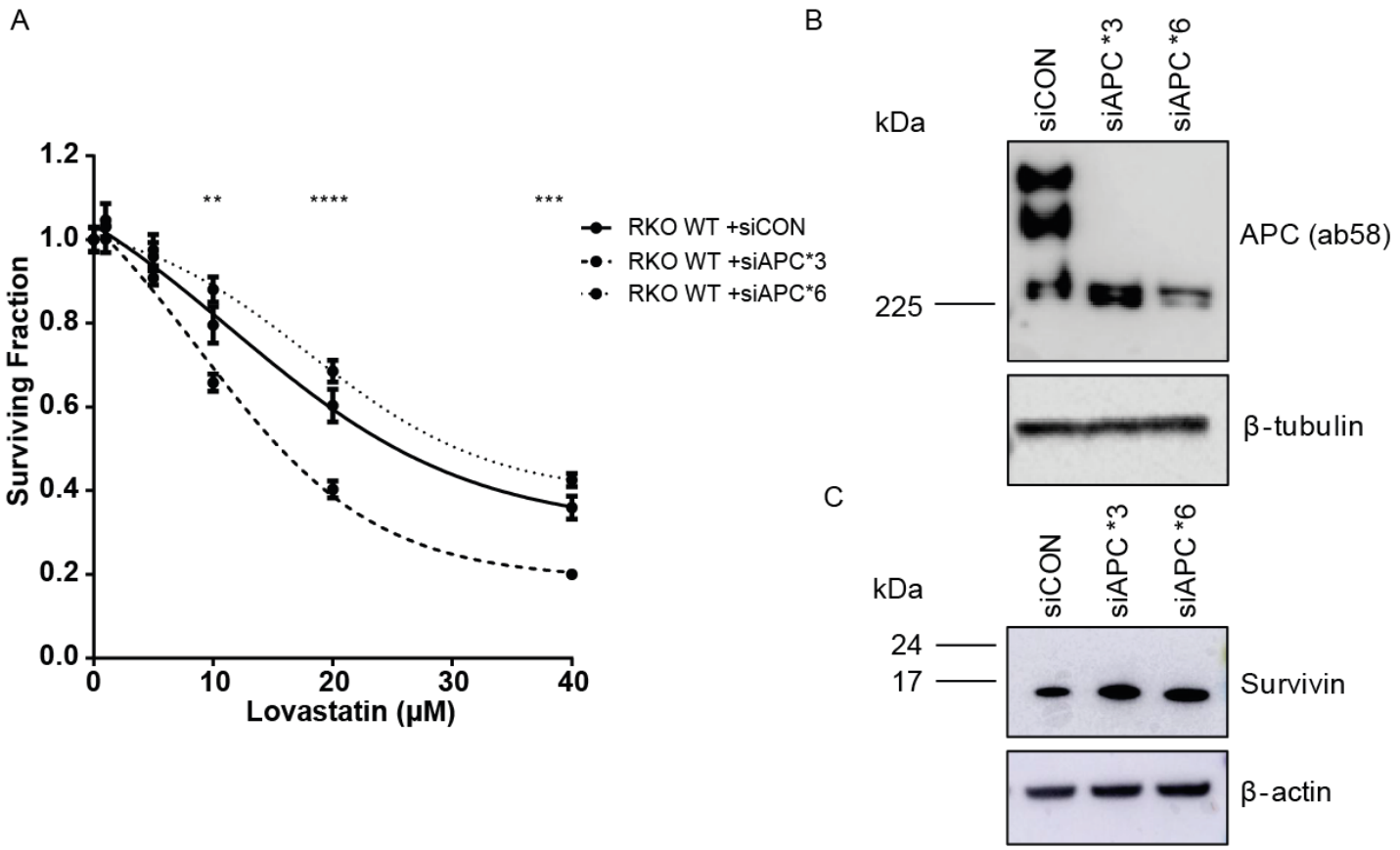

Figure 63 In RKO WT silencing APC does not sensitise cells to lovastatin

A) In a 96 well plate RKO WT cells were transfected with siCON or siAPC, 5 hours later cells were drugged with increasing doses of lovastatin. After 72 hours of drug treatment cell viability was measured using CTG and survival fractions were calculated. Experiment performed in triplicate, error bars are SEM, a two way anova (post hoc Dunnet) was performed and the significance values are shown for siCON vs siAPC*3 (** p≤ 0.01 **** p≤ 0.0001). B) C) In a 6 well plate RKO WT were transfected with siCON, siAPC*3 and siAPC*6 and 72 hours later whole cell lysates were collected. β-tubulin or β-actin used as a loading control B) Levels of APC were detected by western blotting. C) Levels of survivin were detected by western blotting.

8 Investigating the response of a CRC panel to statin treatment

8.1 Response to lovastatin, mevastatin & simvastatin

In our *in vitro* model we have validated a synthetic lethal relationship between statins and the APC mutation. Next we wanted to investigate if this synthetic lethal relationship extended to other CRC cell lines with varying background mutations in addition to APC. In particular we wanted to see if cell lines with an APC mutation were more sensitive than the APC wt cell lines. In our cell line panel, the DLD1, HT29 and SW620 have APC mutations and RKO, HCT116 and SW48 are APC wildtype. In 96 well plates, we performed dose response curves in the DLD1, HCT116, HT29, RKO, SW48 and SW620 cells with increasing concentrations of lovastatin, mevastatin and simvastatin. The cells were drugged twice and the total treatment was for 96 hours. Cell viability was measured using CTG and dose response curves were plotted using survival fractions (Figure 64). We found the six cell lines show the same pattern of sensitivities to each statin such that the DLD1, RKO and SW48 cells were more sensitive than the HCT116, HT29 and SW620 cells to statin treatment. Interestingly, the APC mutant cells were not in general more sensitive to lovastatin, mevastatin and simvastatin (Figure 64 APC mutant = blue, APC wt = black/red). Additionally we analysed whether sensitivity to statins correlated with activation of the Wnt signalling pathway because RKO (shown in red) does not show Wnt activation and this cell line is among the more sensitive cell lines. DLD1, HT29 and SW620 (blue) show Wnt activation due to APC mutations, SW48 and HCT116 (black) show Wnt activation due to β-catenin mutations. However no correlation was seen. We also considered if other common mutations including, mutations in BRAF, KRAS and p53, could correlate with sensitivity to statins. However, these do not explain the pattern of sensitivity (Table 9 shows the status of each line). Therefore the sensitivity of the panel of CRC cell lines is likely to be explained by a combination of factors or a particular APC mutation. Testing more cell lines would help our understanding of this and the impact of different APC mutations.

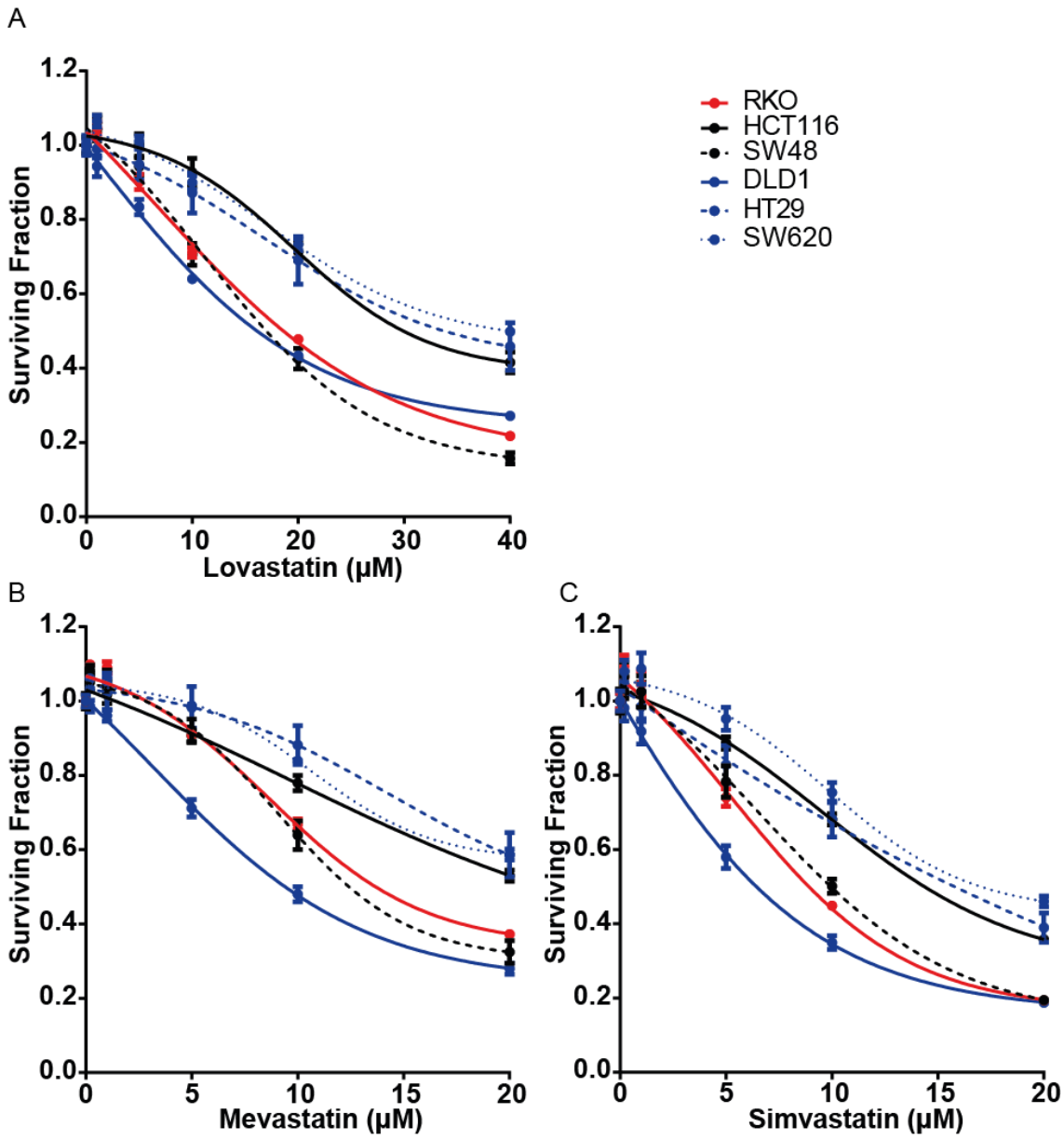

Figure 64 Statin sensitivity in the CRC cell line panel

Dose response curves performed in RKO, HCT116, SW48, DLD1, HT29, SW620 with lovastatin, mevastatin and simvastatin. Colour scheme is; APC and β-catenin wt (red), APC wt & β-catenin mutation (black), APC mutant (blue). Experiments performed in triplicate, error bars SEM. Cell lines were treated with lovastatin A) mevastatin B) simvastatin C).

8.2 Do the basal levels of survivin in the CRC panel and RKO *in vitro* model explain the sensitivities to statins?

We have shown that a decrease in survivin levels induces sensitivity to statin treatment. To further our understanding of the different sensitivities we see in our CRC cell line panel, we analysed the basal levels of survivin in our different cell lines. We hypothesised the differences in statin sensitivities described above could be related to differences in levels of the protein survivin. A summary of the survival fraction at 10 μM lovastatin for all the cell lines is shown in figure 65A. We collected whole cell lysates from the CRC panel and our RKO *in vitro* model cell lines (RKO 7_1, RKO 7 _2, RKO 2_30 and RKO 2_36) and immunoblotted for levels of survivin (Figure 65B). The survivin blots show two bands which could represent three isoforms because wt survivin encodes a 16 kDa protein, survivin ΔEx3 encodes a 15 kDa protein and survivin 2B encodes a 18 kDa protein (Necochea-Campion et al. 2013). Therefore the top band may represent levels of survivin 2B and the lower band could represent wt and survivin ΔEx3. We quantified both bands of survivin together and these are shown in figure 65C. The levels of survivin are very variable across the panel. RKO 2_30 had a lower basal level of survivin then the controls APC wt RKO 7_1 and RKO 7_2, whilst the results for RKO 2_36 show high variability between the repeats. Interestingly the cell lines DLD1 and HT29 appear to express lower levels of survivin than RKO 2_30 and RKO 2_36 but are less sensitive to statins, the reason for this is unclear. In support of our hypothesis one of the most resistant cell lines HCT116 has the highest levels of survivin across the ten cell lines.

To further investigate a possible relationship between basal survivin expression and statin response we first plotted both variables against each other for all cell lines. Figure 66A shows when looking at the data from all the 10 cells lines there is no correlation between survivin expression and statin response. Next we subdivided the cell lines into groups to see if this changed the correlation pattern. Firstly we looked in terms of APC and Wnt signalling status (Figure 66B/C/D/E) and found the strongest correlation (R^2 0.8442) was within the cells showing no Wnt activation. This data suggests a higher survivin level correlates with higher sensitivity to statins, however this finding is limited because it is based on three RKO cell lines. We then looked in terms of KRAS, BRAF and TP53 status and found the highest R^2 value of 0.5532 in the TP53 mutant (DLD1, HT29 and SW620), the greater survivin expression the more resistant to statins, however this result is based on data from three cell lines (Figure 67). Weaker correlations (R^2 ~0.4) were shown in the KRAS mutant, BRAF wildtype and TP53 wildtype. These all suggest a weak positive relationship between survivin

expression and statin response. The correlation strengths are limited because the graphs display data from up to 10 cell lines and the cell lines are biased towards the RKO characteristics. It would be interesting to see if studying more cell lines provides more conclusive data.

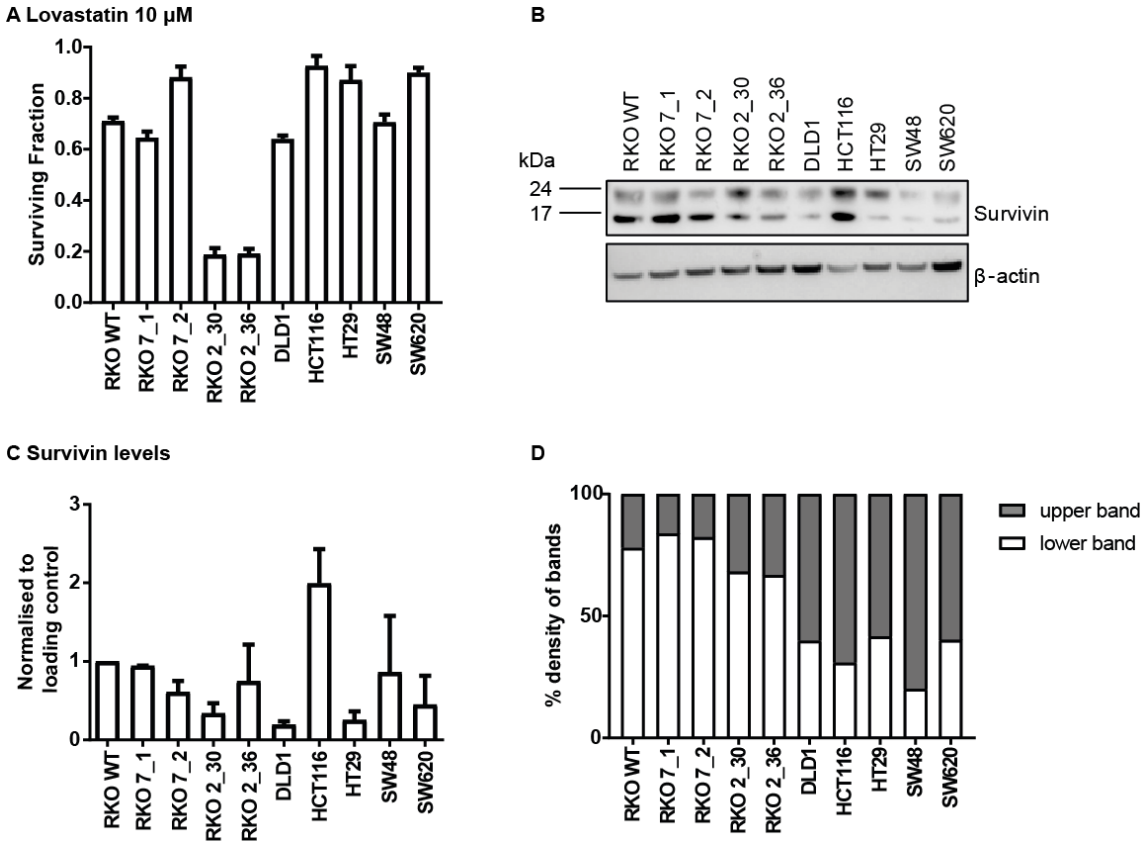

Figure 65 Do survivin levels explain the statin sensitivity in CRC?

A) For all cell lines the survival fraction at 10 µM lovastatin was plotted, data from the dose response curves performed with lovastatin. Combination of three experiments, error bars SEM. B) Whole cell lysates were collected from 6 well plates and immunoblotted. Levels of survivin were detected and normalised to β-actin. Performed twice, representative blot shown. C) Both survivin bands in the western blots from B) were quantified together and normalised to the loading β-actin and RKO WT. Error bars are SEM, one way anova (post hoc Tukey) performed ns. D) For each cell line the % density for the upper and lower survivin bands were calculated and plotted.

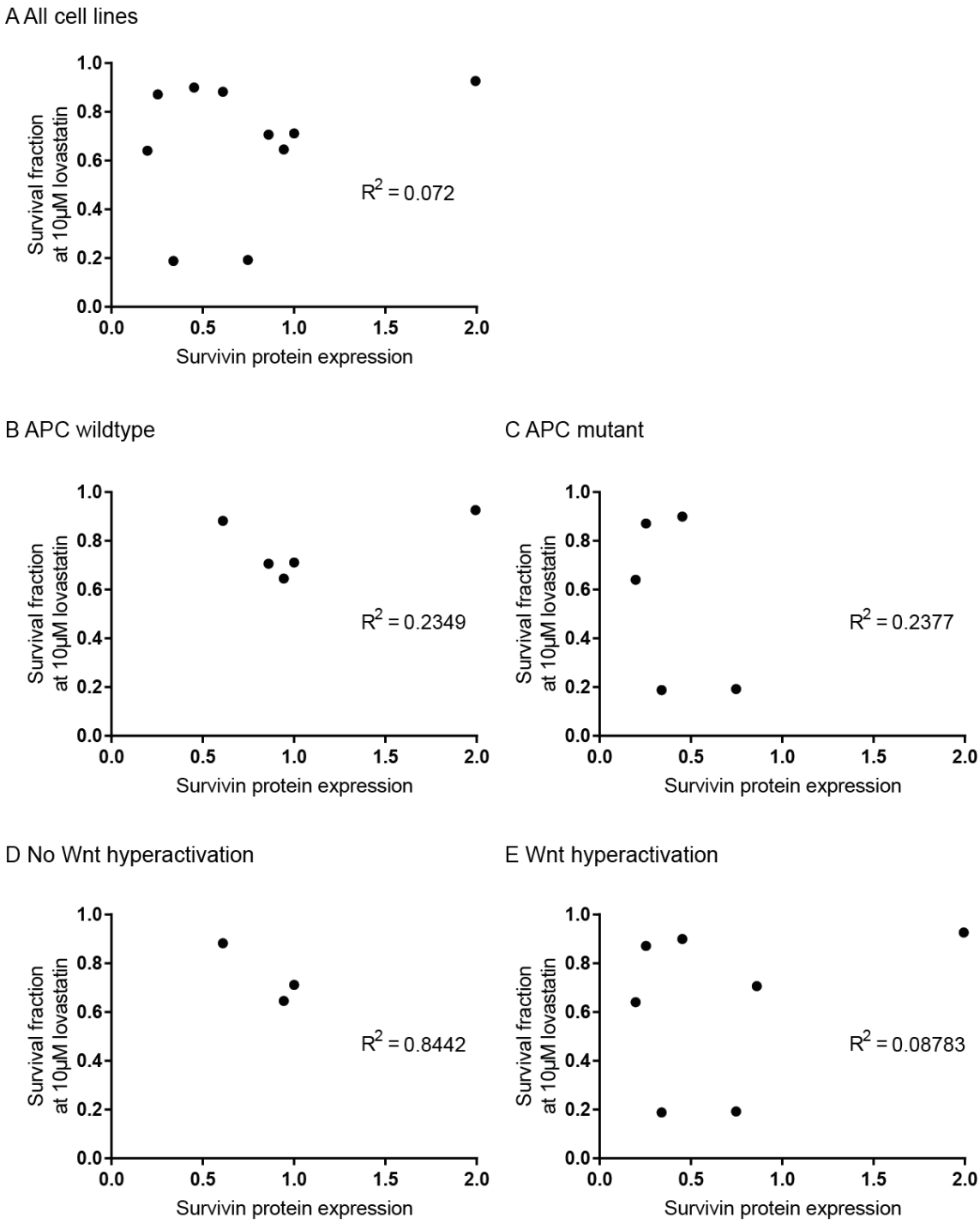

Figure 66 Do survival fractions at 10 μM lovastatin and survivin expression correlate

Plotted survival fraction at 10 μM lovastatin against survivin expression, R^2 values calculated. A) For all cell lines B) For APC wt C) For APC mutant D) For no Wnt hyperactivation E) For Wnt hyperactivation.

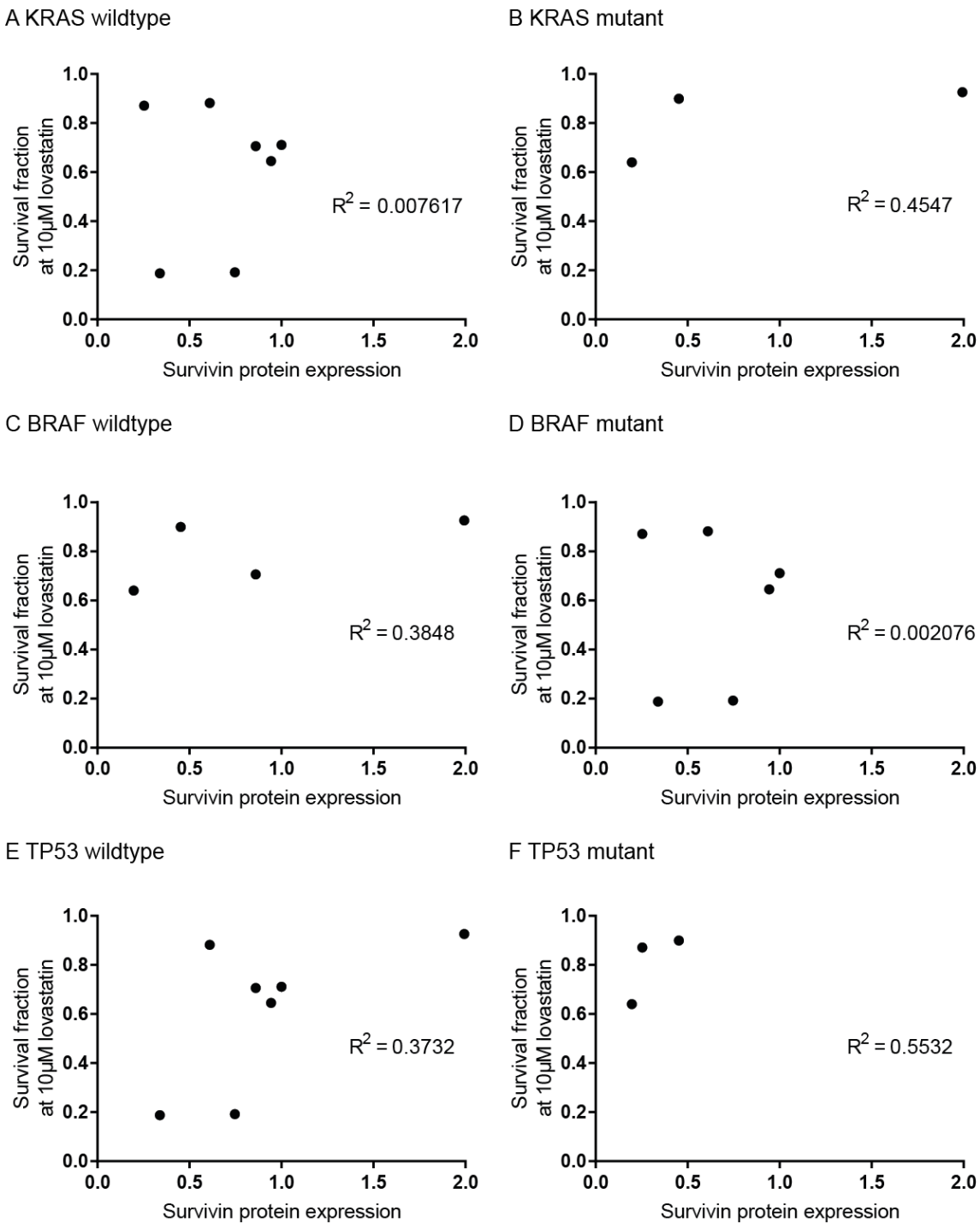

Figure 67 Do survival fractions at 10 μM lovastatin and survivin expression correlate

Plotted survival fraction at 10 μM lovastatin against survivin expression, R^2 values calculated. A) For KRAS wt B) For KRAS mutant C) For BRAF wt D) For BRAF mutant E) For TP53 wt F) For TP53 mutant.

Next we investigated if the pattern of sensitivity to statins was due to the ratio of the top and lower bands. We believe these bands represent different isoforms, the lower band at 16 kDa could be a mixture of wildtype survivin and survivin ΔEx3. The higher band at 18 kDa could represent survivin-2B. Survivin-2B is an interesting isoform because a few studies have shown it is downregulated in later tumour stages (Mahotka et al. 2002; Meng et al. 2004). One study in leukaemia has suggested survivin-2B may have a pro-apoptotic role (Zhu et al. 2004). However, at the moment there is no solid evidence supporting a role for the alternately spliced survivin isoforms in tumourigensis (Li 2005). Figure 65D shows a graph displaying the ratio of upper and lower survivin bands. The results show all the RKO (wildtype and *in vitro* model) cell lines have a higher percentage of the lower than the upper band. In comparison DLD1, HCT116, HT29, SW48 and SW620 all show the opposite and have a higher percentage of the upper than lower band. Additionally, we see a difference when comparing within our *in vitro* model, the APC mutant RKO 2_30 and RKO 2_36 show slightly more upper band than the lower band compared to the controls RKO 7_1 and 7_2. It would be interesting to analyse the RT-PCR levels of each of the survivin splice variants and see if this corresponds to the protein levels we see on the westerns. Additionally it would establish if the lower band represents both wildtype survivin and survivin ΔEx3 and if the higher band is survivin-2B. Overall statin sensitivity doesn't seem to directly correlate to survivin levels or the ratio of the upper and lower survivin bands in our CRC cell line panel and *in vitro* model. It is possible that survivin levels are one of multiple factors which influence response to statins.

In this chapter we have investigated the mechanism responsible for the synthetic lethal relationship between statins and the APC mutation in our *in vitro* model. Figure 68 shows our proposed mechanism. Firstly, statins inhibit HMGCR which lowers levels of isoprenoids. This reduces prenylation of Rac1 causing mislocalisation. We also see an unexplained increase in levels of active Rac1 in just the APC mutant cell lines and this is responsible for driving the transport of β-catenin into the nucleus. However the accumulation of β-catenin into the nucleus does not result in the activation of the Wnt pathway. The Rac1 effector Pak1 showed decreased phosphorylation at ser144 (resulting in less fully active Pak1), which we propose is due to the mislocalisation of Rac1. This results in lower Pak1 activation and potentially this causes a reduction in the phosphorylation of β-catenin at ser675. β-catenin phosphorylated at ser675 is more stable and transcriptionally active. Therefore the reduction in active Pak1 would also decrease levels of Wnt signalling and the Wnt target gene survivin. The decrease in the anti-apoptotic protein survivin below a level the APC mutant cells can tolerate, results

in apoptosis. The APC wt controls are not vulnerable because they do not show hyperactivation of the Wnt signalling pathway.

Further work is required to strengthen our findings and establish how transferrable the mechanism is to other types of APC mutation found in CRC cell lines. Additionally *in vivo* data would help us understand if our findings could translate into patients.

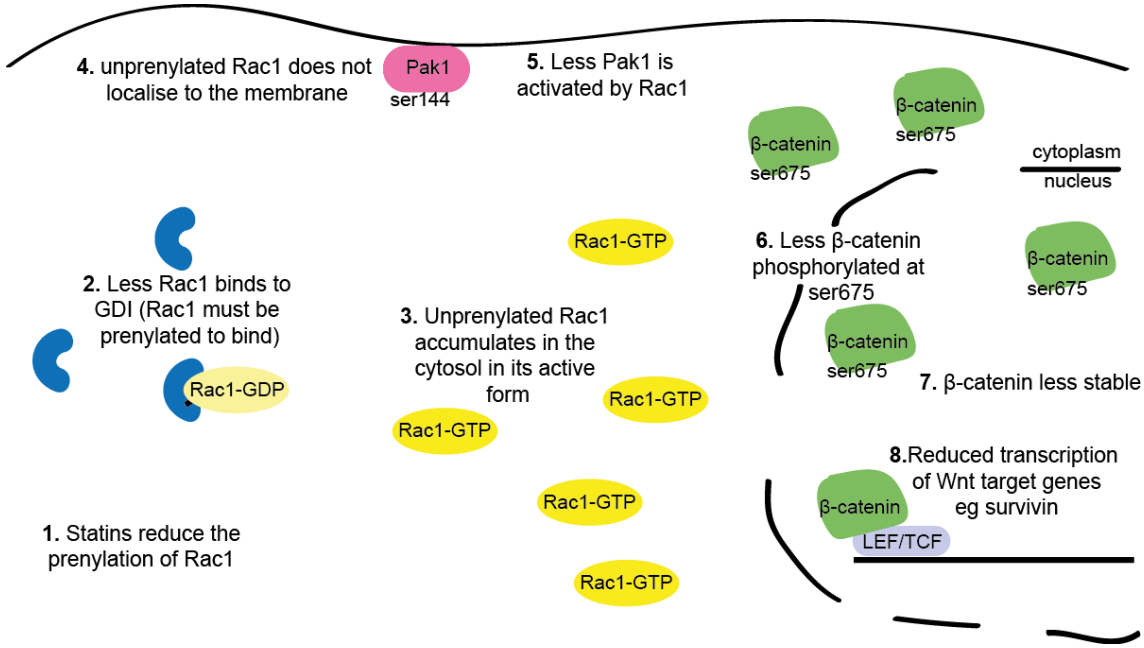

Figure 68 Proposed mechanism of statins in our *in vitro* model

Statins inhibit HMGCR, reducing isoprenoids and levels of prenylated Rac1. Unprenylated Rac1 is unable to bind GDI, therefore Rac1 accumulates in its active form in the cytoplasm. Cytoplasmic Rac1 is unable to interact and activate Pak1. Reduced Pak1 activation reduces Pak1 directed phosphorylation of ser675 on β-catenin. This reduces the stability of β-catenin and reduces transcription of Wnt target genes including survivin which causes apoptosis.

Discussion

1 Creating an *in vitro* model of APC deficiency

There are a wide range of colorectal cancer cell lines available to perform studies in and they represent the broad range of mutations found in CRC. However, to enable us to identify synthetic lethal relationships specific to APC loss we wanted to create a new *in vitro* model where the cell lines only differed in the APC status.

1.1 Use of RKO cell line for our *in vitro* model

As a starting point for our *in vitro* model we wanted to select a cell line which was wildtype for *APC* to enable us to edit this gene. Additionally, we did not want any mutations in other Wnt signalling components, such as the *CTNNB1* gene (encodes β-catenin) to ensure the cell line did not show hyperactivation of the Wnt signalling pathway. After applying this criteria the number of cell lines to select from was limited, this reflects the high rate of APC mutations and the role of the Wnt signalling pathway in driving CRC tumourigenesis. For example, we identified many APC wildtype cell lines which contain β-catenin mutations such as HCT116, SW48 and LS174T (Ilyas et al. 1997; Gayet et al. 2001). We identified both RKO and Co115 cell lines to be APC and β-catenin wildtype (Gayet et al. 2001; da Costa et al. 1999). Our group had experience of working with the RKO cell line, we felt this would be beneficial to us and would help the CRISPR-cas9 process. Research has suggested the RKO cell line has a mutation in the gene *NKD1,* a negative regulator of the Wnt pathway upstream of the β-catenin destruction complex (Guo et al. 2009). The paper identified the mutation in the RKO cell line and then the rest of the work was in either xenopus embryos or cell lines other than RKO (including HEK293T and Co115 cells). We analysed protein levels of total β-catenin and unphosphorylated ser33/ser37/thr41 β-catenin (active) in whole cell lysates from the RKO cell line alongside a panel of CRC cell lines with known APC or β-catenin mutations. The RKO cell lines showed no detectable increase in either total or unphosphorylated β-catenin in comparison to the cell lines with known APC or β-catenin mutations. Therefore, it seems unlikely the *NKD1* mutation identified in the RKO cell line has a phenotypic effect on levels of Wnt signalling. Having confirmed the RKO cell line did not display hyperactivation of the Wnt signalling pathway, we investigated whether the RKO cell line would functionally respond to altered APC expression. We silenced APC with siRNA and measured the level of Wnt signalling through a TCF/LEF reporter assay and found that levels of the pathway increased upon reducing APC expression. This result indicated the RKO cell line was an ideal starting point for our *in vitro* model.

The RKO cell line is characterised as showing MSI and has mutations in key genes known to contribute to the development of CRC including; *BRAF* and *PIK3C*A (Ahmed et al. 2013). This mutational background does not reflect all the mutations found in CRC and therefore our *in vitro* model may behave differently to cell lines displaying MSS and cell lines with mutations in other key genes. To overcome this limitation we tested our findings in a panel of CRC cell lines representing both MSI and MSS and the different key mutations found in CRC. Another important consideration is the RKO cell line is tumourigenic independent of the Wnt signalling pathway, therefore other pathways are important in driving and maintaining the tumourigenic state. The implication of this is manipulating the Wnt pathway by mutating APC may not have the same consequences as in a cell line which has naturally developed hyperactivation of this pathway. Despite the potential limitations of our *in vitro* model, our approach has the advantage that the cell lines have the same mutational background and only differ in their APC status, helping to identify synthetic lethal relationships specific to the APC mutation.

An alternative approach would have involved using a normal colon cell line and editing the *APC* gene using CRISPR-cas9. As with all models this approach had its own limitations, normal cell lines do not grow so well in culture and this would have made the CRISPR-cas9 editing process more difficult, especially during the single colony selection. If we had failed to single colony select we would have had to work with a pool of cells containing a mixture of wildtype *APC* and edited *APC* genes. This would have made it harder to uncover synthetic lethal relationships. Additionally an APC mutation alone is thought to not be sufficient for a cell line to become fully tumourigenic, the cell line would not have any of the additional mutations in key pathways characteristic of CRC and this would have increased the risk that our findings did not translate to a panel of CRC cell lines (Matano et al. 2015). A recent paper used a normal HCEC cell line known as 1CT and the normal colon cell line was modified using a combination of shRNA against TP53 and APC, alongside ectopically expressing plasmids for KRAS G12V and APC1309 (Zhang et al. 2016). This model successfully identified the drug TASIN-1 which shows a synthetic lethal relationship with the APC mutation. This approach did not involve CRISPR-cas9 and therefore did not require single colony selection. Interestingly, the paper also identified a drug targeting the cholesterol synthesis pathway, which supports the use of our *in vitro* model and highlights the potential of targeting this pathway for APC mutant CRC.

1.2 Use of CRISPR-cas9 to generate our *in vitro* model of APC mutation

CRISPR-cas9 has been shown to be an effective gene editing technique and we decided to use it to try to generate a full APC knockout. The APC gene covers 8535 nt and therefore could be difficult to eliminate expression of the entire protein. Matano et al. (2015) used CRISPR-cas9 to edit *APC* along with *TP53*, *KRAS* and *PIK3CA* in human intestinal organoids and demonstrated their resulting tumourigenic potential *in vivo*. The group targeted exon 8 of *APC* resulting in a truncated APC product, it is interesting they did not target exon 15 at the MCR to generate a 'typical' APC mutation. They showed the organoids with altered APC also displayed altered Wnt signalling activation. This was shown by analysing levels of β-catenin by western blotting and because removal of the Wnt factors Wnt and R-spondin from the media only effected growth of the APC wildtype organoids.

We designed gRNA targeting exon 2 and the exon 15 (covers 80 % coding region) using a freely available online tool called dna2.0 CRISPR-cas9 design tool (now called atum) and used two different methods. The gRNA #8 and #9 target exon 2 and we used a transient system from Dharmacon called Edit-R. This system involved transfecting all three components into the cells together. Advantages of this approach are the cas9 is only transiently expressed reducing off target effects and the process is quick because the components are ready to transfect and the selection of edited cells is shorter. However because all 3 components are delivered separately, the selection process will select cells which 1) received the cas9 plasmid, 2) received the cas9 plasmid + tracrRNA 3) received the cas9 plasmid + tracrRNA + crRNA. Therefore the single colony selection process may require more cells to be grown up and analysed. The target sites of the gRNA used with this method were more likely to produce a full APC knockout, however we did not identify any clones with edited APC using this approach.

The gRNA #2 - #6 targeted exon 15 and we used a lentiviral system. This system had the advantage that all components required were delivered on one vector, therefore after the puromycin selection all cells which survived would contain all the components required for editing to have occurred. Using this method we didn't manage to generate a full APC knockout, however the gRNA #2 generated a line with an APC truncation on both alleles resulting in only 25 % of the APC product remaining. An *in vitro* model with an APC truncation represent patients better because this is more common, full loss of APC expression is rare. However, the position of our APC truncation in the armadillo 7th repeat is not in the MCR (region commonly mutated). Additionally, in FAP patients

mutations in this region generate a less severe phenotype than those with mutations in the MCR (Zeineldin & Neufeld 2013). In support of our *in vitro* model generated, there are two *in vivo* mice models (APC^{716} and APC^{min}) with mutations in a similar region of APC which are commonly used to model CRC (Young et al. 2013).

Alongside the RKO APC truncated cell line we generated two matched control cell lines. The control lines were targeted with a non-targeting gRNA and underwent the same process to enable us to minimise the effects of the CRISPR-cas9 editing process. One downside of the cell lines we generated using the lentiviral system was the cell lines still express cas9 and this could result in more off target effects. Papers have reported a wide range of factors contributing to off target effects with the CRISPR-cas9 editing approach, including the type of cas9 used, dose of cas9/gRNA and the design of the gRNA (Fu et al. 2013; Hsu et al. 2013; Wu et al. 2014). At the time of performing the CRISPR-cas9 stage of the project wildtype spCas9 was commonly used and this has been shown to induce more off target effects than other cas9. The main other cas9 available at the time was a cas9 nickase which makes single stranded breaks, reducing off target effects (Sanjana et al. 2014; Hsu et al. 2014). Since completing our CRISPR-cas9 editing, more specific cas9 have been identified including the high fidelity cas9 (HF-cas9) which has been shown to cause no detectable off target effects (Kleinstiver et al. 2016). Despite the potential for off target effects in our *in vitro* model, we have used CRISPR-cas9 to generate two control cell lines and an APC mutant cell line derived from the same RKO parental line.

In retrospect if time was not limited we should have used the gRNA #8 and #9 (targeted exon 2) with the lentiviral method to attempt to generate a full APC knock-out. Although it is possible the region of exon 2 may be less accessible to the cas9 and gRNA due to the chromatin structure (Daer et al. 2017; Wu et al. 2014). Additionally to improve our CRISPR-cas9 methodology we could have used either the T7 endonuclease 1 or surveyor assay, to help us estimate the mutation frequency and determine how many clones to pick. Although these approaches have limitations because they have been shown to underestimate the mutation frequency, they cannot detect events were the same mutation has occurred on both alleles (Kim et al. 2014).

Once we had generated our lines RKO control (7_1 and 7_2), RKO APC mutant (2_6) we checked the cells showed the phenotype we would expect. We analysed the Wnt pathway using the TCF/LEF reporter assay and immunoblotted for levels of β-catenin and found the RKO APC mutant line showed hyperactivation of the Wnt signalling pathway. Unfortunately soon after generating these lines it became apparent that the RKO APC mutant line 2_6 still expressed a low level of full length APC. This could

have happened through poor single colony selection or contamination of the cell line with an APC wildtype line. We decided to re-single colony select the line and generated the RKO APC mutant lines 2_20, 2_21, 2_30 and 2_36, we focused on four cell lines because we were conscious that these cells had undergone two cycles of single colony selection. We confirmed all the lines had the same APC mutation by topocloning and displayed activation of the Wnt signalling pathway. An important consideration of our *in vitro* model cell lines is whether they activate the 'right' level of Wnt signalling. Many studies have supported the hypothesis that the two APC mutations are interdependent, to generate a specific level of Wnt signalling (Zeineldin & Neufeld 2013). In our APC mutant cell lines both APC copies are mutated at the same position in the armadillo 7th repeat, almost identical mutations and mutations in this region are unusual for patients with CRC. This means there is a chance that our *in vitro* model may activate Wnt signalling too little or too much. To help this concern after re-single colony selection we mostly worked with RKO 2_30 and RKO 2_36 because they appeared to have different levels of Wnt signalling, despite having the same mutation in APC. To clarify whether the level of Wnt activation is 'correct' we could perform the TCF/LEF assay in parallel with CRC cell lines harbouring classical APC mutations in the MCR to enable a direct comparison.

1.3 Alternative approaches to generate model

Approaches we could have utilised to generate our *in vitro* model include shRNA, zinc finger nuclease (ZFN) or transcription activator-like effector nuclease (TALENS). shRNA constructs express either miRNA or shRNA and are processed into siRNA resulting in gene silencing. This type of RNAi results in long term gene silencing because the construct is integrated into the host genome. Groups have used this to investigate APC function for example Dow et al. (2015) used an inducible shRNA system in mice to regulate APC expression. The main drawback for us was shRNA reduces protein expression and does not alter the gene. Another approach discussed in section 1.1 used shRNA to silence APC followed by the ectopic expression of APC1309, this reduced full length APC expression whilst inducing the expression of a truncated form of APC. A potential problem of this approach is ensuring the correct level of expression of APC1309 (Zhang et al. 2016).

Alongside CRISPR-cas9 technology there are other nuclease based approaches which can edit genes known as ZFN and TALENs. Both ZFN and TALENS use the Fok1 nuclease and are designed to create a double stranded break which is then repaired by HDR or NHEJ, similar to CRISPR-cas9 technology. Generally ZFN has a lower

success rate than both TALENS and CRISPR-cas9 (Kim & Kim 2014). The target site requirement for the genome editing is one of the major differences which would influence the technology selected. ZFN require GNN repeat regions which are often limited, TALENs can be designed to target any genomic region and require a thymine at the 5' end, whilst CRISPR requires NGG if using wildtype spCas9 (Kim & Kim 2014; Sander & Joung 2014). Despite a wide range of other approaches available to us we selected CRISPR-cas9 because it was an exciting novel approach and our institute had growing expertise in this field.

2 Searching for synthetic lethal interactions with APC in CRC

2.1 Existing synthetic lethal interactions identified with APC mutation

Many studies searching for synthetic lethal relationships in CRC have focused on looking for relationships with other major mutations such as KRAS (Costa-Cabral et al. 2016; Luo et al. 2009; Steckel et al. 2012). Interestingly one group identified *TP53* to be synthetically lethal with two components of the Wnt signalling pathway *CSNK1E (*encodes CK1α*)* and *CTNNB1* (encodes β-catenin) (Tiong et al. 2014). Other research supports this link between *TP53* and Wnt signalling in CRC, Kim et al. (2011) showed loss of *TP53* lead to the reduction in miR-34 repression of TCF/LEF, resulting in Wnt signalling activation. This supports the potential to use inhibitors against either CK1α or β-catenin in patients with *TP53* mutations and this could benefit up to 40-50 % of CRC patients (Tiong et al. 2014).

Some studies have identified specific synthetic lethal relationships with APC mutations. One group identified that APC mutant CRC was synthetically lethal with NSAIDs (Leibowitz et al. 2014). Mutant APC increased levels of the Wnt target gene c-Myc, resulting in higher B3 interacting-domain death agonist (BID) activation and NSAIDs further activated BID, resulting in APC mutant cell specific death, leaving the normal APC wildtype cells unharmed (Leibowitz et al. 2014). Also NSAIDs have been reported to inhibit COX2 which is thought to be synthetically lethal with APC mutations because APC mutant cells show increased expression of COX2 and inhibiting COX2 is effective against APC mutant cells (Lesko et al. 2014; Oshima et al. 1996). Additionally there is potential to target TNKS and upstream of TNKS to selectively kill APC mutant cells. TNKS destabilises Axin which is the rate limiting component of the β-catenin

destruction complex, therefore the inhibition of TNKS increases Axin and levels of the β-catenin destruction complex, resulting in the inhibition of Wnt signalling (Huang et al. 2009). Interestingly, the length of the APC mutation has been linked to the sensitivity to TNKS inhibitors, cell lines lacking all seven 20aa repeats were more sensitive than those with two or more 20aa repeats (Tanaka et al. 2017). Unfortunately TNKS inhibitors are reasonably toxic to normal intestinal cells, a recent paper has identified an approach to exploit this pathway with reduced effects on normal cells (Zhong et al. 2016; Lau et al. 2013; Kang et al. 2017). Kang et al. (2017) identified PrxII regulates TNKS only in APC mutant CRC and the inhibition of PrxII results in APC mutant cell specific death. Another avenue being explored to treat APC mutant cells is the potential of the compound TASIN-1. TASIN-1 inhibits a component of the cholesterol synthesis pathway and it is thought that APC mutant cells are defective in responding to decreases in cholesterol, resulting in APC mutant specific cell death (Zhang et al. 2016). An important consideration when identifying synthetic lethal relationships with APC is that although APC mutations account for up to 80 % of CRC patients, the relationships identified may just be applicable to a subset of patients. Within the 80 %, patients will have different types of APC mutations and different additional mutations in other genes such as *KRAS, BRAF, PIK3CA, PTEN* and *TP53.* To take this into account any synthetic lethal relationships identified in our *in vitro* model were also analysed in a panel of CRC cell lines.

2.2 siRNA kinome screen to identify genes synthetically lethal with APC mutation when silenced

2.2.1 Design of the siRNA kinome screen

To identify potential genes synthetically lethal with the APC mutation we screened a library of 720 siRNA targeting kinases and related genes. We chose to investigate potential synthetic lethal relationships with kinases as target genes identified may have an existing inhibitor available or it would be relatively easy to design one. The library and approach we adopted has been used previously to search for synthetic lethal relationships (Martin et al. 2011; Mendes-Pereira et al. 2012). The library was made up of SMARTpool siRNA, each pool consisted of four individual siRNA targeting different parts of the same gene, using pooled siRNA has been shown to result in a greater phenotypic effect and a higher number of hits identified from the screens (Parsons et al. 2009). The siRNA was used at a concentration of 50 nM, this may not be the optimal concentration for all siRNA in the library, however, this concentration was successfully used to identify synthetic lethal relationships in the papers mentioned

above. Each well contained a different SMARTpooled siRNA and the screen was performed in duplicate because we prioritised biological repeats to increase the number of hits which would validate.

2.2.2 Validation of the hit kinases

From the siRNA screen targeting kinases and related genes we selected seven potential hit genes to follow up. Interestingly one of our potential hits SMG1 also appeared in a transposon screen in APC^{min} mice as a candidate driver gene, however this gene failed to pass our secondary screen validation so we did not investigate it further (March et al. 2011). To confirm the results seen in the screen we ordered a validation plate consisting of the SMARTpool siRNA (used in the screen) alongside the four individual siRNA, which make up the pool. Three of the genes (NAGK, DYRK2 and N4BP2) showed a slight trend of lower survival in the RKO APC mutant lines however the effect is not consistent or large enough for the genes to validate as hits. This result could indicate a limitation of our screening approach or our *in vitro* model. Another consideration is the possibility of limited major synthetic lethal kinases with the APC mutation. Perhaps investigating genes other than kinases may yield a gene, which shows a greater synthetic lethal effect with the APC mutation. However as discussed earlier in section 2.2.1 we chose this approach to improve the chances of translating the finding into the clinic, especially if we identified a kinase which had an inhibitor readily available.

Two of the genes (NAGK and DYKR2) which showed a slight effect upon silencing had inhibitors available which we tested in our *in vitro* model; 3-O-Methyl-N-acetyl-D-glucosamine inhibits NAGK and Harmine inhibits DYRK2. 3-O-Methyl-N-acetyl-D-glucosamine is a competitive inhibitor of NAGK with a Ki of 17 μM, additionally it is a non-competitive inhibitor of N-acetylmannosamine kinase with a Ki of 80 μM (Zeitler et al. 1992). The highest dose we used was 40 μM which would limit the impact of this compound also inhibiting N-acetylmannosamine kinase. Harmine inhibits all the DYRK family, the IC50 for DYRK1 is 80 nM, DYRK3 is 800 nM and DYRK2 is 900 nM, additionally Harmine has also been shown to inhibit PIM3 at 4.3 μM and casein kinase 1 (CK1) at 1.5 μM (Bain et al. 2007). CK1 is involved in the Wnt signalling pathway and research has shown the use of Harmine does inhibit the canonical Wnt signalling pathway when stimulated in HEK293T cells and preadipocytes (Waki et al. 2007). Other research showed Harmine also inhibits Cdk1/Cyclin B, Cdk2/Cyclin A and Cdk5/p25 (IC50 values 17 μM, 33 μM and 20 μM respectively) (Song et al. 2004). The highest Harmine dose we used was 10 μM and therefore this would have limited the

effect on the cyclin-dependent kinases mentioned. This demonstrates the problem with using inhibitors as they often inhibit a broad range of proteins especially at higher concentrations. The inhibitor data agreed with the siRNA data, neither NAGK or DYRK2 validated as hits.

To further understand why none of the potential hits validated it would be interesting to analyse the effectiveness of the siRNA targeting the genes, by investigating the protein level after silencing. If the level of knock-down is not significant then this could explain the lack of validation and we could identify new siRNA targeting the gene which is more effective. Another avenue to explore would be investigating silencing two of the genes which showed a slight effect simultaneously to potentially increase the reduction in cell viability in the APC mutant cell lines. This could be advantageous because targeting different pathways at the same time reduces rates of resistance in therapies.

2.3 Is the mTOR pathway synthetically lethal with APC deficiency

Our siRNA kinome screen data suggested that silencing FLT3 and mTOR may be synthetically lethal with the APC mutation, these genes were potential hits in the first screen replicate only. Additionally research *in vivo* (using two different APC mutant mice models) had suggested mTOR inhibitors such as rapamycin were synthetically lethal with the APC mutation in early stage disease (Faller et al. 2014). Mechanistically without mTOR inhibition the cells showed increased Wnt signalling, increased c-myc, increased inhibition of eEF2K (via mTORC1) and activation of translation elongation, promoting tumourigenesis. The inhibition of mTOR halted this mechanism driving tumourigenesis, resulting in tumour regression (Faller et al. 2014). Based on this we investigated whether silencing FLT3 and mTOR with siRNA resulted in a greater loss of cell viability in the APC mutant cell lines in our *in vitro* model, we did not see an effect. Additionally, we tested the mTOR inhibitors rapamycin and ridaforolimus and again we did not see selectivity in the *in vitro* model or CRC panel cell lines we tested. Our results suggest two possibilities, either the relationship identified by Faller et al. (2014) is only present in mice or there could be a small therapeutic window in early CRC development were mTOR inhibitors would be effective. The human CRC cell lines we used were from established tumours, with many additional mutations (compared to the mice models used in the paper) and protein synthesis through the mTOR pathway may no longer be a driver in tumourigenesis. To further understand the differences in our results we could analyse levels of proteins involved in the mechanism the paper suggested for example c-myc and eEF2K. In support of our data, clinical trials using

mTOR inhibitors as a monotherapy have not been very effective especially in metastatic disease. Clinical trials are exploring the use of mTOR inhibitors in combination with other drugs such as VEGF inhibitors (Wang & Zhang 2014). However, it is possible to gain the full benefit of mTOR inhibitors in CRC, treatment needs to be started early on.

3 Statins are synthetically lethal with APC

3.1 A compound screen of FDA-approved drugs identifies statins to be synthetically lethal with APC mutation

3.1.1 Compound screen design

The compound library and screen design were used previously to successfully identify compounds synthetically lethal in MMR deficient CRC (Guillotin et al. 2017). The library contained 1120 FDA-approved compounds all dissolved in DMSO at 10 μM. Performing a large screen with one drug concentration may result in missing some potential hits, however it allows us to investigate the effect of many drugs in one experiment. As for the siRNA screen we had one well per compound for each biological repeat, we performed three biological repeats to increase our chance of finding a drug showing a synthetic lethal relationship with the APC mutation. Screening an FDA-approved compound library offers the potential to repurpose existing drugs, reducing costs and the time it takes for new treatments to reach the clinic. Identifying the mechanism of the synthetic lethality can be harder in a compound screen compared to a siRNA screen because the main target of the drug may not be responsible for the relationship. In comparison in siRNA screening the target gene responsible is known because multiple siRNA targeting the same gene are used in the validation phase of the screening.

3.1.2 Validation of compounds

We chose to validate 11 compounds, some performed well over each replicate and others performed well in just the first repeat. Potentially some drugs degraded over the course of conducting the repeats. Using a separate batch of compound we performed dose response curves to analyse the behaviour of the compounds in both cell lines. From these we identified lovastatin and mevastatin, which in our *in vitro* model caused a greater decrease in survivial in the RKO APC mutant lines in comparison to the RKO APC wildtype cell lines. Additionally we tested simvastatin, which also showed the

same effect. From the dose response curves we identified the optimal doses for selectivity were lower than the 10 μM used in the screen, emphasising the importance of not ruling out drugs which cause loss of cell viability in both cell lines. Our drug curves show the three statins display different potencies, simvastatin is the most effective at the lowest doses. Mevastatin was derived from *Penicillium citrinum (P.citrinum)*, lovastatin was derived from *Aspergillus terreus (A.terreus)* and scientists modified lovastatin to create simvastatin (Endo 2004; Alberts 1990). Simvastatin has been reported to be more potent then lovastatin, supporting why it shows the best selectivity between our APC wildtype and APC mutant lines at the lowest concentrations (Alberts 1990).

To our knowledge there are no papers, which have identified statins to be synthetically lethal with the APC mutation. Although recently a paper has identified a drug targeting the cholesterol synthesis pathway (known as TASIN-1) showing a synthetic lethal relationship with the APC mutation (discussed further in section 3.2.1) (Zhang et al. 2016). Potentially this indicates cholesterol synthesis is a vulnerability in APC mutant cell lines, which can be exploited. The opportunity to use statins which have FDA-approval means this potential therapy could reach the clinic quicker than using newly developed compounds.

3.2 Statins and CRC

3.2.1 HMGCR dependent or HMGCR independent

Statins exert a wide range of effects on cells and these effects either occur through HMGCR and/or HMGCR independent mechanisms. For our investigations into the mechanism responsible for the synthetic lethal relationship between statins and the APC mutation in our *in vitro* model, we focused on investigating if the effect occurred through HMGCR. We did not rule out HMGCR independent mechanisms and these could occur alongside the mechanism we identified. Our attempts to inhibit HMGCR directly with siRNA to confirm if this mimicked the effect of statins was unsuccessful and needs further optimisation before we can draw conclusions. We investigated the effect of blocking GGPP and FPP prenylation using inhibitors of GGTase and FTase, these steps are downstream of HMGCR. We found the inhibitor of GGPP prenylation GGTI-298 showed a similar effect in our cell lines to statins, especially in RKO 2_30. This finding suggested GGPP prenylated proteins are important in our mechanism. Whereas FTI-277 showed the same level of cell viability in our *in vitro* model cell lines, implying that FPP prenylated proteins do not play a role in our mechanism. Further work is needed to examine if adding in GGPP (and not FPP) whilst treating with statins

rescues the statin sensitivity in our APC mutant RKO 2_30 and RKO 2_36 cell lines. This would fully confirm the importance of GGPP prenylated proteins in the mechanism. Also we investigated if pre-treatment with MVA an hour before statin treatment would rescue the sensitivity in the APC mutant cells lines. Research has shown in CRC that MVA rescues the effects of statins (Zhu et al. 2013; Kaneko et al. 2007). In our *in vitro* model MVA pre-treatment enhances the loss of cell viability in all the cell lines, this could be because RKO cells have not lost all the negative feedback mechanisms controlling HMGCR levels (Demierre et al. 2005; Tsai et al. 2012). Typically cancer cells lose their negative feedback mechanisms enabling upregulation of HMGCR levels to meet cellular demands. Therefore the presence of feedback mechanisms would mean adding MVA may further enhance the effect of statins by decreasing HMGCR levels further.

Other studies into the mechanism of statins in CRC have also shown mechanisms acting through the HMGCR pathway. Lovastatin has been shown to cause apoptosis in HT29, SW480 and LS180 through the HMGCR pathway, the addition of MVA, FPP and GPP reversed the mechanism suggesting both FPP and GPP prenylated proteins are important. The suggested mechanism involved the inhibition of Ras mediated activation of the PI3K pathway, resulting in a decrease in the anti-apoptopic protein survivin (Kaneko et al. 2007). Another study showed mevastatin sensitivity in CaCO-1 cells was through the HMGCR pathway, the sensitivity was reversed by the addition of MVA but not FPP or GGPP (Wächtershäuser et al. 2001). Not all statin sensitivity is thought to occur through the HMGCR pathway. Some studies have suggested statins act through the BMP and NF-kB pathways resulting in effects on cell viability (Kodach et al. 2007; Cho et al. 2008). Another HMGCR independent mechanism involves simvastatin inhibiting angiogenesis by decreasing the expression of VEGF and HER2 (Li et al. 2017). Additionally pitavastatin has been shown to inhibit CRC stem cells, resulting in cell apoptosis (Zhang et al. 2017). Further research is required to understand if all statins have the same effects in cancer cells, whether a few mechanisms occur in parallel or if one key mechanism is responsible for statins anti-proliferative effect in CRC.

Many papers suggest HMGCR is upregulated in cancers, causing hyperactivation of the pathway and promoting tumourigensis (Notarnicola et al. 2004; Chushi et al. 2016; Qiu et al. 2016). It is thought the pathway is hyperactivated because cancer cells require higher levels of cholesterol and isoprenoids for growth (Notarnicola et al. 2004). Isoprenoids are required to prenylate G-proteins promoting a wide range of roles (Notarnicola et al. 2004). Higher HMGCR has been shown in a variety of tumour types including hepatocellular carcinoma, haematological malignancies, brain tumours,

colorectal cancer, gastric cancer and glioblastoma (Notarnicola et al. 2004; Chushi et al. 2016; Qiu et al. 2016). This hyperactivation could make cancer cells more sensitive to statins than normal cells because they are more dependent on the pathway for growth and survivial. It would be interesting to analyse the mRNA and protein levels of HMGCR in our *in vitro* model to see if the RKO APC mutant cell lines express more HMGCR compared to the APC wt controls, this could potentially contribute to the greater sensitivity to statins. Additionally Kaneko et al. (2007) found survivin and HMGCR mRNA levels correlated in colon cancer tissues. High HMGCR and high survivin would suggest more cell survival, whilst low HMGCR and low survivin would cause more apoptosis. As we identified survivin to play an important role in our mechanism it would be interesting to see if the levels of HMGCR and survivin mRNA correlate. Interestingly studies in colorectal, breast and ovarian cancers have suggested high HMGCR expression is associated with favourable tumour characteristics and/or better prognosis (Bengtsson et al. 2014; Borgquist et al. 2008; Brennan et al. 2010). This research doesn't fit with the study by Kaneko et al. (2007) and also questions whether HMGCR expression is a predictor for statin response, further research is required to understand this.

As briefly mentioned a recent paper identified a drug known as TASIN-1 as an inhibitor of EBP which is downstream of HMGCR to show synthetic lethality with the APC mutation (Zhang et al. 2016). The paper shows the APC mutant cell lines (DLD1 and HT29) are more sensitive to TASIN-1 then the APC wildtype cell line (HCT116). The paper shows the same effect with simvastatin, although the effect is less potent than with TASIN-1. The research suggests APC mutant cells are unable to respond to the decrease in cholesterol (consequence of TASIN-1 and statin treatment) by upregulating SERP2 and SERP2 target genes (Zhang et al. 2016). This supports the mechanism of statins in our *in vitro* model is through the HMGCR pathway. It would be interesting to analyse in our *in vitro* model the level of SERP2 and SERP2 target genes and see if this plays a role in the mechanism responsible for the synthetic lethality we identified between statins and APC mutations.

As discussed different studies into the effect of statins on CRC cells have shown either HMGCR dependent or independent mechanisms. It is possible statins could exert their effects through both and the different mechanisms identified could all integrate into a network of statin effects in CRC cells.

3.2.2 Statin sensitivity and APC mutations

In our *in vitro* model APC status is the differing characteristic between the controls and the APC mutant cells. RKO 7_1 and RKO 7_2 are APC wt and RKO 2_6, RKO 2_21, RKO 2_22, RKO 2_30 and RKO 2_36 have an APC mutation in the 7th armadillo repeat in both alleles. The difference in sensitivity to statins in our *in vitro* model must be a result of the difference in APC because all the cell lines have been through the same CRISPR-cas9 process and the pressures of single colony selection. Other studies into statin sensitivity in CRC have not looked at sensitivity to statins in relation to APC status. Kaneko et al. (2007) looked at lovastatin sensitivity in APC mutant lines (HT29 and SW480) and APC wildtype (LS180), SW480 were the most sensitive followed by LS180 and then HT29. Another group looked at lovastatin sensitivity in the APC wildtype HCT116 and APC mutant DLD1, SW480 and HT29 (Kodach et al. 2007). The group found the sensitivity was related to expression of SMAD4, the most sensitive expressed SMAD4, HCT116 (APC wildtype) and DLD1 (APC mutant). The more resistant lines both APC mutant SW480 and HT29 did not express SMAD4 (Kodach et al. 2007). Another study looked at lovastatin in the APC wildtype HCT116 and LOVO and APC mutant SW480 and HT29 (Agarwal, Bhendwal, et al. 1999). The most sensitive lines were SW480 and LOVO followed by HCT116 and HT29. The response to statins in these studies does not relate to APC status alone, additional mutations in these cell lines must contribute. All the APC mutant cell lines in these studies have APC mutations at the MCR and not the 7th armadillo repeat as in our *in vitro* model. The differences between studies could be explained by the type of statin used, dose used and treatment length. Additionally all the studies are small, investigating up to four cell lines in each paper. These studies do not suggest a clear correlation between statin sensitivity and APC mutations.

Part of our study involved comparing statin sensitivity between our *in vitro* model and a CRC panel of cells (DLD1, HCT116, HT29, RKO, SW48 and SW620). These results further support a poor association between statin response and APC status. A key difference between our APC mutant *in vitro* model lines and HT29, DLD1 and SW620 is the location of the APC mutation and this could explain why our APC mutant *in vitro* model cell lines are substantially more sensitive. DLD1 and SW620 have a mutation in the MCR on one allele then the other allele is lost due to loss of heterozygosity. The mutation found in the DLD1 cell line is after the 2nd 20aa repeat and results in a 155 kDa APC protein. The SW620 cell line has a mutation after the 1st 20aa repeat resulting in a 147 kDa protein which retains the 1st 20aa repeat. The HT29 cell line has two different mutations on different alleles. The mutation on allele one retains the armadillo repeats resulting in a 93 kDa protein, the mutation on allele two just after the

3rd 20aa repeat results in a 171 kDa APC protein. These cell lines fit the 'just right' signalling model used to explain the pattern of APC mutations in patients resulting in a specific level of Wnt signalling (Zeineldin & Neufeld 2013). It is possible our APC mutant *in vitro* model cell lines respond differently to statins in comparison to the APC mutant CRC panel cell lines because of too little or too much Wnt signalling. Unfortunately we investigated this within each group (*in vitro* model and CRC panel) separately, as we did not probe for β-catenin levels at the same time on the same blot we are unable to compare between the groups. To enable comparison we should investigate levels of Wnt signalling across our *in vitro* model and the CRC panel together. Research has linked different types of APC mutations to different drug responses. Recent research has suggested this explains why some APC mutant cell lines are sensitive to tankyrase inhibitors whilst others are not. The tankyrase inhibitor sensitive cell lines/tumours lacked the seven 20aa repeats, whilst the resistant cell lines/tumours had 2 or more 20aa repeats. The research linked this effect to the level of Wnt signalling activation, the sensitive cell lines showed higher Wnt signalling than the resistant lines with 2 or more 20aa repeats (Tanaka et al. 2017).

Another possibility is the early location of the mutation in the 7th armadillo repeat of APC in our *in vitro* model results in the loss of an APC function, which is retained in the CRC panel of cell lines tested and this could be responsible for the differences in statin sensitivity. For example, our RKO APC mutant *in vitro* model cell lines would no longer be able to interact with Topo IIα, PCNA, Polβ and Fen-1 through the 15aa repeats, in comparison cell lines mutated at the MCR would still retain this ability (Prosperi & Goss 2011). Additionally there could be unknown interactions with APC between the armadillo repeats and the MCR which are important for explaining the differences in sensitivity to statins. Nelson & Näthke (2013) highlighted over 100 proteins have been reported to interact with APC and understanding these interactions could help uncover new APC roles. To help us decipher whether it is a specific section of APC responsible for the increased statin sensitivity in our APC mutant *in vitro* model we could re-express plasmids containing different sections of APC and see which sections can rescue the effect.

We have discussed two possible contributing factors explaining statin sensitivity in the cell lines we analysed, APC status and expression of HMGCR (discussed earlier in 3.2.1). Another factor which may be involved is additional mutations in key genes known to contribute to CRC. For example, *TP53* status might be involved, research has shown simvastatin might activate p53 through p38MAPK resulting in survivin repression (Chang et al. 2013). We have shown low levels of survivin are important in our mechanism and two of the most sensitive cells are wildtype for *TP53* (RKO and

SW48). However, other research in breast cancer cell lines found *TP53* mutations upregulate levels of the mevalonate pathway, making these cell lines responsive to inhibition of the pathway through statins (Freed-Pastor et al. 2012). Additionally HCT116 which are also *TP53* wildtype are one of the more resistant cell lines. This demonstrates there is no clear pattern with *TP53* status and it could be a combination of factors contributing to statin sensitivity. We looked in terms of KRAS and BRAF mutations, typically many CRC cell lines have a mutation in one or the other and this showed no clear pattern. Interestingly SW48 do not have a mutation in either KRAS or BRAF and is one of the more sensitive lines. Therefore the sensitivity to statins is likely to be more complicated than just looking in terms of one mutation alone. The number of cell lines used to analyse statin sensitivity is low, making it hard to see clear patterns especially when you subdivide into different mutations there are groups with only 1-3 cell lines in. To further our investigation it would be interesting to analyse statin sensitivity in a normal colon cell line and see how this compares to our CRC cell lines. Additionally you could introduce mutations in APC, KRAS, BRAF and TP53 individually and in combination to see if this alters the response of the normal colon cell line to statins.

Identifying the specific reason why our APC mutant *in vitro* model cell lines are more sensitive than other CRC cell lines with APC mutations, would help us to understand who could benefit.

3.2.3 Do statins cause cell arrest or apoptosis?

Statins have been shown to induce cell arrest and apoptosis in a range of tumour types, the two processes are not mutually exclusive because cell arrest can induce apoptosis. Cell arrest occurs when cell cycle regulators (eg cdk4 and cdk6) are downregulated and cell cycle inhibitors are upregulated (eg p21 and p27). Statin induced cell cycle arrest is thought to occur due to the inhibition of ubiquitin proteasome mediated proteolysis resulting in an increase in cell cycle inhibitors p21 and p27 (Rao et al. 1999). Further research is required to understand if there are additional mechanisms.

Most research into statins has focused on the mechanisms leading to apoptosis. Some suggested mechanisms involve the downregulation of members of the IAP family (eg XIAP, cIAP-1, cIAP-2 or survivin) and other anti-apoptopic proteins (eg Bcl-2, Bcl-XL, c-FLIP-S) or the upregulation of pro-apoptotic proteins (eg Bax). We hypothesise the decrease in the anti-apoptotic protein survivin results in the induction of apoptosis in our *in vitro* model upon lovastatin or simvastatin treatment, however further work is

needed to clarify this because we did not analyse levels of apoptosis. Another study supports our hypothesis, the research in the colorectal cancer cell line SW480 found survivin was downregulated in response to lovastatin treatment, whilst other anti-apoptotic proteins were not altered (XIAP, cIAP-1, cIAP-2 Bcl-2 and Bcl-XL) (Kaneko et al. 2007). In comparison other studies in the colorectal cell lines colo205 and HCT116 showed simvastatin treatment caused Bcl-2, Bcl-xL, cIAP1 and cFLIP-S to be downregulated (Cho et al. 2008). Another study found Bcl-2 was downregulated and Bax was increased upon lovastatin treatment in SW480, HCT116, LOVO and HT29 (Agarwal, Bhendwal, et al. 1999). The variation between studies could be due to the use of different cell lines, different statins, different concentrations and treatment lengths. It would be interesting to analyse levels of other anti-apoptotic proteins and pro-apoptotic proteins in our *in vitro* model upon statin treatment to see if they are altered too.

Interestingly research has suggested statins have different effects on apoptosis in different cellular contexts, in normal cells statins are thought to be anti-apoptotic and in tumourigeneic cell lines statins are thought to be pro-apoptotic. Part of this pattern is thought to be due to the statin doses used in the different cell types, tumourigenic lines are typically given higher doses of statins, inducing pro-apoptotic effects (Wood et al. 2013). To investigate this we could analyse the response of normal colon cell lines to statins using the same dose range we used for our *in vitro* model cell lines.

3.3 Statin induced survivin downregulation

3.3.1 Survivin levels decrease upon statin treatment

We investigated levels of survivin in our *in vitro* model of APC mutation and found upon statin treatment levels of survivin decrease more in the APC mutant lines compared to the APC wildtype lines. We hypothesised that in the APC mutant lines the level of survivin decreases below a threshold tolerated, resulting in the induction of apoptosis. This is supported by research by Kaneko et al. (2007) and Chang et al. (2013). Both showed statins induced a decrease in survivin levels, although the upstream mechanisms resulting in the decrease differed. This variation could be due to the use of different cell lines with different mutational backgrounds. Interestingly in different cancer types the downregulation of survivin is also suggested to be part of the mechanism of statins, this has currently been shown in lung, hepatocellular carcinoma and head and neck squamous cell carcinoma (Hwang et al. 2011; Wang et al. 2007; Yen et al. 2016).

We have shown statins cause a decrease in survivin levels and this has been shown by other studies in CRC and additional cancer types. Survivin appears to be key to the mechanism and this is supported by experiments investigating the impact on statin response when either silencing survivin or overexpressing survivin in cell lines. For example, in the APC mutant cell line SW480 silencing survivin increased statin sensitivity, whilst over expressing survivin reduced statin sensitivity (Kaneko et al. 2007). We followed on this research and analysed if silencing survivin in the original RKO cell line (APC wildtype) altered statin sensitivity. We found silencing survivin dramatically sensitised the cells to statins. These results suggest survivin levels play a key role in the response to statins in CRC.

To extend our research we could investigate if overexpression of survivin in our *in vitro* model cell lines makes the cells more resistant to statins and whether this fully rescues the effect. It would be interesting to see if individually overexpressing either survivin or APC fully rescues the effect or if both plasmids are required to rescue the effect of statins in the RKO APC mutant *in vitro* model cell lines. If both are required it would suggest it is a combination of both survivin levels and the APC mutation determining statin sensitivity.

Additionally to investigate if the effect on survivin levels occurs through HMGCR pathway we could analyse the effect on survivin levels when pre-treating with MVA before lovastatin treatment. When we performed these experiments analysing cell viability we found MVA pre-treatment enhanced the decrease in cell viability, which could be due to feedback mechanisms resulting in MVA further enhancing the decrease in HMGCR. Therefore potentially if the cells are pretreated with MVA before statin treatment we might see a greater decrease in survivin levels. It would also be interesting to see if GGTI and not FTI causes a decrease in survivin levels, we found treatment with GGTI had a greater effect on cell viability in just the APC mutant RKO 2_30 cell line compared to FTI.

3.3.2 Survivin is a Wnt target gene

In our paired cell line we also see levels of the Wnt signalling pathway slightly decrease after statin treatment in our *in vitro* model APC mutant lines and this mirrors the decrease in survivin. Survivin is a well known Wnt target gene, therefore if Wnt signalling is inhibited we would also expect a decrease in survivin levels (Zhang et al. 2001; Kim et al. 2003). Research by Zhang et al. (2001) supports a strong interplay between APC and survivin. The group showed in the APC mutant line HT29 the introduction of APC caused apoptosis because it decreased levels of survivin. The

paper also suggests this interplay is important for maintaining crypt homeostasis, survivin expression is high at the crypt with the stem cells whilst APC expression is high at the top of the crypt. It is important to note this study emphasises a link between APC and survivin but is not investigating in terms of statin response. Our data suggests Wnt signalling is inhibited upon statin treatment, to further this we could investigate levels of additional Wnt target genes.

It is possible that Wnt signalling is not responsible for the decrease in survivin levels. The effect of statin treatment on the protein levels of total and unphosphorylated β-catenin are very slight in comparison to the effects on survivin levels at the same statin concentrations. This could suggest other pathways are responsible for the statin induced decrease in survivin. Potential pathways include; microRNA, RTK, PI3K/Akt, MEK/MAPK, NF-kB, mTOR, STAT3, p53, hypoxia, TGF and Notch signalling (Chen et al. 2016). However, research has shown Wnt signalling is key to the regulation of survivin levels in CRC and in section 3.5.1 we discuss a possible explanation for the slight change in protein levels of β-catenin (Kim et al. 2003; Ma et al. 2005). To understand the contribution of Wnt signalling on the regulation of survivin levels in our *in vitro* model, we could use known inhibitors against Wnt signalling at various concentrations and measure the effect on survivin protein levels. Alongside this you could do the same with inhibitors of other pathways shown to regulate survivin levels. It is feasible that statins could be altering several pathways which regulate survivin levels.

3.3.3 Do basal survivin levels in cell lines explain the response to statins?

Generally research has shown survivin expression is low in normal cells and high in tumour cells (Kaneko et al. 2007; Kawasaki et al. 1998; Ambrosini et al. 1997; Sarela et al. 2000). Research suggests in normal tissue survivin expression is concentrated in the crypt (Gianani et al. 2001). We analysed survivin protein levels in our RKO *in vitro* model and a panel of CRC cell lines. We hypothesised the *in vitro* APC mutant RKO 2_30 and RKO 2_36 might have lower survivin levels compared to the rest of the cell lines because these were the most sensitive to statins. This was not the case, DLD1 and HT29 showed lower basal survivin levels, than RKO 2_30 and RKO 2_36 but are less sensitive to statins. Also within our *in vitro* model only RKO 2_30 had a lower basal level of survivin compared to the APC wt controls RKO 7_1 and RKO 7_2. Interestingly RKO 2_30 and RKO 2_36 have different basal levels of survivin which could be explained by the levels of Wnt signalling, RKO 2_30 shows a lower activation of the Wnt signalling pathway and has a lower survivin level than RKO 2_36, however the RKO APC wt controls do not fit this explanation. To investigate the relationship

between survivin levels and statin sensitivity we plotted survivin expression against the survival fraction at 10 μM lovastatin and found no strong correlation. Therefore our data does not show a clear pattern and does not suggest basal survivin levels alone explain statin sensitivity.

It is possible the different survivin isoforms prevent a clear association between statins and basal survivin levels. On western blots our antibody detected two bands, we believe the lower band corresponds to survivin wt and survivin ΔEx3, whilst the upper band may be survivin 2B. Unfortunately there are few antibodies which are specific for the survivin isoforms making it difficult to establish protein levels of each (Necochea-Campion et al. 2013). We analysed the ratio of the upper and lower survivin bands we detected to see if this explained statin sensitivity but it did not. This could be because the lower band represents two isoforms and the different isoforms may have different roles, hiding an effect. Typically papers investigating survivin isoforms use RT-PCR because probes can be designed to target specific isoforms, including expression levels of the two smallest survivin isoforms, which we could not identify on the western due to their size (Suga et al. 2005; Pavlidou et al. 2011). Therefore to further understand if there is an association between basal survivin levels and statin response we could analyse each survivin isoform individually.

To investigate if additional factors contribute to statin sensitivity alongside survivin levels, we subdivided our data into smaller groups (APC status, Wnt signalling, KRAS status, BRAF status and TP53 status) and plotted survivin expression against the survival fraction at 10 μM lovastatin. We did not identify any strong correlations by sub-grouping the data. A key limitation of our investigations into survivin levels is the sample size (as discussed earlier in 3.2.2) because once you sub divide the 10 cell lines into different groups the sample sizes are small and therefore hard to interpret. Increasing our investigation into further cell lines would help solve this. Additionally it would be interesting to analyse survivin levels after statin treatment in all 10 cell lines because we might see the same pattern as in the *in vitro* model, a greater decrease in survivin levels in the more sensitive lines. Further research is needed to understand the extent to which survivin levels can explain the different sensitivities to statins.

3.4 Is Wnt signalling altered upon statin treatment

The involvement of the Wnt signalling pathway in our mechanism is interesting because the majority of our data suggests statins cause a decrease in Wnt signalling. This is supported by the data from the Wnt assay and the western blotting of whole cell lysates for total β-catenin and unphosphorylated β-catenin (active) levels. Additionally we see a decrease in the Wnt target gene survivin upon statin treatment. The immunofluoresence data on total β-catenin localisation upon statin treatment appears to conflict the majority of our data, we see a Rac1 dependent increase in total β-catenin transported from the cytoplasm to the nucleus. Potentially the total β-catenin accumulated in the nucleus is prevented from activating Wnt target genes and a potential mechanism supporting this is discussed in section 3.5.1. To clarify levels of Wnt signalling upon statin treatment investigating levels of other Wnt target genes would help. Interestingly in normal cell contexts (including neural cells and mouse embryonic stem cells) statins have been shown to activate Wnt signalling, however this may not be the same in tumour cells (Robin et al. 2014; Salins et al. 2007; Qiao et al. 2011). The majority of our data supports statins inducing a decrease in Wnt signalling in our *in vitro* model.

3.5 Rac1 and statins

3.5.1 Is Rac1 the link between Wnt signalling and statins

Based on the following, we investigated if Rac1 was involved in the mechanism responsible for the synthetic lethal relationship between statins and the APC mutation in our *in vitro* model. Our data suggested GGPP prenylated proteins are more important in the mechanism than FPP prenylated proteins and Rac1 is one of many proteins which undergo GGPP prenylation (Demierre et al. 2005). Rac1 has been shown to play a role in the canonical Wnt pathway either by promoting nuclear import of β-catenin or the formation of β-catenin-TCF/LEF complexes (Esufali & Bapat 2004; Wu et al. 2008; Jamieson et al. 2015). Additionally, Rac1 has been shown to promote CRC tumourigenesis (Myant et al. 2013; Espina et al. 2008).

We analysed the levels of active RhoA/B/C and active Rac1 before and after statin treatment. Our analysis showed no increase in the activation of RhoA/B/C. However, analysing levels of active Rac1 showed an increase after statin treatment, which was not due to an increase in total Rac1. This is potentially supported by the immunofluorescence data analysing the localisation of active Rac1 upon statin treatment. To further this work we would additionally analyse levels of Cdc42 which is also GGPP prenylated (Demierre et al. 2005). Other studies into statins effects on

cancer cell lines have also shown an increase in the activation of members of the Rho family, including RhoA/B/C, Rac1 and Cdc42. For example, Zhu et al. (2013) found an increase in active Rac1, Cdc42 and RhoA in response to simvastatin treatment in the CRC cell line HCT116. The group linked the increase in active Rho family proteins to a decrease in their interaction with GDI, which normally prevent the activation of Rho proteins. This is thought to be due to a decrease in prenylated Rho proteins because GDI proteins only bind Rho proteins if prenylated and statins decrease prenylation levels (Zhu et al. 2013). Future work would involve confirming if we see a decrease in prenylated Rac1 and if the interaction between Rac1 and GDI is decreased in our *in vitro* model. Interestingly, the increase in activation of members of the Rho family upon statin treatment has also been reported in other cell types including; myeloid lineage cells THP-1 and BV2, the neuroblastoma cell line N2a and the pheochromocytoma (PC12) cell line (Cordle et al. 2005). Different studies see increases in the activation of different members of the Rho family and perhaps this indicates the activation of different pathways upon statin treatment.

Zhu et al. (2013) found treatment with a Rac1 inhibitor in combination with statins reversed the statin sensitivity in HCT116 cells, this indicated the importance of active Rac1 in their mechanism in HCT116 cells. We did not see the same effect in our cell lines when treating with a Rac1 inhibitor and statins at the same time. Additionally a Rac1 inhibitor did not display the same selectivity as statins in our *in vitro* model. This implies the increase in active Rac1 in our *in vitro* model does not explain the selectivity we see between the APC wildtype and APC mutant cell lines. Therefore the mechanism identified by Zhu et al. (2013) which involved active Rac1 and RhoA stimulating superoxide production, leading to JNK mediated activation of BIM and apoptosis, is unlikely to be responsible for the difference in sensitivity we observe. The statin induced decrease in isoprenoids would result in increased unprenylated Rac1 and this would be unable to associate with the plasma membrane. Zhu et al. (2013) showed an increase in cytosolic Rac1 upon statin treatment in HCT116 cells supporting this hypothesis and future work would involve confirming this in our *in vitro* model. It is predicted that the alteration in Rac1 localisation would have implications on downstream effectors. We attempted to analyse Rac1 localisation using microscopy but the data is inconclusive and needs further work. Additionally we analysed the activation of a key Rac1 effector known as Pak1 by analysing levels of phosphorylated ser144 Pak1 which is indicative of active Pak1. We found levels of phosphorylated ser144 Pak1 decreased upon statin treatment in our *in vitro* model, this supports the hypothesis that unprenylated Rac1 is unable to localise to the membrane where Rac1 would normally interact and activate Pak1 (Bustelo et al. 2007). To further confirm this

work it would be interesting to see if introducing active Pak1 into the cells alongside statin treatment rescues the sensitivity of the APC mutant cells to statins. Additionally if Pak1 activation is important for the selectivity we see, treating the cells with a Pak1 inhibitor should cause the same synthetic lethal effect. Investigating the effects of an increase in unprenylated cytosolic active Rac1 on other Rac1 effectors would be interesting too.

We hypothesise that Pak1 activation may explain the discrepancy in the data on Wnt signalling (section 3.4). There is evidence that Pak1 plays a role in the Wnt signalling pathway. Pak1 has been shown to phosphorylate β-catenin at ser675 resulting in stabilisation of β-catenin and enhanced transcription of Wnt target genes (Zhu et al. 2012). Therefore the decrease in Pak1 activation could be responsible for the decrease in levels of the Wnt target gene survivin. This data supports why the immunofluorence data showing an increase in nuclear β-catenin induced by an increase in active Rac1, does not result in an increased expression of Wnt target genes. Also it supports why the protein data on levels of β-catenin before and after statin treatment only show a slight decrease because it is the reduction in phosphorylated ser675 β-catenin which is impacting the level of Wnt target gene transcription. Additionally this supports why we observed the greatest effect on Wnt levels in the TCF/LEF reporter assay. To further support this idea we could probe for levels of phosphorylated β-catenin at ser675 and see if this decreases in our *in vitro* model.

Interestingly, we observed a lower basal level of active Rac1 in the APC mutant lines. This result is conflicting with research showing that APC mutations cause a greater activation of Rac1 in comparison to APC wt cells. In intestinal epithelial cells derived from mice with wt APC and mutant APC, pull down experiments for active Rac1 showed levels were higher in the cells with mutant APC (Myant et al. 2013). This research supports the idea that Rac1 is a key driver in tumourigenesis after APC loss (Myant et al. 2013). There are two factors why our data could be different, firstly the APC wildtype RKO controls in our *in vitro* model appear to express a high level of active Rac1 independent of a APC mutation, although this is speculation and would require comparison to levels of active Rac1 in other CRC cell lines with wt APC and mutant APC. An important consideration is the RKO cell line has become tumourigenic independent of APC and it is possible Rac1 activation is increased through other mechanisms, therefore this could impact the cell lines response to a mutation in APC. Another factor is the position of our APC mutation may cause the lower basal levels of active Rac1. Our *in vitro* model APC mutant cell lines are mutated in the 7th armadillo repeat and this could alter the interaction with binding partners. ASEF and IQGAP are known to interact with APC at the armadillo repeats and both of these proteins interact

and activate Rac1 and Cdc42 (Hanson & Miller 2005; Aoki & Taketo 2007). To investigate this we could perform immunoprecipitation experiments to determine if our APC truncated protein still binds ASEF and IQGAP.

Taken together our results suggest it is the statin induced effect on the localisation of Rac1 and not Rac1 activation, which appears to be important in the mechanism of statin selectivity in APC mutant cells. This reduces Pak1 activation, decreasing the level of Wnt signalling and the expression of the Wnt target gene survivin.

3.5.2 Does Rac1 directly alter survivin levels

It is possible that Rac1 may directly alter survivin levels independent of the Wnt signalling pathway because many pathways have been shown to regulate survivin levels. For example Rac1 regulates NF-kB and NF-kB is a regulator of survivin. A study on breast cancer cell lines supports this because inhibiting Rac1 downregulated survivin levels through NF-kB (Yoshida et al. 2010). Therefore it is possible that the localisation of Rac1 to the cytosol prevents the Rac1-mediated activation of NF-kB and subsequent activation of survivin transcription. To investigate this idea we would investigate whether statin treatment can influence expression of components of the NF-kB pathway.

3.6 The potential of statins for the treatment of APC mutant CRC

Our study highlights statins are synthetically lethal with the APC mutation in our *in vitro* model. Unfortunately the effect in other APC mutant CRC cell lines does not support a clear selectivity. A few other studies have shown the potential of using statins to treat CRC (not in relation to APC mutations). A potential limitation for the use of statins as a therapy is the doses required to see an effect are a lot higher than the doses currently given for CVD (10-200 nM), some studies have used up to 200 μM (Demierre et al. 2005). Our study requires concentrations in the lower μM range to see an effect (simvastatin 2 μM, lovastatin 4 μM). A phase 1 clinical trial investigating lovastatin indicated a concentration range of 0.1-3.9 μM was well tolerated in patients, indicating the dose we see an effect with lovastatin could be a successful therapeutic strategy (Thibault et al. 1996). This highlights if we can identify the reason why our APC mutant *in vitro* model cell lines are more sensitive then we could use statins to treat patients at a tolerated dose.

Many studies have investigated the potential of statins in chemoprevention. Case-control studies have shown varying protective effects, for example one study identified statin treatment resulted in a 47 % decreased risk of CRC, whilst other studies have shown no protective effect (Poynter et al. 2005; Lochhead & Chan 2013). Many randomised studies have not supported a protective effect (Lochhead & Chan 2013). The studies used to investigate the association between statins and CRC have been designed to test the safety of statins to treat CVD, therefore they are not designed to analyse cancer risk, for example the follow up period is often too short. Additionally CVD patients are at higher risk of CRC because CVD risk factors also include low physical activity and a poor diet (Lochhead & Chan 2013). Interestingly a large meta analysis of 42 studies was conducted and included case control studies, cohort studies and randomised control trials. The meta analysis concluded statins have a slight protective effect but long term use does not seem to influence CRC risk (Liu et al. 2014). Recent research has suggested the link between statins and reduced cancer risk may be due to cholesterol levels and not the result of statin treatment (Mamtani et al. 2016). High cholesterol levels (would receive statin treatment) was associated with a reduced cancer risk, whilst low cholesterol levels was associated with a higher cancer risk (Mamtani et al. 2016). Further studies are required to fully understand the link between statins and CRC.

Instead of using statins it is possible that we could exploit the same synthetic lethal relationship by targeting other parts of the mechanism identified. For example, we could investigate if inhibiting GGPP prenylation, survivin or Pak1 shows the same relationship. Another option is targeting another part of the cholesterol synthesis pathway. This is supported by the paper which identified TASIN-1 to inhibit EBP downstream of HMGCR and show a more potent synthetic lethal effect with APC mutations than statins (Zhang et al. 2016). This indicates the cholesterol synthesis pathway could be an ideal target to exploit in APC mutant CRC. The disadvantage of these approaches compared to statins is that statins have FDA-approval and have been used clinically for decades.

In summary we have created a new *in vitro* model of APC mutation in CRC using CRISPR-cas9 (APC wildtype and APC Lys736fs). We used the *in vitro* model to perform a siRNA screen against kinases and an FDA-approved compound screen to help us identify genes showing synthetic lethality with APC mutation. We failed to validate any of the potential hits from the siRNA screen. From the FDA-approved compound screen we successfully identified a synthetic lethal relationship between statins and the APC mutation in our *in vitro* model. The mechanism we propose involves a decrease in prenylated Rac1, which prevents Rac1 from interacting and

activating Pak1 at the membrane. The reduction in Pak1 activation then leads to less β-catenin phosphorylated at ser675 and reduced transcription of Wnt target genes including survivin, leading to apoptosis. The APC mutant cell lines rely more on Wnt signalling and are therefore more susceptible to its inhibition. The potential of targeting the cholesterol synthesis pathway in APC mutant CRC, is strengthened by the research identifying the drug TASIN-1 to be synthetically lethal with the APC mutation. Understanding potential overlap between the different research is essential to translating these findings into the clinic.

References

Agarwal, B., Bhendwal, S., et al., 1999. Lovastatin augments apoptosis induced by chemotherapeutic agents in colon cancer cells. *Clinical Cancer Research*, 5(8), pp.2223–2229.

Agarwal, B., Rao, C. V., et al., 1999. Lovastatin augments sulindac-induced apoptosis in colon cancer cells and potentiates chemopreventive effects of sulindac. *Gastroenterology*, 117(4), pp.838–847.

Ahmed, D. et al., 2013. Epigenetic and genetic features of 24 colon cancer cell lines. *Oncogenesis*, 2(0424), p.e71.

Akiyama, T. & Kawasaki, Y., 2006. Wnt signalling and the actin cytoskeleton. *Oncogene*, 25(57), pp.7538–7544.

Al-Majed, A.-R.A. et al., 2015. Losartan: Comprehensive Profile. *Profiles of drug substances, excipients, and related methodology*, 40, pp.159–194.

Alberts, A.W., 1990. Lovastatin and simvastatin--inhibitors of HMG CoA reductase and cholesterol biosynthesis. *Cardiology*, 77 Suppl 4, pp.14–21.

Albuquerque, C. et al., 2002. The “just-right” signaling model: APC somatic mutations are selected based on a specific level of activation of the beta-catenin signaling cascade. *Human molecular genetics*, 11(13), pp.1549–1560.

Altieri, D.C., 2008. Survivin, cancer networks and pathway-directed drug discovery. *Nature reviews. Cancer*, 8(1), pp.61–70.

Altieri, D.C., 2003. Validating survivin as a cancer therapeutic target. *Nature Reviews Cancer*, 3(1), pp.46–54.

Ambrosini, G., Adida, C. & Altieri, D.C., 1997. A novel anti-apoptosis gene, survivin, expressed in cancer and lymphoma. *Nat Med*, 3(8), pp.917–921.

Aoki, K. & Taketo, M.M., 2007. Adenomatous polyposis coli (APC): a multi-functional tumor suppressor gene. *Journal of cell science*, 120(19), pp.3327–35.

Arenas, R.B. et al., 1996. Introduction of human adenomatous polyposis coli gene into Min mice via cationic liposomes. *Surgery*, 120(4), pp.712–718.

Asanuma, K. et al., 2004. Survivin enhances Fas ligand expression via up-regulation of specificity protein 1-mediated gene transcription in colon cancer cells. *Journal of immunology (Baltimore, Md. : 1950)*, 172(6), pp.3922–3929.

Baan, B. et al., 2012. 5-Aminosalicylic acid inhibits cell cycle progression in a phospholipase D dependent manner in colorectal cancer. *Gut*, 61(12), pp.1708–1715.

Baas, J.M. et al., 2015. Safety and efficacy of the addition of simvastatin to cetuximab in previously treated KRAS mutant metastatic colorectal cancer patients. *Investigational New Drugs*, 33(6), pp.1242–1247.

Bahmanyar, S., Nelson, W.J. & Barth, A.I.M., 2009. Role of APC and its binding partners in regulating microtubules in mitosis. *Adv Exp Med Biol*, 656, pp.65–74.

Bain, J. et al., 2007. The selectivity of protein kinase inhibitors: a further update. *Biochemical Journal*, 408(3), pp.297–315.

Bardou, M., Barkun, A. & Martel, M., 2010. Effect of statin therapy on colorectal cancer. *Gut*, 59(11), pp.1572–1585.

Barrangou, R. et al., 2015. Advances in CRISPR-Cas9 genome engineering: lessons learned from RNA interference. *Nucleic acids research*, (11), pp.1–13.

Bengtsson, E. et al., 2014. HMG-CoA reductase expression in primary colorectal cancer correlates with favourable clinicopathological characteristics and an improved clinical outcome. *Diagnostic Pathology*, 9(1), p.78.

Birmingham, A. et al., 2009. Statistical Methods for Analysis of High-Throughput RNA Interference Screens Amanda. *Nature Methods*, 6(8), pp.569–575.

Bodmer, W.F. et al., 1987. Localization of the gene for familial adenomatous polyposis on chromosome 5. *Nature*, 328(6131), pp.614–616.

Boland, R.C. & Goel, A., 2010. Microsatellite Instability in Colorectal Cancer. *Gastroenterology*, 138(6), pp.2073–2087.

Borgquist, S. et al., 2008. Prognostic impact of tumour-specific HMG-CoA reductase expression in primary breast cancer. *Breast Cancer Research : BCR*, 10(5), pp.R79–R79.

Bose, C.K. & Basu, N., 2015. PARP inhibitors and more. *Journal of the Turkish German Gynecological Association*, 16(2), pp.107–10.

Brault, L. et al., 2010. Pim serine/threonine kinases in the pathogenesis and therapy of hematologic malignancies and solid cancers. *Haematologica*, 95(6), pp.1004–1015.

Brennan, D.J. et al., 2010. Tumour-specific HMG-CoAR is an independent predictor of recurrence free survival in epithelial ovarian cancer. *BMC cancer*, 10, p.125.

Brocardo, M. & Henderson, B.R., 2008. APC shuttling to the membrane, nucleus and beyond. *Trends in Cell Biology*, 18(12), pp.587–596.

Brocardo, M., Näthke, I.S. & Henderson, B.R., 2005. Redefining the subcellular location and transport of APC: new insights using a panel of antibodies. *EMBO reports*, 6(2), pp.184–90.

Bryant, D.M. & Mostov, K.E., 2008. From cells to organs: building polarized tissue. *Nature reviews. Molecular cell biology*, 9(11), pp.887–901.

Buchanan, F.G. et al., 2007. Targeting cyclooxygenase-2 and the epidermal growth factor receptor for the prevention and treatment of intestinal cancer. *Cancer Research*, 67(19), pp.9380–9388.

Burgess, A.W. et al., 2011. Wnt signaling and colon tumorigenesis--a view from the periphery. *Experimental cell research*, 317(19), pp.2748–58.

Bustelo, X.R., Sauzeau, V. & Berenjeno, I.M., 2007. GTP-binding proteins of the Rho/Rac family: Regulation, effectors and functions in vivo. *BioEssays*, 29(4), pp.356–370.

Canaani, D., 2014. Application of the concept synthetic lethality toward anticancer therapy: a promise fulfilled? *Cancer letters*, 352(1), pp.59–65.

Cancer Genom Atlas, 2012. Comprehensive molecular characterization of human colon and rectal cancer. *Nature*, 487(7407), pp.330–337.

Chan, D.A. & Giaccia, A.J., 2011. Harnessing synthetic lethal interactions in anticancer drug discovery. *Nature reviews. Drug discovery*, 10(5), pp.351–64.

Chan, E. et al., 2011. Dual blockade of the EGFR and COX-2 pathways: A phase II trial of cetuximab and celecoxib in patients with chemotherapy refractory metastatic colorectal cancer. *American Journal of Clinical Oncology: Cancer Clinical Trials*, 34(6), pp.581–586.

Chang, H.L. et al., 2013. Simvastatin induced HCT116 colorectal cancer cell apoptosis through p38MAPK-p53-survivin signaling cascade. *Biochimica et Biophysica Acta - General Subjects*, 1830(8), pp.4053–4064.

Chee, C.E. & Sinicrope, F.A., 2010. Targeted Therapeutic Agents for Colorectal Cancer. *Gastroenterology Clinics of North America*, 39(3), pp.601–613.

Chen, X. et al., 2016. Survivin and tumorigenesis: Molecular mechanisms and therapeutic strategies. *Journal of Cancer*, 7(3), pp.314–323.

Cho, S. et al., 2008. Simvastatin induces apoptosis in human colon cancer cells and in tumor xenografts, and attenuates colitis-associated colon cancer in mice. *International journal of cancer. Journal international du cancer*, 123, pp.951–957.

Chong, C. et al., 2001. The mechanism of PAK activation. Autophosphorylation events in both regulatory and kinase domains control activity. *Journal of Biological Chemistry*, 276(20), pp.17347–17353.

Chushi, L. et al., 2016. HMGCR is up-regulated in gastric cancer and promotes the growth and migration of the cancer cells. *Gene*, 587(1), pp.42–47.

Collins, R. et al., 2016. Interpretation of the evidence for the efficacy and safety of statin therapy. *The Lancet*, 388(10059), pp.2532–2561.

Conner, J.R., Beisswenger, P.J. & Szwergold, B.S., 2005. Some clues as to the regulation, expression, function, and distribution of fructosamine-3-kinase and fructosamine-3-kinase-related protein. *Annals of the New York Academy of Sciences*, 1043, pp.824–836.

Copp, J., Manning, G. & Hunter, T., 2010. TORC-specific phosphorylation of mTOR: phospho-Ser2481 is a marker for intact mTORC2. *Cancer Research*, 69(5), pp.1821–1827.
Cordle, A. et al., 2005. Mechanisms of statin-mediated inhibition of small G-protein function. *Journal of Biological Chemistry*, 280(40), pp.34202–34209.
Costa-Cabral, S. et al., 2016. CDK1 Is a Synthetic Lethal Target for KRAS Mutant Tumours. *PloS one*, 11(2), p.e0149099.
da Costa, L.T. et al., 1999. CDX2 is mutated in a colorectal cancer with normal APC/beta-catenin signaling. *Oncogene*, 18(35), pp.5010–5014.
Criscuoli, V. et al., 2013. Mesalazine for the treatment of inflammatory bowel disease. *Expert opinion on pharmacotherapy*, 14(12), pp.1669–1678.
Daer, R.M. et al., 2017. The Impact of Chromatin Dynamics on Cas9-Mediated Genome Editing in Human Cells. *ACS synthetic biology*, 6(3), pp.428–438.
Damin, D.C. & Lazzaron, A.R., 2014. Evolving treatment strategies for colorectal cancer: a critical review of current therapeutic options. *World journal of gastroenterology : WJG*, 20(4), pp.877–87.
Das, S. et al., 2015. Single-molecule tracking of small GTPase Rac1 uncovers spatial regulation of membrane translocation and mechanism for polarized signaling. *Proceedings of the National Academy of Sciences*, 112(3), pp.E267–E276.
Davidson, G. & Niehrs, C., 2010. Emerging links between CDK cell cycle regulators and Wnt signaling. *Trends in Cell Biology*, 20(8), pp.453–460.
Davies, J.T. et al., 2016. Current and Emerging Uses of Statins in Clinical Therapeutics: A Review. *Lipid insights*, 9, pp.13–29.
Demierre, M.-F. et al., 2005. Statins and cancer prevention. *Nature reviews. Cancer*, 5(December), pp.930–42.
DerMardirossian, C. & Bokoch, G.M., 2005. GDIs: Central regulatory molecules in Rho GTPase activation. *Trends in Cell Biology*, 15(7), pp.356–363.
Dhillon, S., 2015. Saxagliptin: A Review in Type 2 Diabetes. *Drugs*, 75(15), pp.1783–1796.
Din, F.V.N. et al., 2012. Aspirin inhibits mTOR signaling, activates AMP-activated protein kinase, and induces autophagy in colorectal cancer cells. *Gastroenterology*, 142(7), p.1504–15.e3.
Doudna, J. a. & Charpentier, E., 2014. The new frontier of genome engineering with CRISPR-Cas9. *Science*, 346(6213), pp.1258096–1258096.
Dow, L.E. et al., 2015. Apc Restoration Promotes Cellular Differentiation and Reestablishes Crypt Homeostasis in Colorectal Cancer. *Cell*, 161(7), pp.1539–1552.
Du, Y. et al., 2014. SMG1 acts as a novel potential tumor suppressor with epigenetic inactivation in acute myeloid leukemia. *International Journal of Molecular Sciences*, 15(9), pp.17065–17076.
Echeverri, C.J. & Perrimon, N., 2006. High-throughput RNAi screening in cultured cells: a user's guide. *Nature Reviews Genetics*, 7(5), pp.373–384.
El-Khoueiry, A.B. et al., 2013. A phase I first-in-human study of PRI-724 in patients (pts) with advanced solid tumors. *Journal of Clinical Oncology*, 31(15_suppl), p.2501.
Emami, K.H. et al., 2004. A small molecule inhibitor of β-catenin/CREB-binding protein transcription. *Proceedings of the National Academy of Sciences*.
Endo, A., 2004. The origin of the statins. *International Congress Series*, 1262(January 1966), pp.3–8.
Endoh, T. et al., 2005. Survivin enhances telomerase activity via up-regulation of specificity protein 1- and c-Myc-mediated human telomerase reverse transcriptase gene transcription. *Experimental Cell Research*, 305(2), pp.300–311.
Espina, C. et al., 2008. A Critical Role for Rac1 in Tumor Progression of Human Colorectal Adenocarcinoma Cells. *The American Journal of Pathology*, 172(1), pp.156–166.

Esufali, S. & Bapat, B., 2004. Cross-talk between Rac1 GTPase and dysregulated Wnt signaling pathway leads to cellular redistribution of β-catenin and TCF/LEF-mediated transcriptional activation. *Oncogene*, 23(50), pp.8260–8271.
Faller, W.J. et al., 2014. mTORC1-mediated translational elongation limits intestinal tumour initiation and growth. *Nature*, 517(7535), pp.497–500.
Falschlehner, C. et al., 2010. High-throughput RNAi screening to dissect cellular pathways: A how-to guide. *Biotechnology Journal*, 5(4), pp.368–376.
Farwell, W.R. et al., 2008. The Association Between Statins and Cancer Incidence in a Veterans Population. *Journal of the National Cancer Institute*, 100(2), pp.134–139.
Fearnhead, N.S. et al., 2001. The ABC of APC. *Human molecular genetics*, 10(7), pp.721–33.
Fearon, E.R., 2011. Molecular genetics of colorectal cancer. *Annual review of pathology*, 6, pp.479–507.
Fearon, E.R. & Vogelstein, B., 1990. A genetic model for colorectal tumorigenesis. *Cell*, 61(5), pp.759–767.
Fellmann, C. & Lowe, S.W., 2014. Stable RNA interference rules for silencing. *Nature cell biology*, 16(1), pp.10–8.
Fiala, O. et al., 2015. G12V and G12A KRAS mutations are associated with poor outcome in patients with metastatic colorectal cancer treated with bevacizumab. *Tumor Biology*, pp.1–8.
Fletcher, D.A. & Mullins, R.D., 2010. Cell mechanics and the cytoskeleton. *Nature*, 463(7280), pp.485–492.
Floquet, C., Rousset, J.-P. & Bidou, L., 2011. Readthrough of Premature Termination Codons in the Adenomatous Polyposis Coli Gene Restores Its Biological Activity in Human Cancer Cells. *PLoS ONE*, 6(8), p.e24125.
Foley, P.J. et al., 2008. Targeted suppression of β-catenin blocks intestinal adenoma formation in APC min mice. *Journal of Gastrointestinal Surgery*.
Freed-Pastor, W.A. et al., 2012. Mutant p53 disrupts mammary tissue architecture via the mevalonate pathway. *Cell*, 148(1–2), pp.244–258.
Fu, Y. et al., 2013. High-frequency off-target mutagenesis induced by CRISPR-Cas nucleases in human cells. *Nature biotechnology*, 31(9), pp.822–6.
Fukata, M. & Kaibuchi, K., 2001. Rho-family GTPases in cadherin-mediated cell-cell adhesion. *Nature Reviews Molecular Cell Biology*, 2(12), pp.887–897.
Gayet, J. et al., 2001. Extensive characterization of genetic alterations in a series of human colorectal cancer cell lines. *Oncogene*, 20(36), pp.5025–5032.
Gelmini, S. et al., 2006. Distribution of Tankyrase-1 mRNA expression in colon cancer and its prospective correlation with progression stage. *Oncology Reports*, 16(6), pp.1261–1266.
Gianani, R. et al., 2001. Expression of survivin in normal, hyperplastic, and neoplastic colonic mucosa. *Human Pathology*, 32(1), pp.119–125.
Greenwood, J., Steinman, L. & Zamvil, S.S., 2006. Statin therapy and autoimmune disease: from protein prenylation to immunomodulation. *Nat Rev Immunol*, 6(5), pp.358–370.
Groden, J. et al., 1991. Identification and characterization of the familial adenomatous polyposis coli gene. *Cell*, 66(3), pp.589–600.
Gubanova, E. et al., 2012. Downregulation of SMG-1 in HPV-positive head and neck squamous cell carcinoma due to promoter hypermethylation correlates with improved survival. *Clinical Cancer Research*, 18(5), pp.1257–1267.
Gubanova, E. et al., 2013. SMG-1 suppresses CDK2 and tumor growth by regulating both the p53 and Cdc25A signaling pathways. *Cell Cycle*, 12(24), pp.3770–3780.
Guillotin, D. et al., 2017. Drug-repositioning screens identify Triamterene as a selective drug for the treatment of DNA Mismatch Repair deficient cells. *Clinical cancer research : an official journal of the American Association for Cancer Research*, 23(11), pp.2880–2890.
Guinney, J. et al., 2015. The consensus molecular subtypes of colorectal cancer. *Nature Medicine*, 21(11), pp.1350–1356.

Guo, J. et al., 2009. Mutations in the human naked cuticle homolog NKD1 found in colorectal cancer alter Wnt/Dvl/β-catenin signaling. *PLoS ONE*, 4(11), pp.2–11.
Hachem, C. et al., 2009. Statins and the Risk of Colorectal Carcinoma: A Nested Case-Control Study in Veterans With Diabetes. *Am J Gastroenterol*, 104(5), pp.1241–1248.
Haikarainen, T., Krauss, S. & Lehtio, L., 2014. Tankyrases: structure, function and therapeutic implications in cancer. *Current pharmaceutical design*, 20(41), pp.6472–88.
Handeli, S. & Simon, J.A., 2008. A small-molecule inhibitor of Tcf/β-catenin signaling down-regulates PPAR and PPAR activities. *Molecular Cancer Therapeutics*, 7(3), pp.521–529.
Hanson, C. a & Miller, J.R., 2005. Non-traditional roles for the Adenomatous Polyposis Coli (APC) tumor suppressor protein. *Gene*, 361, pp.1–12.
Harris, T.J.C. & Tepass, U., 2010. Adherens junctions: from molecules to morphogenesis. *Nature Reviews Molecular Cell Biology*, 11(7), pp.502–514.
Hartwell, L.H., 1997. Integrating Genetic Approaches into the Discovery of Anticancer Drugs. *Science*, 278(5340), pp.1064–1068.
Henney, H.R. 3rd & Runyan, J.D., 2008. A clinically relevant review of tizanidine hydrochloride dose relationships to pharmacokinetics, drug safety and effectiveness in healthy subjects and patients. *International journal of clinical practice*, 62(2), pp.314–324.
Hentosh, P. et al., 2001. Sterol-independent regulation of 3-hydroxy-3-methylglutaryl coenzyme A reductase in tumor cells. *Molecular Carcinogenesis*, 32(3), pp.154–166.
Herrera, L. et al., 1986. Gardner syndrome in a man with an interstitial deletion of 5q. *American journal of medical genetics*, 25(3), pp.473–476.
Heyer, J. et al., 1999. Mouse models for colorectal cancer. *Oncogene*, 18(38), pp.5325–5333.
Hodge, R.G. & Ridley, A.J., 2016. Regulating Rho GTPases and their regulators. *Nature Reviews Molecular Cell Biology*, 17(8), pp.496–510.
Horii, A. et al., 1993. Multiple forms of the APC gene transcripts and their tissue-specific expression. *Human molecular genetics*, 2(3), pp.283–7.
Hsu, P.D. et al., 2013. DNA targeting specificity of RNA-guided Cas9 nucleases. *Nature biotechnology*, 31(9), pp.827–32.
Hsu, P.D., Lander, E.S. & Zhang, F., 2014. Development and Applications of CRISPR-Cas9 for Genome Engineering. *CELL*, 157, pp.1262–1278.
Huang, S.-M.A. et al., 2009. Tankyrase inhibition stabilizes axin and antagonizes Wnt signalling. *Nature*, 461(7264), pp.614–620.
Huntwork-Rodriguez, S. et al., 2013. JNK-mediated phosphorylation of DLK suppresses its ubiquitination to promote neuronal apoptosis. *Journal of Cell Biology*, 202(5), pp.747–763.
Hwang, K.-E. et al., 2011. Apoptotic induction by simvastatin in human lung cancer A549 cells via Akt signaling dependent down-regulation of survivin. *Investigational new drugs*, 29(5), pp.945–952.
Ilyas, M. et al., 1997. Beta-catenin mutations in cell lines established from human colorectal cancers. *Proceedings of the National Academy of Sciences of the United States of America*, 94(19), pp.10330–4.
Jamieson, C. et al., 2015. Rac1 augments Wnt signaling by stimulating B-catenin-LEF-1 complex assembly independent of B-catenin nuclear import. *Journal of Cell Science*, 128(21), pp.3933–3946.
Janzen, W.P., 2014. Screening technologies for small molecule discovery: The state of the art. *Chemistry and Biology*, 21(9), pp.1162–1170.
Jasperson, K.W. et al., 2010. Hereditary and Familial Colon Cancer. *Gastroenterology*, 138(6), pp.2044–2058.
Kahanek, N., Gelbard, C. & Hebert, A., 2008. Desonide: a review of formulations, efficacy and safety. *Expert opinion on investigational drugs*, 17(7), pp.1097–1104.

Kaneko, R. et al., 2007. Survivin down-regulation plays a crucial role in 3-hydroxy-3-methylglutaryl coenzyme A reductase inhibitor-induced apoptosis in cancer. *Journal of Biological Chemistry*, 282(27), pp.19273–19281.
Kang, D.H. et al., 2017. Interaction of tankyrase and peroxiredoxin II is indispensable for the survival of colorectal cancer cells. *Nature Communications*, 8(1), p.40.
Kawasaki, H. et al., 1998. Inhibition of apoptosis by survivin predicts shorter survival rates in colorectal cancer. *Cancer research*, 58(22), pp.5071–5074.
Keating, G.M. & Scott, L.J., 2004. Moxifloxacin: a review of its use in the management of bacterial infections. *Drugs*, 64(20), pp.2347–2377.
Kim, E.R. & Chang, D.K., 2014. Colorectal cancer in inflammatory bowel disease: The risk, pathogenesis, prevention and diagnosis. *World Journal of Gastroenterology : WJG*, 20(29), pp.9872–9881.
Kim, H. & Kim, J.-S., 2014. A guide to genome engineering with programmable nucleases. *Nature Reviews Genetics*, 15(5), pp.321–334.
Kim, J.-S.J.M., Kim, D. & Kim, S., 2014. Genotyping with CRISPR-Cas-derived RNA-guided endonucleases. *Nature communications*, 5, p.3157.
Kim, N.H. et al., 2011. p53 and microRNA-34 are suppressors of canonical Wnt signaling. *Science signaling*, 4(197), p.ra71.
Kim, P.J. et al., 2003. Survivin and molecular pathogenesis of colorectal cancer. *Lancet*, 362(9379), pp.205–209.
Kinzler, K.W. et al., 1991. Identification of a gene located at chromosome 5q21 that is mutated in colorectal cancers. *Science (New York, N.Y.)*, 251(4999), pp.1366–1370.
Klaus, A. & Birchmeier, W., 2008. Wnt signalling and its impact on development and cancer. *Nature Reviews Cancer*, 8(5), pp.387–398.
Kleinstiver, B.P. et al., 2016. High-fidelity CRISPR–Cas9 nucleases with no detectable genome-wide off-target effects. *Nature*, 529(7587), pp.490–495.
Knudson, A.G.J., 1971. Mutation and cancer: statistical study of retinoblastoma. *Proceedings of the National Academy of Sciences of the United States of America*, 68(4), pp.820–823.
Kodach, L.L. et al., 2007. The Effect of Statins in Colorectal Cancer Is Mediated Through the Bone Morphogenetic Protein Pathway. *Gastroenterology*, 133(4), pp.1272–1281.
Kohler, E.M. et al., 2008. Functional definition of the mutation cluster region of adenomatous polyposis coli in colorectal tumours. *Human Molecular Genetics*, 17(13), pp.1978–1987.
Kumar, R., Gururaj, A.E. & Barnes, C.J., 2006. P21-Activated Kinases in Cancer. *Nature Reviews Cancer*, 6(6), pp.459–471.
Kusugami, K. et al., 2000. Troxipide, a novel antiulcer compound, has inhibitory effects on human neutrophil migration and activation induced by various stimulants. *Digestive and liver disease : official journal of the Italian Society of Gastroenterology and the Italian Association for the Study of the Liver*, 32(4), pp.305–311.
Laplante, M. & Sabatini, D.M., 2009. mTOR signaling at a glance. *J Cell Sci*, 122(Pt 20), pp.3589–3594.
Laplante, M. & Sabatini, D.M., 2012. MTOR signaling in growth control and disease. *Cell*, 149(2), pp.274–293.
Lau, T. et al., 2013. A novel tankyrase small-molecule inhibitor suppresses APC mutation-driven colorectal tumor growth. *Cancer Research*, 73(10), pp.3132–3144.
Lee, J. et al., 2011. Effect of simvastatin on cetuximab resistance in human colorectal cancer with KRAS mutations. *Journal of the National Cancer Institute*, 103(8), pp.674–688.
Lee, J. et al., 2004. Liposome-mediated adenomatous polyposis coli gene therapy: A novel anti-adenoma strategy in multiple intestinal neoplasia mouse model. *Diseases of the Colon and Rectum*.

Lehtiö, L., Chi, N.W. & Krauss, S., 2013. Tankyrases as drug targets. *FEBS Journal*, 280(15), pp.3576–3593.
Leibowitz, B. et al., 2014. BID mediates selective killing of APC-deficient cells in intestinal tumor suppression by nonsteroidal antiinflammatory drugs. *Proceedings of the National Academy of Sciences*, 111(46), pp.16520–16525.
Lens, S.M., Vader, G. & Medema, R.H., 2006. The case for Survivin as mitotic regulator. *Current Opinion in Cell Biology*.
Lenz, H.J. & Kahn, M., 2014. Safely targeting cancer stem cells via selective catenin coactivator antagonism. *Cancer Science*, 105(9), pp.1087–1092.
Lepourcelet, M. et al., 2004. Small-molecule antagonists of the oncogenic Tcf/beta-catenin protein complex. *Cancer cell*.
Lesko, A., Goss, K. & Prosperi, J., 2014. Exploiting APC Function as a Novel Cancer Therapy. *Current Drug Targets*, 15(1), pp.90–102.
Li, F., 2005. Role of survivin and its splice variants in tumorigenesis. *British journal of cancer*, 92(2), pp.212–6.
Li, G. et al., 2017. Simvastatin inhibits tumor angiogenesis in HER2-overexpressing human colorectal cancer. *Biomedicine et Pharmacotherapy*, 85, pp.418–424.
Lim, S.H. et al., 2015. A randomised, double-blind, placebo-controlled multi-centre phase III trial of XELIRI/FOLFIRI plus simvastatin for patients with metastatic colorectal cancer. *British journal of cancer*, 113(10), pp.1421–1426.
Linnekamp, J.F. et al., 2015. Colorectal Cancer Heterogeneity and Targeted Therapy: A Case for Molecular Disease Subtypes. *Cancer Research*, 75(2), pp.245–249.
Liu, Y. et al., 2014. Association between statin use and colorectal cancer risk: a meta-analysis of 42 studies. *Cancer causes & control : CCC*, 25(2), pp.237–249.
Lochhead, P. & Chan, A.T., 2013. Statins and colorectal cancer. *Clin Gastroenterol Hepatol*.
Lord, C.J., Martin, S. a & Ashworth, a, 2009. RNA interference screening demystified. *Journal of clinical pathology*, 62(3), pp.195–200.
Lui, C. et al., 2012. APC as a mobile scaffold: Regulation and function at the nucleus, centrosomes, and mitochondria. *IUBMB Life*, 64(3), pp.209–214.
Luo, J. et al., 2009. A Genome-wide RNAi Screen Identifies Multiple Synthetic Lethal Interactions with the Ras Oncogene. *Cell*, 137(5), pp.835–848.
M. Sieber, O., P. Tomlinson, I. & Lamlum, H., 2000. The adenomatous polyposis coli (APC) tumour suppressor – genetics, function and disease. *Molecular Medicine Today*, 6(12), pp.462–469.
Ma, H. et al., 2005. Differential roles for the coactivators CBP and p300 on TCF/beta-catenin-mediated survivin gene expression. *Oncogene*, 24(22), pp.3619–31.
Ma, Y. et al., 2013. Obesity and Risk of Colorectal Cancer: A Systematic Review of Prospective Studies O. Y. Gorlova, ed. *PLoS ONE*, 8(1), p.e53916.
MacDonald, B.T., Tamai, K. & He, X., 2009. Wnt/β-Catenin Signaling: Components, Mechanisms, and Diseases. *Developmental Cell*, 17(1), pp.9–26.
Mahotka, C. et al., 2002. Distinct in vivo expression patterns of survivin splice variants in renal cell carcinomas. *International journal of cancer*, 100(1), pp.30–36.
Mamtani, R. et al., 2016. Disentangling the Association between Statins, Cholesterol, and Colorectal Cancer: A Nested Case-Control Study. *PLOS Medicine*, 13(4), p.e1002007. Available at: https://doi.org/10.1371/journal.pmed.1002007.
Mao, C.-Q. et al., 2014. Synthetic lethal therapy for KRAS mutant non-small-cell lung carcinoma with nanoparticle-mediated CDK4 siRNA delivery. *Molecular therapy : the journal of the American Society of Gene Therapy*, 22(5), pp.964–73.
March, H.N. et al., 2011. Insertional mutagenesis identifies multiple networks of cooperating genes driving intestinal tumorigenesis. *Nature Genetics*, 43(12), pp.1202–1209.
Marginean, E.C. & Melosky, B., 2018. Is there a role for programmed death ligand-1 testing and immunotherapy in colorectal cancer with microsatellite instability?: Part II-the challenge of programmed death ligand-1 testing and its role in microsatellite instability-high colorectal cancer. *Archives of Pathology and Laboratory Medicine*, 142(1), pp.26–34.

Martin, S.A. et al., 2010. DNA Polymerases as Potential Therapeutic Targets for Cancers Deficient in the DNA Mismatch Repair Proteins MSH2 or MLH1. *Cancer Cell*, 17(3), pp.235–248.
Martin, S.A. et al., 2011. Parallel high-throughput RNA interference screens identify PINK1 as a potential therapeutic target for the treatment of DNA mismatch repair-deficient cancers. *Cancer Research*, 71(5), pp.1836–1848.
Mashima, T. et al., 2017. mTOR signaling mediates resistance to tankyrase inhibitors in Wnt-driven colorectal cancer. *Oncotarget*.
Matano, M. et al., 2015. Modeling colorectal cancer using CRISPR-Cas9–mediated engineering of human intestinal organoids. *Nature Medicine*, 21(3), pp.256–62.
McCartney, B.M. & Näthke, I.S., 2008. Cell regulation by the Apc protein. Apc as master regulator of epithelia. *Current Opinion in Cell Biology*, 20(2), pp.186–193.
McNeely, W. & Goa, K.L., 1999. Diclofenac-potassium in migraine: a review. *Drugs*, 57(6), pp.991–1003.
Mendes-Pereira, A.M., Lord, C.J. & Ashworth, A., 2012. NLK Is a Novel Therapeutic Target for PTEN Deficient Tumour Cells. *PLoS ONE*, 7(10), pp.1–6.
Meng, H. et al., 2004. Expression level of wild-type survivin in gastric cancer is an independent predictor of survival. *World Journal of Gastroenterology : WJG*, 10(22), pp.3245–3250.
Mésange, P. et al., 2014. Intrinsic bevacizumab resistance is associated with prolonged activation of autocrine VEGF signaling and hypoxia tolerance in colorectal cancer cells and can be overcome by nintedanib, a small molecule angiokinase inhibitor. *Oncotarget*, 5(13), pp.4709–21.
Michaelson, D. et al., 2005. Postprenylation CAAX processing is required for proper localization of Ras but not Rho GTPases. *Molecular Biology of the Cell*, 16(4), pp.1606–1616.
Miyaki, M. et al., 1994. Characteristics of somatic mutation of the adenomatous polyposis coli gene in colorectal tumors. *Cancer research*, 54(11), pp.3011–20.
Morkel, M. et al., 2015. Similar but different: distinct roles for KRAS and BRAF oncogenes in colorectal cancer development and therapy resistance. *Oncotarget*, 6(25), pp.20785–20800.
Mulcahy, M.F., 2008. Bevacizumab in the therapy for refractory metastatic colorectal cancer. *Biologics : targets & therapy*, 2(1), pp.53–9.
Munguia, R. & Daniel, S.J., 2008. Ototopical antifungals and otomycosis: a review. *International journal of pediatric otorhinolaryngology*, 72(4), pp.453–459.
Myant, K.B. et al., 2013. ROS production and NF-κB activation triggered by RAC1 facilitate WNT-driven intestinal stem cell proliferation and colorectal cancer initiation. *Cell Stem Cell*, 12(6), pp.761–773.
Nakagawa, M. et al., 2001. Recruitment and activation of Rac1 by the formation of E-cadherin-mediated cell-cell adhesion sites. *Journal of cell science*, 114(Pt 10), pp.1829–38.
Naldini, L. et al., 1996. In vivo gene delivery and stable transduction of nondividing cells by a lentiviral vector. *Science (New York, N.Y.)*, 272(5259), pp.263–267.
Narisawa, T. et al., 1996. Chemoprevention by pravastatin, a 3-hydroxy-3-methylglutaryl-coenzyme A reductase inhibitor, of N-methyl-N-nitrosourea-induced colon carcinogenesis in F344 rats. *Japanese journal of cancer research : Gann*, 87(8), pp.798–804.
Näthke, I., 2006. Cytoskeleton out of the cupboard: Colon cancer and cytoskeletal changes induced by loss of APC. *Nature Reviews Cancer*, 6(12), pp.967–974.
Necochea-Campion, R. de et al., 2013. Clinico-pathologic relevance of Survivin splice variant expression in cancer. *Cancer Letters*, 339(2), pp.167–174.
Nelson, S. & Näthke, I.S., 2013. Interactions and functions of the adenomatous polyposis coli (APC) protein at a glance. *Journal of cell science*, 126(Pt 4), pp.873–7.
Nieuwenhuis, M.H. & Vasen, H.F. a, 2007. Correlations between mutation site in APC and phenotype of familial adenomatous polyposis (FAP): A review of the literature. *Critical Reviews in Oncology/Hematology*, 61(2), pp.153–161.

Nihiraa, N.T. & Yoshidaa, K., 2015. Engagement of dyrk2 in proper control for cell division. *Cell Cycle*, 14(6), pp.802–807.
Notarnicola, M. et al., 2004. Up-regulation of 3-hydroxy-3-methylglutaryl coenzyme A reductase activity in left-sided human colon cancer. *Anticancer Research*, 24(6), pp.3837–3842.
Onesto, C. et al., 2008. Characterization of EHT 1864, a novel small molecule inhibitor of Rac family small GTPases. *Methods in enzymology*, 439, pp.111–129.
Oshima, M. et al., 1996. Suppression of intestinal polyposis in Apc(??716) knockout mice by inhibition of cyclooxygenase 2 (COX-2). *Cell*, 87(5), pp.803–809.
Pabla, B., 2015. Colon cancer and the epidermal growth factor receptor: Current treatment paradigms, the importance of diet, and the role of chemoprevention. *World Journal of Clinical Oncology*, 6(5), p.133.
Palamidessi, A. et al., 2008. Endocytic Trafficking of Rac Is Required for the Spatial Restriction of Signaling in Cell Migration. *Cell*, 134(1), pp.135–147.
Parsons, B.D. et al., 2009. A direct phenotypic comparison of siRNA pools and multiple individual duplexes in a functional assay. *PLoS ONE*, 4(12).
Pavlidou, A. et al., 2011. Survivin isoforms and clinicopathological characteristics in colorectal adenocarcinomas using real-time qPCR. *World Journal of Gastroenterology*, 17(12), pp.1614–1621.
Peeters, P.J.H.L. et al., 2015. The risk of colorectal cancer in patients with type 2 diabetes: associations with treatment stage and obesity. *Diabetes care*, 38(3), pp.495–502.
Poynter, J.N. et al., 2005. Statins and the Risk of Colorectal Cancer. *New England Journal of Medicine*, 352(21), pp.2184–2192.
del Pozo, M. a et al., 2000. Adhesion to the extracellular matrix regulates the coupling of the small GTPase Rac to its effector PAK. *The EMBO journal*, 19(9), pp.2008–14.
Del Pozo, M.A. et al., 2002. Integrins regulate GTP-Rac localized effector interactions through dissociation of Rho-GDI. *Nature Cell Biology*, 4(3), pp.232–239.
Prosperi, J.R. & Goss, K.H., 2011. Wnt Pathway-Independent Activities of the APC Tumor Suppressor. *Tumor Suppressors*, pp.105–132.
Qiao, L.J., Kang, K.L. & Heo, J.S., 2011. Simvastatin promotes osteogenic differentiation of mouse embryonic stem cells via canonical Wnt/B-catenin signaling. *Molecules and Cells*, 32(5), pp.437–444.
Qiu, Z. et al., 2016. HMGCR positively regulated the growth and migration of glioblastoma cells. *Gene*, 576(1), pp.22–27.
Rane, C.K. & Minden, A., 2018. P21 activated kinase signaling in cancer. *Seminars in Cancer Biology*.
Rao, C. V & Reddy, B.S., 2004. NSAIDs and chemoprevention. *Current cancer drug targets*, 4(1), pp.29–42.
Rao, C. V & Yamada, H.Y., 2013. Genomic Instability and Colon Carcinogenesis: From the Perspective of Genes. *Frontiers in Oncology*, 3(May), p.130.
Rao, S. et al., 1999. Lovastatin-mediated G 1 arrest is through inhibition of the proteasome, independent of hydroxymethyl glutaryl-CoA reductase. *Biochemistry*, 96(July), pp.7797–7802.
Rao, T.P. & Kühl, M., 2010. An updated overview on Wnt signaling pathways: a prelude for more. *Circulation research*, 106(12), pp.1798–806.
Rego, R.L. et al., 2010. Prognostic effect of activated EGFR expression in human colon carcinomas: comparison with EGFR status. *British journal of cancer*, 102(1), pp.165–72.
Riffell, J.L., Lord, C.J. & Ashworth, A., 2012. Tankyrase-targeted therapeutics: expanding opportunities in the PARP family. *Nature Reviews Drug Discovery*, 11(12), pp.923–936.
Roberts, P.J. et al., 2008. Rho family GTPase modification and dependence on CAAX motif-signaled posttranslational modification. *Journal of Biological Chemistry*, 283(37), pp.25150–25163.

Robin, N.C. et al., 2014. Simvastatin promotes adult hippocampal neurogenesis by enhancing Wnt/B-catenin signaling. *Stem Cell Reports*, 2(1), pp.9–17.
Roh, H. et al., 2001. Suppression of β -Catenin Inhibits the Neoplastic Growth of APC -Mutant Colon Cancer Cells Suppression of ß-Catenin Inhibits the Neoplastic Growth of APC -Mutant Colon. *Cancer research*, 61, pp.6563–6568.
Rohlin, a et al., 2011. Inactivation of promoter 1B of APC causes partial gene silencing: evidence for a significant role of the promoter in regulation and causative of familial adenomatous polyposis. *Oncogene*, 30(50), pp.4977–4989.
De Rosa, M. et al., 2007. Alternative splicing and nonsense-mediated mRNA decay in the regulation of a new adenomatous polyposis coli transcript. *Gene*, 395(1–2), pp.8–14.
Rosner, M. et al., 2010. MTOR phosphorylated at S2448 binds to raptor and rictor. *Amino Acids*, 38(1), pp.223–228.
Rousseaux, C. et al., 2013. The 5-aminosalicylic acid antineoplastic effect in the intestine is mediated by PPARγ. *Carcinogenesis*, 34(11), pp.2580–2586.
Salins, P. et al., 2007. Lovastatin protects human neurons against AB-induced toxicity and causes activation of B-catenin-TCF/LEF signaling. *Neuroscience Letters*, 412(3), pp.211–216.
Samadder, N.J. et al., 2016. Effect of sulindac and erlotinib vs placebo: On duodenal neoplasia in familial adenomatous polyposis: A randomized clinical trial. *JAMA - Journal of the American Medical Association*, 315(12), pp.1266–1275.
Sander, J.D. & Joung, J.K., 2014. CRISPR-Cas systems for editing, regulating and targeting genomes. *Nature biotechnology*, 32(4), pp.347–55.
Sanjana, N.E., Shalem, O. & Zhang, F., 2014. Improved vectors and genome-wide libraries for CRISPR screening. *Nature Methods*, 11(8), pp.783–784.
Santoro, I.M. & Groden, J., 1997. Alternative splicing of the APC gene and its association with terminal differentiation. *Cancer Res*.
Sarela, A.I. et al., 2000. Expression of the antiapoptosis gene, survivin, predicts death from recurrent colorectal carcinoma. *Gut*, 46(5), pp.645–50.
Schubbert, S., Shannon, K. & Bollag, G., 2007. Hyperactive Ras in developmental disorders and cancer. *Nature reviews. Cancer*, 7(4), pp.295–308.
Seabra, M.C., 1998. Membrane association and targeting of prenylated Ras-like GTPases. *Cellular Signalling*, 10(3), pp.167–172.
Shibata, H. et al., 1997. Rapid colorectal adenoma formation initiated by conditional targeting of the Apc gene. *Science (New York, N.Y.)*, 278(5335), pp.120–123.
Shutes, A. et al., 2007. Specificity and mechanism of action of EHT 1864, a novel small molecule inhibitor of Rac family small GTPases. *Journal of Biological Chemistry*, 282(49), pp.35666–35678.
Solomon, E. et al., 1987. Chromosome 5 allele loss in human colorectal carcinomas. *Nature*, 328(19), pp.616–619.
Song, Y. et al., 2004. Specific inhibition of cyclin-dependent kinases and cell proliferation by harmine. *Biochemical and Biophysical Research Communications*, 317(1), pp.128–132.
Spiering, D. & Hodgson, L., 2011. Dynamics of the rho-family small GTPases in actin regulation and motility. *Cell Adhesion and Migration*, 5(2), pp.170–180.
Steckel, M. et al., 2012. Determination of synthetic lethal interactions in KRAS oncogene-dependent cancer cells reveals novel therapeutic targeting strategies. *Cell Research*, 22(8), pp.1227–1245.
Suga, K. et al., 2005. Correlation between transcriptional expression of survivin isoforms and clinicopathological findings in human colorectal carcinomas. *Oncology reports*, 13(5), pp.891–897.
Swamy, M. V. et al., 2006. Chemoprevention of familial adenomatous polyposis by low doses of atorvastatin and celecoxib given individually and in combination to APC Min mice. *Cancer Research*, 66(14), pp.7370–7377.
Symons, M., 2000. Adhesion signaling: PAK meets Rac on solid ground. *Current biology : CB*, 10(14), pp.R535-7.

Tanaka, N. et al., 2017. APC Mutations as a Potential Biomarker for Sensitivity to Tankyrase Inhibitors in Colorectal Cancer. *Molecular Cancer Therapeutics*, 16(4), pp.752–762.
Teraoka, N. et al., 2011. Inhibition of intestinal polyp formation by pitavastatin, a HMG-CoA reductase inhibitor. *Cancer Prevention Research*, 4(3), pp.445–453.
Thibault, A. et al., 1996. Phase I study of lovastatin, an inhibitor of the mevalonate pathway, in patients with cancer. *Clinical cancer research : an official journal of the American Association for Cancer Research*, 2(3), pp.483–91.
Thomson, J.P., 1990. Familial adenomatous polyposis: the large bowel. *Ann R Coll Surg Engl*, 72(3), pp.177–180.
Tiong, K.L. et al., 2014. CSNK1E/CTNNB1 Are Synthetic Lethal To TP53 in Colorectal Cancer and Are Markers for Prognosis. *Neoplasia*, 16(5), pp.441–450.
Tsai, Y.C. et al., 2012. Differential regulation of HMG-CoA reductase and Insig-1 by enzymes of the ubiquitin-proteasome system. *Molecular Biology of the Cell*, 23(23), pp.4484–4494.
Uzbekov, R.E., 2004. Analysis of the cell cycle and a method employing synchronized cells for study of protein expression at various stages of the cell cycle. *Biochemistry. Biokhimiia*, 69(5), pp.485–496.
Vasconcelos-Dos-Santos, A. et al., 2017. Hyperglycemia exacerbates colon cancer malignancy through hexosamine biosynthetic pathway. *Oncogenesis*, 6(December 2016).
Viale, G., Trapani, D. & Curigliano, G., 2017. Mismatch Repair Deficiency as a Predictive Biomarker for Immunotherapy Efficacy. *BioMed Research International*, 2017, pp.1–7.
Voloshanenko, O. et al., 2013. Wnt secretion is required to maintain high levels of Wnt activity in colon cancer cells. *Nature communications*, 4(May), p.2610.
Waaler, J. et al., 2012. A novel tankyrase inhibitor decreases canonical Wnt signaling in colon carcinoma cells and reduces tumor growth in conditional APC mutant mice. *Cancer Research*, 72(11), pp.2822–2832.
Waaler, J. et al., 2011. Novel synthetic antagonists of canonical Wnt signaling inhibit colorectal cancer cell growth. *Cancer Research*, 71(1), pp.197–205.
Wächtershäuser, a, Akoglu, B. & Stein, J., 2001. HMG-CoA reductase inhibitor mevastatin enhances the growth inhibitory effect of butyrate in the colorectal carcinoma cell line Caco-2. *Carcinogenesis*, 22(7), pp.1061–1067.
Waki, H. et al., 2007. The Small Molecule Harmine Is an Antidiabetic Cell-Type-Specific Regulator of PPARγ Expression. *Cell Metabolism*, 5(5), pp.357–370.
Walther, A. et al., 2009. Genetic prognostic and predictive markers in colorectal cancer. *Nature Reviews Cancer*, 9(7), pp.489–499.
Wang, J., Xu, Z. & Zhang, M., 2007. Downregulation of survivin expression and elevation of caspase-3 activity involved in pitavastatin-induced HepG 2 cell apoptosis. *Oncology Reports*, 18(2), pp.383–387.
Wang, M. & Casey, P.J., 2016. Protein prenylation: unique fats make their mark on biology. *Nature Reviews Molecular Cell Biology*, 17(2), pp.110–122.
Wang, X.W. & Zhang, Y.J., 2014. Targeting mTOR network in colorectal cancer therapy. *World Journal of Gastroenterology*, 20(15), pp.4178–4188.
Wang, Y. et al., 2008. Interaction between tumor suppressor adenomatous polyposis coli and topoisomerase IIalpha: implication for the G2/M transition. *Molecular biology of the cell*.
Watanabe, N., Wachi, S. & Fujita, T., 2003. Identification and characterization of BCL-3-binding protein: Implications for transcription and DNA repair or recombination. *Journal of Biological Chemistry*, 278(28), pp.26102–26110.
Wennerberg, K. & Der, C.J., 2004. Rho-family GTPases: it's not only Rac and Rho (and I like it). *Journal of Cell Science*, 117, pp.1301–1312.
Wittrup, A. & Lieberman, J., 2015. Knocking down disease: A progress report on siRNA therapeutics. *Nature Reviews Genetics*, 16(9), pp.543–552.
Wood, W.G. et al., 2013. Statins, Bcl-2, and apoptosis: Cell death or cell protection? In *Molecular Neurobiology*. pp. 308–314.

Wu, X. et al., 2008. Rac1 Activation Controls Nuclear Localization of β-catenin during Canonical Wnt Signaling. *Cell*, 133(2), pp.340–353.
Wu, X., Kriz, A.J. & Sharp, P.A., 2014. Target specificity of the CRISPR-Cas9 system. *Quantitative Biology*, 2(2), pp.59–70.
Yamamoto, Y. & Yamamoto, H., 2015. Enzymatic and non-enzymatic post-translational modifications linking diabetes and heart disease. *Journal of Diabetes Investigation*, 6(1), pp.16–17.
Yan, H. et al., 2016. Low expression of DYRK2 (dual specificity tyrosine phosphorylation regulated kinase 2) correlates with poor prognosis in colorectal cancer. *PLoS ONE*, 11(8), pp.1–18.
Ye, D.Z. & Field, J., 2012. PAK signaling in cancer. *Cellular Logistics*, 2(2), pp.105–116.
Yen, C.S. et al., 2016. Lovastatin causes FaDu hypopharyngeal carcinoma cell death via AMPK-p63-survivin signaling cascade. *Scientific Reports*, 6(April), pp.1–14.
Yoshida, T. et al., 2010. Blockade of Rac1 activity induces G1 cell cycle arrest or apoptosis in breast cancer cells through downregulation of cyclin D1, survivin, and X-linked inhibitor of apoptosis protein. *Molecular cancer therapeutics*, 9(6), pp.1657–1668.
Young, M., Ordonez, L. & Clarke, A.R., 2013. What are the best routes to effectively model human colorectal cancer? *Molecular Oncology*, 7(2), pp.178–189.
Zaytseva, Y.Y. et al., 2012. MTOR inhibitors in cancer therapy. *Cancer Letters*, 319(1), pp.1–7.
Zeineldin, M. & Neufeld, K.L., 2013. Understanding phenotypic variation in rodent models with germline apc mutations. *Cancer Research*, 73(8), pp.2389–2399.
Zeitler, R. et al., 1992. Inhibition of N-acetylglucosamine kinase and N-acetylmannosamine kinase by 3-O-methyl-N-acetyl-D-glucosamine in vitro. *European journal of biochemistry*, 204(3), pp.1165–1168.
Zhang, L. et al., 2016. Selective targeting of mutant adenomatous polyposis coli (APC) in colorectal cancer. *Science Translational Medicine*, 8(361).
Zhang, T. et al., 2001. Evidence that APC regulates survivin expression: A possible mechanism contributing to the stem cell origin of colon cancer. *Cancer Research*, 61(24), pp.8664–8667.
Zhang, X.H. et al., 2015. Pim-2 modulates aerobic glycolysis and energy production during the development of colorectal tumors. *International Journal of Medical Sciences*, 12(6), pp.487–493.
Zhang, Z. et al., 2017. Targeting colon cancer stem cells with novel blood cholesterol drug pitavastatin. *European Review for Medical and Pharmacoogical Sciences*, 21, pp.1226–1233.
Zhong, Y. et al., 2016. Tankyrase Inhibition Causes Reversible Intestinal Toxicity in Mice with a Therapeutic Index < 1. *Toxicologic Pathology*, 44(2), pp.267–278.
Zhu, G. et al., 2012. A Rac1/PAK1 cascade controls β-catenin activation in colon cancer cells. *Oncogene*, 31(8), pp.1001–1012.
Zhu, N. et al., 2004. An alternatively spliced survivin variant is positively regulated by p53 and sensitizes leukemia cells to chemotherapy. *Oncogene*, 23(45), pp.7545–7551.
Zhu, Y. et al., 2013. Deciphering the signaling networks underlying simvastatin-induced apoptosis in human cancer cells: evidence for non-canonical activation of RhoA and Rac1 GTPases. *Cell death & disease*, 4(4), p.e568.
Zhurinsky, J., Shtutman, M. & Ben-Ze'ev, A., 2000. Plakoglobin and beta-catenin: protein interactions, regulation and biological roles. *Journal of cell science*, 113, pp.3127–3139.
Zilberberg, A., Lahav, L. & Rosin-Arbesfeld, R., 2010. Restoration of APC gene function in colorectal cancer cells by aminoglycoside- and macrolide-induced read-through of premature termination codons. *Gut*, 59(4), pp.496–507.

Appendix 1 – siRNA ΔZ scores

Gene Symbol	ΔZ #1	ΔZ #2
AAK1	0.0207	0.4076
AATK	0.3049	0.3148
ABL1	-0.7546	-0.1089
ABL2	1.5950	-0.0745
ACVR1	-0.4410	0.8516
ACVR1B	0.1168	-0.9092
ACVR1C	0.5191	-0.2385
ACVR2	1.1952	0.4685
ACVR2B	0.8114	-0.0706
ACVRL1	-1.8416	-0.1042
ADCK1	1.9246	0.1760
ADCK2	-1.1465	0.1833
ADCK4	-0.2244	1.1683
ADCK5	-0.1157	0.4022
ADK	-0.8548	-0.3839
ADP-GK	-0.0863	0.5113
ADRBK1	-0.5313	-0.4415
ADRBK2	0.1745	-0.1836
AIP1	2.0440	-0.2167
AK1	-1.7381	-0.0093
AK2	1.0797	0.5861
AK3	0.1617	-0.8467
AK3L1	0.6128	0.5407
AK5	0.0804	-0.5688
AK7	2.8852	0.3087
AKT1	-0.0360	0.5634
AKT2	-0.8969	0.1940
AKT3	-0.8157	-0.3387
ALK	-0.3651	-0.2808
ALS2CR2	-0.5948	0.2702
ALS2CR7	1.4414	-0.8302
AMHR2	0.0214	0.7707
ANKK1	-0.3349	-1.6978
ANKRD3	0.9554	1.0115
ARAF1	-0.9947	-0.4194
ARK5	-0.3177	0.1717
ASK	0.7862	1.0378
ATM	-1.6575	1.5452
ATR	-0.0675	0.2176
AURKA	1.0411	-0.4277
AURKB	-1.1576	0.5057
AURKC	0.7281	-1.4502
AXL	1.0691	-1.1434
BAIAP1	-0.9316	0.0545
BCKDK	-0.7754	-1.3950
BCR	-1.2837	-0.6201
BLK	-0.1299	-0.3982
BMP2K	-1.0901	0.4958
BMPR1A	-0.3036	-0.0156
BMPR1B	1.0013	1.0947
BMPR2	-0.6448	-0.1456
BMX	-0.1448	-0.6114
BRAF	-0.1741	0.3854
BRD2	-0.9115	0.1913
BRD3	0.1134	0.2362
BRD4	0.0097	1.4134
BRDT	0.2712	0.2394
BTK	0.9914	-0.4401
BUB1	1.1535	0.3045
BUB1B	-0.2088	-0.9408
C10ORF89	0.8296	0.1969
C14ORF20	-0.2181	0.4831
C7ORF2	1.1502	-0.9487
C9ORF12	1.0822	0.4754
C9ORF96	-0.3216	0.5010
CALM1	-0.1761	-1.7599
CALM2	0.6460	0.5607
CALM3	-2.7097	0.4831
CAMK1	0.1141	0.5504
CAMK1D	0.8515	0.3808
CAMK1G	0.1670	3.0527
CAMK2A	0.4014	0.1848
CAMK2B	-0.1935	-1.8514
CAMK2D	-0.8276	1.8648
CAMK2G	8.2578	0.7788
CAMK4	-0.8978	-0.6048
CAMKIINALPHA	-0.3468	1.0743
CAMKK1	1.3184	-0.0946
CAMKK1	0.5192	0.3201
CAMKK2	2.4682	0.2935
CARKL	-0.9729	-0.3068
CASK	1.5500	1.0916
CCRK	1.2501	0.1994
CDADC1	0.4412	0.7092
CDC2	-0.9477	-0.1360
CDC2L1	0.0532	-0.2128
CDC2L2	1.1667	-0.3800
CDC2L5	0.6710	-0.3242
CDC42BPA	1.4299	-1.2494
CDC42BPB	0.1488	0.5939
CDC7	-1.9995	1.1811
CDK10	-0.2505	0.1314
CDK11	0.8793	0.6134
CDK2	0.4034	0.5871
CDK3	0.5193	0.5577
CDK4	1.2192	1.0595
CDK5	-0.5862	-0.6050
CDK5R1	1.6689	1.0446

CDK5R2	-2.1903	-0.2576
CDK6	0.6172	1.1526
CDK7	-0.6772	-0.3938
CDK8	0.3623	2.0835
CDK9	-0.0305	0.9146
CDKL1	0.1234	0.0743
CDKL2	-0.3403	-1.4356
CDKL3	0.3890	1.0120
CDKL4	-0.4865	1.8375
CDKL5	-0.4491	0.0662
CDKN1A	-0.6112	0.6372
CDKN1B	1.0451	-0.7672
CDKN1C	0.8314	0.7180
CDKN2B	-0.5209	0.3744
CDKN2C	-0.9126	0.8517
CDKN2D	1.7729	1.0600
CERK	-1.3612	0.1829
CHEK1	0.9521	1.4862
CHEK2	0.0836	1.2056
CHKA	-0.3122	0.3581
CHKB	-0.2890	0.6650
CHUK	0.1266	0.8852
CIB2	0.6015	1.9113
CIT	-0.7601	1.4135
CKB	1.2144	-0.9690
CKM	1.6781	-0.3493
CKMT1B	5.5268	0.5229
CKMT2	-1.7247	0.1967
CKS1B	-2.6953	0.4772
CKS2	1.9954	-0.5743
CLK1	0.7243	-1.1949
CLK2	0.6057	0.7622
CLK3	-0.2435	-0.2879
CLK4	-0.4605	-0.2757
COASY	2.1441	0.3017
COL4A3BP	-0.7103	-0.6683
COMMD3	-0.9618	-0.2246
CPNE3	-1.4854	0.4829
CRIM1	1.1896	-1.8044
CRK7	0.2605	-0.9843
CRKL	0.0074	-1.6503
CSF1R	1.5917	0.4552
CSK	-1.9482	-0.5215
CSNK1A1	-1.2462	0.1038
CSNK1A1L	-0.4961	-1.0952
CSNK1D	0.9221	0.9443
CSNK1E	-2.5729	-0.4679
CSNK1G1	-2.3381	0.4222
CSNK1G2	0.7328	0.5733
CSNK1G3	-0.5650	-0.8939
CSNK2A1	-0.8679	0.5954
CSNK2A2	-0.3271	-0.8351
CSNK2B	1.7667	0.2493
DAPK1	1.4826	-0.2079
DAPK2	-0.7558	-0.7508
DAPK3	0.5069	-1.4070
DCAMKL1	2.0263	-0.8903
DCK	0.4990	1.8459
DDR1	-0.2690	-0.0338
DDR2	-1.1659	-1.1110
DGKA	1.1493	-1.0845
DGKB	1.0146	-0.0655
DGKD	0.5455	0.6282
DGKG	-1.8927	-1.5862
DGKH	0.1256	-1.0654
DGKI	-0.0243	-0.7206
DGKK	-1.6827	-0.6996
DGKQ	2.5633	1.3835
DGUOK	-0.1387	-0.8902
DKFZP434C131	-0.5487	-0.4634
DKFZP761P0423	2.1149	1.8044
DLG1	2.4099	-0.7463
DLG2	-0.1246	-0.8630
DLG3	0.1915	-0.6248
DLG4	-0.6804	-2.2348
DMPK	0.0061	-2.2751
DTYMK	1.1569	1.0621
DUSP21	1.8756	-1.3830
DUSTYPK	2.9087	1.5248
DYRK1A	0.0957	-0.0530
DYRK1B	0.8686	1.9135
DYRK2	-2.6865	-1.7969
DYRK3	-0.3056	2.2726
DYRK4	-2.4605	-0.0891
EEF2K	-0.4049	-1.0612
EFNA3	-1.1566	-1.9690
EFNA4	1.0720	2.0711
EFNA5	0.9840	-0.1056
EFNB3	2.2965	-0.6483
EGFR	0.2883	-1.7178
EIF2AK3	3.4591	0.6340
EIF2AK4	0.0493	0.3839
EPHA1	0.7746	0.2111
EPHA10	1.9402	-1.4827
EPHA2	0.8706	0.5747
EPHA3	0.3239	0.1845
EPHA4	-0.2410	0.1299
EPHA5	2.2805	-0.7451
EPHA6	1.2820	0.3529
EPHA7	0.3830	-1.0220
EPHA8	-1.8561	-1.4549
EPHB1	0.8139	0.1038
EPHB2	0.3498	-0.2009
EPHB3	-0.6728	-0.0910
EPHB4	-0.2665	0.4675
EPHB6	-0.9899	0.8936
ERBB2	0.6819	2.3483
ERBB3	-0.7367	-1.2505

ERBB4	0.3196	0.6997
ERK8	7.0267	-1.2375
ERN1	1.6909	1.5773
ERN2	-0.0263	1.0587
ETNK1	-10.4545	0.9367
EXOSC10	-0.4581	0.9206
FASTK	-1.3020	0.4235
FER	-0.9533	0.4039
FES	-0.7756	-0.4263
FGFR1	0.6578	0.2121
FGFR2	-0.7929	-0.7121
FGFR3	-1.4424	-0.8881
FGFR4	-0.1689	0.7127
FGFRL1	0.6983	-0.4342
FGR	0.4852	2.0944
FLJ10761	2.1773	-1.3964
FLJ13052	-0.4805	-0.7147
FLJ23074	1.3183	2.8586
FLJ23356	1.0548	1.1843
FLJ23356	2.2718	-0.0314
FLJ25006	0.2078	0.1477
FLJ32685	0.3422	0.7288
FLJ34389	-1.0803	-0.1108
FLT1	0.2222	0.3075
FLT3	-2.1690	-1.3622
FLT4	-0.3286	-0.5322
FN3K	1.4463	-0.0902
FN3KRP	-2.7146	-1.3204
FRAP1	-2.4170	1.2487
FRDA	-1.7470	-0.3009
FRK	-1.9765	-0.5002
FUK	1.1926	0.2067
FYN	0.3470	-0.7815
GAK	1.1968	1.3860
GALK1	0.7532	-0.7785
GALK2	-0.9196	1.4815
GCK	-0.0608	0.5307
GK	0.3017	2.2365
GK2	-0.2597	-0.1812
GNE	0.0487	-0.5222
GOLGA5	-0.5177	0.7666
GRK1	1.7501	-0.3441
GRK4	-0.2382	1.0811
GRK5	0.2553	1.5986
GRK6	1.5811	0.5113
GRK7	0.3785	-1.3659
GSG2	0.8537	-0.0667
GSK3A	-0.1449	0.6535
GSK3B	-0.8925	-0.1320
GTF2H1	0.3844	0.9356
GUCY2C	-0.4414	0.6049
GUCY2D	0.8047	-0.3544
GUCY2F	-0.0919	2.1656
GUK1	-0.8674	0.1486

HAK	0.0094	0.2019
HCK	3.9743	-0.5492
HIPK1	-3.0275	0.1554
HIPK2	1.3404	0.3132
HIPK3	0.1717	1.1055
HIPK4	0.4998	1.0779
HK1	0.9087	1.8579
HK2	1.9626	-1.7821
HK3	0.5264	0.0874
HRI	-0.4206	0.6330
HSMDPKIN	2.2092	-1.3378
HSPB8	1.4153	-5.1508
HUNK	1.2067	1.2947
HUS1	2.5792	-0.9991
ICK	0.1528	0.0195
IGF1R	1.5653	2.1009
IGF2R	-1.3609	-1.1568
IHPK1	1.3575	1.1626
IHPK2	-1.9821	-1.1357
IHPK3	-0.3587	-0.0650
IKBKAP	0.0428	1.5559
IKBKB	0.3255	0.2937
IKBKE	-0.4098	-1.2371
IKBKG	-0.6995	-0.1837
ILK	-1.7939	0.0013
ILK-2	0.8874	1.6093
INSR	1.2017	0.7668
INSRR	0.4090	-0.6433
IPMK	-0.2008	0.7088
IRAK1	-1.1199	-1.5083
IRAK2	0.1579	0.3657
IRAK3	0.9217	0.3222
IRAK4	-1.7045	-0.3610
ITK	-0.5402	0.1212
ITPK1	-0.7624	-0.0496
ITPKA	-0.6310	-0.7025
ITPKB	0.8553	0.6879
ITPKC	0.4892	0.1205
JAK1	1.0906	1.1155
JAK2	-0.0037	-0.9114
JAK3	-2.2027	-0.4918
JIK	-0.7883	1.1824
KALRN	-0.0988	-0.9417
KCNH2	1.0588	-0.2169
KCNH8	0.1816	1.9249
KDR	-0.1864	0.2464
KHK	-0.9992	-1.5306
KIAA0999	0.3743	-1.5829
KIAA1361	1.3914	-1.3668
KIAA1639	-1.7201	0.7851
KIAA1765	-0.5896	1.2246
KIAA1804	-2.1426	-1.6421
KIAA1811	0.5801	-0.0690
KIAA1811	-0.7282	0.3583

KIAA2002	0.8877	-1.3971
KIT	6.6381	0.2321
KSR	1.3174	-0.5660
KSR2	0.2664	1.5502
KUB3	2.2564	-0.7959
LAK	-0.2482	-1.5811
LATS1	-1.3020	-0.0684
LATS2	-0.3854	0.7198
LCK	0.2586	-0.6286
LIMK1	-0.4854	0.4646
LIMK2	-0.8628	-0.7116
LMTK2	1.0166	1.1331
LMTK3	-0.2492	-0.4022
LOC340156	-0.4589	-0.2159
LOC390226	-0.8583	0.0562
LOC91461	-0.0649	-2.0074
LRRK1	0.2928	-0.2726
LRRK2	0.4383	-0.8842
LTK	0.3384	0.5836
LYK5	-1.4045	0.3597
LYN	-2.1283	1.4570
MAGI-3	-0.2466	-0.6777
MAK	0.3700	1.0239
MAP2K1	-0.2432	0.4944
MAP2K2	-0.4127	0.5085
MAP2K3	-1.7023	0.4875
MAP2K4	-1.1317	-0.5462
MAP2K5	-0.5116	-1.8713
MAP2K6	-1.2467	-0.3892
MAP2K7	-0.6101	0.6193
MAP3K1	0.0433	0.7335
MAP3K10	-0.8687	0.1131
MAP3K11	-1.2710	-0.4635
MAP3K12	-1.9726	-0.5550
MAP3K13	-3.0618	0.6145
MAP3K14	1.1868	0.8845
MAP3K15	-1.5571	-1.2711
MAP3K2	-1.7993	-0.9251
MAP3K3	-0.0604	0.0051
MAP3K4	-0.2423	-0.2288
MAP3K5	-0.3781	-1.4386
MAP3K6	1.5549	0.4712
MAP3K7	2.6330	2.6637
MAP3K7IP1	1.0347	0.3978
MAP3K8	0.2184	0.3208
MAP3K9	2.3233	0.1454
MAP4K1	0.7714	1.0394
MAP4K2	0.2974	-0.5443
MAP4K3	0.0520	-0.1817
MAP4K4	-0.1327	0.7893
MAP4K5	2.4842	2.9439
MAPK1	-0.4575	-0.8857
MAPK10	0.3628	-0.1741
MAPK11	-0.3230	0.4828
MAPK12	0.5198	-0.1457
MAPK13	-0.0350	0.2202
MAPK14	0.1559	0.8594
MAPK3	1.2612	-1.3566
MAPK4	0.2409	-0.9093
MAPK6	-0.3227	0.4396
MAPK7	1.7070	-0.5148
MAPK8	-0.4711	0.3552
MAPK9	-0.5651	0.2768
MAPKAPK2	0.3644	0.4042
MAPKAPK3	0.0880	1.3017
MAPKAPK5	-0.3430	0.4108
MARK1	-1.0412	0.1202
MARK2	-0.8574	-2.8960
MARK3	-0.5679	-0.0754
MARK4	-0.1373	-0.6315
MAST2	0.5411	0.1617
MAST3	-0.3265	0.3412
MAST4	0.2852	1.0901
MASTL	0.6393	0.3473
MATK	-0.1617	0.3711
MELK	-1.2872	-0.7377
MERTK	-0.6920	0.1069
MET	0.0568	0.3094
MGC16169	0.5880	0.1723
MGC42105	-0.2167	0.1701
MGC45428	-0.6582	1.9678
MGC4796	-0.1363	0.3476
MGC4796	-0.1017	-0.4539
MGC8407	-0.9706	-1.5554
MIDORI	0.9201	1.4060
MINK	0.9079	-2.1200
MKNK1	0.8100	-0.4861
MKNK2	-0.7327	0.3316
MLCK	-0.1070	-1.5980
MOS	0.5079	0.0397
MPP1	0.0378	-1.9078
MPP2	0.0473	1.6420
MPP3	-0.6441	2.6564
MST1R	-0.2839	-0.0193
MULK	-1.4537	-1.1230
MUSK	0.4938	0.9801
MVK	-0.4954	-0.8051
MYLK	1.1320	0.7618
MYLK2	3.5947	-1.0569
MYO3A	0.5057	-0.2484
MYO3B	-0.5447	-2.4516
N4BP2	-1.7935	-1.2834
NAGK	-1.0286	-1.8705
NEK1	-0.1733	-1.5400
NEK11	0.8944	-0.8181
NEK2	0.6675	-0.0614
NEK3	-1.2111	-0.7367
NEK4	-0.6918	-1.0361

NEK5	-0.8753	-1.3336
NEK6	-1.2071	-0.9997
NEK7	0.6020	0.5379
NEK8	-1.8003	1.7785
NEK9	-1.5770	-0.0211
NLK	-0.0596	-2.0491
NME1	1.0582	0.2157
NME2	-0.8374	0.3331
NME3	1.0347	-0.8854
NME4	0.3794	0.2626
NME5	0.1361	-1.1809
NME6	-0.1284	0.4566
NME7	-1.0506	-0.4834
NPR2	1.4909	-0.6280
NRBP	-0.9525	-0.9017
NRBP2	-0.6530	-0.3006
NRK	-0.1086	-0.5335
NTRK1	-0.1838	0.7734
NTRK2	1.0145	0.1352
NTRK3	0.7250	-0.4339
NUCKS	-0.8536	-0.9962
NUP62	1.3292	-1.1177
NYD-SP25	-1.6747	-0.6935
OSR1	0.7528	-0.2362
P101-PI3K	-0.9790	-0.2266
PACE-1	0.2287	-0.0455
PACSIN1	0.2379	1.2284
PAK1	-1.1203	1.6218
PAK2	-0.8608	-0.7963
PAK3	-0.4132	-0.7641
PAK4	0.8611	-0.1519
PAK6	0.8155	1.3375
PAK7	-0.1931	1.1663
PANK1	-0.8176	1.0309
PANK2	1.3281	1.1582
PANK3	-0.0175	0.1639
PANK4	-0.3686	-0.6018
PAPSS1	-1.5036	-0.8645
PAPSS2	-0.3550	-0.1693
PASK	-0.9947	0.2214
PCK1	0.9022	0.0575
PCK2	0.7154	0.1014
PCTK1	1.0163	-0.4656
PCTK2	1.0366	0.4460
PCTK3	-1.7213	0.3160
PDGFRA	0.1290	-0.2241
PDGFRB	1.0821	-0.7171
PDGFRL	5.6960	-0.7228
PDIK1L	0.8883	-1.2319
PDK1	-0.8108	-0.3888
PDK2	-1.0857	0.2103
PDK3	-1.2320	-0.0567
PDK4	0.2342	0.6877
PDPK1	0.7128	0.4466
PDXK	0.4941	-2.8593
PFKFB1	-0.8748	-0.6342
PFKFB2	0.0368	-0.6147
PFKFB3	-0.4701	-0.0234
PFKFB4	-1.2981	0.1547
PFKL	-3.2312	0.3997
PFKM	2.6767	-0.6705
PFKP	-1.0121	-0.1843
PFTK1	2.4085	-1.0355
PGK1	0.4904	0.4655
PGK2	-0.1516	0.2207
PHKA1	0.9630	1.1765
PHKA2	-1.9557	-0.1824
PHKB	5.4199	-0.6406
PHKG1	-3.7328	0.4466
PHKG2	1.2455	0.3205
PI4K2B	0.5650	1.7880
PI4KII	2.3102	-1.9592
PIK3C2A	-0.9598	0.4942
PIK3C2B	0.2713	0.7196
PIK3C2G	2.0487	-1.8810
PIK3C3	1.0319	1.3597
PIK3CA	-1.1422	-0.6734
PIK3CB	-0.9178	-0.9784
PIK3CD	0.7888	1.0357
PIK3CG	1.0736	0.4576
PIK3R1	-0.3238	1.2285
PIK3R2	0.4607	-0.6189
PIK3R3	0.0943	-2.4155
PIK3R4	0.5091	0.4358
PIK4CA	1.1548	0.9964
PIK4CB	0.3896	-1.6892
PIM1	-2.2019	0.4096
PIM2	-1.8761	-0.4296
PIM3	-0.1236	1.2530
PINK1	0.6689	1.0958
PIP5K1A	-0.7568	-0.5562
PIP5K1B	-0.7937	-0.5153
PIP5K1C	-0.3878	0.0205
PIP5K2A	0.5934	1.8333
PIP5K2B	1.4990	0.3749
PIP5K2C	-0.9922	0.7276
PIP5K3	0.0034	-0.6753
PIP5KL1	-1.2305	0.7087
PKIA	0.6995	0.3346
PKIB	-0.3679	-1.6227
PKLR	-0.4113	0.5856
PKM2	-1.2578	2.2023
PKMYT1	2.4753	0.0705
PKN3	1.5403	-0.2634
PLK1	-2.7428	0.2187
PLK2	1.1262	-1.3528
PLK3	-0.3758	0.5385
PLK4	-0.2968	0.2823

PMVK	0.3505	-0.2731
PNCK	-0.1162	0.6384
PNKP	-0.1380	1.2622
PRKAA1	-1.4281	-0.7928
PRKAA2	0.4065	-0.3820
PRKAB1	1.4815	0.0186
PRKAB2	0.8994	-0.1919
PRKACA	-0.5758	-0.6679
PRKACB	-0.4413	-0.3245
PRKACG	0.0066	-0.1892
PRKAG1	0.7737	-0.9181
PRKAG2	-0.5232	0.9881
PRKAG3	-3.8244	2.1839
PRKAR1A	-0.7587	0.3556
PRKAR1B	0.2752	-0.3626
PRKAR2A	-0.5415	-0.9677
PRKAR2B	0.6291	0.7424
PRKCA	-0.4827	0.5311
PRKCB1	1.9301	0.0904
PRKCD	1.6623	0.4243
PRKCE	0.7037	-0.8760
PRKCG	1.0195	0.1554
PRKCH	-0.4176	-0.7493
PRKCI	-1.5157	-0.2810
PRKCL1	-0.7923	1.0863
PRKCL2	0.4806	-0.3230
PRKCM	-0.0690	1.4172
PRKCN	0.1708	0.5465
PRKCQ	-0.0676	1.1903
PRKCSH	-0.3696	0.1120
PRKCZ	0.9698	-0.9832
PRKD2	1.8058	0.1133
PRKDC	1.0194	-0.6567
PRKG1	1.7075	0.5131
PRKG2	0.0119	2.6811
PRKR	-0.0997	-0.1799
PRKWNK1	2.0763	-2.2575
PRKWNK2	0.0209	-0.5733
PRKWNK3	0.8691	1.5878
PRKX	-1.0074	-0.5819
PRKY	-0.5524	0.5581
PRPF4B	0.8712	-0.0439
PRPS1	0.1941	-1.0452
PRPS1L1	-0.2898	-1.5210
PRPS2	-0.2139	-0.9939
PSKH1	1.1716	-0.3818
PSKH2	-0.7950	-0.7524
PTK2	-0.3297	-0.7850
PTK2B	-0.0487	0.2569
PTK6	-1.9457	1.2212
PTK7	2.0483	1.0636
PTK9	0.1547	-1.0832
PTK9L	-2.2082	1.3600
PXK	0.3872	1.6570

PYCS	0.2663	0.6687
RAF1	-0.3532	0.6189
RAGE	-0.6500	0.3258
RBKS	-0.0599	0.4125
RELA	-0.5942	1.4561
RET	-0.7233	-0.9937
RFK	0.5473	0.1680
RFP	-1.4112	0.3903
RIOK1	-1.2531	0.2917
RIOK2	-1.2395	0.5149
RIOK3	-0.0710	-0.1895
RIPK1	-1.7215	-0.4865
RIPK2	-4.4636	0.8420
RIPK3	-2.2029	-0.4743
RNASEL	0.6799	1.4997
ROCK1	-0.2381	-1.4065
ROCK2	0.5624	0.8203
ROR1	1.1187	0.1640
ROR2	0.5591	-0.9261
ROS1	1.3953	-0.0931
RP6-213H19.1	-0.7374	-0.4201
RPS6KA1	0.6788	-0.4344
RPS6KA2	0.7966	1.4809
RPS6KA3	-1.7807	-0.8217
RPS6KA4	-0.4628	-0.1861
RPS6KA5	0.3865	1.2880
RPS6KA6	0.6253	0.3951
RPS6KB1	-0.2058	1.1139
RPS6KB2	-1.7411	0.4953
RPS6KC1	-1.4364	-0.1045
RPS6KL1	-0.0455	-2.0881
RYK	-2.8169	0.2582
SAST	-1.5256	0.8837
SBK1	-0.6348	1.1424
SCAP1	-0.3770	2.5630
SCYL1	1.4288	-0.1774
SGK	0.0632	-0.1660
SGK2	-1.7762	-0.3188
SGKL	-1.1889	-1.6646
SIK2	-0.2741	0.9159
SLK	2.7727	0.2067
SMG1	-1.6225	-1.3109
SNARK	0.2147	-0.2921
SNF1LK	-0.8404	-1.2999
SNRK	1.5299	-0.4081
SPEG	0.1440	0.2671
SPHK1	-0.4277	1.0565
SPHK2	0.2414	0.5684
SRC	0.2303	-0.8214
SRMS	-0.6614	0.5002
SRP72	0.8813	0.4873
SRPK1	0.2604	0.5481
SRPK2	0.5908	0.3593
SSTK	0.3041	0.4947

SSTK	-0.7924	-1.7051
STK10	2.4068	-1.1462
STK11	0.4554	-0.0515
STK16	2.0511	2.9406
STK17A	-0.5013	0.2504
STK17B	-0.4423	-0.5595
STK19	2.0996	-1.0614
STK22B	0.5263	1.5188
STK22C	-2.0392	0.1098
STK22D	0.5985	1.9819
STK22D	0.5391	1.9944
STK23	0.3854	2.4375
STK24	-0.5251	0.1933
STK25	-0.2022	1.7538
STK29	1.8053	1.1007
STK3	-0.1324	0.9132
STK31	0.3458	-0.4115
STK32A	-0.9164	0.8710
STK32B	2.8962	0.1802
STK32C	0.3105	0.4587
STK33	1.0405	-1.3796
STK35	0.1390	-0.7244
STK36	0.7367	-1.0666
STK38	0.1468	0.2513
STK38L	-0.7912	-0.0184
STK39	1.0991	-1.7949
STK4	0.1703	1.5708
STYK1	1.2473	1.3938
SYK	-1.2748	-0.6235
TAF1	1.5647	0.1588
TAF1L	0.3473	1.2599
TAO1	1.4512	1.7873
TBK1	1.3228	1.2877
TEC	-0.8803	0.6078
TEK	-0.0192	0.1425
TESK1	-0.2433	-0.0261
TESK2	-0.3709	0.2435
TEX14	0.9597	0.4359
TGFBR1	-2.6567	0.2089
TGFBR2	0.0587	0.2107
TGFBR3	-1.0196	-0.1687
THNSL1	0.1994	-1.7096
TJP2	-0.0818	-0.0856
TK2	-0.2244	-1.1718
TLK1	0.1550	0.6415
TLK2	-0.3280	-0.4490
TNIK	-1.8187	-0.1865
TNK1	-3.2477	0.4269
TNK2	0.2206	1.6887
TNNI3K	1.4093	0.0892
TOPK	1.7739	-0.1181
TP53RK	0.1992	-0.7268
TPK1	0.0194	-0.1080
TRIB1	0.0572	-1.6484
TRIB2	-0.0784	-0.6261
TRIB3	0.4693	0.2263
TRIO	-2.4375	0.4341
TRPM6	-0.6779	-0.3872
TRPM7	0.7709	0.1185
TSKS	-0.7309	-1.3108
TTBK1	2.5677	2.5737
TTBK2	-1.4695	-0.2068
TTK	-1.9768	0.3898
TYK2	-0.1172	-0.5141
TYRO3	-0.2307	-1.4299
UCK1	-0.9025	0.2666
UHMK1	-0.1244	-0.6012
ULK1	-1.0577	-1.2222
ULK2	1.0027	-0.2804
ULK4	0.4486	0.2965
UMP-CMPK	-0.0100	0.6638
UMPK	2.8611	0.6725
URKL1	2.3885	1.1394
VRK1	0.3108	0.3542
VRK2	-2.2871	0.0497
VRK3	0.1525	0.4058
WEE1	1.0142	0.6812
WNK4	-0.2157	0.3298
XYLB	-1.3166	-1.1431
YES1	1.3790	-0.6388
ZAK	0.1750	0.9461
ZAP70	0.6145	-0.5348

Appendix 2 – Compound screen Z scores

	Z SCORES RKO 7_1			Z SCORES RKO 2_36		
GeneSymbol	**REP1**	**REP2**	**REP3**	**REP1**	**REP2**	**REP3**
Procaine (Novocaine) HCl	0.1622	0.2126	0.3561	0.3297	0.9715	0.2202
(+,-)-Octopamine HCl	0.4362	0.8509	0.8462	0.8023	0.6781	0.9496
(R)-(+)-Atenolol	-0.6322	-0.0523	-0.4164	-0.3405	-0.1572	-0.0437
(R)-baclofen	-0.1492	0.7536	1.8347	0.2110	0.0052	0.1413
10-DAB (10-Deacetylbaccatin)	-11.8684	-12.3488	-14.6504	-7.6914	-6.9877	-10.3499
1-Hexadecanol	-1.4850	-0.1672	-1.5434	-0.3510	-0.4106	-1.3155
2-Methoxyestradiol	-14.8565	-18.6584	-19.8087	-10.7349	-12.7432	-15.3284
2-Thiouracil	-1.3519	-1.1993	-0.9526	-0.4600	-0.4455	-1.2402
5-Aminolevulinic acid hydrochloride	-1.1641	-0.7847	-0.2418	-1.4877	-0.4563	-1.5119
9-Aminoacridine	-15.0808	-19.8020	-21.1082	-10.4683	-12.2624	-15.1969
Abacavir sulfate	-0.3080	0.0618	-0.4497	0.3209	0.1792	0.2868
Abiraterone (CB-7598)	0.5831	1.2705	0.6821	1.2603	1.1222	0.7426
Abiraterone Acetate (CB7630)	0.0385	0.0264	-0.5928	0.4249	-0.4249	-0.3054
Abitrexate (Methotrexate)	-5.5437	-7.7046	-8.9878	-1.0992	-2.7438	-4.0782
Acadesine	0.4101	1.7371	0.6392	0.2597	1.1409	0.5914
Acarbose	0.5912	0.9156	1.0395	-0.3101	-0.8517	-0.0969
Acebutolol HCl	-0.6357	-0.0330	-0.6009	-0.2347	-0.8134	-1.3998
Aceclidine HCl	-0.5370	0.3603	-0.4744	-0.6078	-0.7930	-0.2091
Acemetacin (Emflex)	0.8875	0.3692	0.7107	1.0501	0.9640	1.2578
Acetanilide (Antifebrin)	0.0597	-0.3097	0.4639	-0.3210	-0.6579	0.5325
Acetarsone	0.7822	0.0321	0.8144	0.4100	0.0563	-0.0140
Acetylcholine chloride	-0.0820	0.7285	0.9047	0.7654	1.0519	0.7979
Acetylcysteine	-1.1468	-1.0936	-1.2925	-13.0043	-1.0006	-1.2638
Acipimox	0.5132	0.4063	0.9772	0.7616	1.4586	0.7245
Acitretin	0.4541	-0.2480	0.0455	1.2333	0.7277	0.2863
Aclidinium Bromide	-0.2347	-1.1031	-1.3025	-0.1361	-1.0287	-1.0134
Acyclovir (Aciclovir)	0.9704	-0.0295	0.9722	0.6374	1.1131	0.8796
Adapalene	0.6424	0.4383	1.4114	0.2444	-0.3337	0.0969
Adefovir Dipivoxil (Preveon, Hepsera)	-10.9209	0.6208	0.5510	-6.4343	0.7507	0.7109
Adenine	-1.1853	1.0522	0.5671	0.8493	1.1070	0.1621
Adenine hydrochloride	0.5153	1.5205	1.1319	0.8072	1.2709	0.9076
Adenine sulfate	0.8565	2.0071	1.9036	0.7747	1.3605	0.9250
Adenosine (Adenocard)	-0.4718	-0.0488	-0.2486	-1.4550	-0.7427	-1.0150
Adiphenine HCl	0.3781	-0.0251	-1.3218	-0.2236	0.0280	-0.8584
Adrenalone HCl	0.3460	0.7675	0.8432	0.8276	0.3257	0.2780
Adrucil (Fluorouracil)	-2.2657	-5.6376	-5.7841	0.1820	-0.7781	-2.2091
Afatinib (BIBW2992)	-9.2963	-8.6494	-10.0390	-0.7261	-2.0365	-5.7162
Agomelatine	-0.3363	0.2980	1.6004	1.0286	0.0763	0.7933
Albendazole (Albenza)	-2.5687	-4.1677	-5.8641	0.1165	-0.4714	-1.8938
Albendazole Oxide (Ricobendazole)	-3.0051	-6.7886	-7.4202	0.2238	-0.8514	-1.5589
Alendronate (Fosamax)	-0.4991	-0.7247	-0.8065	0.0463	-0.3621	-0.0833
Alexidine HCl	-16.3647	-21.3144	-22.6560	-11.6274	-13.1197	-16.5475
Alfacalcidol	-0.2018	1.1120	0.9843	2.0265	1.4753	0.4263
Alfuzosin hydrochloride (Uroxatral)	-2.5164	-0.3379	-3.2215	-13.8171	-1.3444	-3.4075

Alibendol	-0.9881	-0.7777	-0.6899	-0.9472	-2.3613	-1.0425
Aliskiren hemifumarate	0.3933	0.7944	0.3458	0.6951	0.3217	0.6589
Allopurinol (Zyloprim)	-0.3354	0.4044	0.5186	0.5383	-0.4677	0.4346
Allylthiourea	-0.2604	-0.7577	-0.2124	-1.1681	-2.3783	-1.4432
Almotriptan malate (Axert)	-1.5555	-0.6840	-1.0730	-0.2085	-0.5024	-1.1885
Alprostadil (Caverject)	0.0671	0.8635	0.6324	1.7225	1.3230	0.7021
Altrenogest	-0.3685	-0.5875	0.0943	0.4543	0.6823	0.4129
Altretamine (Hexalen)	-26.4116	-2.2085	-2.5737	-13.6884	-0.5098	-2.7732
Alverine Citrate	-1.2916	-2.4022	-2.0013	-1.2357	-1.5627	-2.1973
Amantadine hydrochloride (Symmetrel)	0.5026	0.4594	0.5816	-0.6634	-0.6578	0.0309
Ambrisentan	-0.7509	0.0819	-0.7079	0.5620	0.1472	-0.2661
Amfebutamone (Bupropion)	-0.3516	0.1298	0.4784	-0.9589	-0.3350	-0.4247
Amfenac Sodium (monohydrate)	-0.5167	-0.3967	-1.5483	-0.6098	-0.1944	-1.8644
AMG-073 HCl (Cinacalcet hydrochloride)	-11.2186	-18.5960	-18.6991	-6.9546	-5.3218	-9.6591
Amidopyrine	-0.4756	0.5461	-0.4670	-0.1816	-0.6751	-0.1716
Amikacin hydrate	-0.5665	-0.2029	-0.6778	-0.8938	-0.4201	-0.0102
Amikacin sulfate	0.0712	-0.0976	-0.8812	-0.4337	-0.3530	-1.2693
Amiloride hydrochloride (Midamor)	0.2137	-0.0094	0.3826	0.2273	1.0703	0.8258
Amiloride hydrochloride dihydrate	-0.3557	-0.9717	-0.1406	-0.9610	-1.0657	-0.7497
Aminocaproic acid (Amicar)	0.8813	0.5535	0.2434	1.3006	1.0709	0.4048
Aminoglutethimide (Cytadren)	0.8896	0.0787	0.4830	0.6839	0.8742	0.1734
Aminophylline (Truphylline)	0.5672	1.0487	0.0774	0.2875	1.0610	0.3098
Aminosalicylate sodium	-0.5021	0.9246	1.6394	1.2725	0.8469	0.8175
Aminothiazole	-0.3272	0.1631	-0.6718	0.6295	0.1927	0.3206
Amiodarone HCl	-8.5381	-4.3546	-13.7941	-4.4164	-5.8016	-12.0128
Amisulpride	-23.0502	-1.2017	-2.3377	-0.5580	0.3489	-1.3871
Amitriptyline HCl	-1.2577	-2.4324	-1.5152	-0.2141	-0.0052	-0.7310
Amlodipine (Norvasc)	-10.6335	-19.8944	-21.0124	-4.6819	-8.1867	-15.0025
Amlodipine besylate (Norvasc)	-6.9964	-19.6254	-21.1197	-4.1129	-9.7419	-14.5436
Ammonium Glycyrrhizinate (AMGZ)	0.5410	-0.3359	0.2755	0.0483	-0.0080	0.1053
Amorolfine Hydrochloride	0.4086	0.9855	0.2827	0.7631	0.7892	0.5917
Amoxapine	-0.5736	-1.3655	-1.2410	0.0283	-0.6083	-0.5763
Amoxicillin (Amoxycillin)	0.2455	-0.9756	-0.8445	-0.0062	-0.4878	-0.4698
Amoxicillin sodium (Amox)	0.6928	-0.5082	-2.1284	-0.0925	-0.3277	-1.5475
Amphotericin B (Abelcet)	0.2271	0.1737	-0.2007	-0.3009	-0.6638	-0.4662
Ampicillin sodium	0.6951	1.0230	0.8708	0.8396	0.5204	0.8924
Ampicillin Trihydrate	0.0547	-0.9027	0.3224	-1.2201	-0.8091	-0.3447
Ampiroxicam	0.3923	0.0714	-0.4615	-0.4737	-1.1870	-1.1566
Amprenavir (Agenerase)	-0.7384	-0.9926	-0.9506	0.6086	-0.3532	-1.1398
Amprolium HCl	1.3163	1.0900	0.1086	-0.2445	0.0095	-0.3281
Anagrelide HCl	1.0244	0.9992	1.0252	1.3012	1.0276	1.2388
Anastrozole	1.3838	0.0371	1.4620	1.9129	1.0007	1.4883
Aniracetam	-17.2209	-0.3112	-1.4136	0.2435	1.0281	-0.4755
Anisindione	1.1662	0.8214	0.3012	0.4044	0.4238	0.5767
Anisotropine Methylbromide	0.5657	0.7490	0.2371	0.6946	0.4433	0.3073
Antazoline HCl	0.5036	0.7304	0.1930	0.6767	0.4853	0.4065
Antipyrine	1.3186	1.2911	1.6409	2.0437	1.4162	2.0758
Apatinib (YN968D1)	-1.4183	-0.1333	-0.0223	0.1994	0.0240	0.1765
Apixaban	0.1090	0.7317	-8.2090	1.6859	0.7888	-1.0410
Aprepitant (MK-0869)	-15.5215	-7.4737	-9.5913	0.8798	-0.0953	-1.4651
Arbidol HCl	-3.1443	-1.6331	-0.2293	0.1403	0.1553	0.4924

Arecoline	-4.6997	1.1677	1.1248	1.5551	1.3420	1.6717
Argatroban	-17.0285	0.4485	-0.2213	-0.2675	0.1893	-0.7880
Aripiprazole (Abilify)	0.9632	-0.5659	-0.0068	-0.1783	-0.4914	0.2724
Artemether (SM-224)	-0.1796	0.0963	-0.5886	0.7267	0.4410	-0.1988
Artemisinin	0.2011	-1.0948	-0.6947	-0.1262	0.6795	-1.0775
Articaine HCl	-0.3517	0.7316	1.3296	0.9214	0.8021	1.0766
Asenapine	-2.1037	-1.7687	-0.7548	1.0998	0.8056	-1.1846
Aspartame	0.2524	0.7893	0.4018	0.3614	0.4334	0.8184
Aspirin (Acetylsalicylic acid)	0.1975	-0.0040	-0.7291	-0.1647	-1.0174	-1.0409
Atazanavir sulfate	0.7235	-0.4014	-0.1638	-0.2894	0.6838	0.6756
Atomoxetine HCl	0.5512	0.2650	0.4023	0.8346	0.3823	0.8568
Atorvastatin calcium (Lipitor)	-1.8403	-4.4027	-4.9718	-6.7340	-7.9268	-11.5011
Atovaquone (Atavaquone)	1.0841	0.2487	0.2335	-0.0433	0.0905	0.0187
ATP (Adenosine-Triphosphate)	0.6305	1.0177	0.7026	0.6710	0.7336	0.9128
Atracurium besylate	-0.8878	0.8314	-0.4724	0.1684	0.9936	0.7161
Atropine	-0.4338	-0.7118	-1.0427	0.9415	0.6370	-0.0931
Auranofin	-11.9213	-19.6144	-20.8104	-10.5175	-11.9832	-14.9399
Avanafil	-1.2640	-2.7880	-1.8648	-0.7150	-0.0381	-2.8816
Avobenzone (Parsol 1789)	0.3450	-0.1940	-0.2738	-0.3756	-0.8691	-0.2398
Axitinib	-5.0412	-1.5133	-4.5447	-2.1244	-2.9112	-3.1033
Azacitidine (Vidaza)	-2.0323	0.1252	1.5655	-1.4760	0.7721	0.5765
Azacyclonol	0.4158	0.1527	0.3302	0.4541	-0.0807	0.7268
Azaguanine-8	1.0503	0.6482	0.3212	0.8159	0.7647	0.8307
Azaperone	-15.9859	-1.9654	-0.8245	-0.0124	-0.9418	-0.2712
Azasetron HCl (Y-25130)	0.7879	0.1787	0.3226	0.7244	0.0785	0.8945
Azatadine dimaleate	-0.4322	0.3265	0.2611	0.3441	-0.0470	0.6155
Azathioprine (Azasan, Imuran)	-3.9787	-5.6306	-6.6368	-1.4592	-2.2611	-3.9012
Azelastine hydrochloride (Astelin)	-18.2738	-5.7539	-9.7728	-3.1137	-3.7709	-11.7123
Azelnidipine	-4.0751	-0.6533	-0.0947	-0.6408	-1.3856	-1.4235
Azilsartan (TAK-536)	-0.2783	-0.1319	-0.1096	-0.7501	-1.2374	-0.1082
Azilsartan Medoxomil (TAK-491)	0.4833	-0.0284	-0.5004	-0.7877	-0.4577	-0.4977
Azithromycin (Zithromax)	0.3132	0.7359	-0.2038	0.2952	0.6940	0.3205
Azithromycin Dihydrate	-0.5347	-0.7108	0.2148	-1.3544	-0.0107	-0.8576
Azlocillin sodium salt	0.9173	0.5548	1.3065	1.0136	0.4443	0.9811
Aztreonam (Azactam, Cayston)	0.7514	1.0940	0.8576	1.9134	0.9779	0.9716
Bacitracin	-15.3874	-0.0042	0.6793	-0.5144	-0.1807	-0.2315
Bacitracin zinc	1.3587	0.0254	0.7085	-0.0016	0.5818	0.6908
Balofloxacin	-0.1063	0.1123	-0.3127	-0.9460	-1.9078	-0.4847
Bazedoxifene HCl	-11.7223	-14.2629	-15.4713	-7.1863	-8.2855	-10.5535
Beclomethasone dipropionate	-0.0937	-5.1421	-0.9349	0.7269	0.2647	-1.2617
Bekanamycin	0.5475	-0.1579	0.0842	0.4042	0.1242	-0.7137
Bemegride	0.2242	0.7300	-0.4612	-0.0480	0.2731	-0.1165
Benazepril hydrochloride	1.2501	0.6455	0.8567	0.0469	0.6463	-0.2662
Bendamustine HCL	1.0241	0.8120	2.2462	1.5909	0.3945	1.6075
Bendroflumethiazide	1.0957	0.3762	0.8693	0.7951	-0.0503	-0.0060
Benfotiamine	-0.9029	-0.6250	-0.8251	0.1019	-1.6081	-0.5223
Benidipine hydrochloride	-0.2596	0.2164	-0.8505	0.6644	1.3400	-0.5572
Benserazide	0.1026	0.5097	0.3264	-1.6193	-0.9367	-0.2939
Bentiromide	1.0237	-0.2159	0.6929	0.5384	-0.0690	0.0115
Benzbromarone	-1.0030	-1.5032	-0.4415	-0.6177	-1.0678	0.1634
Benzethonium chloride	-9.4001	-9.6733	-15.9560	-6.6547	-4.1505	-12.5931
Benzocaine	-0.3476	-0.0978	-0.2864	0.3338	0.1927	-0.3358
Benzoic acid	-0.3156	0.1974	-0.7571	-0.1078	0.9964	-0.0208

Benzthiazide	1.4534	0.6252	0.7549	0.4016	0.3416	0.6676
Benztropine mesylate	-3.1106	-5.3744	-4.8403	-0.7398	-1.8386	-3.2015
Benzydamine Hydrochloride	-0.4857	-0.2921	-0.5285	1.1413	0.9106	0.3865
Benzylpenicillin sodium	-0.5079	-0.2399	-1.1363	-0.2399	-0.0720	-1.3378
Bephenium Hydroxynaphthoate	0.0063	-0.3773	0.0551	-0.2142	-0.7193	-0.7567
Bepotastine Besilate	-1.2736	-3.3231	-1.4632	-0.1306	-1.4115	-1.6305
Bergapten	1.2264	-0.3187	0.1775	0.5769	0.2271	-0.1646
Besifloxacin HCl (Besivance)	-0.1722	-0.7185	-0.9382	-0.3444	-0.5818	-0.7243
Beta Carotene	-1.3069	0.0595	0.7472	-0.2205	-1.8058	-0.4618
Betahistine 2HCl	1.0257	0.7021	0.3098	0.9918	0.3742	1.0439
Betamethasone (Celestone)	-0.6173	-1.4303	-1.2306	-14.7850	-0.3859	-0.9891
Betamethasone Dipropionate (Diprolene)	-0.2511	0.0361	0.5127	1.4213	1.1927	0.4374
Betamethasone valerate (Betnovate)	0.8202	1.1911	-0.1221	1.7378	0.9324	0.7040
Betamipron	0.9932	1.4000	0.8373	1.1649	0.7208	0.9718
Betapar (Meprednisone)	0.0502	0.8733	0.1944	1.8527	1.1645	0.5789
Betaxolol (Betoptic)	0.7473	-0.3756	0.1860	0.2213	0.3630	0.4941
Betaxolol hydrochloride (Betoptic)	0.9187	1.0502	0.5215	0.3684	1.3397	0.4890
Bethanechol chloride	-0.1874	-0.4444	-0.7254	-1.2923	-0.0832	-1.4729
Bexarotene	0.4256	-0.3386	-0.3653	0.9948	0.2988	0.2122
Bextra (valdecoxib)	0.6376	1.7926	1.3902	1.2267	1.0135	0.8738
Bezafibrate	-0.9145	-0.7594	-0.0997	-0.4516	-0.3368	0.4262
Biapenem	0.5106	-0.0715	0.2831	1.6231	0.9094	0.1514
BIBR 953 (Dabigatran etexilate, Pradaxa)	0.6231	0.6672	0.1870	0.6856	0.0753	0.7024
BIBR-1048 (Dabigatran)	-4.0837	-1.3184	-1.2459	0.0066	-0.9088	-1.4864
Bicalutamide (Casodex)	0.0984	0.4426	1.7718	2.0501	0.9293	1.3733
Bifonazole	-0.2931	0.1244	0.2084	0.1424	-0.1974	0.1930
Bimatoprost	0.3782	0.2238	0.1748	-0.0816	-0.6560	0.3945
Bindarit	-1.5449	-0.2418	-1.1475	-0.5110	-0.9706	-1.5976
Biotin (Vitamin B7)	0.2845	0.6993	0.7658	0.4604	0.7628	0.8960
Biperiden HCl	-6.7443	-1.0175	-1.8572	-0.6064	0.1999	-1.8864
Bisacodyl	-2.7901	-0.3528	-0.6271	-0.1508	0.1534	-0.1838
Bismuth Subcitrate Potassium	0.7206	-0.0400	-1.1579	0.0849	-0.5390	-0.0098
Bismuth Subsalicylate	-1.0140	-0.0498	0.0019	-0.4963	-0.6468	-1.3781
Bisoprolol	1.8932	0.2180	1.2923	1.0538	0.7732	1.8257
Bleomycin sulfate	-4.7169	-7.2017	-4.7086	-2.3153	-3.9043	-2.2969
Blonanserin (Lonasen)	-0.2919	0.9803	0.1557	0.7983	0.4444	0.5770
Bortezomib (Velcade)	-18.9038	-20.9956	-20.2880	-9.8179	-11.0859	-14.6831
Bosutinib (SKI-606)	-19.7269	-1.3244	-1.6782	0.3885	0.7850	0.3089
Brinzolamide	1.1308	1.2435	0.4384	0.7979	0.1020	0.7634
Bromhexine HCl	-1.0254	-0.0453	-0.9604	-1.6316	-1.8558	-0.5135
Bromocriptine Mesylate	0.0474	-0.6523	-2.1921	-0.7278	0.3858	-1.6191
Brompheniramine	0.5415	-0.5302	-0.0570	0.6385	0.3162	0.8104
Broxyquinoline	-0.2136	-0.3036	0.1543	0.1503	-0.1306	0.5672
Brucine	0.1381	-0.7832	-0.6118	0.1259	-0.7209	-0.3832
Budesonide	1.0207	-1.4721	-0.3663	0.5190	0.2009	-1.0855
Bufexamac	-2.1067	0.1416	0.2033	0.2909	0.1009	0.4568
Buflomedil HCl	-8.1483	-0.7300	-1.0762	-0.0045	-0.6190	-0.6275
Bumetanide	0.5929	-0.2192	0.0364	-0.0469	0.1150	0.0639
Bupivacaine hydrochloride (Marcain)	-1.2121	-2.3990	-4.1916	-2.2429	-0.9580	-3.8674
Busulfan (Myleran, Busulfex)	0.0084	1.8709	0.4923	1.3880	1.1895	1.2072
Butacaine	0.1826	-0.7474	-0.4471	0.1299	-0.0458	0.1854
Butenafine HCl	-0.8258	0.0145	1.7913	1.9625	1.2235	1.7956

Butoconazole nitrate	-0.2390	-0.7021	-2.1484	0.5822	0.9994	-1.1582
Cabazitaxel (Jevtana)	-14.9912	-16.7893	-16.6494	-8.7442	-9.7098	-12.1952
Calcifediol	-0.0848	0.4540	1.5615	1.8079	1.5481	0.4359
Calcitriol (Rocaltrol)	-1.4371	0.5232	0.6960	-0.1075	0.8855	0.4593
Calcium Gluceptate	-0.0678	-0.0666	0.4537	-0.2685	-0.4754	-0.0053
Calcium levofolinate (Calcium Folinate)	1.0317	0.3577	0.1607	0.5156	0.6667	0.9121
Camptothecin	-13.6721	-18.5241	-20.1805	-9.1975	-10.9609	-14.1493
Camylofin Chlorhydrate	-0.5058	-2.1563	-2.4512	-1.5535	-0.9289	-2.1351
Candesartan (Atacand)	-0.1422	0.0450	0.3129	0.5843	0.2742	0.5333
Candesartan cilexetil (Atacand)	-14.9835	1.0334	0.7739	0.5608	0.3125	0.6780
Capecitabine (Xeloda)	0.1875	0.9310	1.5442	1.3344	0.9169	1.3532
Captopril (Capoten)	0.7760	0.2028	0.3799	0.0116	-0.9807	0.0239
Carbachol	-1.1198	0.1267	-0.3831	-0.6024	0.1300	-0.5982
Carbadox	-1.5746	-1.6076	-0.3680	-0.1382	-1.2951	-0.4653
Carbamazepine (Carbatrol)	-0.2902	1.8084	0.0586	1.2979	0.6495	0.7170
Carbazochrome sodium sulfonate	-0.4654	0.1751	0.5070	1.0224	0.7331	1.0480
Carbenicillin disodium	0.2716	0.4658	-0.4742	-0.3984	-0.6561	-0.0999
Carbenoxolone Sodium	-0.2565	0.0733	0.1364	-0.4325	-0.6791	-0.4364
Carbidopa	0.2867	1.2914	0.2481	0.1736	0.2058	0.6617
Carbimazole	-0.4429	0.9393	1.3791	0.5441	1.1681	1.0088
Carboplatin	0.4167	-1.1246	-1.1805	1.1583	-0.3601	-0.3574
Carfilzomib (PR-171)	-18.0611	-20.4626	-22.0115	-10.7297	-12.2674	-15.2139
Carmofur	-1.9882	-5.2142	-7.5099	-0.7639	-2.8992	-5.6296
Carprofen	1.0910	1.4097	0.2173	-0.3879	0.1077	-0.2880
Carvedilol	0.1959	-2.0285	-3.4256	-0.2726	0.0402	-2.6876
Caspofungin acetate	0.8507	0.1916	0.8522	-0.0917	0.2144	0.0392
Catharanthine	-1.4641	-3.1059	-3.6941	-0.4900	-0.8735	-2.0280
Cefaclor (Ceclor)	-8.1520	-9.5028	-12.0223	-2.9849	-4.4705	-5.7510
Cefdinir (Omnicef)	0.1156	1.4452	1.0647	1.9483	0.7336	0.7889
Cefditoren pivoxil	-1.0279	0.0155	-0.0049	-1.3517	-0.8943	-0.3444
Cefoperazone (Cefobid)	1.0666	-0.1085	0.4508	1.1466	0.6257	0.5455
Cefoselis sulfate	1.1246	0.8443	0.6879	1.8463	0.9701	0.6721
Cefprozil hydrate (Cefzil)	0.2810	0.0288	0.2085	0.4591	0.0461	-0.0483
Ceftazidime Pentahydrate	-0.2740	0.1970	0.0310	0.3895	0.1659	0.1312
Ceftiofur hydrochloride	0.3483	0.1065	0.9052	0.0032	-0.3533	0.1340
Celecoxib	1.0022	0.4066	1.0815	0.6068	0.0853	0.2192
Cephalexin (Cefalexin)	0.5725	0.7517	0.6162	1.0785	1.1843	0.6589
Cephalomannine	-13.5720	-23.8257	-25.2395	-13.1532	-14.7074	-18.1675
Cephapirin Sodium	-0.0587	-0.1250	0.1664	0.0008	0.3102	0.1413
Cepharanthine	0.7508	-0.3108	-2.6140	0.0124	0.1207	-3.3523
Cetirizine Dihydrochloride	-9.3594	-2.0760	-1.7198	-14.1653	-0.1878	-2.0202
Cetrimonium Bromide	-13.3925	-18.1436	-18.9717	-7.7224	-10.8479	-13.2248
Cetylpyridinium Chloride	-15.4059	-19.8812	-21.4477	-11.3375	-12.4066	-15.1635
Chenodeoxycholic acid	-0.9214	1.0622	0.4571	0.2443	1.5830	1.2001
Chloramphenicol (Chloromycetin)	0.4176	0.2680	0.0996	0.7245	0.5257	0.5146
Chlormezanone (Trancopal)	0.9083	0.8274	0.3486	0.4607	0.8143	0.8340
Chlorocresol	-0.9166	-0.2858	-0.4701	-0.0920	-0.1142	-0.7220
Chloroquine Phosphate	1.0149	0.7334	-0.2114	0.6118	0.3157	0.6722
Chlorothiazide	0.8150	0.2395	-0.5694	-0.3994	-0.2393	-1.2443
Chloroxine	-0.8821	-4.4658	-7.5147	-0.7460	0.2088	-3.3201
Chlorpheniramine Maleate	-0.4145	-0.4994	0.0267	-0.1265	0.1050	0.1863
Chlorpromazine (Sonazine)	-11.6692	-11.4532	-18.2642	-7.4661	-7.4087	-14.0343
Chlorpropamide	1.3185	1.1400	0.9007	1.3082	1.1272	1.3107
Chlorprothixene	-1.5456	-0.4243	-0.1635	-1.5641	-0.9099	-1.3132

Chlorquinaldol	-8.1736	-14.1329	-17.5343	-6.7519	-6.2780	-11.0264
Chlortetracycline HCl	0.5064	0.8222	0.4765	0.3618	0.4651	0.6622
Chlorzoxazone	0.9827	1.0842	0.4499	1.0226	0.5142	0.7305
Cholesterol	0.9534	0.9369	0.4080	1.1110	0.7530	1.0523
Choline Chloride	0.1275	0.6172	0.7041	0.1780	0.3797	0.8333
Chromocarb	-1.8130	-1.0506	-1.4559	-0.4512	-0.6244	-1.9505
Ciclopirox (Penlac)	-10.9037	-16.7473	-16.7789	-4.1814	-9.0407	-11.9996
Ciclopirox ethanolamine	-15.1966	-17.8054	-18.8827	-6.2333	-8.3477	-13.1308
Cidofovir (Vistide)	-1.7849	-2.1909	-1.6968	-10.5834	-0.0098	-0.6586
Cilazapril monohydrate (Inhibace)	-0.4069	-1.1724	-1.0454	-1.0350	-0.7239	-1.5733
Cilnidipine	-9.4801	-1.7831	-1.2979	-2.3010	0.3454	-1.3216
Cilostazol	-0.1667	0.6480	-0.3470	0.9946	0.9203	-0.3151
Cimetidine (Tagamet)	1.0515	0.9169	0.4024	0.3987	1.6882	0.9352
Cinchophen	1.4484	1.3736	1.3271	1.5813	0.9095	1.3996
Cinepazide maleate	0.3033	-0.4016	0.0666	-0.1112	-1.1375	-0.2010
Cinoxacin	-0.0357	-0.0155	-0.1227	-0.1500	0.7239	-0.1553
Ciprofloxacin (Cipro)	0.1968	0.6568	-0.3773	0.1142	-0.0807	-0.4219
Cisatracurium besylate (Nimbex)	-2.3236	0.7700	0.1359	0.8629	0.3547	0.0539
Cisplatin	0.5906	1.2701	1.8670	1.1070	0.6946	1.2895
Cladribine	-15.8501	-17.7529	-20.9595	-11.1080	-12.5189	-14.9737
Clafen (Cyclophosphamide)	1.6957	0.7462	0.6137	1.0393	0.5838	0.5191
Clarithromycin (Biaxin, Klacid)	-0.9047	-0.1390	-0.2596	-0.7555	0.1212	-1.1764
Clemastine Fumarate	-11.1801	-16.2232	-16.1032	-8.0984	-8.9347	-11.7662
Cleviprex (Clevidipine)	0.5830	0.1826	0.4109	-1.2260	-0.0545	-0.4468
Climbazole	0.4450	1.5039	1.2908	1.0697	1.4629	1.1895
Clinafloxacin (PD127391)	-0.1033	-0.3184	-0.3252	-0.7687	-1.4019	-0.0740
Clinafoxacin HCl	-0.8082	0.5121	0.6356	0.4344	0.7213	0.4856
Clindamycin	0.1364	-0.5541	-0.8635	-0.2949	-0.6048	-1.2294
Clindamycin hydrochloride (Dalacin)	0.8196	0.4710	-0.5200	-0.2548	0.5481	-0.8640
Clindamycin palmitate HCl	-16.7863	0.2128	-0.0064	0.8233	0.8366	0.6141
Clindamycin phosphate	-0.4662	-0.0545	0.2770	0.3663	-0.3297	-0.0749
Clobetasol propionate	-0.5630	-0.5491	-0.5187	1.1205	1.4247	0.7754
Clodronate Disodium	-2.4555	-1.7356	-1.8678	-1.1789	-0.8715	-1.5089
Clofarabine	-13.4568	-19.4684	-18.1162	-9.3040	-11.0447	-12.2790
Clofazimine	-3.1193	-3.0348	-4.7994	-1.6789	-0.9909	-3.3037
Clofibrate (Atromid-S)	0.0199	-0.1909	0.5665	-0.1623	-0.2552	0.2948
Clofibric acid	-0.5679	-0.1776	0.2199	0.1324	-0.4244	0.5975
Clofoctol	-0.1012	-0.3620	0.0232	0.1970	0.0053	-0.2612
Clomifene citrate (Serophene)	-14.1878	-17.9639	-18.6574	-9.7207	-11.0496	-13.8927
Clomipramine hydrochloride (Anafranil)	-4.4217	-1.3439	-2.3141	-3.4594	-1.0800	-2.1991
Clonidine hydrochloride (Catapres)	0.3846	0.2261	0.3223	-0.2937	0.4555	-0.1964
Clopamide	0.8818	0.4264	0.4056	0.8478	0.5877	0.5757
Clopidogrel (Plavix)	-4.9672	-0.3845	-2.6323	-1.5323	-1.6238	-2.3005
Clorgyline HCl	1.2388	0.9094	0.8559	0.9789	1.0758	0.8300
Clorprenaline HCL	1.4668	0.2511	0.1526	-0.0597	0.6007	-0.5387
Clorsulon	0.3141	0.6079	0.6380	1.4983	1.1337	1.3760
Closantel	0.3840	-0.7216	-0.8635	-0.5020	-1.6350	-0.4670
Closantel Sodium	0.6651	-0.0203	-0.1889	-0.3345	-0.8573	-0.1335
Clotrimazole (Canesten)	-5.0189	-4.8524	-8.4438	-1.2731	-1.9813	-8.2663
Cloxacillin sodium (Cloxacap)	-0.7619	-0.6632	0.4061	-1.8629	-1.1292	-0.6756
Clozapine (Clozaril)	-0.0145	-0.3768	-2.5106	0.0806	0.8625	-1.6263

Cobicistat (GS-9350)	-4.9726	0.0597	-0.5334	0.8173	0.7341	0.1661
Colistimethate Sodium	0.8921	0.9324	0.7031	1.1961	1.1803	0.5060
Colistin Sulfate	0.4355	-0.1754	1.2355	0.7412	0.4477	0.6248
Conivaptan HCl (Vaprisol)	-1.0113	1.2407	1.3067	1.4121	1.1416	0.1586
Cortisone acetate (Cortone)	-0.9496	-0.1303	0.1163	-0.6347	-0.8893	-0.7595
Coumarin	1.5791	1.1790	0.9120	1.0112	0.3299	0.8791
Creatinine	-0.2584	-0.1944	-0.6494	-0.6744	0.3339	-0.2253
Crizotinib (PF-02341066)	-15.2921	-21.2435	-21.9181	-10.9600	-12.9553	-15.2946
Crystal violet	-14.4666	-19.4228	-20.3584	-10.5469	-13.1443	-14.6120
Curcumin	0.0529	-13.9428	-14.4655	0.0260	-7.9628	-11.2884
Cyclamic acid	-0.4634	-0.7212	0.2615	-0.9096	-1.3542	-1.0694
Cyclandelate	1.6909	2.4272	1.5650	1.7539	1.2522	1.5013
Cyclophosphamide monohydrate	-1.6210	0.7505	-0.8174	-0.9050	-1.9406	-0.8463
Cyclosporine (Neoral)	-5.0803	-6.3557	-5.7836	1.8357	-3.6409	-5.0723
Cyproheptadine HCl (Periactin)	-7.5071	-2.6071	-2.2792	-0.9044	-1.2345	-2.4841
Cyromazine	0.9093	1.4541	0.4936	1.5291	0.6838	1.0575
Cysteamine HCl	0.7060	0.1240	0.7938	0.2909	0.6255	0.8206
Cytarabine	-16.3276	-19.9782	-22.3615	-12.0422	-11.9558	-17.1878
Cytidine	-22.6062	0.0933	-3.1822	-2.4697	-1.7446	-2.3762
Dabrafenib (GSK2118436)	-3.9378	-5.1932	-3.8231	-0.0725	-0.3042	-1.6154
Dacarbazine (DTIC-Dome)	2.3533	0.0463	1.3184	0.6419	0.2655	1.3577
Daidzein	0.3956	0.9556	0.8233	0.4944	1.3954	0.9975
Danofloxacin Mesylate	0.1475	-0.2602	-0.5716	-0.6225	-1.2893	-1.6831
Dapoxetine hydrochloride (Priligy)	-0.0125	-3.6755	-1.5953	-0.4346	0.9213	-0.2476
DAPT (GSI-IX)	0.6307	-0.0009	0.4447	0.5832	0.6847	0.1475
Daptomycin	0.9784	1.6536	1.1764	1.8511	0.8751	0.7587
Darifenacin HBr	-1.1972	-4.3303	-3.4385	0.3516	-0.0511	-1.2693
Darunavir Ethanolate (Prezista)	-0.2678	-0.3057	-0.1478	1.7380	-0.2590	0.1305
Dasatinib (BMS-354825)	-4.0556	-13.1842	-8.8843	0.5369	-2.6262	-5.4324
Daunorubicin HCl (Daunomycin HCl)	-19.2045	-21.8824	-22.9886	-11.2825	-13.3896	-16.0797
D-Cycloserine	0.3439	2.1588	1.7495	1.0206	1.7869	1.2655
Decamethonium bromide	-1.5946	0.9537	0.9093	0.5649	0.8636	0.3014
Decitabine	-2.5186	-2.0314	-0.3640	-0.8319	-0.8400	-0.4672
Decoquinate	1.2616	0.7351	0.4322	0.0124	0.2758	-0.0410
Deferasirox (Exjade)	-6.2130	-6.7461	-10.1991	-1.6623	-2.3407	-5.9663
Deferiprone	0.1042	1.4676	1.4228	1.3185	0.5988	0.9423
Deflazacort (Calcort)	0.4651	1.0433	0.4902	0.6263	0.8576	0.3520
Dehydroepiandrosterone (DHEA)	0.7118	0.1944	0.2787	0.6170	0.7102	0.9017
Deoxyarbutin	-0.5603	-0.2998	-2.0882	-1.4437	0.0058	-2.8966
Deoxycorticosterone acetate	1.2522	-0.3258	0.1797	0.1554	-0.0203	0.2163
Dequalinium chloride	-7.2642	1.0812	0.9837	-6.7320	0.8130	0.4403
Desloratadine	-2.3305	-3.0598	-3.2789	-0.7318	-1.8027	-3.7860
Desonide	-0.2624	-0.0802	0.0049	-15.1495	-0.2940	0.2133
Detomidine HCl	0.4258	-0.2634	0.2769	-0.0248	-0.0799	-0.0248
Dexamethasone	-4.9290	-1.5203	-1.3839	-9.1297	-0.3095	-0.8698
Dexamethasone acetate	-0.3528	-1.4666	-0.2998	0.1315	-0.6643	-1.1134
Dexlansoprazole	0.1633	0.2088	-0.1162	-0.3138	-0.2604	-0.5200
Dexmedetomidine	0.7162	-0.1953	0.7339	0.6859	0.3051	-0.0297
Dexmedetomidine HCl (Precedex)	1.0614	-0.3724	0.3059	0.4574	0.2801	0.1908
Dexrazoxane Hydrochloride	1.9516	0.5882	1.2241	1.5396	0.5250	1.2053
Dextrose (D-glucose)	-0.5447	-0.2120	-0.7810	-0.0556	-0.6270	-0.9150
Dibenzepine HCl	1.7101	1.1440	0.7020	1.1774	0.5672	0.8145

Dibenzothiophene	1.4560	1.0398	0.1107	1.1607	-0.1006	0.6461
Dibucaine HCL	-1.4976	-0.3754	-0.4680	0.0151	1.0805	-0.4381
Dichlorisone Acetate	0.5580	0.0027	0.4951	0.1367	0.0241	0.0977
Dichlorphenamide (Diclofenamide)	1.3679	1.2221	0.5821	0.8590	0.3883	0.6843
Diclazuril	0.2051	0.5650	-0.3588	0.5572	0.4621	0.1160
Diclofenac	-0.1168	0.1684	-0.0198	0.2789	-0.6297	-0.1644
Diclofenac Diethylamine	-0.6467	-0.1140	-0.7753	-0.7848	-0.7500	-2.4278
Diclofenac Potassium	0.2364	0.4000	0.0064	-1.4101	-1.5970	-0.7271
Dicloxacillin Sodium	-0.7885	-1.5714	-0.9835	-1.0542	-0.5836	-1.2384
Dicyclomine HCl	-1.4387	0.1678	-1.0523	-0.9204	-0.6268	-0.7029
Didanosine (Videx)	-0.4098	-1.0309	-0.6075	-0.3799	-0.2311	-1.0866
Dienogest	0.1238	0.0243	1.0724	0.2442	-0.5343	0.1003
Diethylstilbestrol (Stilbestrol)	0.2156	-0.9149	-4.1415	0.4913	0.8750	-0.5867
Difloxacin HCl	0.0570	-0.7795	-1.4080	-0.0077	0.1486	-1.7090
Difluprednate	-2.6577	-0.8932	-1.3865	-0.2636	-0.4300	-0.7936
Digoxigenin	-15.4290	-19.4685	-19.8133	-10.5151	-11.2464	-13.9755
Diltiazem HCl (Tiazac)	-0.1450	0.2520	0.0148	-0.1372	1.3057	-0.3060
Dimaprit 2HCl	1.0791	1.0308	0.1428	1.2952	0.4451	0.8147
Dimethyl Fumarate	0.8881	0.7698	0.7995	0.6452	0.5802	0.7038
Diminazene Aceturate	0.2012	-0.1057	-0.8972	0.1254	-0.9492	-0.7332
Diperodon HCl	-0.2656	-0.0027	0.0669	-0.2313	0.3142	-0.1124
Diphemanil methylsulfate	-1.5153	-0.2819	-0.4362	-0.4334	-0.0217	-0.3563
Diphenhydramine HCl (Benadryl)	0.2894	0.8916	0.1515	0.6685	1.6297	0.7152
Diphenylpyraline HCl	0.6826	-0.5012	-1.1648	0.1000	0.2813	0.0205
Dipyridamole (Persantine)	0.0669	0.7563	0.1941	0.3673	0.0178	0.3979
Dirithromycin	-0.0174	-0.0908	-0.3203	0.6147	-0.3745	0.1154
Disodium Cromoglycate	-0.5231	-0.5659	-1.7879	-1.5995	-1.4367	-1.6052
Disopyramide Phosphate	0.5669	-0.3191	0.1378	0.3573	-0.1448	0.4486
Disulfiram (Antabuse)	-7.9672	-20.3400	-16.8864	-5.4661	-12.5624	-9.4431
Divalproex sodium	-0.5233	0.6385	-0.0756	0.8722	0.4123	-0.1535
DL-Adrenaline	-0.0118	-0.2352	0.0162	-0.0944	-0.5315	0.5794
DL-Carnitine hydrochloride	-0.2573	-0.5029	0.3925	0.3505	-0.1051	0.1291
DL-Mevalonic Acid Lactone	0.2350	-0.7352	0.5594	-0.0158	-0.7413	0.4069
D-Mannitol (Osmitrol)	0.4593	-0.3055	-0.1213	-0.1168	-0.9355	0.1550
Docetaxel (Taxotere)	-15.1958	-20.0611	-19.4495	-9.2052	-10.8575	-13.2620
Docosanol (Abreva)	-1.8434	-0.2783	-1.3717	-14.0907	-1.1113	-2.8871
Dofetilide (Tikosyn)	-0.2448	-1.4133	-1.1075	-1.9172	-0.0995	-2.3763
Domiphen Bromide	-7.5761	-5.9195	-15.7650	-5.4265	-2.6346	-12.8630
Domperidone (Motilium)	0.4016	-0.1153	-0.3785	0.8196	0.4432	-0.1712
Donepezil HCl (Aricept)	-0.8987	-2.4599	-2.0393	-0.0032	-0.7101	-1.1545
Dopamine hydrochloride (Inotropin)	0.4119	0.7283	0.2538	0.3408	0.7300	0.2528
Doripenem Hydrate	-2.2127	1.9058	1.2256	2.1245	1.3824	1.3143
Dorzolamide HCL	-0.0334	-0.5714	-0.7132	1.4282	0.8841	-0.4893
Doxapram HCl	-0.1564	0.7978	1.2615	1.1795	1.2574	0.6459
Doxazosin mesylate	-8.1741	-2.5661	-2.7497	-3.2104	-0.3543	-2.0814
Doxercalciferol (Hectorol)	0.9399	0.6127	0.5279	0.4245	1.3235	0.6746
Doxifluridine	-5.3527	-3.3779	-3.3550	-4.6394	-3.9544	-4.9251
Doxofylline	0.7793	0.7412	0.7205	0.9316	0.9303	0.9364
Doxorubicin (Adriamycin)	-14.4094	-19.5300	-20.2657	-9.1604	-10.9781	-13.3064
Doxycycline HCl	0.1278	-0.6300	-0.4505	0.0165	-0.9412	-0.3593
Doxylamine Succinate	1.3024	-0.1994	-0.1633	0.3074	-0.2958	0.2045
D-Phenylalanine	0.7521	0.7252	0.4384	0.7807	0.8935	0.3516
Dronedarone HCl (Multaq)	-12.9741	-14.4409	-15.8376	-7.7557	-9.2255	-11.0494
Droperidol	-1.3051	-0.6576	-0.4348	-0.2393	-0.7454	-0.6167
Dropropizine	0.8020	1.2917	0.2102	-0.6177	0.7935	-0.0130

Drospirenone	0.8346	0.4465	0.7033	1.5689	0.6062	1.0423
Droxidopa (L-DOPS)	0.7130	0.1449	0.2519	0.0318	-0.5283	-0.1589
Duloxetine HCl (Cymbalta)	-13.6294	-11.7984	-18.7323	-4.2365	-6.7303	-12.7428
Dutasteride	1.7945	1.1967	0.8784	1.2563	0.6502	0.9251
Dyclonine HCl	-18.4983	-0.1748	-1.6287	-0.3549	-0.6069	-1.4024
Dydrogesterone	0.2243	-0.1989	0.2395	-0.0814	-0.2950	-0.3618
Dyphylline (Dilor)	0.1922	-10.3086	0.7808	1.6180	0.9839	0.8007
Econazole nitrate (Spectazole)	-0.6540	-1.6959	-2.2708	0.0792	-0.4826	-1.7110
Edaravone (MCI-186)	-0.9361	0.4038	-0.1968	0.8181	1.0439	0.2254
Ellagic acid	-15.9969	0.6380	0.2814	-2.0561	1.2234	0.5650
Eltrombopag (SB-497115-GR)	-3.7662	-4.7620	-7.0491	-2.5600	-2.6493	-3.7897
Elvitegravir (GS-9137)	-0.9644	0.8322	0.5697	0.4772	1.0547	0.0471
Emetine	-15.5395	-20.7078	-21.6164	-11.3343	-12.9869	-15.2299
Emtricitabine (Emtriva)	-0.0033	0.5673	0.6919	1.3756	0.8802	0.5897
Enalapril maleate (Vasotec)	2.2971	-0.8129	0.6458	-0.2524	0.4572	0.2136
Enalaprilat dihydrate	0.4232	-0.2166	0.2931	-0.9432	0.8775	-1.1913
Enoxacin (Penetrex)	0.0033	0.8189	-0.2607	0.0253	-0.6606	0.1818
Enrofloxacin	-0.0818	-0.1224	-0.2142	-1.2852	-1.1476	-0.7451
Entacapone	-1.3027	-0.5828	-0.3753	-0.1706	-0.5188	-0.7387
Entecavir hydrate	-1.6296	-0.0243	-1.7011	-0.0475	-0.4074	-1.2559
Epalrestat	0.7038	1.6044	0.9301	0.4210	0.3113	0.8392
Epinephrine bitartrate (Adrenalinium)	-15.2071	0.3064	-0.1494	0.2593	0.2908	0.6756
Epirubicin Hydrochloride	-15.4791	-19.6445	-20.2139	-10.3724	-11.6198	-14.5850
Eplerenone	0.6367	1.8440	1.6870	1.1789	1.5255	1.2936
Eprazinone 2HCl	0.7202	0.5186	-0.6983	-0.8310	-0.0083	-0.6895
Eprosartan Mesylate	0.4943	-0.0997	0.2420	-0.1996	-0.6427	-0.1348
Erdosteine	-0.7754	1.2481	-0.0592	-0.7655	0.8347	0.2919
Erlotinib HCl	1.6170	0.9861	0.7146	-0.2086	1.2128	1.2447
Erythromycin (E-Mycin)	0.2265	0.0996	-0.0107	1.0850	-0.6268	0.0759
Erythromycin Ethylsuccinate	-0.3149	0.8060	0.9012	0.9422	1.2298	0.6867
Escitalopram oxalate	0.4293	1.2723	1.2896	0.9766	1.2108	0.7223
Esmolol HCl	0.6795	0.1304	0.3364	0.0749	-0.4425	-0.3836
Esomeprazole magnesium (Nexium)	-1.1866	-0.3520	-1.4074	0.7364	-0.1189	-0.2210
Esomeprazole sodium (Nexium)	-1.1833	-0.5953	-0.5778	-0.0066	-0.9088	-0.6184
Estradiol	0.0359	1.5015	0.4123	0.8022	0.6534	0.7003
Estradiol valerate	-1.6512	0.7646	1.0058	-0.8229	0.6817	0.9024
Estriol	0.3361	0.0350	-0.3890	-0.2577	-0.4190	-0.2795
Estrone	-0.3682	-1.2128	-0.2328	-13.1768	-0.5449	-1.5674
Ethacridine lactate monohydrate	-13.9470	-16.6158	-19.3961	-8.0572	-7.4497	-13.5361
Ethambutol HCl	0.1942	-0.4357	0.0321	-0.0165	-0.8248	-0.2200
Ethamsylate	0.4972	0.7174	0.6580	0.6765	0.6211	0.6131
Ethinyl Estradiol	-4.2122	-4.8760	-7.4334	-0.9944	-1.5639	-0.8565
Ethionamide	-19.8093	-0.8982	-0.5389	-2.2093	-0.8726	-1.5695
Ethisterone	-4.5386	0.5006	0.4328	1.1370	0.7037	1.1627
Ethoxzolamide	-0.6429	0.3566	0.0031	0.0679	0.7151	0.0018
Ethynodiol diacetate	0.4068	0.1410	0.4159	0.5686	0.1243	0.3424
Etidronate (Didronel)	1.3926	0.6989	0.1990	0.6259	0.9637	0.6504
Etodolac (Lodine)	0.7981	1.2450	0.5333	0.6823	1.2637	0.5688
Etomidate	1.0789	1.1569	0.4990	1.9790	1.2360	0.7985
Etoposide (VP-16)	-10.4238	-13.7146	-8.7377	-6.0473	-8.2853	-10.0720
Etravirine (TMC125)	-11.5373	-15.9187	-11.2334	-4.9578	-2.3131	-5.2097
Everolimus (RAD001)	-4.6198	-5.2525	-4.2277	-0.2628	-1.0743	-2.4355
Evista (Raloxifene	0.2537	-0.1284	0.7097	1.2504	0.0285	0.6540

Hydrochloride)						
Exemestane	-3.8310	-3.8389	-1.9273	-0.8740	-0.9222	-0.7664
Ezetimibe (Zetia)	0.7204	-0.1472	-0.5020	-1.1706	0.5447	-1.7364
Famciclovir (Famvir)	0.2048	0.0492	-0.9223	-0.6204	-0.7512	-0.4584
Famotidine (Pepcid)	1.0341	-0.0489	-0.2363	-0.1169	0.2811	-0.0248
Famprofazone	-0.0002	0.6216	-0.0721	0.2686	0.6624	0.4507
Febuxostat (Uloric)	0.0281	1.0877	1.5579	-0.9459	1.1183	0.9997
Felbamate	1.0499	1.0641	0.6443	1.6527	1.1600	1.0312
Felodipine (Plendil)	0.4304	1.0187	0.5962	0.6184	1.0657	0.7861
Fenbendazole (Panacur)	-16.2105	-20.5474	-20.5367	-11.7349	-12.4479	-16.8960
Fenofibrate (Tricor, Trilipix)	1.2773	-0.2210	0.2062	-0.5218	-0.5915	0.0513
Fenoprofen calcium	0.0017	-1.0460	-0.1403	-0.6187	-0.4030	-0.7819
Fenoprofen calcium hydrate	-0.2476	0.4294	-0.2782	0.3326	0.0806	0.6197
Fenspiride HCl	0.8945	1.2419	0.3782	0.5658	0.6129	0.7240
Fenticonazole nitrate	-2.7232	-1.1279	-1.7818	-1.2295	-0.5769	-3.4037
Fesoterodine fumarate (Toviaz)	-15.5232	-1.0975	-0.6859	-0.0180	-0.4043	-0.6708
Fexofenadine HCl	0.2357	0.1436	-0.1741	-0.2821	-0.5621	-0.1956
Fidaxomicin	-0.1699	-0.7922	-1.1535	-0.5699	-0.3667	-1.5810
Finasteride	-0.7147	0.3655	1.7691	1.1409	0.5834	1.4399
FK-506 (Tacrolimus)	-0.2649	1.5154	0.8975	0.5259	1.0640	0.7902
Flavoxate HCl	0.8845	0.2472	0.4296	1.0319	0.3218	0.3847
Fleroxacin (Quinodis)	0.5340	-0.2196	-0.1621	-0.8200	0.4753	-0.7150
Florfenicol	0.3748	1.1150	0.6749	-0.4225	-0.8123	-0.5660
Floxuridine	-16.0811	-8.7570	-11.2684	-2.8708	-3.9931	-8.4896
Flubendazole (Flutelmium)	-15.3100	-18.3149	-10.0407	-10.1088	-4.1458	-5.8952
Fluconazole	0.5680	1.2214	0.4350	1.1948	0.9330	0.8633
Flucytosine (Ancobon)	-0.0176	-1.6428	-0.6923	-1.4695	-0.2320	-2.2145
Fludarabine (Fludara)	-1.1565	-9.4185	-16.4303	-5.2339	-11.2766	-14.5040
Fludarabine Phosphate (Fludara)	-0.0914	0.2341	-11.8682	0.5179	-2.7831	-13.1029
Flumazenil	0.2741	0.2190	0.5855	1.6663	0.8278	0.8311
Flumequine	-0.5717	-1.1479	-0.6925	-0.4206	-0.7455	-1.1074
Flumethasone	0.2599	1.2328	0.9975	0.8744	0.7446	0.7469
Flunarizine 2HCl	-3.4982	-0.5798	-2.8256	-0.4537	0.1520	-2.7148
Flunixin meglumin	0.6935	-0.2553	0.3741	-0.3542	-0.1043	0.1604
Fluocinolone acetonide (Flucort-N)	0.4425	-0.0041	-0.1001	0.1137	0.5073	-0.3986
Fluocinonide (Vanos)	-2.6597	0.3132	0.0552	0.2418	0.7985	0.4646
Fluorometholone Acetate	-0.5941	-1.2487	-0.8268	-0.4730	-0.7499	-1.1106
Fluoxetine HCl	-11.3325	-8.5124	-14.7462	-7.6157	-4.5745	-10.3968
Flurbiprofen (Ansaid)	0.4032	-0.0447	-0.0492	0.2125	0.1379	0.2505
Flutamide (Eulexin)	-0.0872	-0.0072	-0.2448	-0.5300	-1.0409	-0.3092
Fluticasone propionate (Flonase, Veramyst)	-23.7230	-1.4421	-0.8071	-0.2579	-0.1743	-1.1425
Fluvastatin sodium (Lescol)	-8.8460	-12.9437	-13.6339	-11.0069	-12.6580	-14.6145
Fluvoxamine maleate	-2.0057	-1.8617	-1.7058	0.1878	-0.6880	-0.3749
Formoterol hemifumarate	0.7688	1.4789	1.0098	0.6409	1.0360	0.9850
Fosaprepitant dimeglumine	-0.8642	-0.6387	-1.0652	0.0298	-0.8826	-0.7486
Fosfomycin Tromethamine	-6.7932	0.2049	0.1321	0.2798	-0.2701	-0.1831
Fosinopril sodium (Monopril)	0.5059	-0.1726	0.5923	-0.6999	-0.1125	-0.1917
Ftorafur	0.9269	1.1926	-0.0292	1.5359	0.9846	0.0455
Fudosteine	1.1786	1.3596	1.5793	0.9913	0.6518	1.2059
Fulvestrant (Faslodex)	1.4361	0.9815	1.8215	1.8653	0.7159	1.9987
Furaltadone HCl	-1.2914	0.4231	-1.6773	1.1807	0.8656	0.2078
Furosemide (Lasix)	1.7311	1.8864	1.7751	2.3518	1.5402	1.5091
Gabapentin (Neurontin)	0.6307	0.6915	0.2564	0.5207	0.2933	0.6118
Gabapentin Hydrochloride	-3.1134	-1.3827	-1.2855	-12.8004	-0.2560	-1.2348

Gabexate mesylate	0.3358	1.1231	0.3031	1.0169	0.6945	0.5311
Gadodiamide (Omniscan)	0.1374	1.0525	0.1212	0.2017	-0.4073	0.3440
Gallamine triethiodide (Flaxedil)	0.5240	0.5729	-0.0714	0.0680	0.9062	0.0002
Ganciclovir	0.3570	0.4756	0.2053	0.5319	-0.8849	0.4070
Gatifloxacin	-1.0360	-0.0356	-0.0292	-0.0927	0.6544	-0.0030
Gefitinib (Iressa)	0.2412	0.5113	1.0701	0.4575	1.2907	1.0662
Gemcitabine (Gemzar)	-14.5593	-19.1529	-19.4363	-14.1531	-11.3536	-13.9292
Gemcitabine HCl (Gemzar)	-16.0814	-22.1106	-20.4528	-9.9750	-12.0502	-13.8284
Gemfibrozil (Lopid)	0.5368	-0.2334	-0.0136	-2.1706	-0.2813	0.4883
Genipin	-0.4762	0.6656	-0.7973	-0.3786	-0.2105	-0.0057
Geniposide	-1.3793	0.1163	-0.7063	-0.4088	-0.4339	-0.1467
Geniposidic acid	-0.6540	-0.2048	-0.4054	-0.1661	-0.4195	-0.3598
Genistein	-5.2849	-0.8852	-1.2623	1.1188	0.7407	-1.3727
Gestodene	0.0334	0.8086	0.8285	1.4888	0.8121	0.3041
Gimeracil	-1.8555	0.9196	-1.4302	-0.8469	-1.9980	-0.7476
Ginkgolide A	-16.7096	-0.3850	-1.1562	-0.5019	-0.5040	-1.4139
Glafenine HCl	-0.2357	-0.0067	-0.3128	0.0263	0.3539	-0.2137
Gliclazide (Diamicron)	0.0096	0.2735	0.7459	1.2326	1.0469	1.3310
Glimepiride	0.7576	0.7071	0.6405	1.1779	1.0166	0.4460
Glipizide (Glucotrol)	-3.5358	-5.8073	-6.9278	0.0307	-0.8688	-3.3012
Gliquidone	-0.0670	0.8150	1.3019	1.0823	0.7593	1.1140
Glyburide (Diabeta)	-1.1956	0.5814	-0.2373	0.5417	0.6577	0.0847
Granisetron HCl	0.6277	1.3556	0.3181	1.6649	1.0929	0.8485
Guaifenesin (Guaiphenesin)	0.6319	0.4624	0.1485	0.7944	-0.4626	0.7153
Guanabenz acetate	-0.2458	1.6634	1.2038	0.7836	1.1989	0.9910
Guanethidine Sulfate	0.7473	0.9973	0.4091	0.7758	0.7320	0.6306
Guanidine HCl	-1.0879	-1.1327	0.1651	-0.1489	-0.2882	-0.9010
Halobetasol Propionate	-0.0570	0.1674	0.4068	1.1478	1.0555	0.4168
Haloperidol (Haldol)	-0.3058	-0.8762	-1.3535	-1.2030	-2.1633	-1.1478
Hemicholinium Bromide	1.3073	1.2034	0.9153	1.0327	0.9202	0.7816
Hexamethonium bromide	0.0276	0.1245	-0.1902	-0.1330	-0.1280	0.0098
Histamine Phosphate	-0.3098	-0.7482	-1.5333	-0.7587	-1.0749	-1.1237
Homatropine Bromide	0.6190	0.5928	1.1959	0.8044	1.1500	0.2786
Hydralazine hydrochloride	-0.0668	0.4035	-0.2754	-0.9096	-0.8720	-0.3279
Hydrastinine HCl	-8.8155	-0.6547	-2.7037	-0.9999	-0.2504	-2.2171
Hydrochlorothiazide	0.4490	2.3820	1.3385	1.6083	1.4321	1.8096
Hydrocortisone (Cortisol)	-0.3933	1.1514	0.2291	0.8753	0.5629	0.7961
Hydroxyurea (Cytodrox)	0.3860	-0.1291	-0.0148	0.1342	-0.6134	-0.2006
Hydroxyzine 2HCl	-0.4911	-0.6558	-0.1777	0.5959	0.1025	-0.4189
Hygromycin B	-6.8979	0.2631	0.0658	0.8228	0.4600	0.9265
Hyoscyamine (Daturine)	0.7903	-0.3261	0.1195	-0.6142	-1.0778	-0.7835
Ibandronate sodium	-0.1469	-0.6511	-1.1506	0.1265	0.2234	0.0053
Ibuprofen (Advil)	-1.0237	-1.1458	-0.8151	-1.4892	-0.9961	-1.5265
Ibuprofen Lysine (NeoProfen)	0.3898	0.4361	0.2718	-11.9433	1.1981	0.5371
Ibutilide fumarate	-14.5554	-0.2512	-1.0817	0.4853	0.0080	-0.1340
Idarubicin HCl	-15.5734	-21.0031	-22.3033	-10.6653	-13.3241	-15.8876
Idebenone	1.0801	0.1617	0.8142	1.0417	0.6729	0.5264
Idoxuridine	-0.1411	-1.4714	-2.1804	0.5950	0.5147	-0.5372
Ifosfamide	0.9025	0.8140	0.1972	1.6112	0.8861	0.3658
Iloperidone (Fanapt)	-0.9749	-0.1867	-0.2953	1.0014	0.9168	0.3020
Imatinib (Gleevec)	0.7774	0.6362	0.5764	0.4591	0.7489	0.2870
Imatinib Mesylate	-1.6133	-4.0062	-0.2591	-1.0867	1.1149	0.8262
Imidapril (Tanatril)	-0.5802	-0.0476	-0.6218	-0.3301	-0.5628	-0.8162
Imipramine HCl	-0.8304	-0.4992	-1.7375	-0.9188	-0.8235	-0.4403
Imiquimod	1.3218	0.7266	1.7321	1.3770	0.7066	1.4803

Indacaterol Maleate	-0.9319	-4.3317	-2.2611	0.5853	-0.5421	-1.4628
Indapamide (Lozol)	0.3967	-1.0726	-0.3532	0.1316	-0.2042	-0.1393
Indomethacin (Indocid, Indocin)	1.3166	1.6252	2.0126	1.5363	1.2002	1.3843
Ipratropium bromide	-0.1745	-1.6423	-1.3464	-0.9799	-0.2456	-1.6032
Irbesartan (Avapro)	0.5105	0.9186	0.9411	1.5803	1.2817	0.8915
Irinotecan	-12.5543	-18.0149	-19.3948	-6.1833	-8.6883	-11.9457
Irinotecan HCl Trihydrate (Campto)	-14.5704	-17.6514	-17.8728	-5.4812	-8.0787	-11.4649
Irsogladine	-0.9109	-0.2292	-0.2238	-0.8201	-2.5463	-0.7758
Isoconazole nitrate (Travogen)	-0.0733	-0.8002	-0.0967	-0.0166	0.2908	0.0716
Isoetharine Mesylate	1.3567	1.6666	0.9329	1.1442	1.6148	1.2089
Isoniazid (Tubizid)	0.8242	-0.3823	-0.0420	-0.0069	0.4581	-1.0209
Isoprenaline hydrochloride	-5.8869	0.1693	-0.4708	-0.6270	0.6439	-0.7317
Isosorbide	1.0491	1.0662	0.4445	0.8567	0.3371	0.6059
Isotretinoin	0.5326	0.1425	0.2756	-0.0677	-0.4459	0.6580
Isovaleramide	0.2731	-0.4841	-0.7349	-0.9938	-0.8435	-1.3541
Isoxicam	0.5016	0.8161	1.0875	0.1637	0.0910	0.5517
Isradipine (Dynacirc)	0.0179	-1.0137	-0.0550	-1.5413	0.6089	-0.8666
Itraconazole (Sporanox)	0.6660	0.3838	0.4376	0.5327	0.6551	0.4358
Ivabradine HCl (Procoralan)	-0.3552	-0.0211	0.0461	0.4376	0.2013	-0.0465
Ivacaftor (VX-770)	0.9727	0.6271	1.1303	1.6798	0.9594	0.5016
Ivermectin	-1.7352	1.6864	1.5111	1.8168	1.3866	0.8571
Ketoconazole	0.7737	1.4392	1.2720	1.7083	1.0968	0.9089
Ketoprofen (Actron)	0.5992	0.3545	0.3134	-1.4550	-0.3959	-0.9281
Ketorolac (Toradol)	-0.4581	-0.3124	-0.1153	-1.0854	-0.9821	-1.1398
Ketotifen fumarate (Zaditor)	-0.0446	0.0423	-0.7810	0.3505	0.1889	0.1457
Lacidipine (Lacipil, Motens)	-19.9185	0.5034	-0.3038	0.0099	0.5264	-0.7342
L-Adrenaline (Epinephrine)	0.2139	0.2874	-0.5724	0.6423	0.2334	0.6142
Lafutidine	-0.2782	-0.8015	-0.5526	-1.3525	-1.8190	-0.3420
Lamivudine (Epivir)	0.2877	1.1986	0.2120	1.5251	1.0894	0.9392
Lamotrigine	0.6719	0.2983	0.2052	0.3274	-0.0094	0.6133
Lansoprazole	-0.2914	0.9368	0.7893	1.1157	0.8499	0.5676
Lapatinib	-14.9973	-0.0405	-3.8396	-9.7540	0.6779	-7.4882
Lapatinib Ditosylate (Tykerb)	0.5592	1.5408	0.4795	0.1233	0.7313	1.1676
L-Arginine HCl	1.0027	1.2163	1.4016	1.5807	0.7939	1.5039
L-carnitine (Levocarnitine)	0.1378	-0.8939	0.3500	-0.2837	-0.6541	-0.0079
Leflunomide	0.9959	0.4523	1.7410	1.3279	0.2175	0.8087
Lenalidomide	1.3938	1.4515	0.3380	-0.7753	0.8069	0.6329
Letrozole	-4.7950	0.0718	-0.0206	0.2061	0.1106	0.2442
Leucovorin Calcium	1.3848	0.9248	1.8873	-0.0728	0.5780	0.8537
Levamisole Hydrochloride (Ergamisol)	1.1944	-1.7421	0.1803	0.2990	0.1452	-0.0992
Levetiracetam	0.0974	0.6676	1.2974	1.1670	0.6382	0.9697
Levobetaxolol HCl	-1.1179	0.3330	0.1772	0.6960	0.1940	0.3526
Levodopa (Sinemet)	0.3323	1.3819	0.6655	1.3237	0.4731	0.9396
Levofloxacin (Levaquin)	1.8676	-1.5168	1.0926	0.0979	0.4541	-0.0825
Levonorgestrel (Levonelle)	0.6384	0.7807	1.0733	0.5264	0.0492	0.7822
Levosimendan	-3.7755	-8.9451	-5.3226	0.9666	-0.7276	-0.9766
Levosulpiride (Levogastrol)	0.7310	0.6335	0.0646	0.9149	0.5121	0.9766
L-Glutamine	-0.0345	0.5801	0.5901	0.2038	-0.6601	0.0486
Licofelone	0.1521	-0.5939	-0.1501	-0.2638	-0.0398	-0.4499
Lidocaine (Alphacaine)	-0.2434	0.7212	0.7245	0.8553	0.2257	0.9175
Linagliptin (BI-1356)	0.0781	-0.0511	-0.3924	-0.3370	-0.4035	-0.0752
Lincomycin hydrochloride (Lincocin)	0.4038	-0.0509	0.1924	0.3557	0.5207	0.3627
Linezolid (Zyvox)	-0.3870	-0.9899	-0.0068	-2.0216	-0.7034	-0.5155

Liothyronine Sodium	0.1701	-0.6291	-0.1383	0.5471	-0.0277	0.2477
Liranaftate	-0.1692	1.6129	1.0383	0.3381	1.1832	0.7049
Lisinopril (Zestril)	0.5276	0.3581	0.1508	0.0094	0.2256	0.0071
Lithium Citrate	0.9418	0.1498	0.8507	0.6605	-0.1105	0.6586
Lithocholic acid	0.5122	-0.2353	0.0131	-0.3066	-0.5955	0.0525
Lofexidine HCl	0.7819	0.2879	0.5858	-0.0267	-0.3070	0.5251
Lomefloxacin hydrochloride (Maxaquin)	-1.3090	-1.2067	-0.5003	-1.3427	-1.1654	-1.2566
Lomerizine HCl	-6.0190	-1.8567	-3.1430	-0.8090	-0.3672	-1.8093
Lomustine (CeeNU)	0.7110	1.0453	0.3584	0.3690	1.3381	0.6933
Lonidamine	-1.0933	0.3149	0.0219	1.0925	0.9571	0.6817
Loperamide hydrochloride	-1.6465	-3.2059	-4.2386	-0.5466	-0.4240	-4.2492
Lopinavir (ABT-378)	-6.4202	-0.6315	-1.3693	-12.8225	0.0597	-1.1820
Loratadine	0.1198	0.4932	0.3798	-0.5805	-0.0597	0.8725
Lornoxicam (Xefo)	-0.9590	0.1959	0.5317	-0.3070	-0.7285	-0.0066
Losartan potassium	-0.6905	-0.8488	-1.4241	-12.4703	-0.1374	-0.9076
Loteprednol etabonate	0.5580	0.2708	0.3885	0.8446	0.9335	-0.0928
Lovastatin (Mevacor)	-3.2518	-4.7577	-5.9034	-8.0289	-10.1331	-12.2193
Loxapine Succinate	-0.0568	0.1480	-0.4951	0.8167	0.4565	0.1710
L-Thyroxine	-0.3852	0.7310	0.2833	1.1362	0.8187	1.2430
Lurasidone HCl	-0.4005	-1.0843	-0.7522	-0.4261	-0.6721	-0.1198
Malotilate	-17.5674	0.7215	1.6739	1.2209	0.9771	1.0163
Manidipine (Manyper)	0.5841	-0.3398	0.0210	0.3361	-0.1988	0.4469
Maprotiline hydrochloride	-3.7875	-14.3239	-15.9320	0.7378	-8.5244	-12.0014
Maraviroc	0.0472	0.2083	0.0527	0.1034	0.5233	0.5217
Marbofloxacin	0.0181	-1.4163	-0.5939	-1.6114	-0.0845	-0.6479
Masitinib (AB1010)	-3.4527	-11.1173	-11.4852	-1.3519	-5.5434	-7.8142
MDV3100 (Enzalutamide)	0.6067	0.6693	1.2377	0.4465	-0.0274	0.2325
Mecarbinate	0.9813	0.8134	-0.0655	0.1437	0.2143	-0.3867
Meclizine 2HCl	-1.0601	-0.4290	-1.3018	-0.2641	0.5634	-1.7991
Meclocycline Sulfosalicylate	1.7366	1.2935	0.5721	1.3737	1.3598	1.2517
Medetomidine HCl	-0.0362	-0.8774	-0.2085	-1.6273	-1.4414	-0.8067
Medroxyprogesterone acetate	1.7614	0.5330	-0.1060	0.1652	0.9521	0.0776
Medrysone	1.2029	1.2958	0.7221	1.1231	0.7814	0.8424
Mefenamic acid	1.0093	1.4727	1.3932	1.2314	0.9646	0.8921
Megestrol Acetate	0.5733	0.3127	0.0373	1.1338	1.1282	0.6482
Meglumine	0.7657	-1.0666	0.0100	0.5066	0.1879	0.3649
Melatonin	1.9918	0.2130	1.5891	1.3335	1.0725	1.2855
Meloxicam (Mobic)	0.4708	0.7746	0.1390	1.6747	0.2378	0.7409
Memantine HCl (Namenda)	-2.3951	0.1403	-0.8337	-0.1529	-0.3786	-0.8463
Menadione	1.8089	-0.8143	0.7616	-0.3051	0.3968	0.1092
Mepenzolate Bromide	-0.9249	0.0304	-1.0543	-0.3685	-0.6558	-0.4226
Mepiroxol	1.2397	0.8045	0.6016	0.6533	0.4710	0.5198
Mepivacaine HCl	0.4111	0.8683	1.5686	1.6085	0.9251	1.6606
Meptazinol HCl	-0.2377	0.0373	-1.0001	-0.2282	-0.7716	-0.5856
Mequinol	0.7705	1.6381	1.8884	1.6350	1.3901	1.1863
Mercaptopurine	-6.4568	-10.0261	-11.6080	-2.1011	-3.6267	-7.0696
Meropenem	-5.8929	-0.9924	-0.3762	0.4280	-0.1037	-0.2649
Mesalamine (Lialda)	0.2591	-1.2911	0.1538	-15.2441	-0.6824	-0.1616
Mesna (Uromitexan, Mesnex)	0.5854	0.9509	0.8044	1.1309	0.0920	0.7568
Mesoridazine Besylate	0.3937	0.1263	0.2399	0.2031	0.2057	0.4387
Mestranol	1.5999	0.8110	0.6559	0.7129	0.4084	0.5393
Metaproterenol Sulfate	-0.1964	0.5266	0.6711	-1.6034	-0.5074	0.4272
Metaraminol Bitartrate	-1.2187	-0.3726	-0.3312	0.0358	-0.8355	-0.6001
Metformin hydrochloride (Glucophage)	2.0855	1.0757	0.4198	0.2540	0.3731	0.1030

Methacycline hydrochloride (Physiomycine)	0.4659	0.2628	-0.1074	-0.3503	-0.0021	-0.0002
Methapyrilene HCl	-1.0123	-0.2385	-0.7850	0.1961	-0.0200	-0.1951
Methazolamide	-0.0048	0.8383	1.2543	0.2826	1.0294	0.0301
Methazolastone	0.6721	-0.1140	1.2321	0.9122	-0.0978	0.7018
Methenamine (Mandelamine)	0.7448	0.8340	0.9104	0.9931	0.8167	1.1229
Methimazole (Tapazole, Northyx)	-0.1077	-2.3372	-1.5740	-12.9831	-0.4995	-1.2090
Methocarbamol (Robaxin)	0.6581	1.1082	1.1897	0.7874	0.3090	0.7272
Methoxamine HCl	0.0509	0.2404	0.1518	0.4043	0.5518	0.3222
Methoxsalen (Oxsoralen)	2.1586	-2.2475	0.0686	0.1496	0.0492	-0.0233
Methscopolamine (Pamine)	-17.0303	0.6273	-0.6351	0.3007	0.4117	-0.4267
Methyclothiazide	-0.0042	0.9599	0.1404	-0.0715	-0.0796	0.3444
Methyldopa (Aldomet)	0.0043	0.7205	-0.6793	-0.5411	-0.5071	-1.2889
Methylhydantoin-5-(D)	-0.5415	-0.0193	0.0024	-0.2127	-0.8746	-0.4087
Methylprednisolone	0.6756	0.4363	0.2344	0.9337	0.4017	0.5101
Methylthiouracil	0.2048	0.2316	1.5198	1.2989	1.1320	1.4251
Meticrane	1.0260	0.6849	0.4909	0.7190	0.7997	0.5417
Metolazone (Zaroxolyn)	-0.1918	0.1608	0.0685	0.4085	0.3308	0.3306
Metoprolol tartrate	-0.4905	0.6551	-0.1204	0.2698	0.4751	0.1715
Metrizamide	-1.2132	0.0067	-0.1176	-1.1206	-1.2404	-0.3253
Metronidazole (Flagyl)	0.1126	0.2219	-0.4442	0.0322	-0.4804	-0.1696
Mevastatin	-3.9117	-4.1191	-5.8697	-7.3662	-6.6369	-13.4623
Mexiletine HCl	-1.0152	-1.4454	-1.1760	-0.4464	-1.3683	-1.6912
Mezlocillin Sodium	0.8910	1.5908	1.1424	1.7003	1.3709	1.4887
Mianserin hydrochloride	-6.4130	-0.6419	-0.3918	1.6596	0.4409	-0.1953
Miconazole (Monistat)	0.1984	-0.5109	-1.1822	0.2659	-0.1552	-0.0582
Miconazole nitrate	-1.1147	-3.3779	-1.1567	-3.0015	-1.3255	-1.1851
Mifepristone (Mifeprex)	0.1169	-0.8245	0.5975	-0.0901	0.2681	-0.2623
Miglitol (Glyset)	1.0720	0.4204	0.1367	0.5292	0.6479	0.6259
Milnacipran HCl	0.6267	0.7561	0.4469	1.0073	0.8394	1.1794
Milrinone (Primacor)	0.2935	-0.6179	-0.3027	0.5116	-0.0862	0.0665
Minocycline HCl	0.3840	-1.0589	-1.4426	-0.9517	-0.4944	-1.6462
Minoxidil	0.4410	0.7402	0.6623	0.9330	0.4200	0.1421
Mirabegron (YM178)	0.0409	-0.9308	-0.1614	-0.5994	-1.5030	-1.2571
Mirtazapine (Remeron, Avanza)	1.1928	1.8027	1.3254	0.7198	1.5655	0.8307
Misoprostol	-0.3288	0.4067	-0.1960	-0.1016	0.4505	-0.1482
Mitiglinide calcium	1.4900	0.5738	-0.4156	-0.1749	0.3458	-0.4270
Mitotane (Lysodren)	-1.8173	-0.1993	-0.4827	-0.4009	-0.0999	-0.2660
Mitoxantrone Hydrochloride	-16.4397	-21.3701	-22.7289	-11.9894	-13.1412	-15.9883
Mizolastine (Mizollen)	0.1255	-0.4825	0.3320	0.5080	-0.1270	0.1136
Mizoribine (Bredinin)	0.6673	1.0569	0.9826	1.1326	0.4381	0.5586
Moclobemide	0.3724	-0.6328	-0.9451	0.7447	0.1789	0.4149
Moexipril HCl	0.4793	0.5954	-0.3202	-0.7336	0.2196	-0.1955
Moguisteine	0.3409	0.4318	0.5424	0.0982	0.7484	0.4149
Mometasone furoate	-1.2434	-1.7790	-1.4245	0.6238	0.5625	0.0066
Monobenzone (Benoquin)	-1.9348	-4.7348	-4.0244	1.2368	-0.2307	-2.8530
Montelukast Sodium	-0.0573	-0.1030	0.0738	0.5461	-0.0058	0.3331
Moroxydine	-5.3783	-0.1322	-0.6010	-1.1736	-0.2290	-1.1306
Mosapride citrate	-2.8543	1.0965	1.0335	1.1769	0.4244	0.7018
Moxalactam Disodium	1.1719	1.4537	0.6864	0.7345	1.1190	0.8122
Moxifloxacin hydrochloride	-0.0337	-1.8151	-0.6220	-13.8659	0.2505	-0.4028
Moxonidine	0.0829	-0.0737	-1.3096	-1.9944	-1.1336	-2.9759
Mycophenolate mofetil (CellCept)	-9.3939	-11.4656	-10.3635	-6.0970	-6.8133	-8.3940
Mycophenolic (Mycophenolate)	-7.6569	-9.6620	-10.1976	-5.6809	-4.1499	-8.5527

Nabumetone	0.8938	2.0053	1.9785	1.3440	1.3547	1.2212
Nadifloxacin	0.4771	1.1154	1.0058	1.0372	0.8094	0.7078
Nafamostat mesylate	1.0042	0.3424	0.9909	1.1089	0.3922	0.7976
nafcillin sodium monohydrate	0.0286	0.8281	0.9245	0.6495	0.5654	0.3378
Naftifine HCl	-0.2052	0.3592	0.5612	0.8198	0.8231	1.4472
Naftopidil (Flivas)	-0.3100	-0.3984	-0.6922	1.1596	0.3217	0.0057
Nalidixic acid (NegGram)	-0.0385	-0.4122	0.1937	0.1371	-0.3231	0.0404
Nalmefene HCl	1.4980	1.3651	0.9794	0.9982	1.5791	1.1264
Naloxone HCl	-5.8963	-0.5062	0.6112	0.3237	0.6257	-0.0909
Naltrexone HCl	-0.1465	0.0009	0.1484	0.8910	0.7256	0.7253
Naphazoline hydrochloride (Naphcon)	0.9565	0.6540	0.5063	-7.9706	0.5559	0.5226
Naproxen (Aleve)	-0.0043	-0.2100	0.0929	0.7485	-0.2223	0.1061
Naratriptan HCl	0.4308	0.7040	0.2985	1.0110	1.2454	0.5949
Natamycin (Pimaricin)	-1.5993	-0.0765	0.3624	-13.7604	0.8134	0.2781
Nateglinide (Starlix)	0.5649	0.7743	0.5727	0.6117	0.9514	0.0799
Nebivolol (Bystolic)	-15.1549	-10.2550	-3.8440	-9.5709	-5.1347	-3.0481
Nefiracetam (Translon)	0.8057	0.9557	0.8144	0.2537	0.6851	0.4172
Nefopam HCl	0.3226	1.1624	0.6480	1.3147	1.0163	1.0401
Nelarabine (Arranon)	1.5556	0.1091	1.6266	0.7708	0.5314	1.4367
Neomycin sulfate	1.5861	0.6850	0.3428	0.5388	0.9159	0.7223
Neostigmine bromide (Prostigmin)	0.4905	0.7061	0.6849	0.6432	0.8518	0.3581
Nepafenac	0.1059	1.2766	-0.4194	-0.5897	0.0274	-0.5935
Netilmicin Sulfate	0.2367	0.7278	1.4150	1.0815	1.1120	1.2215
Nevirapine (Viramune)	-0.9165	-0.3403	-1.5711	-1.0432	-0.7751	-0.9747
Niacin (Nicotinic acid)	-0.1222	-0.2272	-0.6395	0.9853	-0.6882	0.3727
Nialamide	1.6468	1.1725	0.5456	0.9167	1.2772	1.0421
Nicardipine HCl	-0.0492	0.8551	0.4785	0.6771	0.5875	0.8474
Niclosamide (Niclocide)	-13.5934	-17.6291	-19.4847	-7.4789	-10.9830	-13.6458
Nicorandil (Ikorel)	1.0290	-0.0563	0.0993	0.5789	0.4962	0.3156
Nicotinamide (Niacinamide)	-15.7510	0.0072	-0.3958	-0.2181	-0.3724	-0.3407
Nicotine Ditartrate	-1.7219	-0.2033	-1.2477	-1.0965	-0.5572	-1.2488
Nifedipine (Adalat)	1.2319	0.4786	1.1611	0.3408	1.4306	1.2880
Nifenazone	-0.1987	-0.3709	0.8604	-0.2604	-0.7687	0.0945
Niflumic acid	-0.3866	-2.6978	-1.0599	-0.0717	-2.2558	-0.2250
Nifuroxazide	-3.6785	0.0042	-3.9980	0.0593	0.9147	-1.1710
Nilotinib (AMN-107)	1.2357	0.6318	0.0211	-0.8833	0.3627	0.8954
Nilvadipine (ARC029)	0.1618	-0.0515	0.4717	1.0746	0.7180	0.2344
Nimesulide	-24.9744	-0.7653	-1.2359	-0.4690	-0.7529	-1.5325
Nimodipine (Nimotop)	-0.4760	0.1340	0.0199	1.2784	-0.4351	0.4431
Nisoldipine (Sular)	-0.4145	0.4224	0.2647	0.6537	-1.0415	-0.1252
Nitarsone	-0.9714	-0.8113	-1.2065	-0.5485	-0.2571	-0.8418
Nitazoxanide (Alinia, Annita)	-3.3001	-5.0858	-6.0246	1.3378	-1.0208	-2.1935
Nithiamide	-1.4070	-1.9229	-0.3269	-1.1703	-1.6410	-0.7524
Nitrendipine	0.8889	0.8043	1.0858	0.3253	0.9722	0.5162
Nitrofurazone (Nitrofural)	-0.2790	0.3527	-0.2639	-1.1200	-0.8802	-0.7889
Nizatidine	-14.0715	0.7765	0.6066	0.5100	0.6592	0.6551
Nomifensine Maleate	0.2962	-0.5320	-3.1018	-1.2864	0.0153	-3.2472
Noradrenaline bitartrate monohydrate (Levophed)	0.5498	1.1476	0.9487	1.2721	1.3749	1.3651
norethindrone	0.0827	0.8743	1.4420	0.6075	0.7635	0.6345
Norfloxacin (Norxacin)	0.5259	0.4767	0.7692	1.2011	0.5415	0.6599
Noscapine HCl	-0.6372	-0.7763	-1.1506	-0.2429	0.4247	-0.3235
Novobiocin sodium (Albamycin)	1.2087	1.1229	1.5132	0.3231	1.1196	0.6846
Nystatin (Mycostatin)	-0.0001	-1.5886	-2.4411	0.0069	-0.1212	-1.9744
Ofloxacin (Floxin)	0.0309	-0.6313	-0.7540	-1.3672	0.0696	0.0113

Olanzapine (Zyprexa)	0.8715	1.1182	0.8985	0.6223	0.7523	0.6722
Olmesartan medoxomil (Benicar)	1.4476	1.2968	1.5279	2.4843	1.4362	1.1777
Olopatadine hydrochloride (Opatanol)	0.5049	0.9688	0.5283	1.8727	0.4519	0.4517
olsalazine sodium	0.1465	1.4144	0.9566	0.5681	0.8963	0.2314
Omeprazole (Prilosec)	0.3195	1.1112	1.0442	0.9468	0.4091	0.7286
Ondansetron (Zofran)	-1.8462	0.9597	0.7709	0.5250	1.2037	0.3674
Ondansetron hydrochloride (Zofran)	0.2477	-0.1865	1.0388	0.7673	0.1117	0.7001
Orbifloxacin	-0.9690	0.3994	-0.9983	0.2063	0.4908	-0.2752
Orlistat (Alli, Xenical)	-0.7589	-0.1326	0.2809	1.2321	-0.5951	0.2866
Ornidazole	0.1947	-0.5991	-0.3448	-0.0255	0.2956	0.1299
Orphenadrine citrate (Norflex)	-4.4906	-0.5172	-2.5087	-1.6129	-2.0676	-2.3608
Oseltamivir phosphate (Tamiflu)	-7.4738	0.3306	0.3528	0.8960	0.8117	1.3019
OSI-420 (Desmethyl Erlotinib)	-1.5099	-0.6595	0.9641	1.2755	0.6951	0.6633
Otilonium Bromide	-1.2193	-0.2414	-1.7478	-0.9189	-1.7478	-2.8283
Ouabain	-14.5743	-18.0745	-19.2405	-10.0950	-12.5043	-14.4039
Oxacillin sodium monohydrate	-0.6476	-1.2618	0.0369	-0.3570	-1.2752	-0.2110
Oxaliplatin (Eloxatin)	-0.7504	-0.0677	1.4068	0.6545	0.1237	1.2832
Oxaprozin	-0.8664	-0.1966	-0.8630	-0.3333	-1.0071	-0.9231
Oxcarbazepine	0.1096	0.2924	0.8247	0.7113	-0.1768	0.7700
Oxeladin Citrate	-0.6670	-1.5358	-2.3931	-0.8380	-0.3145	-1.6921
Oxethazaine	-0.2183	-1.8077	-8.0459	-0.1711	0.1226	-1.7440
Oxfendazole	0.9351	0.6358	0.3050	0.8920	1.4005	0.9249
Oxibendazole	-0.4314	1.3571	-0.5924	-0.0390	1.4583	0.0031
Oxiglutatione Disodium Salt	-0.4167	0.0786	-0.8058	0.1384	0.2405	-0.1867
Oxprenolol HCl	0.6476	0.6352	0.1968	0.3262	0.5298	0.6280
Oxybuprocaine HCl	-1.1119	-1.7029	-0.8640	-0.3615	-1.3055	-1.6063
Oxybutynin (Ditropan)	-1.1268	0.4866	-0.6737	-0.0253	-0.7096	-0.6264
Oxybutynin chloride	0.0629	-1.5079	-0.6009	0.2528	0.1415	-0.2153
Oxymetazoline hydrochloride	0.0788	-0.1453	0.0176	0.2595	0.2610	0.3053
Oxymetholone	0.0599	0.8367	0.1115	0.9051	0.7172	0.5864
Oxytetracycline (Terramycin)	-0.9289	-0.0968	-0.3417	-0.9432	-1.6819	-0.6744
Oxytetracycline dihydrate	-0.3435	-0.9994	-0.4360	-1.1971	-1.2357	-0.1012
Ozagrel	0.6009	0.5612	0.5755	0.4966	0.1513	0.7182
Ozagrel HCl	0.2331	0.1683	-1.4577	-0.8050	-0.1954	-1.3992
Paclitaxel (Taxol)	-12.8785	-17.1843	-16.4073	-8.8346	-11.1252	-13.2573
Paeoniflorin	-0.6244	0.2938	-0.7730	-0.4118	-0.3996	-0.7013
Paliperidone (Invega)	0.4410	1.1861	-0.2612	1.1181	0.7660	0.9333
Palonosetron HCl	-5.8641	-6.1709	-6.8281	-2.1667	-2.6293	-4.3563
Pamidronate Disodium	0.4522	0.4354	-0.0342	1.0050	0.4047	0.3374
Pancuronium (Pavulon)	-0.3022	-0.8007	0.2151	0.1327	-0.4609	0.0060
Pantothenic acid (pantothenate)	-1.0140	0.2312	-0.8017	-0.7533	0.0021	-0.8418
Paromomycin Sulfate	-0.8305	-0.2118	0.2433	-0.0648	-0.5269	0.5092
Paroxetine HCl	-13.0419	-15.9596	-16.6356	-8.1625	-9.6875	-12.2333
Pasiniazid	0.6628	0.5245	0.0773	0.1334	0.5500	0.2879
Pazopanib	0.4753	0.6961	0.5134	0.7989	0.1466	0.5163
Pazopanib HCl	0.8175	-0.1727	-0.7941	1.2082	0.5266	-0.7185
PCI-32765 (Ibrutinib)	-0.9143	-0.3300	0.2523	1.3940	0.8922	0.6820
Pefloxacin mesylate	0.1934	-1.3740	-1.3483	-1.0458	-0.2048	-1.1091
Pemetrexed	-8.3408	-9.3603	-6.0839	-2.3502	-2.7256	-6.3718
Pemirolast (BMY 26517) potassium	-0.5690	-0.7828	-1.8418	-1.4751	-1.4124	-1.9791
Penciclovir	-0.2291	0.3927	-1.2501	-0.1750	0.1188	-1.3269

Penfluridol	-14.6812	-19.9258	-21.7764	-10.2445	-11.4777	-15.1825
Penicillamine (Cuprimine)	0.8139	0.9125	0.2428	0.0016	0.4523	0.4961
Pentamidine	-4.7780	-3.6510	-9.3059	-2.6711	-2.0928	-8.8573
Pentoxifylline	0.6608	0.5147	0.9734	0.4862	0.4669	0.5956
Peramivir Trihydrate	0.5068	0.4188	0.3508	1.0863	0.4416	0.9279
Pergolide mesylate	-0.6748	-1.4834	-1.2294	-0.3814	-0.7083	-0.5675
Perindopril Erbumine (Aceon)	0.9944	1.6793	0.9195	1.8764	1.2225	0.9405
Phenacetin	-0.0096	0.4840	-0.1733	0.2597	-0.0746	-0.5460
Phenazopyridine HCl	0.9771	-0.1117	-1.1794	-0.0543	0.0251	-1.4994
Phenformin hydrochloride	-0.4917	-0.6063	-0.2034	-1.1986	-0.5123	-1.4205
Phenindione (Rectadione)	0.6505	0.0116	-0.2986	-0.8571	-1.4212	-0.4176
Pheniramine Maleate	-0.8460	-0.6062	-0.5040	-0.2424	-0.8993	-1.2353
Phenothrin	0.1431	0.0938	-0.4342	-0.0333	0.4877	0.1796
Phenoxybenzamine HCl	-0.6104	0.5661	0.0839	-1.0296	0.8907	-0.1275
Phentolamine mesilate	-0.0399	-0.9385	-1.6902	-0.4793	-1.3528	-2.5783
Phenylbutazone (Butazolidin, Butatron)	0.3493	-0.6435	-0.0389	-0.9702	0.5795	-0.8802
Phenylephrine HCl	1.4557	0.8394	0.1701	0.2514	1.0205	0.9653
Phenytoin (Lepitoin)	-15.6653	0.3760	0.4469	0.0149	0.2124	-0.1008
Phenytoin sodium (Dilantin)	-8.3459	0.0188	-0.4664	-0.9750	-0.5063	-0.8932
Phosphatidylcholine	0.7486	-0.2638	0.8080	0.1006	-0.1265	0.6654
Phthalylsulfacetamide	0.0002	0.2456	-0.1165	0.2668	0.0200	-0.1590
Physostigmine Hemisulfate Salt	-2.4906	-1.4973	-0.6770	-0.3387	-0.4534	-0.3389
Physostigmine Salicylate	-0.4498	0.4403	0.1209	-0.1353	0.0920	0.3493
Picrotoxinin	-0.7382	0.5429	0.3543	0.3433	0.5879	0.2889
Pidotimod	0.5384	0.1358	1.0541	0.5613	1.1500	0.4307
Pilocarpine HCl	-0.2897	0.0312	-0.6741	-0.6525	-0.8902	-0.4611
Pimecrolimus	-7.1664	-5.1884	-2.7224	-2.8749	0.2719	-4.3037
Pimobendan (Vetmedin)	-7.4951	-11.3442	-9.6497	1.0051	-2.1632	-3.7072
Pimozide	-5.5403	-7.9833	-6.4931	-3.2058	-4.0109	-11.8801
Pinacidil	-0.0030	-0.0159	-0.2378	-0.2406	0.0933	-0.1140
Pindolol	0.7316	0.3280	0.4775	0.2759	0.1513	0.4046
Pioglitazone (Actos)	0.3096	-0.2606	-0.4554	-0.2954	0.0094	0.2255
Pioglitazone hydrochloride (Actos)	-0.2140	0.4098	-0.1159	-0.3515	-0.5956	-0.0497
Pipenzolate Bromide	-1.1435	-1.3185	-0.3805	-0.1970	-1.2618	-0.9323
Piperacillin Sodium	-2.5386	-1.2224	-2.5921	-1.7634	-1.2305	-3.5359
Piromidic Acid	-0.9554	-0.3496	0.4944	0.3035	0.1194	0.0595
Piroxicam (Feldene)	-0.1764	0.6728	-0.3346	-0.5002	0.0286	0.6975
Pitavastatin calcium (Livalo)	-10.9673	-17.6993	-18.1431	-13.0390	-12.3249	-15.0414
Pizotifen malate	-2.1729	-1.7416	-1.1946	-0.7454	-0.8759	0.0030
Plerixafor (AMD3100)	0.2404	0.6959	0.5270	0.1475	0.5979	0.6804
PMSF (Phenylmethylsulfonyl Fluoride)	0.5742	0.3975	0.2465	0.6384	-0.0328	0.4858
Pomalidomide	-0.1228	0.1783	0.8687	1.4097	0.0300	0.5493
Ponatinib (AP24534)	-14.9295	-21.0552	-21.9585	-11.0630	-12.4707	-15.8762
Posaconazole	0.0772	-4.4954	-2.7065	-2.8185	-5.7219	-2.2523
Potassium Canrenoate	-0.7129	-0.0458	-0.8916	-0.2846	-0.0349	-0.3838
Potassium iodide	-1.3407	-1.5949	-1.8276	-1.3180	-1.0868	-1.4865
Pralatrexate (Folotyn)	-7.0099	-9.1791	-12.3447	-2.4599	-4.2683	-5.6332
Pramipexole (Mirapex)	0.6048	0.5706	-0.0162	0.0486	0.2252	0.0137
Pramipexole dihydrochloride monohydrate	-1.6646	1.3245	0.6115	0.3492	1.0289	0.1967
Pramiracetam	-3.4857	0.0219	-0.3105	0.2508	0.5970	0.4345
Pramoxine HCl	0.4879	0.5675	-0.2330	0.4029	-0.2226	0.3190
Pranlukast	1.0182	1.4116	0.3914	1.0636	1.6563	0.9575
Pranoprofen	-1.7660	-0.0423	0.0532	0.4337	0.8268	-0.1798

Prasugrel (Effient)	0.6883	0.9017	1.1983	0.0170	0.2907	0.1115
Pravastatin sodium	-5.8246	-0.0609	-0.3767	0.1150	-0.9230	-0.2732
Praziquantel (Biltricide)	0.4910	1.3827	0.6541	1.0352	1.0962	1.0500
Prazosin HCl	-3.5996	-11.9036	-14.4620	-2.5371	-5.7377	-10.6782
Prednisolone (Hydroretrocortine)	0.1320	1.3434	0.8654	0.8653	0.2491	0.9620
Prednisolone acetate (Omnipred)	1.1314	1.1126	0.9010	-0.0764	1.2460	0.6622
Prednisone (Adasone)	0.4220	0.2340	0.9953	0.1608	-0.4529	0.3595
Pregnenolone	-0.4338	-0.8738	-0.6165	-0.6295	-1.3508	-0.5412
Pridinol Methanesulfonate	-2.9844	-0.6429	-2.1782	-1.0893	-0.3719	-1.1474
Prilocaine	0.9331	0.5006	0.2265	1.2107	0.0626	0.6559
Primaquine Diphosphate	-0.1537	-0.7108	-3.9813	0.0889	-0.2118	-2.8064
Primidone (Mysoline)	1.0301	0.5736	0.7332	0.4645	1.0396	0.3611
Proadifen HCl	-2.8932	-1.0677	-3.5078	-1.3642	0.0570	-2.6619
Probenecid (Benemid)	0.1518	0.1531	0.8227	0.7382	0.7584	0.1889
Probucol	0.6603	0.7927	0.0996	0.7371	0.2623	0.7628
Procarbazine HCl (Matulane)	-2.9997	1.1889	0.6616	0.4390	1.0309	0.0647
Prochlorperazine Dimaleate	-9.3795	-4.0504	-2.8504	-7.1394	-1.5488	-7.6176
Procodazole	1.1067	1.0539	0.7886	0.4284	0.4850	0.6505
Procyclidine HCl	-1.6216	-0.4259	-0.0490	0.5204	0.6190	0.0845
Progesterone (Prometrium)	-0.2043	0.4601	-0.1699	1.9343	0.8584	0.5737
Propafenone (Rytmonorm)	-1.8425	-0.3274	-1.4112	0.5132	0.6316	-1.0670
Proparacaine HCl	-0.5326	1.3887	0.5837	0.8054	1.5780	1.0934
Propranolol HCl	0.8246	2.1710	2.4687	1.7071	1.5033	0.9864
Propylthiouracil	0.4786	-0.3592	0.0332	-0.1893	-0.7518	0.2031
Protionamide (Prothionamide)	0.4225	0.1062	-0.4800	-0.0293	0.1883	-0.0261
Pyrazinamide (Pyrazinoic acid amide)	-1.9976	-0.3219	-0.9526	-1.0257	-0.9386	-1.7169
Pyridostigmine Bromide (Mestinon)	-0.0741	0.5740	0.2791	0.4352	-0.5575	0.4819
Pyridoxine hydrochloride	0.5858	-0.0145	0.8971	0.7114	1.0884	0.7497
Pyrilamine Maleate	-0.1681	-0.0132	-1.6759	-0.6833	0.6706	-1.8132
Pyrimethamine	-23.2058	-12.3167	-12.7116	-5.1386	-6.4014	-9.0433
Pyrithione zinc	-13.1152	-16.2778	-16.9965	-8.6108	-9.7110	-12.3542
Quetiapine fumarate (Seroquel)	-1.1563	-1.4225	-0.6602	-0.0631	-1.1614	-0.8044
Quinapril HCl (Accupril)	-1.1034	0.9810	0.6148	0.8141	1.0829	0.8164
Quinine hydrochloride dihydrate	-0.0338	1.2508	-0.2685	0.5823	0.7610	0.1462
Quipazine Maleate	0.2261	0.6420	0.4532	0.5235	0.2644	0.5835
R-(-)-Apomorphine HCl Hemihydrate	-1.1344	-0.2397	0.0318	0.5001	0.8607	0.1270
Racecadotril (Acetorphan)	0.6980	1.3116	1.2611	0.2452	0.9290	0.7142
Ractopamine HCl	0.2049	0.8035	0.6677	0.2655	0.8546	0.2378
Raltegravir (MK-0518)	0.2832	-0.2019	-0.0269	-0.4572	-0.4148	0.5144
Ramelteon (TAK-375)	-0.2020	0.3558	-1.9394	-0.2715	-1.5582	-0.4714
Ramipril (Altace)	0.9190	-0.8412	0.1775	-0.2452	-0.0178	0.2737
Ranitidine (Zantac)	-0.3774	0.9548	0.0680	-0.1583	0.6060	0.1575
Ranolazine (Ranexa)	0.2699	-0.7738	-0.0997	-0.7582	-0.1088	-1.0055
Ranolazine dihydrochloride	-21.2032	0.3931	-0.7201	-0.5572	-0.8782	-1.3096
Rapamycin (Sirolimus)	-2.0838	-2.8404	-4.2730	0.1587	-0.2349	-2.1860
Rasagiline mesylate	0.0642	0.1766	0.2062	1.0312	0.8094	0.6404
Rebamipide	0.9836	0.9676	0.9280	0.4369	0.4968	0.7786
Reboxetine mesylate	0.6952	-0.2903	0.2014	0.3726	0.0328	0.5659
Regorafenib (BAY 73-4506)	-0.4735	-2.1645	-1.4530	-7.2809	-0.1247	-1.0484
Repaglinide	-20.3068	0.1275	-0.4008	-0.5817	-0.7440	-0.7265
Reserpine	-0.9825	0.9674	0.3848	1.8150	0.9776	0.4329

Resveratrol	-3.0915	-2.0404	-2.5731	-13.2592	-1.1826	-1.7971
Retapamulin	-1.6026	-1.0408	-1.9213	0.9268	0.9057	-1.0371
Ribavirin (Copegus)	1.4720	2.0087	2.0970	1.4410	2.3943	1.5193
Riboflavin (Vitamin B2)	0.3625	-0.0327	-0.4146	-0.2016	0.0435	-0.5832
Rifabutin (Mycobutin)	-0.2230	-1.5760	-0.9281	-0.1798	-0.4263	-0.2241
Rifampin (Rifadin, Rimactane)	-0.8561	-0.1850	-2.3559	-0.3167	-0.7120	-0.2303
Rifapentine (Priftin)	0.1738	-0.7129	-1.6533	-14.8838	-0.0316	-0.3223
Rifaximin (Xifaxan)	1.4886	0.2959	2.0263	1.0790	1.7531	1.5210
Riluzole (Rilutek)	0.4491	0.5370	0.6734	1.5705	0.0958	-0.4078
Rimantadine (Flumadine)	0.6038	0.7421	0.9442	0.4206	0.7864	0.1637
Rimonabant (SR141716)	-12.3898	-1.2240	-1.5645	0.3802	-0.2126	-0.4827
Risedronate sodium	-18.6245	-0.2306	-1.0737	-1.4712	-0.7689	-1.2340
Risedronic acid (Actonel)	0.3610	1.3575	0.3443	0.4757	1.1677	0.9427
Risperidone (Risperdal)	-0.1296	-0.6363	-0.4469	0.8628	-0.2088	0.2199
Ritodrine hydrochloride (Yutopar)	0.7599	0.0041	0.4962	0.5038	0.7205	0.5574
Ritonavir	0.5097	1.5156	1.3551	2.0487	0.8373	0.9030
Rivaroxaban (Xarelto)	0.4667	0.9279	1.5442	1.3117	0.9681	1.2651
Rivastigmine tartrate (Exelon)	-0.1252	0.3088	0.0144	0.5546	0.2564	0.4487
Rizatriptan Benzoate (Maxalt)	0.8305	0.4437	0.4330	1.6024	0.0147	0.6029
Rocuronium bromide	-1.3781	-0.9850	-1.0258	-0.0743	-0.5491	-0.8191
Rofecoxib (Vioxx)	0.6950	0.1016	0.0631	0.0045	-0.6943	-0.2299
Roflumilast (Daxas)	0.8606	0.4829	0.3958	0.5624	0.4718	0.5956
Rolipram	-15.7604	0.2046	-0.4037	-0.7499	-0.9644	-0.5895
Rolitetracycline	0.7307	0.4132	0.9046	0.4935	1.0098	0.5536
Ronidazole	0.3466	1.1507	1.4050	1.0209	1.1759	1.1208
Ropinirole HCl	0.2806	0.0193	0.5148	1.1459	0.2257	0.9247
Ropivacaine HCl	-1.5426	-1.9709	-0.0019	-0.1932	-0.7425	-1.0591
Rosiglitazone (Avandia)	-0.4915	-0.5265	-0.1832	-0.7581	-0.5375	-0.9160
Rosiglitazone HCl	0.3912	0.6956	-0.2278	0.0337	0.2769	0.0258
Rosiglitazone maleate	0.5367	1.4346	1.9136	0.7826	1.0419	1.0506
Rosuvastatin calcium (Crestor)	1.2033	0.0509	0.2812	0.6823	0.5067	0.3627
Roxatidine acetate HCl	-0.0441	-0.3539	-1.2594	-0.7589	-0.8154	-1.5306
Roxithromycin (Roxl-150)	0.7301	0.8074	0.9902	0.9688	0.2782	0.6508
Rufinamide (Banzel)	1.1217	0.2242	1.0027	-0.0393	0.3846	-0.4340
Ruxolitinib (INCB018424)	0.2456	0.9242	0.6832	0.9978	0.1503	0.8252
S-(+)-Rolipram	-0.1382	0.5493	0.5992	0.7801	0.3293	0.5423
Salbutamol sulfate (Albuterol)	0.4281	0.6106	0.6722	0.3745	0.2597	0.7520
Salicylanilide	1.2394	1.7550	0.8814	0.9112	0.4610	0.8506
Sarafloxacin HCl	-23.3387	-1.5896	-1.1165	-1.2056	-0.3445	-1.1524
Sasapyrine	1.5599	1.5670	1.0843	1.3838	1.1449	1.1772
Saxagliptin (BMS-477118,Onglyza)	0.9208	1.9538	1.6308	-7.9878	1.6912	1.2600
Scopine	0.0608	-0.4669	0.6151	0.2328	-0.4305	0.2397
Scopolamine hydrobromide	0.4136	0.0326	0.5100	0.1055	0.0673	0.7834
Secnidazole (Flagentyl)	0.4136	0.6808	0.4672	0.2418	-0.0875	0.7106
Serotonin HCl	0.7749	-0.4823	0.9803	0.0087	-0.0962	0.2731
Sertaconazole nitrate	-1.9846	0.1041	0.0103	-0.6132	0.2455	0.9180
Sertraline HCl	-14.3300	-17.3068	-18.7919	-9.5329	-10.3890	-13.6602
Sevelamer HCl	0.0042	-0.7846	-0.7937	-0.9916	-2.1171	-1.5093
Sildenafil citrate	-0.3024	0.5604	-0.3056	-0.0582	-0.5725	-0.1197
Silodosin (Rapaflo)	-0.6481	-0.2439	-0.6843	0.9417	0.0495	-0.1466
Simvastatin (Zocor)	-4.1669	-0.3975	0.4566	-0.0862	0.5942	0.9729
Sitafloxacin hydrate	0.7478	-0.1614	0.3287	-0.0652	-0.0571	-0.1389

Sodium 4-aminohippurate Hydrate	-1.8234	-0.0835	-0.2280	0.3131	0.6639	-0.1642
Sodium ascorbate	1.0541	-0.2115	0.0129	-0.3492	-0.6866	-0.3113
Sodium butyrate	0.4997	2.1532	1.7584	0.7282	1.1733	1.1867
Sodium Gluconate	-0.0123	0.7602	-0.5456	0.1324	0.8765	0.1185
Sodium Monofluorophosphate	0.0315	-0.9173	0.1582	-0.0535	-0.9001	-0.6232
Sodium nitrite	0.3855	0.7445	1.2182	1.2518	0.5994	1.0280
Sodium Nitroprusside	-2.0278	0.9129	0.5594	-0.0545	0.9934	0.5694
Sodium orthovanadate	0.0137	1.5381	0.9317	0.6533	1.2105	0.7653
Sodium Picosulfate	-1.0616	-0.3998	-1.1442	-0.7073	0.1314	-1.4616
Sodium salicylate	0.4145	0.7459	1.2687	1.6868	1.2732	1.4091
Solifenacin succinate	-6.3335	-3.6164	-4.2369	-2.3957	-2.2532	-4.4557
Sorafenib (Nexavar)	-0.0772	-4.1520	-0.5537	0.1793	0.8935	-0.1636
Sorbitol (Glucitol)	-0.0645	-1.8897	-0.3876	-0.4601	-0.8969	-0.2859
Sotalol (Betapace)	-0.0089	-0.4959	0.0666	-0.2504	0.0231	0.4620
Sparfloxacin	0.6894	0.7761	-0.1463	1.0080	0.8344	0.6648
Spectinomycin hydrochloride	-8.8095	-0.4604	-1.1606	-0.4353	-0.2041	-0.7340
Spiramycin	-1.5858	-0.6685	-0.9756	-0.6482	-0.6739	-1.7190
Spironolactone	0.4000	0.7238	0.7204	1.8319	0.9885	0.6930
Stavudine	-0.2635	-0.1205	-0.6947	0.9842	-0.3940	-0.2997
Streptomycin sulfate	1.5559	0.0040	0.7987	-0.1194	0.6851	0.8084
Streptozotocin (Zanosar)	0.2182	0.2980	0.0068	0.6017	0.1042	0.3080
Strontium ranelate (Protelos)	0.0593	-0.6530	0.6787	-0.1459	-0.7762	0.3226
Sucralose	-0.2400	-0.6009	0.1598	0.3307	-0.5282	0.1758
Sulbactam	-20.8159	-1.1543	-1.0452	-0.7365	-0.0492	-1.5937
Sulbactam sodium (Unasyn)	0.0828	-0.6729	0.3978	-0.4897	-1.0989	0.0312
Sulconazole Nitrate	-1.7696	-1.8737	-9.9213	-2.5111	-2.4339	-8.3635
sulfacetamide sodium	0.5984	0.4580	-0.1239	-0.2320	-0.2859	0.0177
Sulfadiazine	-1.4876	0.6120	0.1548	-0.5983	-0.8230	-0.4235
Sulfadoxine (Sulphadoxine)	0.1468	0.7403	-0.1235	0.2328	0.6728	-0.0310
Sulfaguanidine	0.6133	1.1126	0.4039	0.9832	0.6946	0.7056
Sulfamerazine	0.6072	0.9816	1.0618	0.8865	1.0242	1.0455
Sulfameter (Bayrena)	0.1612	0.9754	0.8645	1.4448	0.3888	0.8458
Sulfamethazine	0.7198	0.9349	1.1243	1.0188	1.0862	1.3384
Sulfamethizole (Proklar)	1.6284	-1.4647	0.2535	-0.5927	-0.6460	-0.0656
Sulfamethoxazole	-0.0625	-0.5305	-0.1616	-0.5138	-1.6148	-1.2774
Sulfanilamide	0.3776	-0.0155	-0.3562	0.7459	0.8652	0.0781
Sulfapyridine (Dagenan)	1.1899	0.6761	1.3683	1.4084	0.7888	0.8617
Sulfasalazine (Azulfidine)	0.5118	-1.9050	-1.5411	-13.5020	-0.4684	-0.7711
Sulfathiazole	0.1647	-0.1016	0.7868	0.8922	0.4691	0.4815
Sulfisoxazole	-0.6085	-1.0853	-0.7977	-0.5110	-2.5494	-0.9496
Sulindac (Clinoril)	-14.3232	0.5320	-0.1566	0.2377	0.1873	-0.3050
Sulphadimethoxine	-0.3585	-0.2420	0.7043	0.4071	1.0550	0.2142
Sumatriptan succinate	0.6742	0.5684	0.1511	-0.7894	-0.7296	0.0071
Sunitinib Malate (Sutent)	-18.3043	-8.4696	-0.8621	-8.8448	-0.1817	-0.9142
Suplatast tosylate	0.0577	1.2955	0.9088	0.4311	1.2363	0.6488
Suprofen (Profenal)	-1.9810	-1.5397	-1.0477	-2.6881	-1.4308	-1.6256
Suxibuzone	0.0220	-0.0870	0.6492	-0.2336	-0.2102	-0.0018
Tacrine HCl	-0.4939	-0.2409	-0.7408	-0.2316	-0.3537	-0.1994
Tadalafil (Cialis)	-0.6354	0.0306	0.0107	1.5244	-1.5666	0.2616
Talc	-0.8733	0.2859	0.0157	0.0462	-0.1591	-0.0831
TAME	-0.2084	0.1692	-0.0144	-0.4412	-0.2274	0.1489
Tamoxifen Citrate (Nolvadex)	-8.0163	-13.2273	-11.6527	-7.0781	-8.7592	-11.5833
Taurine	-7.6979	1.2333	0.2823	0.5272	0.8320	0.3342
Tazarotene (Avage)	0.2460	0.3455	0.3309	1.2830	0.0098	0.5851
Tebipenem pivoxil (L-084)	-0.8139	-0.2458	-0.1859	0.6900	0.0986	0.0415

Teicoplanin	0.7130	0.5549	0.1511	0.6418	-0.0814	-0.4903
Telaprevir (VX-950)	-2.8497	0.5179	-0.2481	-1.7497	1.2616	-0.0113
Telbivudine (Sebivo, Tyzeka)	0.4662	-0.5397	-0.4710	-0.8404	0.6480	-1.3204
Telmisartan (Micardis)	-0.2511	1.8174	0.5395	0.6164	-0.5525	1.0045
Temocapril HCl	0.7419	0.4925	0.3031	1.0713	0.7745	0.4563
Temsirolimus (Torisel)	-1.4587	-3.9046	-4.0159	1.1109	-0.2800	-1.5080
Teniposide (Vumon)	-8.5722	-13.5231	-12.7606	-5.9087	-7.8824	-11.2931
Tenofovir (Viread)	-0.1361	0.1871	0.6875	0.0523	-0.4906	-0.0673
Tenofovir Disoproxil Fumarate	-0.1314	0.5106	0.6777	0.5057	-0.3486	-0.3525
Tenoxicam (Mobiflex)	0.2360	0.3558	0.0767	0.7603	0.5867	0.5604
Terazosin HCl (Hytrin)	0.6843	0.1183	-1.2205	-0.8982	-1.6507	-0.8732
Terbinafine (Lamisil, Terbinex)	0.2713	1.7072	0.4524	1.2610	0.6639	1.0360
Terbinafine hydrochloride (Lamisil)	-0.5926	0.0469	-0.7177	0.0683	0.4012	-1.2926
Terfenadine	0.4883	0.1286	-0.0024	0.4027	0.6233	0.0234
Teriflunomide	1.5640	1.1230	0.9874	1.5730	1.1938	1.0563
Tetracaine hydrochloride (Pontocaine)	0.8198	0.3446	0.3289	0.1362	0.7044	0.0459
Tetracycline HCl	1.2966	0.3396	0.2705	-0.3325	0.5631	0.3245
Tetraethylenepentamine 5HCl	0.1429	0.5058	0.5729	0.9433	0.2542	0.6430
tetrahydrozoline hydrochloride	-0.3160	0.1963	0.6142	0.3970	0.7288	0.5062
Tetramisole HCl	-1.9362	-1.4306	-1.3328	-1.5622	-0.8745	-2.0342
Thalidomide	0.4338	1.0102	2.5887	1.7490	1.0926	1.7994
Thiabendazole	0.0740	1.5144	0.1958	1.2173	0.0561	0.8563
Thiamine HCl (Vitamin B1)	0.6005	0.1436	-0.1696	-0.3408	-0.5856	-0.0169
Thiamphenicol (Thiophenicol)	0.5713	0.9481	0.1567	0.6271	0.3528	0.0564
Thioguanine	-10.6754	-18.6801	-19.3266	-11.8787	-8.7696	-13.2564
Thioridazine HCl	-14.3721	-17.6312	-18.9537	-9.8349	-11.2616	-13.2029
Thiostrepton	-1.5274	-0.4571	-0.6533	-0.4097	0.5411	0.0044
Thonzonium Bromide	-14.6826	-19.0153	-19.6885	-10.4547	-11.6925	-14.7018
Tianeptine sodium	0.1323	-0.0854	-0.3033	-0.7091	-1.2236	0.3251
Ticagrelor	0.2968	0.9273	0.4771	1.1020	0.6277	-0.6683
Ticlopidine HCl	0.7578	1.2686	1.3419	0.7520	1.0767	0.9951
Tigecycline	0.5229	-0.0379	-0.0544	-0.2171	-1.1177	-0.2263
Tilmicosin	-0.2803	-0.8337	-2.1575	-1.0501	-1.4708	-1.8336
tinidazole	-0.1654	1.3554	0.4206	0.8061	0.6773	0.6993
Tioconazole	-1.1510	-4.6871	-5.4471	-2.8846	-2.4332	-5.4613
Tiopronin (Thiola)	0.0001	0.4324	-0.0201	-1.1301	-1.6682	-0.3965
Tiotropium Bromide hydrate	-0.2944	-0.0663	0.2217	0.8727	-0.3515	0.1606
Tioxolone	0.2458	0.5802	0.5523	0.9108	0.7728	1.2103
Tiratricol	-0.5310	0.6887	-0.1218	0.6566	0.6200	0.1355
Tizanidine HCl	-0.1981	-0.6929	-0.9257	-1.8554	-1.5368	-0.0780
Tobramycin	0.3409	0.5142	0.1530	0.6361	0.7934	0.3867
Tofacitinib citrate (CP-690550 citrate)	-0.0063	0.5538	0.2630	0.2393	-0.1870	0.1760
Tolazamide	0.0895	0.2799	0.6102	0.0033	-0.0481	0.3839
Tolbutamide	-7.9273	0.4561	-0.4100	-0.0202	-1.0098	0.0894
Tolcapone	-0.5236	0.0203	-0.6280	0.8103	0.2372	-0.8214
Tolfenamic acid	-12.8670	-0.1833	-0.3504	0.2971	0.3590	-0.5956
Tolmetin Sodium	-0.5122	0.0752	0.1126	-0.4837	0.4454	-0.3404
Tolnaftate	-0.3002	-0.2139	-0.9659	-1.5711	-1.7873	-1.2121
Tolperisone HCl	0.9059	1.0494	0.4712	1.2326	0.3812	0.8112
Tolterodine tartrate (Detrol LA)	-15.8034	-1.6497	-0.6102	-0.5262	-1.0245	-0.8177
toltrazuril	-0.2160	-0.5931	-0.9426	-0.2409	-0.2973	-0.0448

Tolvaptan (OPC-41061)	-0.2330	-0.6401	-0.3850	-0.0050	-0.1256	-0.5980
Topiramate	0.3169	-1.0138	-1.0400	-14.1428	0.4690	-0.8537
Topotecan HCl	-19.1564	-25.4352	-25.9321	-12.8996	-15.0655	-18.4084
Toremifene Citrate (Fareston, Acapodene)	-8.1031	-10.0865	-21.3402	-14.7827	-3.7350	-13.2901
Torsemide (Demadex)	0.0488	1.2981	0.4478	-0.6186	0.1927	0.5935
Tranexamic acid (Transamin)	0.5869	1.4007	0.5743	0.5751	1.2300	0.9116
Tranilast (SB 252218)	0.5426	-0.5867	-0.9495	-1.9010	0.5293	-0.4760
Trazodone hydrochloride (Desyrel)	-4.4070	0.5802	-0.2594	1.0389	0.7016	1.2154
Tretinoin (Aberela)	0.2615	-1.2410	-0.5434	0.9334	0.7457	0.0918
Triamcinolone (Aristocort)	0.6691	-2.2040	-3.5674	-1.5431	-0.6645	-2.5491
Triamcinolone Acetonide	0.4516	0.4949	0.6062	1.0078	-0.7867	-0.0534
triamterene	-0.4317	-0.3462	-0.8222	-0.0284	-0.0045	-1.3301
Trichlormethiazide (Achletin)	-0.2803	0.5863	-0.0214	0.6647	0.6573	-0.1677
Triclabendazole	-0.3169	-1.3623	-0.5384	-0.5262	-0.6642	-1.4201
Trifluoperazine 2HCl	-12.4443	-20.4697	-20.0311	-10.6819	-12.2645	-15.1529
Triflupromazine HCl	-3.6447	-1.1984	-2.5632	-3.1550	-0.7165	-2.1006
Trifluridine (Viroptic)	-7.8237	-8.0698	-8.5713	-5.9743	-5.7880	-7.6520
Triflusal	0.5578	-0.3703	0.1351	0.1202	-0.3466	0.6253
Trilostane	0.1628	-0.1956	0.4013	-0.0827	-0.3741	-0.1603
Trimebutine	0.5261	0.1285	-0.4319	0.6042	0.5468	0.3410
Trimethoprim	-0.2672	0.0692	0.0107	-0.2053	0.2676	0.2528
Trimipramine Maleate	-3.0886	0.0529	-0.9640	-0.4192	0.5568	-0.1457
Tripelennamine HCl	-0.4674	-0.9816	-1.2531	-0.2738	-0.6829	-0.5013
Trometamol	0.5255	0.9644	0.8254	1.0545	0.9348	0.6548
Tropicamide	0.3905	-0.0215	-1.2738	-0.9978	-1.5877	-1.1546
Tropisetron	-1.9289	-0.5182	-1.9710	-1.1950	-0.8983	-1.1366
Trospium chloride (Sanctura)	-0.0347	-0.4854	-0.0660	-0.3564	-0.9295	0.5192
Troxipide	-0.3087	-0.0228	-0.7805	-1.4357	-2.0241	-1.0025
Tylosin tartrate	-0.3513	0.2346	-0.4949	-0.1687	-0.4019	0.0214
Ubenimex (Bestatin)	-0.0126	0.0306	-0.0414	1.3151	0.7308	0.1894
Ulipristal	-0.0773	-0.8348	-0.0768	0.6294	0.0278	-0.0053
Uracil	0.3813	1.5231	0.9578	1.2550	1.0479	1.1241
Urapidil HCl	0.3941	-0.1944	-0.0727	-0.0779	-0.2718	0.3222
Uridine	1.1014	1.0035	0.4796	0.5166	0.7053	0.1444
Ursodiol (Actigal Urso)	0.3791	0.4151	-0.2567	-0.2424	0.0324	-1.2785
Valaciclovir HCl	0.2907	1.1761	0.2934	0.6461	0.5604	0.8218
valganciclovir hydrochloride	0.7427	1.8778	1.6495	1.0220	1.3068	1.1894
Valnemulin HCl	-0.5703	-1.1411	-0.8998	0.1473	-0.5932	-1.0175
Valproic acid sodium salt (Sodium valproate)	1.2722	1.3571	1.0362	0.5096	0.4526	0.8541
Valsartan (Diovan)	0.2528	0.8536	0.4164	0.1891	1.1646	0.5016
Vancomycin HCl (Vancocin)	0.7436	0.4881	0.2290	-0.1949	0.4639	0.0858
Vandetanib (Zactima)	-18.8177	-0.5205	0.0206	1.0220	0.7915	0.9327
Vardenafil (Vivanza)	-0.2340	0.7937	1.0396	0.9427	0.6865	0.4538
Varenicline tartrate	1.2635	-0.0306	-0.6962	-1.5200	0.9415	-0.0421
Vecuronium Bromide	0.4690	-0.3273	0.2302	0.2624	-0.3408	0.1581
Vemurafenib (PLX4032)	-2.4712	-2.9188	-3.7219	1.2111	-0.3111	-2.0052
Venlafaxine	-0.0376	-1.1432	-0.5689	-0.4086	0.8412	-0.0527
Verteporfin (Visudyne)	0.3460	-0.8762	0.4357	0.3427	0.5967	-0.0031
Vidarabine (Vira-A)	0.1149	-0.5432	1.8450	0.6286	0.4033	0.6199
Vildagliptin (LAF-237)	-5.0916	-1.5867	-2.3325	-0.7464	-0.9535	-1.4701
Vinblastine	-1.8177	-2.4508	-1.7816	0.0048	-0.6253	-0.3697
Vincristine	-15.5400	-20.7794	-21.4008	-10.4383	-12.2999	-14.2448
Vinorelbine (Navelbine)	-14.0284	-18.2673	-19.1868	-10.5352	-10.2902	-13.0422
Vinpocetine (Cavinton)	-2.0092	0.0066	-1.0378	0.1040	-0.0560	-0.3579
Vismodegib (GDC-0449)	0.7813	1.1719	1.1563	1.1409	0.5140	0.7940

Vitamin B12	-0.0126	0.1085	0.1488	0.1702	-0.2612	-0.0973
Vitamin C (Ascorbic acid)	0.1053	-0.2871	0.9282	0.6365	0.4848	0.8302
Vitamin D2	-0.2546	1.0336	1.3545	0.1938	1.0011	0.6224
Vitamin D3 (Cholecalciferol)	0.6533	1.2663	1.2622	1.1128	1.2766	1.0088
Voglibose	0.6834	-0.4078	-0.4658	-0.0557	-0.1209	-0.2199
Voriconazole	1.0313	-0.2458	0.6097	-0.0463	1.1358	0.1926
Vorinostat (SAHA)	-15.6294	-22.6029	-19.8585	-8.2366	-10.9909	-13.4676
XL-184 (Cabozantinib)	-9.3567	-13.2101	-4.5088	-6.9803	-6.5942	-2.8801
Xylazine HCl	1.1747	1.2848	1.3148	0.5511	1.1307	0.7242
Xylometazoline HCl	0.5477	-0.9357	-0.3742	-0.7681	-0.0258	-0.4396
Xylose	-0.1057	0.0202	0.2936	0.4408	0.4071	0.0767
Zafirlukast (Accolate)	0.8814	0.9712	0.8478	0.4647	-0.5360	0.2771
Zalcitabine	0.0311	1.0892	0.9087	-0.2077	0.1205	-0.9001
Zaltoprofen	0.2294	0.2963	0.1265	0.9460	0.4797	0.9672
Zanamivir (Relenza)	0.9905	0.4025	0.4202	1.2118	0.3637	0.9135
Zidovudine (Retrovir)	-3.6228	-0.5415	-0.8731	0.5537	0.7704	0.3104
Zileuton	1.5071	-0.4374	0.0690	-0.0521	0.9552	0.4325
Ziprasidone hydrochloride	1.0023	-0.7674	-0.0839	0.0877	0.8746	0.3755
Zoledronic Acid (Zoledronate)	0.4653	-0.5775	-1.5486	-0.5115	-0.3691	-0.5783
Zolmitriptan (Zomig)	-0.9763	-1.1847	-1.2869	-1.4627	0.2249	-2.6822
Zonisamide	1.1410	-0.6502	0.4285	0.0783	0.9000	0.3394
Zoxazolamine	-1.1918	-1.7772	-0.7709	-0.7736	-2.3510	-0.7684